Dissertation

submitted to the

Combined Faculty of Natural Sciences and for Mathematics

of the Ruperto Carola University Heidelberg, Germany

for the degree of

Doctor of Natural Sciences

Presented by

M.Sc. Sarah Simone Bunten

Born in Darmstadt, Germany

Oral examination: 14th September 2020

Host Cell Peptidylprolyl *cis-trans* Isomerases as Immune Modulators of HIV-1 Infection

1 Acknowledgement

Dankeschön geht an meinen Opa. Danke für deine nie endende Unterstützung, dein Interesse und deine aufmunternden Worte. Ohne euch hätte ich das alles nicht geschafft. Danke dass ihr mir die nötige Kraft gegeben habt.

2 Summary

Since the 1980s, the human immunodeficiency virus 1 (HIV-1) has been acknowledged as the trigger for AIDS, the acquired immunodeficiency syndrome. Every year, worldwide approximately 700,000 people die from late effects of HIV-1 infection and AIDS (UNAIDS, 2018). Thus, continuous research is important to better understand the interaction of the virus with the human host and to develop a cure. Host cell proteins that promote or fight infection are referred to as co- and restriction factors, respectively. Innate immunity restriction factors are, for example, TRIM5α or tetherin and some of them are induced by interferons (IFNs). Cyclophilin A (CypA), a small protein that influences the folding and thus the function of several cellular proteins, is a co-factor for HIV-1 infection. According to current knowledge, CypA shields cellular HIV-1 capsid cores form restriction factors after viral cell entry and thus ensures the safe transport of the virus genome into the cell nucleus. There, the HIV-1 genome can integrate into the host genome.

In addition to CypA, the protein family of cyclophilins (Cyps) contains at least 16 other proteins in humans, all of which have similar cyclophilin domain structures, but have diverse cellular functions. While the role of CypA during HIV-1 infection is reasonably well characterized, almost no information is available for the other Cyps. This work investigated the influence of Cyps on early HIV-1 infection events in connection with the antiviral effects of type I IFNs. In general, some type I IFN-stimulated cells exert a significantly reduced HIV-1 infection. Interestingly, this early block to infection is amplified in CypA deficient cells. This indicates a role of CypA in the immune defense against HIV-1. Furthermore, an increase in infection after treatment with a cyclophilin inhibitor, Cyclosporin A (CsA) was observed. This can also be observed in the absence of CypA, the supposedly main target of CsA inhibition. This suggested the presence of CsA-sensitive factors that affect HIV-1 infection in type I IFN treated cells. Since both, CsA and type I IFNs have been proposed and tested as possible therapy strategies, however with little success, this observation warrants further investigation to reveal the underlying mechanisms, which could lead towards an adapted therapeutic strategy.

The most obvious candidate targets are other members of the cyclophilin family. Therefore, CypB, CypC, CypD, CypE and CypH deficient THP-1 cells were generated using CRISPR/Cas9, and the effect of type I IFN treatment and CsA stimulation on HIV-1 infection was examined. While knockout of CypB, CypC and CypD modulated infection but showed no effect in response to IFN or CsA, CypE and CypH knockout cells showed a significantly increased sensitivity of HIV-1 infection to type I IFN-induced blocks. Due to these different

phenotypes, the interplay of several Cyps was examined by generating double knockout cell lines. Depletion of CypB alone had no effect on HIV-1 infection, but a significantly increased sensitivity to type I IFN-induced post entry blocks was observed in the absence of both, CypA and CypB. The same could be observed for the double knockout of CypA and CypE. This suggests that Cyp functions on early HIV-1 infection events are complex and that some functions may depend on other members of this protein family. Furthermore, the results of this study show that CypA is not the only member of this family that has a function during early HIV-1 infection.

The results from this study suggest that knockout of single cyclophilin genes was insufficient to render THP-1 cells insensitive to the CsA-induced increase in HIV-1 infection in type I IFN-induced cells, i.e. the phenotype could not be explained by one the candidates tested. To conduct a more unbiased approach, a mass spectrometry screen based on thermal protein stability was carried out covering the entire cellular proteome. In addition to known CsA targets, several new factors could be identified for which protein stability was sometimes dramatically altered upon CsA treatment of cells, indicating possible functional sensitivity to CsA. Some of these were IFN-induced proteins, such as members of the Retinoic Acid inducible gene I (RIG-I) signaling pathway. RIG-I recognizes viral RNA and induces an antiviral signaling cascade within the cell, which among other things leads to type I IFN production. Since this signaling pathway has been already associated with HIV-1 infection in the literature, some members of this signaling pathway were examined in more detail regarding HIV-1 infection and sensitivity to type I IFN and CsA. Knockout of RIG-I, MDA5, MAVS, TRADD or IRF3 in CypA deficient THP-1 cells showed increased sensitivity to type I IFN-induced early infection blocks. In addition, an increased infection in IRF3 knockout cells was observed, which indicates a function of IRF3 in the restriction of HIV-1. It was also seen that the CsA-induced effects in CypA knockout cells were no longer observable when either RIG-I, MDA5, MAVS or IRF3 were knocked out on top. While a mechanism of action of CsA on the RIG-I signaling pathway could unfortunately not be identified due to time limitations, the generated cell lines in this study are excellent tools for future studies that will aim to reveal mechanistic insights. The complex interplay between HIV-1 co-factors and type I IFN-induced cellular restriction factors in early infection events may yet again underline how perfectly well HIV-1 has adapted to exploit cellular pathways.

3 Zusammenfassung

Seit den 1980er Jahren gilt das humane Immunschwächevirus 1 (HIV-1) als der Auslöser von AIDS, dem Acquired Immunodeficiency Syndrom. Da weltweit jährlich ca. 700 000 Menschen an den Spätfolgen der HIV-1 Infektion und AIDS sterben (UNAIDS, 2018), ist die kontinuierliche Forschungsarbeit zum besseren Verständnis der Interaktion des Virus mit dem humanen Wirt wichtig. Wirtszellenproteine, die eine Infektion fördern, werden als Co-Faktoren und Proteine, die dagegen ankämpfen werden als Restriktionsfaktoren bezeichnet. Restriktionsfaktoren sind beispielsweise TRIM5α und Tetherin, wobei die Expression einiger Restriktionsfaktoren durch Interferone (IFNs) induziert wird. Cyclophilin A (CypA), ein kleines Protein, das die Faltung und somit die Funktion anderer zellulärer Proteine beeinflussen kann, ist ein solcher Co-Faktor der HIV-1 Infektion. Nach aktuellem Kenntnisstand schirmt CypA zelluläre HIV-1 Kapsid Strukturen nach dem viralen Zelleintritt vor Restriktionsfaktoren ab und stellt somit den sicheren Transport des Virusgenoms in den Zellkern sicher. Dort kann das HIV-1 Genom sich in das Wirtsgenom integrieren.

Neben CypA beinhaltet die Proteinfamilie der Cyclophiline beim Menschen noch mindesten 16 weitere Proteine, die alle CypA ähnliche Cyclophilin Domänenstrukturen aufweisen, jedoch zahlreiche zelluläre Funktionen besitzen. Während die Rolle von CypA während der HIV-1 Infektion einigermaßen gut charakterisiert ist, fehlt für die andern Cyclophiline nahezu jegliche Information. Diese Arbeit untersuchte den Einfluss von Cyclophilinen auf Ereignisse direkt nach der Infektion von HIV-1, die im Zusammenhang mit der antiviralen Wirkung von Typ I IFNs stehen. Im Allgemeinen weisen einige Typ I IFN stimulierten Zellen eine signifikant reduzierte HIV-1 Infektion auf. Interessanterweise ist dieser frühe Block der Infektion in CypA defizienten Zellen verstärkt. Dies deutet auf eine Funktion von CypA in der Immunabwehr gegen HIV-1 hin. Des Weiteren konnte eine Erhöhung der Infektionsrate nach Stimulation mit einem Cyclophilin Inhibitor, Cyclosporin A (CsA) beobachtet werden. Dies ist auch in Abwesenheit von CypA, dem vermeintlich hauptsächlichen Ziel der CsA Inhibition, zu beobachten. Dies deutet auf einen weiteren CsA-sensitiven Faktor hin, der die HIV-1 Infektion in Type I IFN stimulierten Zellen beeinflusst. Dies stellt die Grundlage für weiterführende Untersuchungen dar, da sowohl CsA als auch type I IFN als möglich HIV-1 Medikamente untersucht worden sind, leider jedoch mit wenig Erfolg. Das Verständnis der zugrundeliegenden Mechanismen könnte jedoch wichtige Erkenntnisse für eine angepasste HIV-1 Therapie bieten.

Die naheliegendsten alternativen CsA-Targets waren weitere Mitglieder der Cyclophilin

Familie. Deshalb wurden CypB, CypC, CypD, CypE und CypH defiziente THP-1 Zellen mit Hilfe der CRISPR/Cas9 Technologie generiert und der Effekt von Typ I IFNs und CsA Stimulation auf die HIV-1 Infektion untersucht. Während ein Knockout von CypB, CypC und CypD zwar die Infektion beeinflusste aber keinen Effekt bei IFN oder CsA Stimulation hatte, zeigten CypE und CypH knockout Zellen eine signifikant erhöhte Sensitivität der HIV-1 Infektion für den Typ I IFN induzierten Infektionsblock. Durch diese unterschiedlichen Phänotypen wurde das Zusammenspiel mehrerer Cyps mit Hilfe von Doppelknockoutzelllinien untersucht. Knockout von CypB alleine zeigte keinen Effekt auf die HIV-1 Infektion, allerdings konnte eine signifikant erhöhte Sensitivität gegenüber Typ I IFNs in Abwesenheit von CypA und CypB beobachtet werden. Ähnliches konnte auch für den doppelten Knockout von CypA und CypE beobachtet werden. Dies deutet darauf hin, dass Cyclophilin-Funktionen während eins frühen Stadiums der HIV-1 Infektion in komplexen Zusammenhang stehen und eventuell einige Funktionen von anderen Mitgliedern dieser Proteinfamilie abhängen. Des Weiteren zeigen die Ergebnisse dieser Studie, dass CypA nicht das einzige Mitglied der Cyclophilin Familie mit einer Funktion während der frühen HIV-1 Infektion ist. Die Ergebnisse dieser Studie legen nahe, dass der Knockout eines einzelnen Cyclophilins nicht ausreichend ist, um die CsA-induzierte erhöhte HIV-1 Infektion in Typ I IFN stimulierten THP-1 Zellen zu verhindern, beziehungsweise konnte dieser Phänotyp durch keinen der hier untersuchten Kandidaten erklärt werden.

Zur Identifizierung weiter möglicher CsA-sensitiven Faktoren wurde ein neutraler Ansatz gewählt, bei dem das gesamte zelluläre Proteom auf seine thermische Proteinstabilität mit Hilfe von Massenspektrometrie untersucht wurde. Neben bekannten CsA Targets konnten auch einige neue Faktoren identifiziert werden, deren Proteinstabilität deutlich durch die Zugabe von CsA beeinflusst wurde und somit eine mögliche Sensitivität dieser Kandidaten für CsA gegeben ist. Einige dieser Kandidaten waren type I IFN-induzierte Proteine, wie Mitglieder des Retinoic acid inducible gene (RIG-I) Signalweges. RIG-I erkennt virale RNA und induziert eine antivirale Signalkaskade innerhalb der Zelle, die unter anderem zur Typ I IFN-Produktion führt. Da dieser Signalweg in der Literatur bereits im Zusammenhang mit der HIV-1 Infektion beschrieben ist, wurden einige Mitglieder dieses Signalweges genauer in Bezug auf die HIV-1 Infektion und die Sensitivität gegenüber Typ I IFNs und CsA untersucht. Knockout von RIG-I, MDA5, MAVS, TRADD und IRF3 in CypA defizienten THP-1 Zellen zeigten alle eine erhöhte Sensitivität gegenüber dem Typ I IFN-induzierten frühen Block der HIV-1 Infektion. Zusätzlich konnte eine erhöhte Infektion in IRF3 Knockout Zellen beobachtet werden, was auf eine Funktion von IRF3 in der Restriktion von HIV-1 hindeutet. Zudem konnten die CsA-

induzierten Effekte in CypA knockout Zellen nicht mehr beobachtet werden, wenn entweder RIG-I, MDA5, MAVS oder IRF3 zusätzlich ausgeknockt waren. Ein Wirkmechanismus von CsA auf den RIG-I Signalweg konnte leider aus Zeitgründen nicht identifiziert werden. Allerdings stellen die in dieser Studie hergestellten Zelllinien exzellente Werkzeuge für zukünftige Studien zur Aufdeckung der zugrunde liegenden Mechanismen dar. Das komplexe Zusammenspiel zwischen Ko-Faktoren der HIV-1 Infektion und den zellulären Typ I IFN-induzierten Restriktionsfaktoren während den frühen Phasen der Infektion zeigt wieder einmal, wie gut HIV-1 an die humanen zellulären Prozesse angepasst ist.

Table of contents

4 Abbreviation

AIDS	acquired immune deficiency syndrome
APOBEC3G	apolipoprotein B mRNA-editing enzyme catalytic polypeptide like 3G
APS	ammonium persulfate
Arp2/3	actin-related protein 2/3
ASK1	Apoptosis signal-relating kinase 1
ATP	Adenosine triphosphate
BSA	bovine serum albumin
CA	Capsid protein
CARD	caspase activation and recruitment domains
CCR5	C-C motif chemokine receptor 5
CLK	CDC28/cdc2-like-kinase
CPSF6	cleavage and polyadenylation specific factor 6
CsA	Cyclosporin A
CTD	C-terminal domain
CXCR4	C-X-C motif chemokine receptor type 4
CypX	Cyclophilin X
CypX -/-	knockout of Cyclophilin X
DMEM	Dulbecco's Modified Eagle Medium
DMSO	dimethyl sulfoxide
(ds)DNA	(double stranded) deoxyribonucleic acid
dNTP	deoxynucleotide triphosphate
ECL	electrochemiluminescence
EDTA	ethylenediaminetetraacetic acid
Env	Envelope protein or *env* gene
ER	endoplasmic reticulum
ERAD	endoplasmic-reticulum-associated protein degradation
ESCRT	endosomal sorting complex required for transport
EtOH	ethanol
FACS	fluorescence-activated cell sorter
FADD	Fas-associated protein with death domain

FCS	fetal calf serum
FIV	Feline immunodeficiency virus
FKBPs	FK506 binding protein
fwd	forward
Gag	group specific antigen
GFP	green fluorescent protein
gRNA	guide ribonucleic acid
GTPase	guanosine triphosphate hydrolase
HAART	highly active antiretroviral therapy
HBV	Hepatitis B virus
HIV-1	human immunodeficiency virus 1
Hsp90	heat shock protein 90
IAV	Influenza A virus
IFITM	interferon induced transmembrane protein
IFN(s)	type I interferon(s)
IN	Integrase
IRF3	interferon regulatory factor 3
ISG(s)	Interferon stimulated gen(s)
JAK-STAT	Janus kinase/signal transducers and activators of transcription
JNK	c-Jun N-terminal kinase
kDa	kilo Dalton
LB	Luria broth
LTR	long terminal repeats
LV	lentiviral vector
MA	Matrix protein
MAPK	mitogen-activated protein kinase
MAVS	mitochondrial antiviral signaling protein
MDA5	myeloma differentiation-associated protein 5
MDM	monocyte derived macrophages
MHC I	major histocompatibility complex I
MLL1	mixed lineage leukemia 1
mM	millimolar

mRNA	messenger ribonucleic acid
MS	mass spectrometry
MX	myxovirus resistance protein
NC	Nucleocapsid protein
NEB	New England Biolabs
Nef	Negative factor
NFAT	Nuclear factor of activated T cells
NFκB	nuclear factor kappa-light-chain enhancer of activated B-cells
NMR	nuclear magnetic resonance
N-WASP	neural Wiskott-Aldrich syndrome protein
ORF	open reading frame
PAMPs	pathogen-associated molecular patterns
PBMCs	peripheral blood mononuclear cells
PBS	phosphate buffered saline
PCR	polymerase chain reaction
PEI	polyethyleneimine
PFA	paraformaldehyde
PIC	pre-integration complex
pol	HIV-1 polymerase ORF
PPIase	peptidylprolyl *cis-trans* isomerase
PR	Protease
PVDF	polyvinylidene fluoride
RACK1	receptor for activated C kinase 1
rev	reverse
Rev	Regulator of infection protein
RIG-I	Retinoic-acid-inducible gene 1
RIP1	receptor-interacting serine/threonine protein kinase 1
RLR	RIG-1-like receptors
(t)RNA	(transfer) ribonucleic acid
RPMI	Roswell Park Memorila Institute 1640
RS	arginine/serine rich
RT	Reverse transcriptase

SDS	sodium dodecyl sulfate
SDS-PAGE	sodium dodecyl sulfate polyacrylamide gel electrophoresis
SEM	standard error of the mean
SG-Pert	SYBR Green based PCR enhanced reverse transcription assay
snRNP	small nuclear ribonucleoprotein particle
ssRNA	single stranded ribonucleic acid
STAT3	signal transducer and activator of transcription 3
TAE	tris-acetate ethylenediaminetetraacetic acid
Tat	Transactivator of transcription protein
TBK1	TANK-binding kinase 1
TEMED	N'-tetramethylethylenediamine
TLR	toll-like receptor
TNFR	tumor necrosis factor receptor
TOR	target of rapamycin
TRADD	TNF receptor type 1-associated DEATH domain protein
TRAF	TNF receptor-associated factor
TRIM5	Tripartite motif-containing protein 5
UV	ultraviolet light
Vif	Virion infectivity factor
Vpr	Viral protein R
Vpu	Viral protein U
VSV	Vesicular stomatitis virus
WB	Western blot
wt	wild type

5   Introduction

5.1   Human Immunodeficient Virus Type 1 (HIV-1)

Human immunodeficient virus type 1 (HIV-1) was first isolated and characterized in 1983 [1], [2] and named HIV-1 three years after its first isolation [3]. HIV-1 infection causes the acquired immunodeficiency syndrome (AIDS), a condition characterized by the progressive failure of the immune system. This makes patients susceptible to life-threatening opportunistic infections, which eventually lead to a patient's death. Transmission of the virus occurs from person to person by transfer of blood, breast milk, pre-ejaculate, semen or vaginal fluid. HIV-1 infects a subset of human immune cells, mainly $CD4^+$ T cells and macrophages but also myeloid cells [4]. The infection can be categorized into three stages [5]: First, the acute early infection, in which the virus replicates rapidly. The initial phase is characterized by a dramatic depletion of $CD4^+$ T cells, accompanied by the production of large quantities of proinflammatory cytokines including type I interferons (IFNs) [6]. Secondly, in the clinical latency phase a rebound of T cell count occurs. The virus remains silent and no viral replication is detectable thus, the virus evades the immune system, which can last for several years. The last stage is marked by the onset of AIDS. The viral load increases accompanied by $CD4^+$ T cell depletion.

Despite intensive research, 37.9 million people are infected with HIV-1 worldwide as by the UNIDAS report form 2019 and since the discovery of the virus approximately 32 million patients died from AIDS related illnesses [7]. In 2018 alone, 1.7 million new infections were recorded and recent data from June 2019 indicate that 65 % of infected people are currently undergoing highly active antiretroviral therapy (HAART) [7]. HAART is a cocktail of at least three different antiviral drugs, blocking HIV-1 replication and resulting in a decreased viral load. So far, there is no cure for HIV-1 and AIDS, despite two singular cases (see below). The required life-long therapy, the high mutation rates of the virus and its latency promote the evolution of drug-resistant virus variants and side effects of drug toxicity over the long treatment period [8]. At the current stage, no vaccine is available, and treatment and diagnostics remain expensive.

Recently, a promising breakthrough was discovered. The total remission of HIV-1 was not only achieved in the "Berlin patient", but also in the "London patient". Both received allogeneic hematopoietic stem-cell transplantations from a homozygous CCR5Δ32 donor [9], [10]. The 32 base-pair deletion in the C-C motif chemokine receptor 5 (CCR5) gene prevents the interaction of the virus with its host coreceptor, leading to HIV-1 resistance of these cells [11].

These are very promising results. However, suitable donors are uncommon, and this therapy is not applicable for everybody. The goal for the current HIV-1 research is the complete understanding of the viral life cycle, its latency and the development of an affordable commercial cure for HIV-1 infection and AIDS.

5.1.1 Classification, genome organization and virion structure

HIV-1 is an enveloped virus belonging to the family of *Retroviridae* and the genus *Lentivirus*. The genome contains two copies of a single stranded positive-sense ribonucleic acid (RNA) of 9.7 kilo bases (kb) in size [12], [13]. A unique feature of the virus family *Retroviridae* is the viral enzyme reverse transcriptase (RT), which transcribes the viral RNA into double stranded deoxyribonucleic acid (dsDNA). Until now, two types of human immunodeficiency viruses have been discovered: HIV-1 and HIV-2. Both versions share around 50 % sequence homology, but HIV-2 shows lower virulence and infectivity [14]. Worldwide multiple HIV-1 strains circulate and are divided into four groups: M (major), N (non-M-non-O), O (outlier) and P (putative) [15]. Members of the M group are responsible for 90 % of infections, while the majority of strains belonging to the remaining groups are mostly locally restricted to sub regions of the African continent [15], Portugal and France [16]–[18].
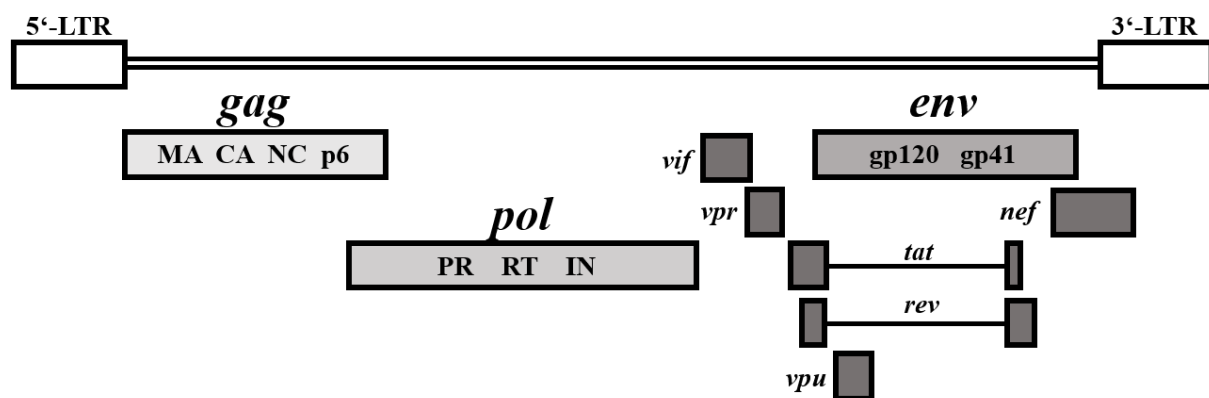
Figure 1: Genomic organization of HIV-1.

The HIV-1 genome is flanked by 5' and 3' LTRs. The ORFs for *gag, pol* and *env* genes are represented as rectangles at the respective position in the HIV-1 genome. HIV-1 accessory and regulatory genes are represented by dark grey rectangles and the introns of tat and rev are depicted as horizontal lines. The *gag* ORF encodes for matrix (MA), capsid (CA), nucleocapsid (NC) and p6 protein. The viral proteins protease (PR), reverse transcriptase (RT) and integrase (IN) are encoded by the *pol* ORF. HIV-1 glycoproteins gp120 (surface) and gp41 (transmembrane) are encoded by the *env* ORF. Modified from [19].

The HIV-1 genome is depicted in Figure 1. The genome is flanked by long terminal repeats (LTRs), which are duplicated during reverse transcription. The 5'LTR contains the active promotor, which is essential for viral gene transcription from the provirus integrated in the host genome. Viral proteins are encoded from nine open reading frames (ORFs). The first one is the group specific antigen (*gag*) ORF, encoding for the structural polyprotein, which is processed

during maturation by the viral protease (PR) into matrix (MA), capsid (CA), nucleocapsid (NC) and the p6 protein [20]. The polymerase (*pol*) ORF encodes the viral enzymes PR, RT and integrase (IN). The structural glycoproteins are encoded by the envelope (*env*) ORF: surface protein gp120 and transmembrane protein gp41. These two glycoproteins define the host tropism and mediate virus entry dependent on two human cell surface receptors: CCR5 or C-X-C motif chemokine receptor type 4 (CXCR4), which are differentially expressed on HIV-1 target cells [21]. The remaining six ORFs encode the accessory and regulatory proteins of HIV-1, the virion infectivity factor (Vif), viral protein R (Vpr), viral protein U (Vpu), negative factor (Nef), transactivator of transcription (Tat) and regulator of infection (Rev), [22]. HIV-1 virions are spherical particles with a diameter of 120 - 140 nm [23], [24]. The lipid envelope is generated from host cell plasma membrane during the budding process [23]. Budded particles are immature. Maturation is initiated upon PR activation in the viral particle. After the PR processes the Gag-polyprotein, the structural proteins MA, CA and NC undergo major reorganization leading to a cone shaped CA core inside the virion. These mature, infectious particles contain in addition the viral genome, IN, RT, Vpr, Nef and Env as well as host cell proteins [25]

5.1.2   HIV-1 life cycle

Like all viruses, HIV-1 is an intracellular obligate parasite that hijacks the host cell machinery during its life cycle (full cycle is shown in Figure 2). HIV-1 facilitates the host cell entry by binding of the viral surface glycoprotein Env to the CD4 receptor of its target cell [26], [27]. The Env protein forms a trimer of heterodimers containing the gp120 and gp41 proteins and 7-14 trimers are incorporated into each virion [28], [29]. Virion attachment is facilitated by the binding of gp120 to the CD4 receptor as an essential prerequisite for major structural rearrangements of gp41. This process is required for the engagement of the CCR5 or CXCR4 co-receptor [30], [31]. Binding of the co-receptor induces a conformational change in gp41 enabeling the fusion peptide, a N-terminal hydrophobic region, to insert into the host cell plasma membrane [32]–[34]. A fusion pore is formed by a six-helix bundle that brings the opposing membranes into close proximity. In the process of fusion the viral core containing the ribonucleoprotein complex as well as viral proteins being relevant for replication and virion structure are released into the cytoplasm [35], [36].

The early HIV-1 infection steps include processes occurring in the cytoplasm, such as the reverse transcription of the viral genome by the viral enzyme RT and the formation of the pre-integration complex (PIC). Reverse transcription of the viral single stranded RNA genome into dsDNA takes place in reverse transcription complexes [37]. These complexes contain the viral

genome, ribonucleoproteins, IN, RT and cellular host factors. RT also harbors a ribonuclease H (RNasH) activity, important for transfer RNA (tRNA) primer processing used to start minus-strand DNA synthesis [38]. After viral DNA flanked with LTRs is generated, the PIC is formed. It contains the newly synthesized viral DNA, several viral proteins (RT, IN, CA, Vpr) as well as cellular proteins. The PIC is shuttled to the nucleus [39].
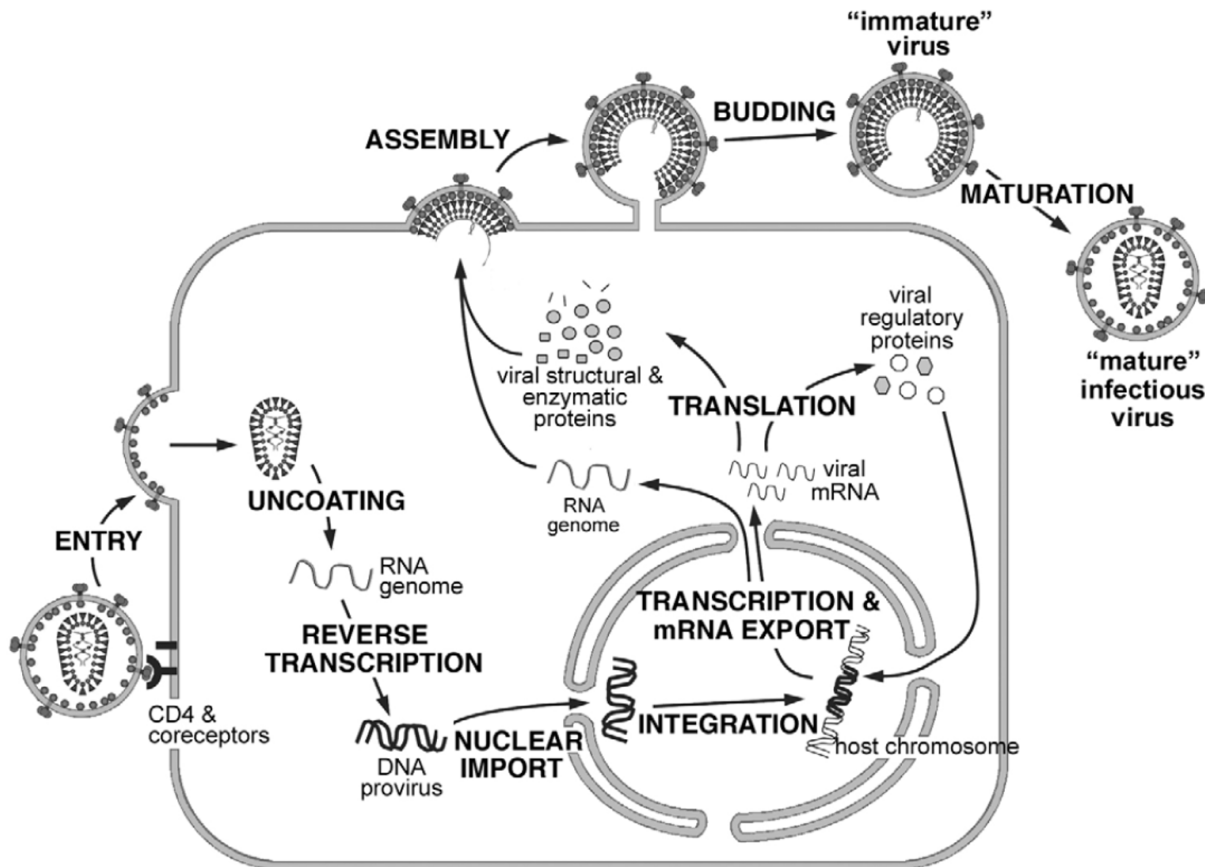
Figure 2: HIV-1 life cycle.

HIV-1 virions attach to the cell surface of their host cells by CD4 receptor and co-receptor binding. Fusion with the plasma membrane releases the viral core into the cytoplasm of the host cell. Uncoating of the viral core is induced and the viral RNA genome can be reverse transcribed into the dsDNA provirus. Host and viral proteins form the PIC. The provirus is imported into the nucleus and integrated into the host cell genome by the viral protein IN. The provirus is used as template during transcription of the viral genes resulting in viral mRNA and viral genome generation. Translation of viral mRNA into viral proteins takes place in the cytosol. Some of the accessory and regulatory proteins are imported into the nucleus and regulate viral transcription. Novel immature viral particles assemble at the plasma membrane. After budding with the help of the cellular endosomal sorting complex required for transport (ESCRT) machinery, the viral PR incorporated into viral particles becomes active, processes the structural proteins and thus, mature viral particles are formed. Adapted from [40].

The early post-entry steps of HIV-1 infection are accompanied by a process referred to as uncoating, during which parts or the entire viral capsid core break down, so that the viral PIC can traffic across the nuclear membrane. While under certain circumstances also entire viral capsid cores can be seen in cells (unpublished work from Robin Burk in the Kräusslich lab, personal communication 2017 - 2019), uncoating before nuclear entry is still considered to be the predominant way of HIV-1 nuclear import. After nuclear entry through nuclear pores [41]

a characteristic hallmark of retroviruses takes place, the viral DNA is integrated into the host cell genome. This process is catalyzed by the viral enzyme IN and is preferably found in transcriptionally active regions of the host genome [42], [43]. The integrated viral genome is referred to as provirus and becomes part of the cellular genome for the cell's lifespan. The provirus serves as a template for viral messenger RNA (mRNA) transcription and remains in the host genome, either as a latent provirus or transcriptionally active [44], [45]. Transcription of viral mRNA is dependent on the recruitment of transcription factors to the viral promoter sitting in the 5'LTR region of the provirus. This leads to the initiation of proviral gene expression starting with a single viral transcript. It encodes the accessory proteins Tat, Rev and Nef. Transcribed RNA is spliced multiple times and exported by the nuclear export pathway as cellular mRNAs. Tat enhances the viral transcription efficiency by binding to the transactivation response RNA structure (tar) and thereby facilitating the recruitment of the cellular RNA polymerase II [46], [47]. Rev is responsible for the export of viral unspliced and partially spliced mRNAs, which cannot take the cellular export route. These mRNA variants encode Gag, Gag-Pol, Env, Vpr, Vif and Vpu [48]–[50].

After translation of viral proteins by the cellular machinery, Env is transported to the plasma membrane via the secretory pathway [51]. Gag and Gag-Pol are recruited to the plasma membrane after binding two copies of the ssRNA genome initializing the assembly of novel HIV-1 particles. Gag binding to the plasma membrane mediates Env, viral Gag-Pol, Nef, Vpr and Vif recruitment. These viral proteins are all incorporated into viral particles [52]. Hijacking the cellular endosomal sorting complex required for transport (ESCRT) machinery an immature viral particle is pinched off the plasma membrane [53]. The formation of infectious particles relies on a maturation process after virion budding [54], [55] which is initiated by the activation of the viral PR. At six distinct sites PR cleaves Gag and Gag-Pol into their components CA, NC, MA, p6, PR, RT and IN, in a concerted order. Major structural rearrangements of the Gag subunits and Env take place [56]. The mature HIV-1 particles are formed consisting of a viral core formed by CA encapsulating the RNA-NC complex.

5.1.3 HIV-1 and the type I interferon (IFN) response

The human immune system is comprised of two arms, the innate and adaptive immune system. Both arms are essential for the protection from infections caused by pathogens as well as for resolving infections. The innate immune system acts immediately after bacteria or viruses enter the host. This includes for example the activation of the complement system or the production of interferons (IFNs). IFNs are small molecules belonging to the cytokine family, that can induce an antiviral state by promoting the expression of interferon stimulated genes (ISGs) [57].

IFNs are signaling molecules produced and released by the host cell upon pathogen infection to heighten antiviral senses of the surrounding cells and activate immune cells. IFNs can be divided into three classes based on their signaling receptor: type I IFNs (IFN α/β receptor (IFNAR)), type II IFNs (IFNγ receptor (IFNGR)) and type III IFNs [58]. The innate system acts rapidly and limits virus replication. Therefore, it provides time for the organism to induce the second arm of defense, the adaptive immune system. This includes the selection and expansion of specific B- and T cells as well as the production of specific antibodies directed against a particular pathogen. The innate immune system comprises a heterogeneous group of intracellular factors, called restriction factors. These factors counteract viral infection in multiple ways. Many restriction factors are IFN induced and usually upregulated during early infection [59], [60]. They also share some characteristics as self-sufficient activity, a cell type specific expression, their ability to decrease viral infection and the antagonistic effects of viral proteins against them [61].

Type I IFNs (from here on referred to as IFNs) are released during the acute phase of an infection and signal through the heterodimeric interferon alpha receptor [58]. This group includes at least 13 distinct IFNα subtypes as well as IFNβ, IFNω, IFNε and IFNκ [62]. IFNα subtypes are genetically and structurally very similar. They lack introns, are clustered on chromosome nine and share an amino acid sequence similarity between 75 - 99 % [63]. After recognition by its receptor, IFNs trigger the Janus kinase/signal transducers and activators of transcription (JAK-STAT) pathway and induce the expression of hundreds of ISGs. These antiviral genes can reduce infection of many viruses including HIV-1. ISGs inhibit HIV-1 replication in cell culture systems [64]–[67] and impair reverse transcription and nuclear import of the viral genome [68]. In monocyte derived macrophages (MDM) or lymphocytic cells HIV-1 infection is blocked prior or during reverse transcription upon IFNα treatment, but some factors involved in the IFN response to HIV-1 are still unknown [69]–[72]. However, *in vitro*, different cell types respond differently to IFNα treatment while the timing of IFNα treatment and viral infection plays a crucial role. For example, an inhibition of viral protein synthesis could only be detected in T cells, when they were treated with IFN prior to infection or 10 h post infection at the latest [69]. Recombinant IFNα therapy has been tested in clinical trials, leading to a reduction in viral load, but viral rebound overtime was detected. Thus, HIV-1 can overcome effects of IFN induced restriction factors [73], [74]. What exactly the viral determinants for overcoming the IFNα induced block to HIV-1 infection are, is unknown. To date all what is known is that IFN exerts a dual role in HIV-1 infection. IFN is produced during HIV-1 infection but is not able to inhibit early infection effectively. The negative effects of IFN

on progression to disease are most evident in the chronic phase of the infection. Constant high levels of ISG lead to a more rapid CD4$^+$ T cell depletion and increased viremia [75], [76]. This is probably due to the activation of a IFN-related desensitization mechanism [6]. Consequently, it is of great interest to identify host cell effectors induced by ISGs to understand the interplay between host and virus after IFNα treatment.

5.1.4   HIV-1 restriction factors

Antiviral factors expressed by the host cell are also called restriction factors. These are usually constantly expressed at low doses. However, when incoming viruses are sensed expression of these restriction factors is enhanced. Host restriction factors are usually virus specific and their goal is to block viral replication and viral life cycle propagation. For HIV-1 a variety of restriction factors are known and have been deeply investigated over the last decades. Many of the known restriction factors are known to be antagonized by at least one HIV-1 accessory protein and a few are described below [61]. These restriction factors are highly regulated, expression levels vary between cell types and it is not astonishing, that HIV-1 infectivity differs amongst target cells at least to some degree due to the variety of restriction factors.

The apolipoprotein B mRNA-editing enzyme catalytic polypeptide like (APOBEC) 3G protein [77] belongs to the apolipoprotein B mRNA editing enzyme, catalytic polypeptide-like family of cytidine deaminase enzymes. APOBEC3G is a major player in innate anti-viral immunity, as it induced G-to-A hypermutations by deamination of cytosine residues in single stranded viral DNA. Therefore, both proteins restrict a broad variety of viruses including hepatitis B virus (HBV), human T cell leukemia virus type 1, endogenous retroviruses and HIV-1 [78]–[80]. In the HIV-1 life cycle, APOBEC3G becomes catalytically active during reverse transcription of the viral RNA. Amino acid substitutions and the incorporation of premature STOP codons as result of hypermutation by APOBEC3G in the newly transcribed single stranded DNA occur and lead to the production of defective viral proteins [81]–[83]. A second, perhaps the more important mechanism by which APOBEC3G interferes with viral reverse transcription is by binding to viral DNA and to RT directly and thus, blocking reverse transcriptase [81]. This leads to vastly reduced viral reverse transcription products in the presence of APOBEC3G when Vif is absent. Furthermore, APOBEC3G is encapsulated into newly produced HIV-1 virions when they lack the viral protein Vif. HIV-1 counteracts the activities of APOBEC3G through its accessory protein Vif. Vif recruits a ubiquitin ligase complex that facilitates proteasomal degradation of APOBEC3G, thus preventing its incorporation into HIV-1 virions [84].

Another restriction factor induced by IFN is tetherin/BST-2 (tetherin). It is an unusual type II

single-pass transmembrane protein incorporated into the plasma membrane. It carries a transmembrane anchor at its N-terminus and a glycophosphatidylinositol lipid anchor at its C-terminus [85]. With this anchor it blocks the budding of various viruses from different families, indicating that its function is independent of viral protein structure or sequence [86], [87]. Most likely tetherin hinders HIV-1 virions from budding by attaching its C-terminal glycosyl-phosphatidylinositol group to the viral membrane, whereas its N-terminal anchor remains in the plasma membrane. Virions are eventually internalized and degraded via the endosomal/lysosomal pathway. The effects of this protein are encountered by the viral protein Vpu, which colocalizes with tetherin and reduces its levels at the cell surface [88].

The interferon-induced transmembrane (IFITM) protein family contains three members with immune-related functions: IFITM1, IFITM2 and IFITM3 [89]. These proteins do not only restrict HIV-1 but also Dengue virus, Influenza A virus (IAV), West Nile virus, SARS coronavirus, Ebola virus and Vesicular Stomatitis virus (VSV) [59], [90]–[93]. The mechanism by which IFITMs inhibit HIV-1 are not completely understood and experimental evidence is providing contradicting results. Overexpression of IFITMs in TZMbl cells does not impede HIV-1 entry [91] but in Huh and SupT1 cells IFITM2 and IFITM3 do inhibit HIV-1 replication [59], [90]. In viral producer cells IFITM2 and IFITM3 antagonize Env by impairing Env processing and its incorporation into virions. Interestingly, upon IFITM overexpression in these cells, Env mutants arise, that overcome IFITM restriction [94], indicating an important function for the viral life cycle.

Myxovirus resistance (Mx) proteins are dynamin-like guanosine triphosphate hydrolases (GTPases). In human there are two gene variants: MX1 and MX2 (Haller and Kochs 2011). MX1 and MX2 differ in their cellular localization and activity. MX1 shows a broad antiviral activity against RNA and DNA viruses [95], [96], whereas MX2 has a potent antiviral activity only against a few viruses like VSV [97] and HIV-1 [98], [99]. MX2 is localized at the cytoplasmic site of the nuclear pore complex [100]. It possesses a C-terminal GTPase domain and an N-terminal triple-arginine motif. Crucial for its antiviral activity is only the N-terminal region. [98], [99]. It has been suggested that MX2 targets the HIV-1 CA protein, as CA can bind to those motifs [101], [102]. Interestingly the antiviral function of MX2 is linked to Cyclophilin A (CypA) and/or cleavage and polyadenylation specific factor 6 (CPSF6). CypA can bind HIV-1 CA and is incorporated into HIV-1 virions as will be explained in chapter 5.2.2. CPSF6 is also an HIV-1 CA binding protein. For both proteins, HIV-1 specific CA mutants unable to interact with the respective protein exist. These mutants have been shown to be less sensitive to MX2 inhibition and the depletion of CypA terminates the antiviral activity of MX2

[103] as CypA binding to CA might alter its conformation and makes it more accessible for MX2 binding. Overexpression of MX2 inhibits HIV-1 replication and MX2 silencing decreases the IFN-induced block to HIV-1 infection in some cell types. CypA and CPSF6 are both bound to CA until nuclear entry, therefore, a function of MX2 at the stage of nuclear import [72], [99] or integration [104] is likely.

Tripartite motif-containing protein 5 (TRIM5), specifically the alpha isoform (TRIM5α), is another IFN inducible retrovirus restriction factor, blocking early infection [105], [106]. The TRIM protein family is a large protein family which members have diverse functions. A shared feature between all family members is the tripartite motif, a domain containing the RING, the B-box and a coiled-coil domain. TRIM5α also has a C-terminal PRY-SPRY domain, which is responsible for the antiviral function, as dimeric TRIM5α complexes bind viral capsids with this domain. TRIM5α blocks HIV-1 infection before reverse transcription is complete [107], but its effects on reverse transcription can be abrogated by inhibition of the proteasome [108]. TRIM5α is also a good example for the co-evolution theory of host and retroviruses. Many species-specific TRIM5α variants have been found [109], [110] and viruses evade TRIM5α restriction by changing their CA sequence. Rhesus TRIM5α for example strongly blocks HIV-1 infection, whereas the human TRIM5α shows only weak inhibition [105]. Recent studies identified TRIM5a as a HIV-1 CA-specific Cyclophilin A sensitive restriction factor. In the absence of CypA, TRIM5a potently restricts HIV-1 prior to reverse transcription [60], [111]. Furthermore, other members of this family have also been investigated as restriction factors. TRIM22 can decrease HIV-1 production [112], [113] and TRIM11 as well as TRIM15 can inhibit HIV-1 virus release [114].

5.2 Peptidylprolyl *cis trans* isomerases (PPIases)

Peptidylprolyl *cis-trans* isomerases (PPIases) are highly conserved proteins, that are ubiquitously expressed in all organisms, prokaryotic and eukaryotic [115]–[117], which indicates an important cellular function. However, until now the assignment of specific cellular functions to specific members of this protein family has been proven difficult [118], as sequence similarity amongst them is high and experiments investigating redundancy are missing. PPIases can be classified into three distinct groups: Cyclophilins (Cyps), FK506 binding proteins (FKBPs) and parvulin like PPIases. FKBPs and Cyps are also referred to as immunophilins, as they can suppress immune responses in a complex with their inhibitors, FK506 and cyclosporin A (CsA), respectively. Many members of all three classes carry out an enzymatic activity, after

which this protein family is named. They catalyze the adenosine triphosphate (ATP)-independent isomerization of specific bonds in oligopeptides or proteins. These bonds must be N-terminal of a proline residues and in case of parvulins the amino acid N-terminal of the proline has to be phosphorylated which can be seen in Figure 3: Prolyl *cis-trans* isomerase activity of PPIases. [119].
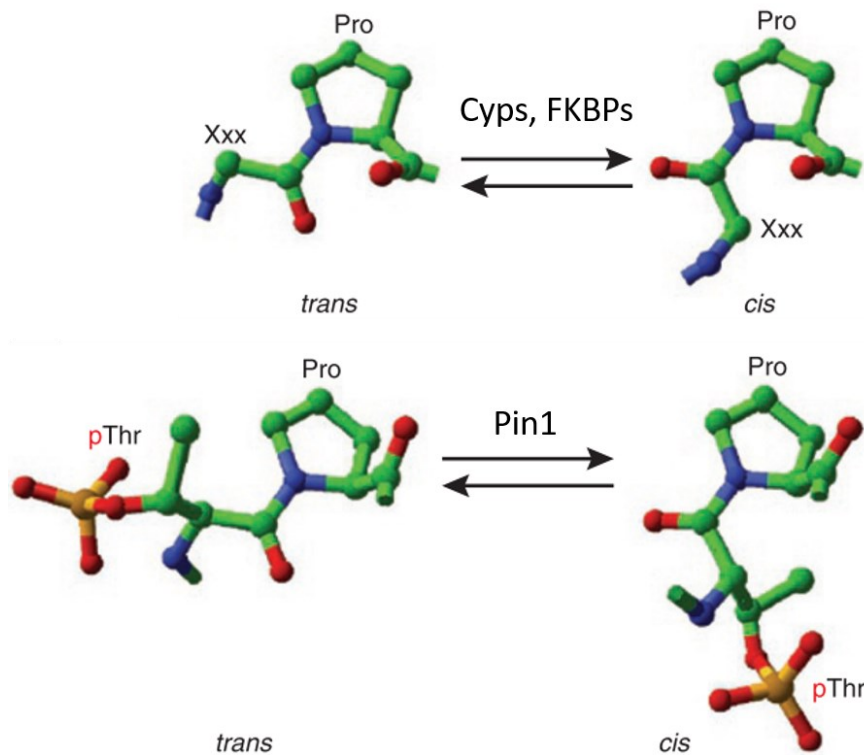
Figure 3: Prolyl *cis-trans* isomerase activity of PPIases.

PPIases can be divided into two groups by their substrate specificity into phosphorylation-independent and phosphorylation-dependent enzymes. The first group catalyzes the isomerization of Xxx-Pro motifs. Xxx stands for three amino acids except Xxx being phosphorylated Serine or Threonine. All Cyps and all FKBPs belong to this group. The second group is the phosphorylation-dependent group containing Pin1. A phosphorylated Serine or Threonine residue followed by a Proline is required. Figure adapted from [120].

The enzymatic activity has been first shown in 1989 [121] and leads to accelerated protein folding, as PPIases catalyze one of the rate limiting steps in protein folding [122]. Known substrates are for example ribonuclease T1 and collagen [123], [124]. In addition, PPIases can also impact the secondary structure of proteins by the isomerization of peptide bonds which include prolines. This might serve as a timed trigger for proteins involved in signal transduction [120]. PPIases execute their enzymatic function as monomers but how exactly remains elusive [120], [125], [126]. They most likely bind the substrate in the binding pocket and lower the transition barrier by desolvating the substrates. PPIases can catalyze the reaction from cis to trans and vice versa. Since the free energy of the cis state is higher than the one of the trans state the catalyzed reaction from trans to cis is more likely. Cyclophilins are named after their ability to bind the immunosuppressive drug CsA. In fact, the first Cyp was discovered by an

affinity purification using a CsA column in 1984 [127]. This protein group is evolutionary well conserved, as members can be found in all eukaryotes, prokaryotes, archea and even a virus encoded Cyp (Mimicyp) has been found [128]. This provides evidence for their conserved and important functions and discriminates them from FKBP. Cyps and FKBP differ in their sequences between species and might have species-specific functions [129]. In human cells at least 17 different proteins harboring a cyclophilin domain are expressed. CypA, the most prominent member and predominant CsA target, is an 18 kilo Dalton (kDa) cytosolic and nuclear protein. The biggest protein categorized as Cyp is the nuclear pore protein Nup358, also called RanBP2 with 358 kDa. All have the common cyclophilin domain structure, consisting of an eight-strand b-barrel forming a hydrophobic pocket, which is shown in Figure 4. In this pocket a loop containing aromatic residues is localized [130]. Cyps share a high sequence similarity in this domain and differ in their N- and C-terminal sequences flanking the core domain. These contain for example signaling peptides which locate them to certain cell compartments.

The second group of PPIases are FKBPs, a protein family which was discovered approximately at the same time as Cyps. In humans, 16 different FKBPs can be found ranging from 12 to 132 kDa in size. They are all inhibited by FK506 or rapamycin and exert a gain-of-function mechanism when bound to their inhibitor. FK506 and CsA are immunosuppressant molecules, which are used to treat patients after organ transplantations [131]. The binding of FKBP to FK506 inhibits calcineurin, a phosphatase involved in signal transduction of lymphatic T cells. This leads to the delayed production of interleukin 2 and blocks T cell activation by preventing the dephosphorylation of the nuclear factor of activated T cells (NFAT) [132]. The complex of CsA with Cyclophilins has the same effect on calcineurin and both effects are independent of the PPIase activity [133]. FKBPs share only little sequence homology with Cyps but their domain structure is conserved over all members and consists of a curved five-stranded antiparallel b-sheet that wraps around a short a-helix [130]. The second inhibitor of FKBPs is rapamycin, also an immunosuppressant which signals through the target of rapamycin (TOR) signaling pathway. This pathway is essential for cell growth and cell proliferation [134].

The third group of PPIases is the smallest one with only three members found in humans. These parvulin-like PPIases (parvulins) are not sensitive to inhibition by CsA or FK506 and only seem to be present in higher organisms. Parvulins can be inhibited by juglone [135] and encode small proteins (10-20 kDa) which have a preference for phosphorylated residues preceding the proline as their substrates [136]. The most prominent member is Pin1, which was first identified as the protein interacting with never-in-mitosis-A (NIMA) in a two-hybrid assay. Dysfunction of Pin1

influences immune response, apoptosis, cancer and Alzheimer's disease [137], [138]. The structure of Pin1 reveals not only a PPIase domain but also a WW domain, which might facilitate substrate binding. Thereby Pin1 influences catalytic activity, subcellular localization and protein stability of its substrates [138], [139]. As Pin1 recognizes only phosphorylated substrates, a role in cell signaling is suggested, as phosphorylation is the most common post-translational modification and a crucial mechanism of signal transduction [140].

5.2.1 Cyclophilin A

CypA is the most prominent member of the Cyp family. It can be found extracellularly as well as intracellularly in the cytosol and nucleus and its function has been studied in different research fields for decades. A role of CypA in viral infection, cardiovascular and inflammatory diseases as well as a link of CypA to various types of cancers has been described [141]–[143]. In 1984 CypA was originally purified from bovine thymocytes by CsA affinity purification identifying it as the primary binding protein of this immunosuppressive drug [127]. The nuclear magnetic resonance (NMR) structure of this complex was solved ten years later [144] and is shown in Figure 4.
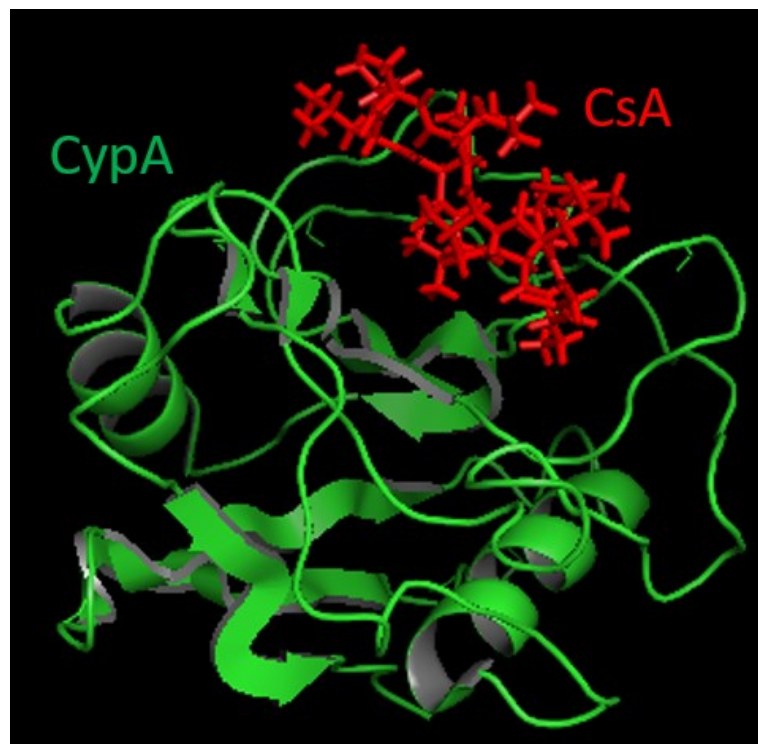
Figure 4: Cyclophilin A in complex with the inhibitor cyclosporin A.

NMR structure of human cyclophilin A (CypA, depicted in green) complexed with the drug cyclosporin A (CsA, depicted in red). The structure was obtained from PDB file 3CYS and was analyzed with Pymol. The binding site for CsA is a pocket formed by flexible loops of CypA. The bottom of the binding pocket is formed by a signature feature of Cyps: a base formed by five β-sheets, which are conserved within all members of the Cyp family.

CsA is a cyclic undecapeptide that binds to the active site of Cyps inhibiting their enzymatic function as PPIases. Although CsA can inhibit every Cyp, its predominant target is CypA. In complex with CsA, CypA can bind to Calcineurin, a Ca^{2+}/calmodulin-dependent protein phosphatase. As Calcineurin targets NFAT, this complex formation leads to suppression of T cell activation after antigen recognition and interleukin 2 production [133]. This immune modulating effect is independent of the PPIase activity and has been used in clinical approaches since the early eighties to suppress rejection after organs transplantation. The NMR structure of CypA (Figure 4) reveals, that additionally to the Cyp domain structure described in section 5.2, the protein contains two additional α-helices and a β-sheet. These additional structural features do not influence the catalytic activity of CypA as a PPIase. However, a clear mechanism how CypA isomerizes and recognizes its substrates is unknown. It is conceivable, that the recognition sequence is flexible but the suggested consensus sequence FGPXL can be found in various cellular proteins [145]. The PPIase activity is crucial for the function of CypA as a molecular chaperone, its involvement in protein folding and trafficking and signal transduction. CypA acts most likely as a molecular chaperone for one of the cellular most basic components, the actin skeleton. It has been shown that neural Wiskott-Aldrich syndrome protein (N-WASP), which is crucial for the nucleation of actin via the actin-related protein 2/3 (Arp2/3) complex, has a binding motif for CypA.Knockdown experiments resulted in a disruption of the F-actin structure and an enhanced degradation of N-WASP via the proteasomal pathway [146].

Another important function of CypA is the inhibition of signal transduction in CD4$^+$ T cells via interleukin-2-inducible T cell kinase, a interleukin 2 tyrosine kinase crucial for CD4$^+$ T helper cells [147]. Additionally, CypA can act as a modulator of transcription, as it has been identified as an interaction partner of YY1, a zinc finger transcription factor [148]. Furthermore, CypA influences dependent of its PPIase activity nuclear factor kappa-light-chain-enhancer of activated B cells (NFκB) signaling by promoting the nuclear translocation of NFκB/p65. This plays for example a critical role in chondrogenic differentiation [149], [150]. The ability of CypA to regulate the transcriptional activity of NFκB is also important for macrophage polarization towards a pro-inflammatory phenotype with significantly elevates levels of several cytokines [151]. Notably not all functions of CypA are dependent on its PPIase activity. CypA is also involved in apoptosis regulation through the direct binding to apoptosis signaling-regulating kinase 1 (ASK1), a member of mitogen-activated protein kinase (MAPK) family which activates the c-Jun N-terminal kinase (JNK) and the p38 signaling pathway. CypA negatively regulates the phosphorylation of ASK1 and inhibits ASK1-mediated apoptosis by

decreasing the caspase 3 activity [152]. In addition CypA seems to be upregulated in response to oxidative stress, hypoxia and viral infections in macrophages and is involved in the regulation of autophagy and apoptosis in these cells [153]. Another pathway which seems to be regulated by CypA is the WNT/β-catenin signaling pathway [154]. CypA as well as Pin1 can bind β-catenin. CypA increases the interaction of β-catenin with the transcription factor TCF4, which enhances transcriptional activity of WNT target genes. Furthermore, the involvement of CypA not only in protein folding but also in cell cycle progression, regulation of apoptosis, and cell migration and invasion makes it a central player of the cellular metabolism [146], [155], [156]. Therefore, it is not surprising that CypA is overexpressed in several human cancers types including non-small lung cancer, pancreatic adenocarcinoma, hepatocellular carcinoma and glioblastoma [154], [157]–[160]. As the function of CypA is manifold, an overview is shown in Figure 5.
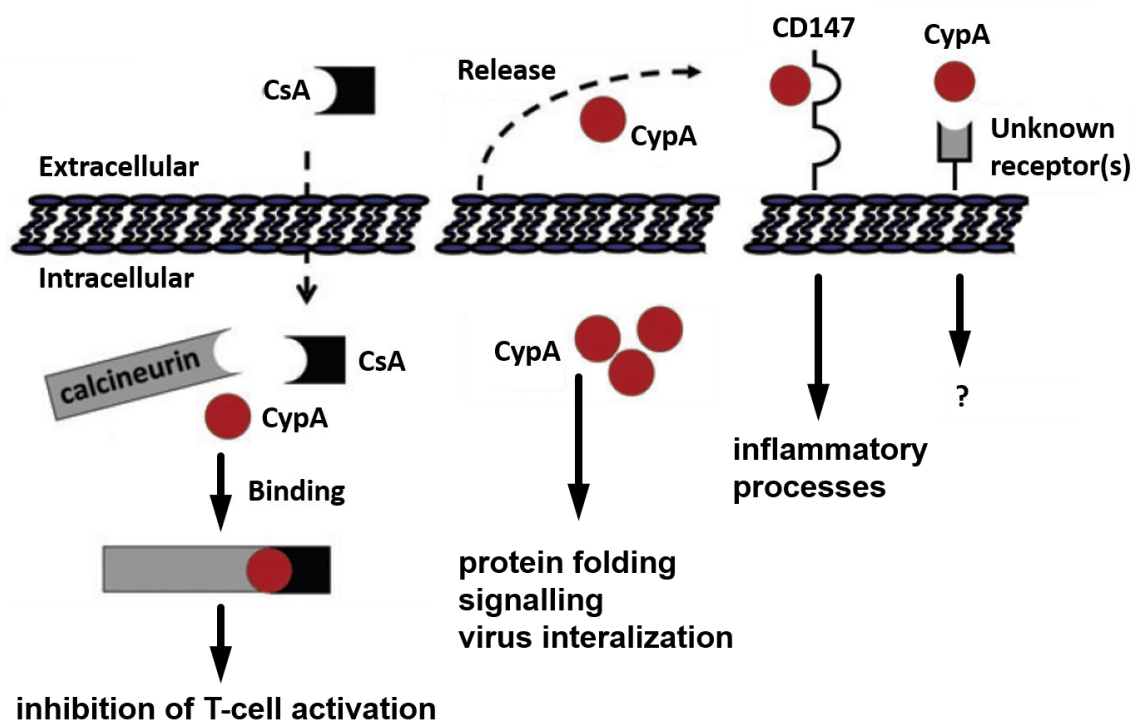
Figure 5: Intra- and extracellular CypA activities.

CsA can pass the cell membrane and intracellular binding to CypA forms a complex with calcineurin. This complex inhibits the NFAT mediated T cell activation. Various cell types secrete CypA. Extracellular CypA induces inflammatory pathways by signaling through CD147 or unidentified other receptors. Intracellular CypA exerts many functions like protein folding, signaling and an involvement in viral infection. Figure adapted from [161].

Besides its broad cellular activity and the immunosuppressive effect in complex with CsA, CypA is secreted by various cell types including macrophages [162], [163] to exert signaling through its receptor EMMPRIN/CD147 or a currently unknown novel receptor. CD147 is an extracellular matrix metalloproteinase inducer important for tumorigenesis, metastasis and

tumor invasion [159], [164] or chemotaxis of activated CD4$^+$ T cells and leukocytes [143], [165]. CypA might be marked for secretion by acetylation in response to inflammatory stimuli [166]. Through its signaling via the cell surface receptor CD147, which is apparently dependent on the PPIase activity [167], CypA promotes proinflammatory signaling pathways. Extracellular CypA leads to the activation of MAPK including ERK1/2, JNK and p38 [168]. The functions of CypA described above and the conserved distribution across several species would indicate that this protein is essential for cell, but several knockout experiments in different cell lines and the existence of knockout CypA mice show the opposite [151], [169]. This might be explained by redundancy amongst Cyps and/or more than 50 processed pseudogenes as revealed by a computer based analysis [170]. This makes CypA one of the top five proteins with the highest number of processed pseudogenes in the human genome [170]. Some of them have intact ORF and might be expressed, as for example some fusion proteins show (e.g. TRIMCyp) [171], but how this affects the function of CypA and impacts its function in disease progression is currently unknown and unstudied. As CypA is involved in several cellular processes it is not astonishing, that various viruses have evolved to use CypA during their life cycle including Vaccinia virus, VSV, Cytomegalovirus, Hepatitis C virus (HCV), IAV and HIV-1 [172]–[176]. A study from 2012 identifies CypA as a major component for human cytomegalovirus reactivation from a non-productive infection state in THP-1 cells [177]. Furthermore, CsA treatment revealed an immunosuppressive and antiviral effect for Cytomegalovirus infection [178]. For HCV infection PPIase activity of CypA seems to be involved in double membrane vesicle formation, a crucial step for the virus life cycle [179]. In context of HCV infection variants of the gene coding for CypA have been found, that destabilize CypA and prevent HCV replication and infection [180]. A function of CypA as an inhibitor of viral replication in case of IAV has also been reported [173] as well as a function as co-factor that stimulates viral replication for example in HCV and HIV-1 infection [174], [181].

5.2.2 CypA and HIV-1

Since the early nineties, the role of CypA as a co-factor for HIV-1 infection has been discussed. A yeast-two hybrid screen identified not only CypA but also CypB as HIV-1 Gag binding proteins [182]. In fact, additional studies showed that CypA is incorporated into newly produced HIV-1 particles (Franke, Yuan, and Luban 1994b; Luban et al. 1993). A crystal structure solved in 1996 showing CypA in complex with the N-terminal domain of HIV-1 CA [184] can be seen in Figure 6. An exposed proline rich CA loop facing the exterior of the capsid shell harboring the amino acids AGPIA can bind CypA at its active site, which is also the CsA binding site. This loop is referred to as Cyp-binding loop [181]. Interestingly, these amino acids

differ from the previously assumed substrate recognition motif discussed in 5.2.1, indicating a flexibility in the CypA binding motif. The crystal structure revealed the proline residue P90 in an unprecedented *trans* conformation, which suggest a catalytic function of CypA on CA P90 isomerization [183], [185], [186]. Further studies of the HIV-1 virion revealed a packaging of CypA into HIV-1 virions in a ratio of 1:10 to CA molecules [183].

A comparison with other lentiviruses showed, that all lentiviruses have a CypA binding loop in their CA protein structure, however not all package CypA into their virions or require CypA for efficient replication [141], [182], [187]. This might indicate, that although HIV-1 virions incorporate CypA, the cellular effects in the target cell are more important for viral replication than the packaging of CypA into virions [188], [189]. In fact, virions depleted of CypA showed no defects in infectivity [190].
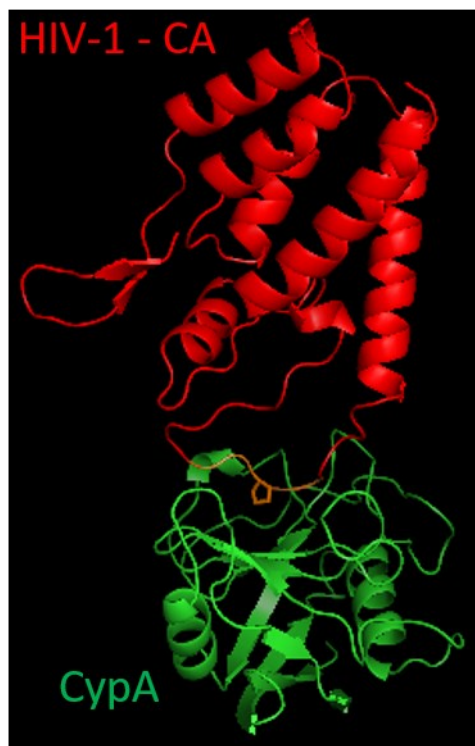
Figure 6: CypA in complex with HIV-1 CA protein.

HIV-1 CA protein (depicted in red) is bound to the active site of human CypA (depicted in green). The structure is obtained from PDB file 1AK4. The Cyp-binding loop of HIV-1 CA is highlighted in orange and the P90 residue of HIV-1 CA is shown with its side chain. The structure was obtained with Pymol.

A crucial step for HIV-1 infectivity is uncoating, a process where the conical capsid core undergoes morphological changes resulting in the disassociation of CA from the viral genome [191], [192]. This process is not yet fully understood, but uncoating seems to be directly linked to HIV-1 infectivity efficiency and CA stability. Therefore, it is not surprising, that cellular binding of CypA to CA influences this process. Contradictory results show on the one side a destabilizing effect of CypA on CA-NC complex or HIV-1 CA assembly [193], [194] and on

the other side HIV-1 core stabilizing effects [195], which results in a delayed uncoating of the virion [196], [197]. A model suggests that the binding of CypA causes steric hindrance to adjacent CA hexamers in the CA core. This could lead to accelerated disassembly of the viral core [194]. Interestingly the infection promoting activity of CypA seems to be cell type dependent [188], [198].

The interaction of CypA with the Cyp-binding loop of CA could be prohibited by CsA, and hence CsA was investigated as an antiviral drug. CsA treatment of CD4$^+$ Hela cells resulted in reduced HIV-1 DNA levels and reduced infectivity in peripheral blood mononuclear cells (PBMCs) and Jurkat cells which indicate an involvement in uncoating [199], [200]. Yet, in H9 T cells HIV-1 replication was not blocked by CsA [201] pointing at a cell type specific effect of CsA [196]. To exclude that the effects of CsA on HIV-1 infectivity are related to its immunosuppressive function, non-immunosuppressive analogues unable to interact with calcineurin were used. These analogous inhibited or promoted HIV-1 infection as well leading to the assumption that the interaction of CypA with HIV-1 CA plays a crucial role in HIV-1 infection independent of a immunosuppressive role of CsA [199], [202], [203]. This observation was reassured by the finding of resistant CA variants, which arise when HIV-1 is propagated in the presence of CsA [187], [204], [205]. These variants (A92E and G94D) could still bind CypA but efficient viral replication is dependent on CypA inactivation by CsA. Hence, the effects on viral replication are dependent on CypA expression levels, which differ amongst cell lines. Consequently, CsA was required for replication in HeLa and H9 T cells but not in Jurkat or 293T cells [197], [201], [206]. Until now, this cell-type specific effect and the differences in HIV-1 restriction are not fully understood. Interestingly most of these variants were unable to infect non-dividing cells, usually a feature of lentiviruses [201], [205], [206]. The binding of CypA to HIV-1 CA could also be abrogated by mutations in the CypA binding loop of HIV-1 CA. The P90A CA variant can still bind CypA but is resistant to isomerization by it and, therefore infects cells independently of CypA enzymatic activity [187], [189], [198]. This caused reduced viral replication efficiencies in macrophages and CD4$^+$ T cells accompanied by a retargeted integration site selection, but did not block HIV-1 infection completely [187], [207]. Furthermore, manipulating the CypA cellular levels by knockdown or genetic deletion of the CypA gene inhibits an early HIV-1 infection step and alters reverse transcription [181], [187], [189], [198], [200], [202]. A CypA knockout (CypA -/-) in Jurkat cells could impair viral infectivity [181], [208], [209] and furthermore, deletion of CypA in CD4$^+$ T by homologous recombination decreased HIV-1 replication, which could not be further decreased by CsA treatment. Re-expression of CypA restored HIV-1 replication in these cells

[181]. Taken together, a single role for CypA in uncoating could not be demonstrated. It is more likely that CypA will influence almost every post-entry step by altering CA stability and competing with other host factors for CA binding.

Further studies identified that the CypA-CA interaction not only affects reverse transcription or impacts integration site selection, but also regulates the utilization of other HIV-1 co-factors, like Nup358, MX2, CypB and Pin1, two other PPIases, PDZD8 or TRIM5 and TRIM11 [196], [207], [210]–[213]. However, CypA alone does not function as a potent restriction factor of HIV-1. In some new world owl monkeys a fusion protein of CypA with TRIM5α has been found. Through alternative splicing and retrotransposition CypA was inserted into intron 7 of TRIM5α [214], [215]. This TRIMCyp fusion protein potently restricts not only HIV-1 but also feline immunodeficiency virus (FIV). A treatment of owl monkey infected cells with CsA rescues HIV-1 infectivity, indicating that binding of TRIMCyp is responsible for viral restriction [216]. Furthermore, a second fusion protein of TRIM5α with CypA has been found in rhesus, pigtail and cynomolgus macaques [217]–[219]. The insertion of CypA into TRIM5α occurred downstream of exon 8 [220] and independently by LINE-1 mediated retrotransposition. This second fusion protein is not able to restrict HIV-1 but restricts HIV-2 and FIV potently.

The ability of lentiviruses to infect non-dividing cells was genetically mapped to the CA protein [221], [222]. It was shown that HIV-1 infection of macrophages or dendritic cells is not accompanied by activation of the innate immunity through pathogen-associated molecular patterns (PAMPs) [203], [223], [224]. This lack of immunity in myeloid cells could be linked to CA, more specifically to the CypA-CA interaction. CsA treatment or the CA mutants P90A and G89V resulted in an innate immune response in these cells indicating a mechanism for HIV-1 to escape immune sensing in a CypA-CA dependent manner [203], [224]. Infecting non-dividing cells with different CA mutants upregulated the cytoplasmic DNA sensor cyclic GMP-AMP synthase, which is responsible for interferon regulatory factor 3 (IRF3) nuclear translocation. IRF3 is a member of the interferon regulated transcription factor family. It signals through the retinoic-acid-inducible gene 1 (RIG1) signaling pathway and induces the expression of IFNα, IFNβ and ISGs [203], [223]. ISGs play a critical role in HIV-1 restriction. So does MX2 restrict HIV-1 in a CA dependent manner [98], [99], [103], resulting in reduced viral DNA amounts and integration. Interestingly this effect appears to be CypA dependent, as CypA depletion prevented MX2 mediated restriction [103]. Another factor involved in innate sensing and interferon production is CPSF6. Depletion of CPSF6 triggers innate sensing and interferon production which might also be regulated by CypA-CA binding [203], [225].

Altogether, CypA can regulate pathways directly by binding to HIV-1 CA protein or indirectly by mediating signaling through its extracellular binding receptor CD147 [167] or the effect on other host restriction factors. However, these effects and implications on the virus life cycle remain poorly characterized and understood.

5.2.3 Other Cyclophilins and PPIases

The human genome alone contains at least 17 different Cyps. All of them harbor the cyclophilin domain core structure described in 5.2.1 but they differ in their subcellular localization. This is mostly due to additional N- or C-terminal accessory domains carrying protein localization signals and specific target recruitment domains.

Cyclophilin B (CypB) for example is a 22 kDa protein, that shares 64% sequence homology with CypA and has an additional N-terminal hydrophobic leader sequence, which is responsible for its endoplasmic reticulum (ER) localization [117]. The high sequence homology can be explained by the conserved Cyp domain structure. It is therefore not surprising, that CypB can also be inhibited by CsA [117]. As this region is mainly responsible for HIV-1 CA protein binding, an interaction that is sensitive to CsA could be observed [182]. *In vitro* studies showed an even higher affinity to CA for CypB compared to CypA and surprisingly CA mutants exist, that only bind to CypB but not to CypA [141], [182]. The differences in the binding capacity of HIV-1 are mainly due to the leader sequence, since deletion of this sequence did not show any altered binding compared to CypA [226]. For that reason, a function of CypB on the HIV-1 life cycle is under discussion. Although increased CypB amounts in human plasma from HIV-1 positive patients has been found [227], no further involvement of CypB in HIV-1 infectivity could be shown. However, CypB is associated with the secretory pathway and can be released into biological fluids like milk, plasma or cell culture supernatants [228]–[230], which indicates a role in signaling. It has been found, that CypB can specifically bind to human peripheral T-lymphocytes and might function as an inflammatory mediator [231]. This is consistent with the finding, that both CypB and CypA appear to be involved in tumor development. CypB is highly elevated in pancreatic cancer patient sera. CypB silencing inhibited cell proliferation, migration and invasion via inhibition of the signal transducer and activator of transcription 3 (STAT3) pathway [232]. This is consistent with the finding, that CypB plays a role in STAT3 phosphorylation and translocation to the nucleus [233]. As CypB is located in the ER, it is not surprising, that CypB functions in attenuating oxidative stress and thereby inhibits hypoxia-induced apoptosis, which is also a stimulating factor for tumor growth and can be used to evade viral infection [234], [235].

Cyclophilin C (CypC) is a primarily cytoplasmic member of the PPIase family [236]. The 33

kDa protein can also be secreted and is found in the ER[236], [237]. Like CypB, CypC seems to be involved in mediating ER protein folding and regulating the oxidative status [238]. However, CypC might play a role in immune evasion, as it seems to be involved in the degradation of major histocompatibility complex class I molecules (MHC I). This degradation is induced by the immune evasion protein US2, marking newly synthesized MHC I molecules for degradation by the endoplasmic-reticulum-associated protein degradation machinery (ERAD) [239]. The involvement of CypC in innate immunity is also supported by the binding of calcineurin in presence of CsA [133], [237] and possible expression induction by interferons. Furthermore, CypC binds to Mac-2BP, which was originally identified as CypC binding protein in mice and interaction with it can be disrupted by CsA [240], [241]. It belongs to the scavenger-receptor cysteine-rich domain superfamily and the secreted glycoprotein modulates the host response to endotoxins [241]. Mac-2BP is upregulated in tumor cells and by HIV-1 and HCV infection [242], [243]. Mac-2BP stimulates MHC I expression which in turn can be suppressed by a non-immunosuppressive analogue of CsA [237] linking the function of Mac-2BP to US2. In addition, a binding of Mac-2BP in complex with CypC to NFAT was shown and a function in dephosphorylation of NFAT mediating macrophage activation was suggested [244].

A two-domain Cyp is Cyclophilin D (CypD), also often referred to as Cyp40. It is a 40 kDa cytosolic protein, that carries an additional heat shock protein 90 (Hsp90) binding domain including three tetratricopeptide repeat motifs [245]. Hsp90 is involved in protein folding and protein degradation. Interestingly, it can also bind other immunophilins like FKBPs and a glucocorticoid receptor. An isolated complex of Hsp90 with the glucocorticoid receptor had also bound CypD, suggesting a role for CypD in transcriptional activity of steroid receptors by controlling steroid ligand binding [246], [247]. The TRP domains facilitates CypD to interact with a variety of ligands additional to the PPIase binding capacity. A tandem affinity purification approach identified several new CypD interacting proteins including a hypoxia-inducible factor and receptor for activated C kinase 1 (RACK1), which is involved in translation [248]. All findings indicate putative activities of cytosolic CypD but lack evidence of a clear function.

Cyclophilins are also located in the nucleus. A 33 kDa member originally purified from T cells is called CypE [249]. It shares 83 % sequence similarity with CypA in the core domain and harbors an additional N-terminal RNA binding domain [250]. With this RNA binding domain, CypE can bind specifically poly(A)+RNA and binding of RNA stimulates the PPIase activity [251]. Furthermore, CypE has been identified as part of the spliceosome complex. This is a highly dynamic, macromolecular machinery required for the removal of introns from nascent

transcripts [252]. In this context it is not surprising that CypE also has been identified as an interaction partner of mixed lineage leukemia 1 (MLL1) protein, a histone methyltransferase [253]. So does CypE binding mediate the downregulation of MLL1 target genes like HOXC8 and c-myc in a PPIase dependent manner [254]. HOXC8 and c-myc are transcription factors involved in cell proliferation and morphogenesis. In context of viral infection, CypE has been discussed as a possible host factor for HIV-1, HCV and IAV infection. CypE plays a role in HCV replication and can bind the nucleoprotein of IAV which results in the inhibition of viral replication and transcription [237], [255]. For HIV-1 CypE has been identified in a yeast two-hybrid screen as a CA interaction partner like CypA and CypB [256]. If CypE is involved in the splicing of HIV-1 gene products, is currently unknown.

CypF is a small cyclophilin located in mitochondria. Its expression is upregulated in response to IFN. It is often also referred to as CypD although it is expressed from the PPIF gene. CypF is known to play a critical role in mitochondrial homeostasis and cell death. It is located at the membrane permeability transition pore in the inner mitochondrial membrane [257]. An opening of this pore leads to mitochondrial swelling and release of small molecules like calcium, apoptotic mediators and reactive oxidative species, which induce cell death. This swelling is not possible in CypF knockout mice suggesting CypF as an important mediator of apoptosis [257], [258]. If CypF is involved in viral infection and plays a role in the HIV-1 life cycle is currently unknown.

Cyclophilin G (CypG), also called SR-Cyp or CARS-Cyp, is an 89 kDa large member of the Cyp family, which is involved in mRNA mediated gene expression. It has a CypA-like N-terminal domain, two Nopp140 repeats that are important for nuclear import and a C-terminal arginine/serine rich (RS-) domain. The protein was first identified in a yeast two-hybrid screen using CDC28/cdc2-like-kinase (CLK) [259]. CLK is involved in pre-mRNA splicing as it phosphorylates RS rich splicing factors. This observation was confirmed by co-localization of CypG and nuclear pinin, a SR-related protein involved in pre-mRNA splicing. Interestingly the modulation of CypG expression levels resulted in altered nuclear distribution of SR proteins, indicating an important role for CypG in splicing [260]. Furthermore, CypG interacts directly via the RS domain with the phosphorylated C-terminal domain (CTD) of RNA Pol II [261].

Cyclophilin H (CypH) is a 19 kDa cytoplasmic and nuclear protein with a single Cyp domain. However, its PPIase activity is significantly reduced compared to CypA [262]. It is reported to be a component of the U4/U6 small nuclear ribonucleoprotein particle (snRNP) suggesting an involvement in splicing events [263], [264]. The binding of CypH to U4/U6 snRNP leaves the PPIase active side unaffected, allowing CypH to mediate interactions with other proteins inside

the spliceosome and initiate chaperoning activities.

Another protein is worthwhile to mention, even if it is not a classical cyclophilin. Nup358 is a nuclear pore protein, which has a C-terminal Cyp domain. It is the largest member of the PPIase family and named Ran-binding protein 2 (RanBP2) as well. Nup358 most likely binds HIV-1 CA due to its Cyp domain [265], [266], however one study suggests otherwise [267]. The current understanding of Nup358 function is an involvement in synchronizing HIV-1 uncoating and nuclear import. A depletion of Nup358 resulted in reduced HIV-1 infectivity, 2-LTR circle formation and proviral integration, indicating an involvement in nuclear entry of HIV-1 [207], [266], [268].

For FKBPs little is known about their ability to affect HIV-1. FKBP12 can bind the Env protein [227] and FKBP4 interacts with HIV-1 protease [269]. An RNAi mediated knockdown of FKBP6 resulted in a moderately increased HIV-1 infectivity which might makes FKBP6 a negative regulator in HIV-1 infection [270]. Taken together, there is no indication for the involvement of FKBPs in early HIV-1 infection steps and a crosstalk with Cyps.

Another PPIase involved in the HIV-1 life cycle is Pin1, a parvulin-like PPIase. Pin1 was suggested to bind the CA protein and isomerize the peptide bond between S16 and P17. In fact CA mutations at these positions severely reduced HIV-1 infectivity and downregulation of Pin1 by RNAi inhibited HIV-1 infection in certain studies [210], [271]. Furthermore, a phosphorylation of HIV-1 IN by JNK generates an additional target for Pin1 in CD4$^+$ T cells. Phosphorylation of IN increases its stability and thereby modulates infectivity and proviral DNA integration [272]. Pin1 could therefore execute a dual role in HIV-1 infectivity and a crosstalk between Cyps and Pin1 has been proposed [273]. However, every direct effect of Pin1 on HIV-1 infection is independent of CsA, as CsA exclusively inhibits Cyps.

5.3 RIG-I Signaling pathway

The most efficient way to control viral infection is the innate immune system. It is essential for infection control and every virus has evolved measures to fight against it. It is a very complex system, varies within different cell types and the various pathways involved are highly crosslinked. The RIG-I-like receptors (RLRs) signaling pathway is one of them, triggering IFN production and expression of antiviral genes. RLRs are DExD/H box RNA helicases that function as cytoplasmic sensors for PAMPs of viral RNA. Retinoic-acid-inducible gene 1 (RIG-I) and myeloma differentiation-associated protein 5 (MDA5) are two of these receptors, that detect viral RNA in the cytoplasm. They are highly active in myeloid and epithelial cells, but not in plasmacytoid dendritic cells and their expression is linked to IFN exposure and viral

infection. RLRs have two caspase activation and recruitment domains (CARDs), a helicase domain and a CTD. The helicase and CTD are essential for dsRNA binding [274], and signaling occurs through the CARDs by binding to mitochondrial antiviral signaling protein (MAVS) [275]–[277]. It is known that RIG-I and MDA5 both recognize certain viruses exclusively, whilst other viruses like Dengue virus or reovirus are recognized by both RLRs [278], [279]. RIG-I was initially found to bind dsRNA and trigger IFN induction. Later it was identified as a major factor involved in HCV replication [276]. RIG-I recognizes shorter ssRNA or dsRNA sequences marked with at least one phosphate at the 5' end of the RNA, but full signaling capacity is fulfilled with 5'triphosphorylated ends [280], [281]. MDA5 on the other hand recognizes longer dsRNA fragments.
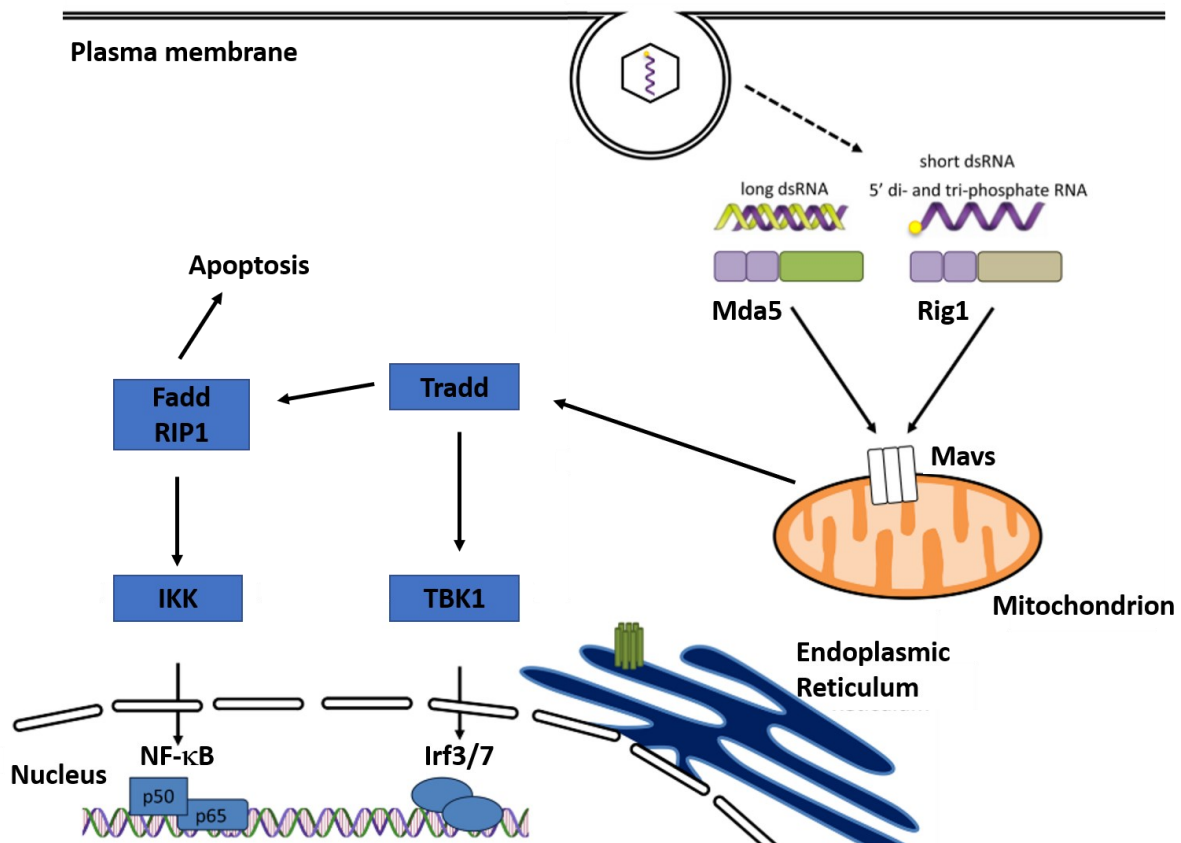
Figure 7: Schematic overview of the RIG-I signaling pathway.

Upon viral infection, viral RNA is sensed in the cytosol by MDA5 or RIG-I. Activation of their CARD domains facilitate complex formation with the mitochondrial protein MAVS which recruits other proteins to the signalosome. Through TNF receptor type 1-associated DEATH domain protein (TRADD) either apoptosis or a pro-inflammatory response is facilitated. The recruitment of kinases leads to activation of the transcription factors IRF3/7 and NFκB. These travel to the nucleus and stimulate ISG production as well was IFNβ production. Figure adapted from [282].

TANK-binding kinase 1 (TBK1) is another kinase, that phosphorylates IRF3 facilitating its transport to the nucleus. As IRF3 is expressed constitutively a function in the immediate early antiviral transcription is suggested. IRF3 is activated through phosphorylation by the non-

canonical IκB kinases IKK-ε or TBK1 and translocated to the nucleus, where it drives gene transcription [283]. The activation of NFκB requires the phosphorylation of its inhibitory subunit by IκB kinases, which is degraded by the proteasome. Activated NFκB is imported to the nucleus, where it activates the expression of several ISGs and IFNβ production which leads to autocrine and paracrine IFN receptor signaling through JAK-STAT. The components involved in the RIG-I signaling pathway are also shared with other cellular pathways involved in cellular immunity. MAVS can also be activated through transmembrane toll-like receptor 3 (TLR3) signaling upon viral infection and IRF3 and NFκB play a role in tumor necrosis factor receptor I (TNFRI) and TLR signaling pathways.

To shed some light on the involvement of the RIG-I signaling pathway in HIV-1 signaling macrophages were stimulated with a synthetic dsRNA known to signal through RIG-I. RIG-I expression was induced as well as IFNβ production. Furthermore, RIG-I activation resulted in the expression of several HIV-1 restriction factors including several ISG, APOBEC3 and tetherin, all able to at least partly inhibited HIV-1 replication [284]. These results have been recently confirmed by a study, that identified a 58 nucleotide-long capped RNA that emerges from abortive HIV-1 transcripts to induce IRF3 and NFκB through RLR signaling [285]. In addition, HIV-1 derived dimeric and monomeric forms of viral RNA were shown to be recognized by RIG-I [286]. In addition, for primary human PBMCs and macrophages it was shown that genomic HIV-1 secondary structured RNA was able to induce an innate immune response through RIG-I-dependent signaling [287]. However, HIV-1 can inhibit this signaling pathway by protease mediated sequestration of RIG-I [286]. Furthermore, IRF3 or TBK1 can be marked for cellular degradation. The HIV-1 accessory proteins Vpr and Vif have been shown to bind TBK1 and prevent signaling [288]. Another accessory protein involved in preventing the pro-inflammatory state of an infected cell is Vpu. Its involvement in the IFN response by degradation of IRF3 is discussed controversially. Some studies indicate that Vpu facilitates IRF3 degradation through a lysosome-dependent pathway and/or induces a caspase-dependent cleavage of IRF3 [289], [290]. Other studies find IRF3 unaffected by HIV-1 infection. However, Vpu is able to inhibit NFκB activity [291], [292]. How exactly HIV-1 interferes with the Rig-1 signaling pathway remains elusive. The ability of HIV-1 RNA recognition by RLRs is given, but at which stages of the viral replication cycle the pathway inhibits replication or integration remains unknown.

5.4 CETSA-Cellular thermal shift assay

Thermal shift assays (TSAs) have long been used as a biochemistry method to investigate thermostability of proteins based on their unfolding behavior with increasing temperatures [293]. Correctly folded proteins are only stable until a certain protein-specific temperature, their melting temperature (Tm). Protein exposure at higher temperatures results in unfolding and aggregation. These heat-dependent unfolding processes can be trailed by measuring intrinsic protein fluorescence intensity over time. The aromatic amino acid Tryptophan possesses an autofluorescence. Due to its apolarity, Tryptophan is often buried in the protein core, to avoid electrostatic interactions with the surrounding medium. Upon unfolding processes, the surroundings of Tryptophans change thus affecting their autofluorescence resulting in a shift in fluorescence intensity. Alternatively, to measure heat-induced unfolding processes in proteins with a low Tryptophan content, it is possible to use fluorescent dyes that only bind to correctly folded proteins [294], [295]. Changes in fluorescence intensity can be measured for example with a real-time cycler or differential static light scattering or differential scanning fluorometry. All mentioned detection methods provide sigmoidal melting curves resulting in a distinct Tm. The thermal shift assay (TSA) is often used in protein characterization studies as well as for protein engineering and drug design studies, as binding of additional components to the protein of interest frequently stabilizes the protein. These additional components can be small molecules like drugs, lipids or even DNA or other proteins. Small molecule or drug binding to a protein target results in thermal stabilization or destabilization and thus in a melting curve shift and consequently a shift in Tm (ΔTm) [293]. Thus, TSAs are frequently applied to investigate protein-protein, protein-DNA, protein-lipid and protein-drug interactions as it is an easy to use method which requires no specific technical equipment or chemically modified ligands. However, these basic assays rely on purified proteins and can only characterize binding effects of known interaction partners.

The cellular thermal shift assay (CETSA) is a novel variant of TSAs, using cell culture systems instead of purified proteins (Figure 8). Molina and colleagues showed a similar heat-dependent behavior of proteins in vivo as known for purified proteins, thus providing a more natural insight of protein interactions [296]. For CETSA experiments, cells are treated with the compound of interest or a vehicle control. After heat treatment cell lysis occurs followed by precipitation of aggregated proteins. Initial protocols used immunoblotting as a quantification method of stabilization events for the remaining soluble proteins, thus limiting target evaluation to suitable antibody availability. Melting curves and ΔTm shifts are inferred from blotting the amount of soluble protein against the temperature.
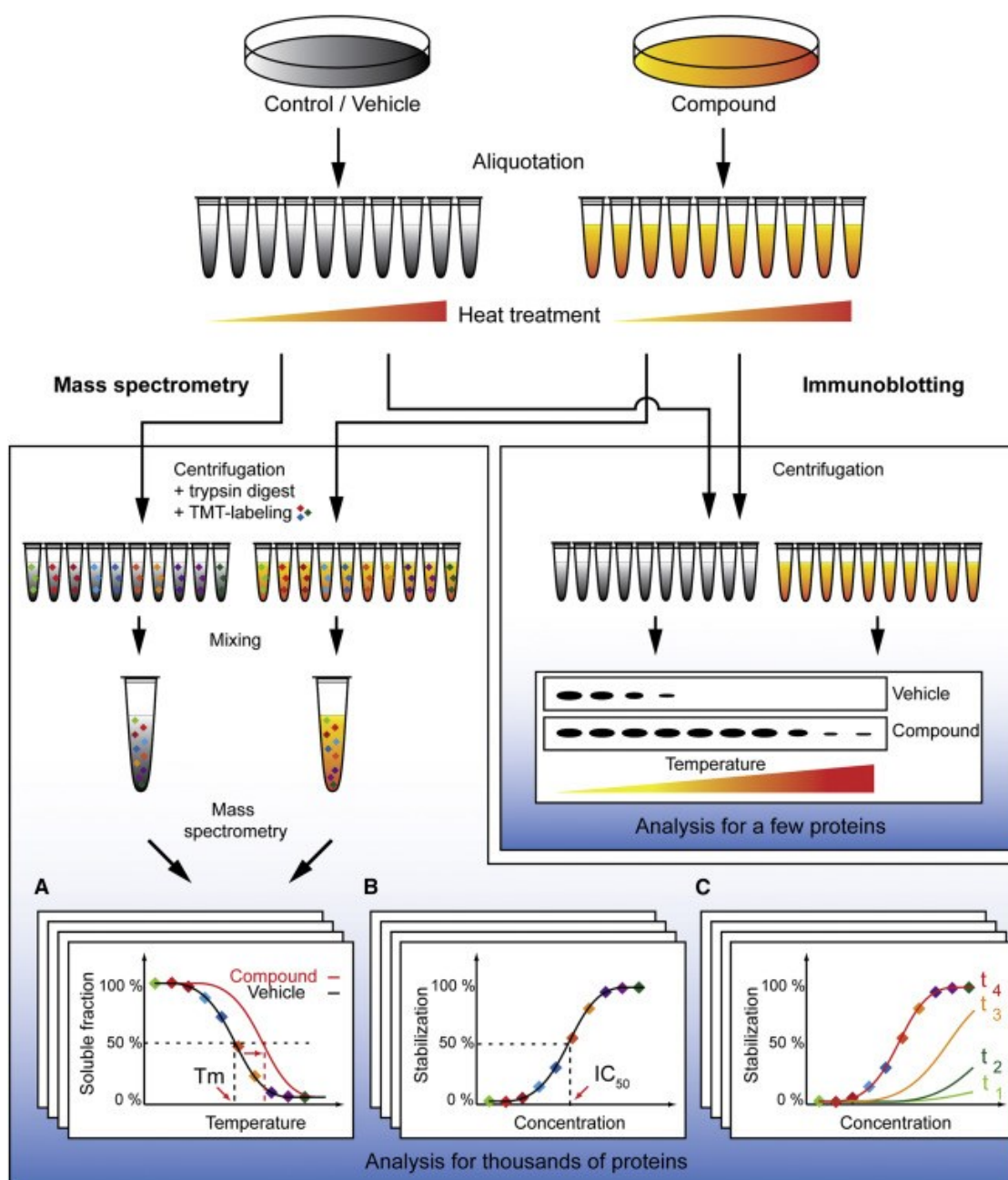
Figure 8: Cellular thermal shift assay (CETSA).

Cells are incubated with a compound or a vehicle control. Afterwards, cells are aliquoted and heated at ten different temperatures. Post-heating cells are lysed to separate denatured and soluble protein fractions by centrifugation. The remaining soluble protein fraction is analyzed by immunoblotting or mass spectrometry (MS). For MS-analysis soluble fractions are enzymatically digested and labeled with a specific mass-tag according to the heating temperature. MS-analysis provides a parallel readout for thousands of proteins using thermal proteome profiling (TPP) experiments as well as isothermal-dose-response relation (ITDR) or time-resolved ITDR experiments. Figure adapted from [297].

Therefore, a quantitative mass spectrometry (MS) approach has been developed. This MS-based detection method enables parallel binding studies for the whole cellular proteome in an unbiased approach, called thermal proteome profiling (TPP) [298]. Isobaric tandem-mass-tag (TMT) labeling allows simultaneous quantification of proteins from up to ten different experimental conditions, e.g. varying temperatures. A common temperature range from 37°C to 67°C was suggested, as most human proteins show sigmoidal melting curves for this

temperature range [298]–[300].

First experimental setups used a fixed compound concentration and ten different temperature points. The used compound concentration should ideally be sufficient to saturate all binding sites to ensure maximal stabilization of the compound target proteins, resulting in maximal melting curve shifts and consequently maximal ΔTm shifts. Another experimental setup employs a compound concentration range at a fixed temperature, ideally the Tm, providing information about an isothermal-dose response relation (ITDR). At low compound concentrations most proteins should be denatured while most proteins should be present upon compound treatment. Thus, ITDR experiments could also be used to determine ligand affinities in living cells. With a slightly altered experimental setup cellular compound uptake can be investigated by measuring different time intervals upon compound treatment. At early time-points intracellular compound concentration should be low, resulting in no protein stabilization whereas high intracellular compound concentration and major stabilization should occur at later time-points. Therefore, no increase in ΔTm is observed after reaching the maximal intracellular compound concentration.

Some major limitations of this method are the restriction to soluble proteins. However, modified protocols use mild detergent during protein extraction to stabilize membrane or membrane associated proteins [300], [301]. Overall behavior of soluble proteins is almost not affected allowing detection of cytosolic and membrane bound proteins in parallel. However, low abundance proteins are hard to detect due to instrument limitations and small proteins might not aggregate in the used temperature range (Savitski 2014). Furthermore, detergents reduce MS instrument capacity and specificity [302]. A few limitations remain as not all ligand binding events result in changes in thermal stability especially in large proteins. However, in theory melting curves for the whole human genome containing ~ 20,000 proteins could be obtained in a single experiment [303].

6   Objectives of this study

CypA is a known co-factor of HIV-1 infection (reviewed in [304]). Furthermore, Cyps are known immune modulators for several other viruses including HCV and IAV [172], [174]–[176], [305] and play crucial roles in organ rejection after transplantation [133]. Previous studies showed the involvement of CypA in type I IFN-mediated immunity against HIV-1 and interestingly, CsA could increase HIV-1 infection in THP-1 CypA knockout cells after a type I IFN-induced early block [209]. Therefore, the aim of this study was to identify the CsA-sensitive target responsible for the observed effects. To investigate the influence of other Cyps, several cyclophilin CRISPR/Cas9 knockout cells were generated. In addition, an unbiased mass spectrometry screen for cellular proteins that change in thermal stability after CsA treatment of cells was employed to reveal possible candidates that could be involved in the observed infection phenotype and to understand the interplay of cyclophilins with HIV-1. This screen not only revealed many cellular proteins as yet unknown to shift in thermal stability in cells treated with CsA but also identified members of the RIG-I pathway as possible candidates involved in early HIV-1 infection steps.

7 Material and Methods

7.1 Material

7.1.1 Laboratory equipment

Name	Company
Bacteria Incubator (IN75)	Memmert, Schwabach, Germany
C1000 Touch Thermal Cycler	BioRad, Hercules, USA
Cell culture Centrifuge (MegaFuge 40R)	Heraeus, Hanau, Germany
Centrifuge J2HS with JA-10 rotor	Beckman Coulter, Brea, USA
CFX 96 Real Time PCR detector	BioRad, Hercules, USA
Electrochemiluminescence (ECL) ChemoCam Imager system	INTAS Science Imaging, Göttingen, Germany
Flow Cytometer fluorescence-activated cell sorter (FACS) Verse	BD Biosciences, Franklin Lakes, USA
Flow Cytometer FACS Celesta	BD Biosciences, Franklin Lakes, USA
Gel iX Imager (Agarose gel ultra violett (UV)-imager)	INTAS Science Imaging, Göttingen, Germany
Ice Maker AF 103	Scotsman, Sprockhövel
Incubator C200	Labotect , Rosdorf, Germany
L8-70M Ultracentrifuge with SW32 rotor	Beckman Coulter, Brea, USA
Leica DMIL Led Fluorescent Microscope	Leica Microsystems, Wetzlar, Germany
Light Microscope EL WD 0.3 T1-SNCP	Leica Microsystems, Wetzlar, Germany
NanoPhotometer	Implen, München, Germany
Neubauer Counting Chamber	Marienfeld, Lauda-Köngshofen, Germany
PCR Cycler	BioRad, Hercules, USA
pH-Meter (FiveEasy)	Mettler-Toleda, Columbus, USA
Plate Reader Infinite M200 Pro	Tecan, Männedorf, Switzerland
Thermoblock Eppendorf ThermoMixer® comfort	Eppendorf, Hamburg, Germany

Standard equipment, such as freezers, balances or gel chambers are not listed here and were purchased from commercial sources.

7.1.2 Laboratory materials

Name	Company
Blotting paper 3MM Chr	Whatman, Dassel, Germany
Cell Culture Dishes (100 x 20 mm) CELLSTAR®	Greiner Bio-One, Kremsmünster, Austria
Cell Culture Flasks (25, 75, 175 cm^2) CELLSTAR®	Greiner Bio-One, Kremsmünster, Austria
Cell Culture Multiwell Plates (6, 12, 24, 48, 96 well) CELLSTAR®	Greiner Bio-One, Kremsmünster, Austria
Fluid aspiration system BVC professional	VACUUBRAND, Wertheim, Germany
polyvinylidene fluoride (PVDF) membrane, Immobilon-FL 0.45µm	Merck Milipore, Billerica, USA
Surgical disposable scalpel	B. Braun, Melsungen, Germany
Syringe filters units (0.22 µM) Millex	Merck, Millipore, Billerica, USA
Syringe filters units (0.45 µM) Rotilabo® KH55.1	Carl Roth, Karlsruhe, Germany
Syringes (1 ml – 60 ml) BD Luer-Lok™	Becton Dickinson, Franklin Lakes, USA

Standard laboratory materials, such as gloves or filter tips are not listed here and were purchased from commercial sources.

7.1.3 Kits

Name	Company
Acrylamide Solutions TGX™ Fast Cast™	BioRad, Hercules, USA
DC™ Protein Assay	BioRad, Hercules, USA
DNeasy® Blood & tissue Kit	Qiagen, Hilden, Germany
MycoAlert Mycoplasma Detection Kit	Lonza, Basel, Switzerland
NucleoBond® Xtra Midi EF	Macherey-Nagel, Düren, Germany
NucleoSpin® Gel and PCR Clean-up	Macherey-Nagel, Düren, Germany
QIAamp DNA Mini	Qiagen, Hilden, Germany

7.1.4 Chemicals and reagents

Name	Company
Agarose	Fisher Bio Reagents, USA

Ammonium persulfate (APS)	Sigma-Aldrich, St. Louis, USA)
β-Mercaptoethanol	Sigma-Aldrich, St. Louis, USA
Blasticidin	ThermoFisher Scientific, Rockford, USA
Bovine Serum Albumin (BSA)	Carl Roth, Karlsruhe, Germany
Bromophenol blue	Chroma, Fürstenfeldbruck, Germany
Clarity Western ECL Substrate	BioRad, Hercules, USA
Dimethyl sulfoxide (DMSO)	Merck, Darmstadt, Germany
GeneRuler 1kb Plus DNA Ladder	ThermoFisher Scientific, Rockford, USA
Deoxynucleotide triphosphate (dNTP) Set	ThermoFisher Scientific, Rockford, USA
Ethylenediaminetetraacetic acid (EDTA)	Merck, Darmstadt, Germany
Gel Loading Dye, Purple (6x) for DNA	New England Biolabs (NEB), USA
Glycerol	AppliChem GmbH, Darmstadt, Germany
MIDORI[Green] Advance	Nippon Genetics, Dueren, Germany
Paraformaldehyde (PFA)	Merck, Darmstadt, Germany
Phosphate buffered saline (PBS) Dulbecco Powder	Biochrom GmbH, Berlin, Germany
Polyethylenimine (PEI)	Sigma-Aldrich, St. Louis, USA
cOmplete protease inhibitor, EDTA-free	Roche, Mannheim, Germany
Prestained PageRuler™	ThermoFisher Scientific, Rockford, USA
Puromycin	Merck Millipore, Darmstadt, Germany
Sodium dodecyl sulfate (SDS)	Applichem, Karlsruhe, Germany
SYBR Green	ThermoFisher Scientific, Rockford, USA
Triton X-100	Sigma-Aldrich, St. Louis, USA
Tween 20	Carl Roth, Karlsruhe, Germany

All standard chemicals and reagents not listed above were purchased form Carl Roth, Karlsruhe, Germany, Sigma-Aldrich, St. Louis, USA or Merck, Darmstadt, Germany.

7.1.5 Buffers, solutions and drugs

Name	Component	Concentration
PBS 1x	ddH$_2$0	
	NaCl	140 mM
	KCl	2.7 mM
	Na$_2$HPO$_4$	8 mM

	KH$_2$PO$_4$	1.8 mM
PBST	PBS 1x	
	Tween-20	0.05 % (v/v)
SDS blotting buffer	ddH$_2$0	
	Tris	48 mM
	Glycine	39 mM
	Methanol	20 % (v/v)
SDS running buffer	ddH$_2$0	
	Glycine	190 mM
	SDS	0.1 % (w/v)
	Tris-HCl	25 mM
SDS sample buffer 3x	ddH$_2$0	
	Tris-HCl pH 6.8	150 mM
	SDS	6 % (w/v)
	Glycerol	30 % (w/v)
	Bromophenol blue	0.02 % (w/v)
	β-Mercaptoethanol	5 % (v/v)
SYBR Green based PCR enhanced reverse transcription assay (SG-Pert) dilution buffer 1x (pH 8.0)	ddH$_2$0	
	(NH$_4$)$_2$SO$_4$	5 mM
	KCL	20 mM
	Tris-HCl	20 mM
SG-Pert reaction buffer 2x	SG-Pert dilution buffer	
	MgCl$_2$	10 mM
	BSA	0.2 mg/ml
	dNTPs	400 μM
	Primer RT-Assay-fwd	1 pmol
	Primer RT-Assay-rev	1 pmol
	MS2 RNA	8 ng
	SYBR Green	1: 10000
	GoTaq Hotstart Polymerase	0.5 U
SG-Pert lysis buffer (pH 7.5 with HCl)	ddH$_2$0	
	Tris	25 mM

	EDTA	1 mM
	EGTA	1 mM
	NaCl	100 mM
	Triton X-100	1 % (v/v)
	NP40	0.5 % (v/v)
tris-acetate ethylenediaminetetraacetic acid (TAE) buffer, 50x, pH 8.3	ddH$_2$0	
	EDTA	0.1 M
	NaAc	1 M
	Tris	2 M
Western blot (WB) stripping buffer pH 2.5	ddH$_2$0	
	Glycine	200 mM
	SDS	1 % (w/v)
WB blocking buffer	1x PBS	
	Milk powder	5 % (w/v)

Name	Company
Cyclosporin A	Sigma-Aldrich, St. Louis, USA
IFNα2	Dr. Kathrin Sutter (Universitätsklinikum Essen)

7.1.6 Bacterial strains and culture media

For plasmid preparation and cloning, the chemo competent *E. coli* strain Stbl2 (Invitrogen, genotype F- mcrA Δ(mcrBChsdRMSmrr) recA1 endA1 lon gyrA96 thi supE44 relA1 λ- Δ(lac-proAB)) was used.

Name	Component	Concentration
Luria broth (LB) medium	H$_2$O	
	NaCl	5 g/l
	Tryptone	10 g/l
	Yeast extract	5 g/l
	Adjust to pH 7.2, autoclave	

LB agar plates	Agar	12.5 g/l
	LB	

For selection, Ampicillin (0.1 mg/ml) was added to the medium or LB-agar plates.

7.1.7 Cell lines and culture media

Name	Description	Growth mode	Reference
HEK293T	human embryonic kidney cell line expressing large T antigen of SV40	adherent	[306], [307] RRID:CVCL_0063
THP-1 wild type (wt)	human peripheral blood monocyte cell line	suspension	ATCC® TIB-202™

Name	Medium	Supplements
DMEM+++	Dulbecco's Modified Eagle Medium (DMEM), high glucose (GIBCO)	10% heat inactivated fetal calf serum (FCS) 100 U/ml penicillin 100 µg/ml streptomycin
RPMI+++	Roswell Park Memorila Institute 1640 (RPMI) (GIBCO)	10% FCS heat inactivated 100 U/ml penicillin 100 µg/ml streptomycin
Freezing media	Heat inactivated FCS	10% DMSO or glycerol based on cell type
Optimem	OptiMem (GIBCO)	
Selection media	RPMI (GIBCO)	1 µg/ml Puromycin or 5 µg/ml Blasticidin

All adherent cell lines were cultured in DMEM+++ and frozen in freezing media supplemented with DMSO. All suspension cell lines were cultured in RPMI+++ and frozen in freezing media supplemented with glycerol. Cell lines were grown from mycoplasma free liquid nitrogen stocks. Cultured cells were checked for mycoplasma contamination four times a year. All cell lines used were contamination free.

7.1.8   Plasmids

Name	Description	Source
pGSGW	HIV-1 vector encoding green fluorescent protein (GFP)	[308]
pCSxW	HIV-1 vector	[309]
pCMVΔR8.91	HIV GagPol encoding plasmid	[310]
plentiCRISPRv2	puromycin resistance marker to express guide RNAs (gRNAs) constructs for CRISPR-mediated genome editing	Addgene, Cambridge, USA
plentiCRISPRv2bla	blasticidin resistance marker to express gRNA constructs for CRISPR-mediated genome editing	gift from Steeve Boulant
plentiCRISPR-CypAg1	plentiCRISPRv2 expressing gRNA targeting CypA	Luis Apolonia, (UCL, London, UK)
plentiCRISPR-CypBg1	plentiCRISPRv2 expressing gRNA targeting CypB	Luis Apolonia, (UCL, London, UK)
plentiCRISPR-CypCg1	plentiCRISPRv2 expressing gRNA targeting CypC	Luis Apolonia, (UCL, London, UK)
plentiCRISPR-CypDg1	plentiCRISPRv2 expressing gRNA targeting CypD	Luis Apolonia, (UCL, London, UK)
plentiCRISPR-CypEg1	plentiCRISPRv2 expressing gRNA targeting CypE	Luis Apolonia, (UCL, London, UK)
plentiCRISPR-CypFg1	plentiCRISPRv2 expressing gRNA targeting CypF	Luis Apolonia, (UCL, London, UK)
plentiCRISPR-CypGg1	plentiCRISPRv2 expressing gRNA targeting CypG	Luis Apolonia, (UCL, London, UK)
plentiCRISPR-CypHg1	plentiCRISPRv2 expressing gRNA targeting CypH	Luis Apolonia, (UCL, London, UK)
plentiCRISPRbla-CypBg1	plentiCRISPRv2bla expressing gRNA targeting CypB	this study
plentiCRISPRbla-CypEg1	plentiCRISPRv2bla expressing gRNA targeting CypE	this study
plentiCRISPRbla-RIG-Ig1	plentiCRISPRv2bla expressing gRNA targeting RIG-I	this study
plentiCRISPRbla-MDA5g1	plentiCRISPRv2bla expressing gRNA targeting MDA5	this study

plentiCRISPRbla-MAVSg1	plentiCRISPRv2bla expressing gRNA targeting MAVS	this study	
plentiCRISPRbla-IRF3g1	plentiCRISPRv2bla expressing gRNA targeting IRF3	this study	
plentiCRISPRbla-TRADDg1	plentiCRISPRv2bla expressing gRNA targeting TRADD	this study	
plentiCRISPRbla-Cas10g1	plentiCRISPRv2bla expressing gRNA targeting Caspase 10	this study	
pNL4.3GFP	Full-length HIV-1 encoding GFP in place of Nef followed by an IRES-Nef cassette	Torsten Schaller (UCL London, UK)	
pMD.G2	VSV-G expression plasmid	Didier Trono lab	

7.1.9 Oligonucleotides

Name	Sequence	Purpose	Publication
SB1	aaacCGTCTCCTTTGAGGTCGGGCc	gRNA vs CypA fwd	
SB2	caccgGCCCGACCTCAAAGGAGACG	gRNA vs CypA rev	
SB3	aaacCTCCGAACGCAACATGAAGGc	gRNA vs CypB fwd	
SB4	caccgCCTTCATGTTGCGTTCGGAG	gRNA vs CypB rev	
SB5	aaacgGTCACCTTGGCCGTCACCGAc	gRNA vs CypC fwd	
SB6	caccCAGTGGAACCGGCAGTGGCT	gRNA vs CypC rev	
SB7	aaacCCCTCGAGTCTTCTTTGACGc	gRNA vs CypD fwd	
SB8	caccgGGGAGCTCAGAAGAAACTGC	gRNA vs CypD rev	
SB9	aaacCCAAGCGCGTCTTGTACGTGc	gRNA vs CypE fwd	
SB10	caccgCACGTACAAGACGCGCTTGG	gRNA vs CypE rev	
SB11	aaacTGATGTCAGTATTGGCGGTCc	gRNA vs CypH fwd	
SB12	caccgGACCGCCAATACTGACATCA	gRNA vs CypH rev	
SB13	aaacGCCCTGGCTGGTGTCGCAGCc	gRNA vs IRF3 fwd	[311]
SB14	caccgGCTGCGACACCAGCCAGGGC	gRNA vs IRF3 rev	
SB15	aaacATAAGTATATCTGCCGCAATc	gRNA vs MAVS fwd	
SB16	caccgATTGCGGCAGATATACTTAT	gRNA vs MAVS rev	[311]
SB17	aaacTCTCCATCGTTTGAGAACGCc	gRNA vs MDA5 fwd	[312]
SB18	caccgGCGTTCTCAAACGATGGAGA	gRNA vs MDA5 rev	

SB19	aaacGGATTATATCCGGAAGACCCc	gRNA vs RIG-I fwd	[313]
SB20	caccgGGGTCTTCCGGATATAATCC	gRNA vs RIG-I rev	
SB21	aaacGTCGGATGCCTACGCGCACCc	gRNA vs TRADD fwd	
SB22	caccgGGTGCGCGTAGGCATCCGAC	gRNA vs TRADD rev	
SB23	caccgGCACTACCAGAGCTAACTCA	non targeting gRNA fwd	
SB24	aaacTGAGTTAGCTCTGGTAGTGCc	non targeting gRNA rev	
SB25	ACTGTCACTCTGGCGAAGTC	PCR CypA fwd	
SB26	CTAGGCAGAGGGACAATCGG	PCR CypA rev	
SB27	GGCTTCCGTCTATAGGCCAG	Sequencing CypA	
SB28	GAGCCCAATGAGGGAGCAAT	PCR CypB fwd	
SB29	GTTGCGGGGAAATTTCTTCGA	PCR CypB rev	
SB30	ACGTSTTTHCTAACCTCAAGCG	Sequencing CypB	
SB31	CTTTAGGTTCGCCGGAATCC	PCR CypD fwd	
SB32	GCATTGARACAAGGGGCTG	PCR CypD rev	
SB33	CATGGCTTCCGGTTCTTG	Sequencing CypD	
SB34	GGACCACGTCCCTTGGTTTA	PCR CypE fwd	
SB35	AGAGGATCCGAAGGGCCATA	PCR CypE rev	
SB36	CCACGTCCCTTGGTTTACCA	Sequencing CypE	
SB37	ACCCTAGCAGTCTCAGCACA	PCR CypH fwd	
SB38	TGCATGGAGGAATCAGGTCT	PCR CypH rev	
SB39	CTTTAGGTTCGCCGGAATCC	Sequencing CypH	
SB40	GACTATCATATGCTTACCGTAAC	Sequencing CRISPR Vector	
SB41	TCCTGCTCAACTTCCTGTCGAG	SG-Pert fwd	
SB42	CACAGGTCAAACCTCCTAGGAATG	SG-Pert rev	
SB43	aaacGGGGGTCCAAGATGTGGAGAc	gRNA vs Casp10 fwd	[314]
SB44	caccgTCTCCACATCTTGGACCCCC	gRNA vs Casp10 rev	
SB45	aaacTCCCGTTGGCGTCCACGTCCc	gRNA vs CypF fwd	
SB46	caccgGGACGTGGACGCCAACGGGA	gRNA vs CypF rev	
SB47	aaacACGAAAGTTCTCGCATGTTTc	gRNA vs CypG fwd	
SB48	caccgAAACATGCGAGAACTTTCGT	gRNA vs CypG rev	

7.1.10 Enzymes

Name	Company
BsmBI	New England Biolabs, USA
EcoRI	New England Biolabs, USA
GoTaq Hot Start DNA Polymerase	Promega, USA
HindIII	New England Biolabs, USA
NotI	New England Biolabs, USA
Phusion High Fidelity DNA Polymerase	New England Biolabs, USA
RiboLock RNAse Inhibitor	ThermoFisher Scientific, Rockford, USA
T4 DNA Ligase	New England Biolabs, USA

7.1.11 Antibodies

Name	Company	Application
β-Actin AC-74 (mouse)	Sigma-Aldrich, St. Louis, USA	1:2000 WB
CypA (rabbit)	Enzo Life Sciences, Farmingdale, USA	1:3000 WB
CypB k2E2 (mouse)	Santa Cruz Biotechnology, Dallas, USA	1:1000 WB
CypC (rabbit)	ThermoFisher Scientific, Rockford, USA	1:1000 WB
CypD (rabbit)	ThermoFisher Scientific, Rockford, USA	1:1000 WB
CypE (rabbit)	ThermoFisher Scientific, Rockford, USA	1:1000 WB
CypH (rabbit)	ThermoFisher Scientific, Rockford, USA	1:1000 WB
IRF3 SL-12 (mouse)	Santa Cruz Biotechnology, Dallas, USA	1:1000 WB
MAVS AT107 (rabbit)	Enzo Life Sciences, Farmingdale, USA	1:1000 WB
MDA5 AT113 (rabbit)	Enzo Life Sciences, Farmingdale, USA	1:1000 WB
Peroxidase goat anti-mouse	Jackson ImmunoResearch, Ely, UK	1:10000 WB
Peroxidase goat anti-rabbit	Jackson ImmunoResearch, Ely, UK	1:10000 WB
RIG-I (mouse)	AdipoGen Life Sciences, Liestal, Switzerland	1:1000 WB
TRADD A-5 (mouse)	SantaCruz Biotechnology, Dallas, USA	1:1000 WB

7.1.12 Software

Name	Company
CFX Manager	Biorad, Herkules, USA
DNA Dynamo	BlueTractorSoftware Ltd
Excel	Microsoft, Redmond, USA
FACSDiva	BD, Franklin Lakes, USA; RRID:SCR_001456
FACSSuite	BD, Franklin Lakes, USA; ????
FIJI	(Schindelin et al., 2012); RRID:SCR_002285
FlowJo V10	FlowJo LLC, Ashland, USA; RRID:SCR_00852
Graph Pad Prism 5	GraphPad Software, Inc., La Jolla, USA; RRID:SCR_002798

7.2 Molecular biology methods

7.2.1 Bacteria and DNA preparation

20 µl to 80 µl chemically competent *E. coli* Stbl2 bacteria were thawed on ice and subsequently mixed with 1 µl of plasmid DNA or 5 µl of ligation mix. The solution was kept on ice for 10 min or 40 min, respectively. Heat shock was performed in a water bath at 42°C for 90 sec, followed by incubation on ice for 2 min or 15 min for a ligation mix. Transformed bacteria were plated on pre-warmed LB agar plates containing 0.1 mg/ml ampicillin and incubated at 37°C overnight.

To amplify plasmid DNA, a single cell colony was picked to inoculate LB medium supplemented with 0.1 mg/ml ampicillin at 37°C overnight. For small scale productions 2 ml bacterial culture was grown and purification was performed with QIAamp DNA Mini Kit (Qiagen, Hilden, Germany) according to the manufacturers protocol. For large scale productions 100 ml bacterial culture was grown and purification was performed with NucleoBond® Xtra Midi EF Kit (Macherey-Nagel, Düren, Germany) according to the manufacturers protocol. Concentration and purity of the produced plasmid DNA was controlled using a NanoPhotometer (Implen, München, Germany). Sufficient DNA quality was archived by an OD260 nm/280 nm ratio between 1.8 and 2.0.

7.2.2 Polymerase chain reaction (PCR)

Reaction mixtures were prepared on ice and the following components were mixed in a 0.2 ml PCR tube:

Name	Final concentration
Nuclease-free water	to 50 µl
5x Phusion HF or GC buffer	1x
10 mM dNTPs	250 µM each
10 µM Forward Primer	10 pmol
10 µM Reverse Primer	10 pmol
DMSO	3 %
Phusion Polymerase	1 U
Template DNA	100 ng – 1 µg

Annealing temperatures and elongation times were set depending on the primer compositions and the length of the amplified sequence, respectively. Usually 35 reaction cycles of the following thermocycling protocol were performed:

Step	Temperature	Duration
1) Initial denaturation	98°C	30 sec
2) Denaturation	98°C	10 sec
3) Annealing	variable	30 sec
4) Elongation	72°C	15 - 30 sec per kilo bp
Repeat steps 2-4 35 times		
5) Final extension	72°C	10 min
6) store	12°C	
Lid temperature	105°C	

All nucleotide sequences of PCR production were gel purified and confirmed by sequencing (Eurofins Genomics, Ebersberg, Germany).

7.2.3 DNA separation by agarose gel electrophoresis and purification

DNA fragments were separated by electrophoresis using gels containing 1 % agarose in 1 x TAE buffer supplemented with MIDORI[Green] Advance to stain DNA (5 µl for a 100 ml agarose gel prior to polymerization). DNA samples were mixed with DNA loading buffer and loaded into the wells. Gels were run at 80 V for 30 min. A DNA standard (DNA ladder 1kb Plus) was used to compare DNA fragment sizes. Loaded DNA was visualized under UV light and analyzed with a Gel iX Imager.

Extraction of DNA bands was performed using surgical disposable scalpels and purification

was performed with NucleoSpin® Gel and PCR Clean-up kit (Macherey-Nagel, Düren, Germany) according to the manufacturers protocol. Purified DNA was eluted from the column with 30-50 µl of water.

7.2.4   Ligation of DNA fragments

For ligation 2-4 µg plasmid DNA was digested with appropriate restriction enzymes according to the manufacturer's protocols. Digested DNA was gel purified and eluted with 50 µl of water. 1 µl purified vector DNA was mixed with 5 µl of insert DNA, 2 µl 10 x ligase buffer, 1 µl (3 U) T4 ligase and water to a final volume of 20 µl. After 20 min incubation at room temperature 5 µl of the ligation mix was added directly to 80 µl competent bacteria for transformation.

7.2.5   Analysis of DNA with restriction enzymes

Restriction digests were conducted using 1 µg plasmid DNA, 0.5 µl of each restriction enzyme and 2 µl 10 x NEB buffer recommended for the respective enzyme used. Reactions were filled up with water to 20 µl and incubated at the optimal temperature for each enzyme.

7.2.6   Cloning of gRNAs into retroviral vector plentiCRISPRv2

10 µg of FWD and REV gRNA sequence was mixed with 2.5 µl of 2 M NaCl and filled up with water to a final reaction volume of 22.5 µl in a 0.2 ml PCR tube. After incubation at 98°C for 5 min the mixture was subsequently cooled down at a rate of 0.1°C/s. The annealed oligos were transferred to a 1.5 ml reaction tube and mixed with 40 µl 3 M NaAC, 1 ml of absolute ethanol (EtOH) and 350 µl water. After brief vortexing, the sample was placed at -80°C for 30 min or overnight. To pellet the DNA, the ice-cold sample was centrifuged with 14000 rpm for 15 min at 4°C, the DNA pellet was air dried and resuspended in 50 µl water.

8 µg of the CRISPR backbone vector plentiCRISPRv2 or plentiCRISPRv2bla was digested with 1 µl BsmbI, 2 µl 3.1 buffer in a final reaction volume of 18 µl for 1.5 h at 55°C. 1 µl of the cut vector was mixed with 5 µl of annealed oligos. For ligation 2 µl of T4 ligation buffer and 1 µl of T4 ligase was added and filled up with water to 20 µl. The reaction was performed at room temperature for 10 min followed by transformation in *E. coli*. The next day at least 5 clones per plate were picked for a small-scale production of plasmid DNA. Successful cloning was confirmed by digestion with HindIII and EcoRI and sequencing.

7.3 Cell biology methods

7.3.1 Cell culture

THP-1 wt cells and their CRISPR/Cas9 derivates were grown in RPMI+++ medium at 37°C. Passaging of the cells was performed every 2-4 days in a ratio of 1:5. HEK293T were grown in DMEM+++ at 37°C. Passaging of these cells was performed every 2-3 days. Cells were washed once with PBS followed by detachment from the cell culture dish surface by 0.05 % Trypsin/EDTA in PBS for 5-10 min. Cells were resuspended in fresh medium and diluted in 1:4 (2 days) or 1:6 (3 days).

Cell line stocks were maintained by cryo-conservation. Therefore, cells were pelleted (1200 rpm for 5 min) and resuspended in freezing medium supplemented with 10 % DMSO (adherent cells) or 10 % glycerol (suspension cells). Cells were transferred into a cryo-conservation tube and slowly cooled to -80°C in freezing Styrofoam boxes. For long term storage, tubes were transferred to a liquid nitrogen tank. Cells were thawed rapidly and transferred into 75 cm² flasks (suspension cells) containing 15 ml fresh, pre-warmed RPMI+++ or 10 cm dishes (adherent cells) with 10 ml fresh, pre-warmed DMEM+++. Medium was changed after 6 h (suspension cells) or 18 h (adherent cells).

7.3.2 Virus and vector preparation

HEK293T cells were seeded in 10 cm dishes. After 24 h at 75 % confluency cells were transfected with 4 µg PEI per µg DNA in 1 ml Optimem. For lentiviral vector (LV) production 4.5 µg of HIV-1 viral plasmid (pGSGW, plentiCRISPRv2 or plentiCRISPRv2bla vectors, encoding the gRNA od interest), 3 µg of pCMVΔR8.91 GagPol encoding plasmid and 3 µg of VSV-G Env expression plasmid pMD.G2 per plate were mixed into a reaction tube with 0.5 ml Optimem. PEI was mixed with 0.5 ml Optimem in a separate reaction tube. Both were combined and mixed by vortexing and incubated at room temperature for 15 min. The mixture was added dropwise to 8 ml fresh DMEM+++ on top of HEK293T cells. For VSV-G pseudotyped full-length HIV-1 GFP reporter virus production 8 µg pNL4.3GFP was cotransfected with 2 µg of pMD.G2 per plate. For all productions, the media was replaced with 6ml fresh medium 24 h post transfection. Supernatant was harvested 48 h and 72 h post transfection. Both collections were pooled and filtered using a 0.45 µm cellulose filter to remove cell debris. All viral supernatants were subjected to sucrose purification as described before [315].

Analysis of RT activity in concentrated supernatants was performed by SG-PERT [316]. Concentrated supernatant and a RT standard were diluted 1:500 and 1:1000 and 5 µl of each

dilution was lysed by incubation with 5 µl SG-Pert lysis buffer containing 2 U Ribolock RNAse inhibitor. Subsequently, 90 µl SG-Pert dilution buffer were added. From this mixture 10 µl were mixed with 10 µl SG-Pert reaction buffer containing 0.5 U GoTaq Hot Start DNA Polymerase. RT-PCR was performed, using a CFX 96 Real Time PCR detector (BioRad, Hercules, USA) with the following conditions: 42°C for 20 min, 95°C for 2 min, 40 cycles of 95°C for 5 sec, 60°C for 5 sec, 72°C for 15 sec and 80°C for 7 sec. A final melting curve step was included. Results were analyzed with the CFX Manager software (BioRad, Hercules, USA).

7.3.3 Generation of CRISPR/Cas9 THP-1 knockout cell lines

THP-1 wt or THP-1 CypA -/- cells were transduced with VSV-G pseudotyped HIV-1 LV delivering plentiCRISPR vectors with the respective gRNA against the target proteins in a 12-well format. A medium change was performed 24 h post transduction and selection for at least 2 weeks either with 1 µg/ml puromycin or 5 µg/ml blasticidin was started 48 h post transduction. Single cell clones were generated by limiting dilution and grown in 96 well plates for at least 4 weeks in the absence of selection medium. Afterwards, cells were expanded, and expression of the targeted proteins was analyzed by Western blot. Genomic DNA from cell clones with no detectable protein expression was isolated, the corresponding gene amplified by PCR (used oligonucleotides are listed in 7.1.9). PCR products were gel purified and send for sequencing at Eurofins Genomics. Used oligonucleotides are listed in 7.1.9.

7.3.4 Infection assays

100 µl containing 1×10^5 THP-1 based cells were plated per well in a 96-well plate and treated or not with 500 U IFNα2 in a final volume of 200 µl for 24 h. The next day 100 µl of supernatant was removed and cells were treated or not with 2.5 µM CsA. Purified VSV-G pseudotyped GFP-reporter lentiviral vector or NL4.3GFP reporter virus (see 7.3.2) corresponding to 100 mU of RT activity were added to each well. Cells were fixed 48 h later in 4 % PFA. Infectivity was determined from the percentage of GFP positive cells by flow cytometry using a FACSVerse or FACSCelesta (BD Biosciences, Franklin Lakes, USA).

7.4 Biochemistry methods

7.4.1 SDS-polyacrylamide-gel electrophoresis (SDS-PAGE)

Samples for SDS-PAGE were boiled in SDS sample buffer at 98°C for 10 min. Polyacrylamide gels were generated using Acrylamide Solutions TGX™ Fast Cast™ (BioRad, Hercules, USA)

according to the manufacturers protocol using an acrylamide concentration of 10 % or 12 % for the separating and 4 % for the stacking gel. For the separation gel 3 ml Resolver A was mixed with 3 ml Resolver B, 3 µl N'-tetramethylethylenediamine (TEMED) and 30 µl of 20 % APS and quickly poured into the gel chamber of the Biorad PAGE gel casting system. Air bubble formation was prevented by overlaying the separation gel with a thin layer of isopropanol. After polymerization, isopropanol was discarded. The stacking gel was prepared by mixing 1 ml of Stacker A with 1 ml of Stacker B, 2 µl TEMED and 10 µl APS. The stacking gel solution was transferred quickly in the gel chamber on top of the polymerized separation gel. After polymerization, the glass slides were installed into the running chamber which was filled with SDS running buffer. 10 µl of boiled protein samples was loaded per lane. Gel electrophoresis was performed between 80 V and 120 V for 60 min.

7.4.2 Western Blot

SDS-gels were transferred after gel electrophoresis to a 0.45 µm PVDF membrane (Merck Milipore, Billerica, USA) using the Electrophoretic Transfer Cell Mini Trans-Blot® system (BioRad, Hercules, USA) at 100 V for 60 min in a cold room (4°C). After transfer, membranes were incubated for at least 20 min in PBST supplemented with 5 % non-fat milk powder to saturate non-specific binding sites. Membranes were washed three times for at least 5 min with PBST. Primary antibodies were diluted in PBST in the respective concentrations and incubated with the membrane at 4°C over-night. After washing three times with PBST, the membrane was incubated with the secondary antibody in PBST shaking at room temperature for 1 h. After three times washing with PBST, membrane bound secondary antibody was detected with Clarity Western ECL Substrate (BioRad, Hercules, USA) at an ECL ChemoCam Imager system (INTAS Science Imaging, Göttingen, Germany).

7.4.3 Cellular thermal shift assay

10 ml containing 1×10^7 THP-1 based CypA -/- cells were seeded in T25 flasks and stimulated or not with 500 U IFNα2 for 24 h. The next day one IFN treated flask was stimulated with 2.5 µM CsA and a second one with DMSO for 1.5 h. In parallel, an infection assay with full-length HIV-1 GFP reporter virus using THP-1 cells described in 7.3.4 was conducted for quality control.

After treatment, cells were centrifuged with 300 rpm for 5 min and washed once with PBS. CsA and DMSO treated samples were each resuspended in 1.5 ml PBS containing a protease inhibitor cocktail. Samples were aliquoted in 10 PCR tubes containing 150 µl sample each. Tubes were placed in a PCR Cycler (BioRad, Hercules, USA) and each tube was heated to one

temperature between 37°C and 67°C for 3 min followed by cooling to 20°C for 3 min. Samples were placed directly in liquid nitrogen and three cycles of freeze/thaw were performed, using a water bath at 25°C. Between each cycle cells were kept on ice and briefly vortex. Afterwards, samples were kept on ice and transferred into a 1.5 ml reaction tube. Denatured proteins were separated by centrifugation at 21xg for 2 min at a pre-cooled centrifuge at 4°C. The supernatant (100 µl) was carefully transferred to a new pre-cooled PCR tube without disruption of the protein pellet and placed on ice. 10 µl were transferred to a new tube and mixed with SDS-sample buffer for Western blot analysis. Another 10 µl were used to determine the protein concentration using DC™ Protein Assay (BioRad, Hercules, USA) and a Plate Reader Infinite M200 Pro (Tecan, Männedorf, Switzerland) following the manufacturers protocol. The remaining sample was frozen in liquid nitrogen, stored at –(80°C), and shipped for further sample processing and mass spectrometry (MS) analysis to SciLifeLab at the Carolinska Institutet, Soln, Sweden. Sample processing and MS was performed as published previously [298], [299].

7.5 Statistical analysis

Statistical analysis was performed using Graph Pad Prism software. Datapoints are plotted as mean ± SD. Statistical significance was calculated using two-tailed unpaired t-tests. Values of $p < 0.05$ are considered as significant.

8 Results

8.1 The role of Cyclophilins in a type I IFN-induced block of HIV-1 infection

To test the hypothesis, that Cyclophilins play a role in the type I IFN related innate immunity against HIV-1 infection, several Cyp knockout THP-1 cell lines were generated using CRISPR/Cas9. THP-1 cells are human monocytic suspension cells, derived from peripheral blood of a one-year-old infant male with acute monocytic leukemia. They are used as an easy accessible cell model for human monocytes and macrophages [317]. Except CypA -/- cells, all knockout cell lines were generated in the course of this study. For all experiments several single cell clones have been tested and at least two individual experiments for one representative clone are shown in all presented experiments.

8.1.1 CypA modulates HIV-1 infectivity

CypA has been thoroughly investigated as a co-factor for HIV-1 infection. However, its role in type I IFN-mediated innate immunity against HIV-1 infection is not well understood. Therefore, we used CypA knockout (CypA -/-) THP-1 cells to investigate the response to IFNα2.

Figure 9: Validation of CRISPR/Cas9 CypA knockout cell line.

A: THP-1 parental cells (THP-1 wt) and a THP-1 based CypA knockout cell line (CypA -/-) were analyzed by Western blot for CypA or β-actin expression. **B:** PCR amplification of the CypA gene from genomic DNA of THP-1 wt and CypA -/- cells revealed disruption of the CypA gene in CypA -/- cells. Data was analyzed by ICE analysis from synthego.com as well as with DNADynamo.

CypA -/- single cell clones were generated previously [209]. However, full evaluation of the knockout clones was missing. Therefore, gene disruption was validated by immunoblotting and sequencing across the gRNA target site. To this end, genomic DNA was isolated and the CypA gene was amplified by PCR. The product was purified and sent for sequencing. Sequencing results were analyzed with the ICE tool from synthego.com and DNADynamo.
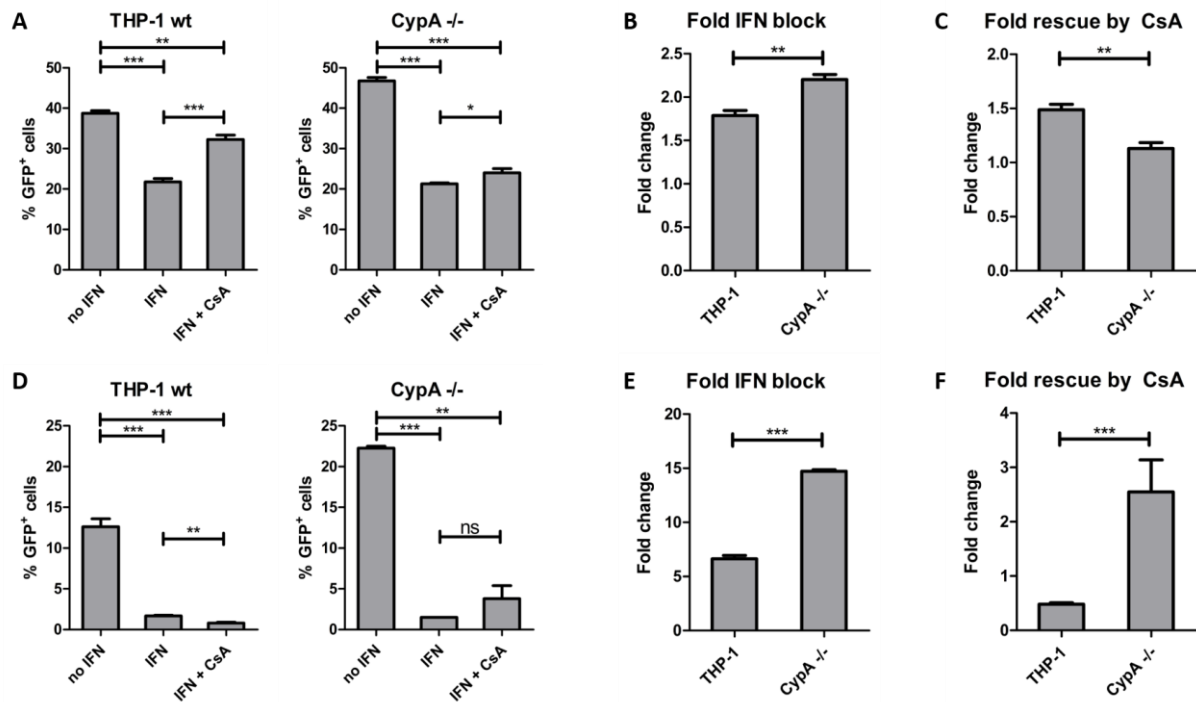

Figure 10: Cyclophilin A (CypA) knockout THP-1 cells show hypersensitivity to the type I IFN-induced block of HIV-1infection.

A: THP-1 wt cells or CypA -/- cells were treated or not with 500 U/ml IFNα2. 24 h post IFN stimulation cells were treated with 2.5 μM CsA. At the time of CsA addition, cells were infected with VSV-G pseudotyped HIV-1 8.91 GFP reporter lentiviral vector (HIV-1 LV) for 48 h. Percentage of GFP positive cells was determined by flow cytometry. Bars indicate the average infectivity determined from three independent experiments and error bars indicate standard deviation. Unpaired two-tailed t test was performed (*, p< 0.05; **, p< 0.01; ***, p< 0.001). **B:** Calculated fold changes of IFNα2 induced block to HIV-1 LV infection. Bars indicate the average fold changes and error bars indicate standard deviation. Unpaired two-tailed t test was performed (**, p< 0.01). **C:** Calculated fold changes of the rescue from the IFN-induced block to HIV-1 LV infection by CsA. Bars indicate the average fold changes and error bars indicate standard deviation. Unpaired two-tailed t test was performed (**, p< 0.01). **D:** THP-1 wt cells or CypA -/- cells were treated or not with 500 U/ml IFNα2. 24 h post IFN stimulation cells were treated with 2.5 μM CsA. At the time of CsA addition, cells were infected with VSV-G pseudotyped HIV-1 NL4.3 GFP reporter virus (NL4.3) for 48 h. Percentage of GFP positive cells was determined by flow cytometry. Bars indicate the average infectivity determined from at least three independent experiments and error bars indicate standard deviation. Unpaired two-tailed t test was performed (**, p< 0.01; ***, p< 0.001; ns, not significant). **E:** Calculated fold changes of IFNα2 induced block to NL4.3 infection. Bars indicate the average fold changes and error bars indicate standard deviation. Unpaired two-tailed t test was performed (***, p< 0.001). **F:** Calculated fold changes of the rescue from the IFN-induced block to NL4.3 infection by CsA. Bars indicate the average fold changes and error bars indicate standard deviation. Unpaired two-tailed t test was performed (***, p< 0.001).

Alignment of wt and knockout sequences revealed an eight-nucleotide deletion in the first exon of the CypA gene (Figure 9B). The induced frameshift destroyed the first splicing site and generated an early stop codon preventing full-length protein expression. This can be seen on the Western blot in Figure 9A. An anti-CypA antibody, produced with full CypA protein as

immunogen, was used to detect cellular CypA protein (7.1.11). Immunoblotting against β-actin served as a loading control for THP-1 parental and knockout cells. Next, the involvement of CypA on HIV-1 infection in THP-1 cells was investigated. Therefore, THP-1 wt cells and CypA -/- cells were challenged with equal doses of (i) VSV-G pseudotyped HIV-1 GFP lentiviral vector (HIV-1 LV) or (ii) VSV-G pseudotyped HIV-1 full-length NL4.3 GFP virus (NL4.3). Pseudotyping with VSV-G was necessary, as THP-1 cells do not express sufficient CD4 and the corresponding co-receptors for either CXCR4 or CCR5 HIV-1 strains. Thus, detectable infection with natural HIV-1 Env proteins was not achieved. The used LV reporter virus lacks all HIV-1 accessory proteins and therefore, served as a reduced and easier model of HIV-1 infection. However, HIV-1 accessory proteins play essential roles during immune evasion. Therefore, the NL4.3 full-length virus was investigated as well, in particular since some accessory proteins have been associated with CypA [318]–[320]. To provide better comparison between the two used HIV-1 constructs (i) HIV-1 LV and (ii) NL4.3, equal viral doses measured in RT activity (see 7.3.2) were used for all infection assays. Infected cells were identified as GFP positive cells 48 h post viral infection by FACS analysis and percentages of GFP-positive cells were determined.

To exclude general effects of the knockout procedure a previously generated CRISPR/Cas9 control cell line (Ctr) utilizing a non-targeting gRNA [209] was infected in parallel to THP-1 parental and THP-1 CypA -/- cells. This cell line was generated along with the used CypA -/- cell line. Likewise, for every other cell line produced in this study a corresponding CRISPR/Cas9 control cell line was generated, using the same non-targeting gRNA used for the Ctr cell line shown in Figure 11. For all Ctr cell lines, no changes in infectivity compared to the corresponding THP-1 wt cell lines were observed (data not shown). In Figure 11A one exemplary dataset is shown. CypA -/- increased the permissivity of cells to HIV-1 LV and HIV-1 NL4.3 infection. THP-1 parental cells showed 38.8 % HIV-1 LV and 12.6 % NL4.3 infection, whereas Cyp A -/- cells showed 46.8 % HIV-1 LV infection and 22.3 % NL4.3 infection (Figure 10A and D), indicating a role for CypA in cellular immunity against HIV-1 infection in THP-1 cells. To investigate whether this is related to the type I IFN response, cells were treated with 500 U IFNα2 24 h prior to infection. Infection was significantly reduced in THP-1 wt and CypA -/- cells for both viral constructs (Figure 10A and D). However, the block of infection by type I IFN was explicitly stronger in NL4.3 infection for both cell lines. For THP-1 wt cells a 1.8-fold IFN-induced block to HIV-1 LV infection was observed and full-length HIV-1 infection was reduced by 6.6-fold. There was a significantly enhanced blocking effect for CypA

-/- cells (Figure 10B and E). For NL4.3 infection a reduction in infectivity upon IFN treatment of 14.7-fold was monitored for CypA -/- cells.
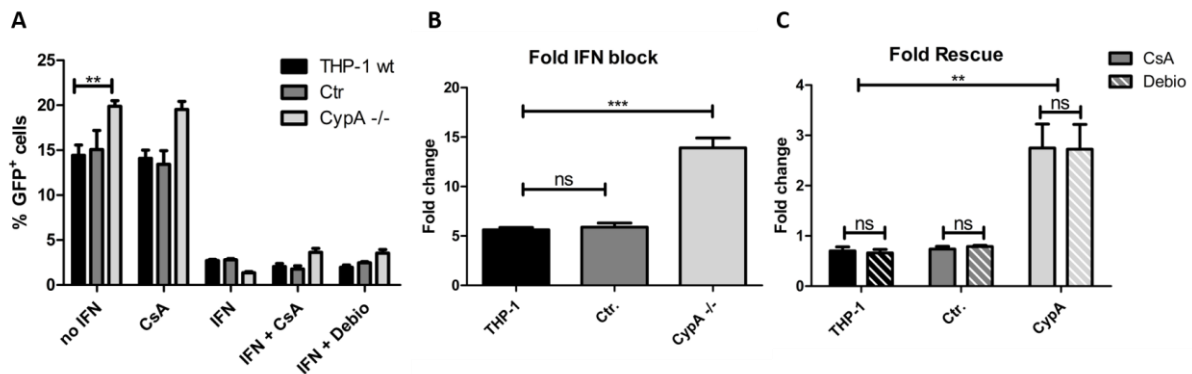

Figure 11: Effects of CsA are independent of its immunosuppressive role.

A: THP-1 wt cells, CRISPR/Cas9 control cells (Ctr) or CypA -/- cells were treated or not with 500 U/ml IFNα2. 24 h post IFN stimulation cells were treated with 2.5 µM CsA or 2.5 µM Debio-025 (Debio). At the time of CsA/Debio addition, cells were infected with VSV-G pseudotyped NL4.3 for 48 h. Percentage of GFP positive cells was determined by flow cytometry. Bars indicate the average infectivity determined from two independent experiments and error bars indicate standard deviation. Unpaired two-tailed t test was performed (**, p< 0.01). **B:** Calculated fold changes of IFNα2 induced block to HIV-1 NL4.3 infection. Bars indicate the average fold changes and error bars indicate standard deviation. Unpaired two-tailed t test was performed (***, p< 0.001; ns, not significant).**C:** Calculated fold rescue of the IFN-induced block to NL4.3 infection by CsA or Debio, respectively. Bars indicate the average fold changes and error bars indicate standard deviation. Unpaired two-tailed t test was performed (**, p< 0.01; ns, not significant).

To confirm the involvement of CypA in the type I IFN-induced block of HIV-1 infection, cells were treated at the time of HIV-1 LV or NL4.3 challenge with CsA, an inhibitor that targets Cyclophilins, however its main cellular target is believed to be CypA [127], [321]. CsA treatment without previous IFN stimulation had no effect on any investigated cell line, as can be seen for THP-1 parental, CRISPR/Cas Ctr cells and CypA -/- cells in Figure 11 (compare no IFN and CsA columns). In THP-1 wt cells CsA treatment could increase HIV-1 LV infection from the type I IFN-induced block by a factor of 1.5-fold (Figure 10C). This indicates a protective role of CypA against IFN induced cellular restriction factors, as inhibiting CypA increased HIV-1 LV infection. Indeed, in CypA -/- cells this rescue ability was significantly reduced (Figure 10C). For HIV-1 NL4.3 the response to CsA treatment was quite different. In THP-1 wt cells CsA treatment resulted in a further reduction of infection. With IFN stimulation 1.7 % infected cells could be detected, whereas additional CsA stimulation resulted in 0.8 % infected cells (Figure 10D). Given that CypA is the main cellular target for CsA, CsA treatment of CypA knockout cells should not affect HIV-1 infection of CypA -/- cells. However, in CypA -/- cells a rescue from the type I IFN-induced HIV-1 infection block upon CsA treatment of 2.6-fold was observed (Figure 10F). These results reveal differences between the two used viral constructs and a possible involvement of HIV-1 accessory proteins. Furthermore, these results confirm a role of CypA in protecting HIV-1 from type I IFN-induced host restriction factors

and moreover suggest another CsA target aside from CypA being involved in protecting HIV-1 from IFN induced restriction factors.

To exclude a contribution of the immunosuppressive function of CsA, a non-immunosuppressive analogue of CsA, Debio-025 was used in the infection assays. THP-1 wt cells, THP-1 Ctr and CypA -/- cells were stimulated with IFNα2 as previously described (7.3.4). Cells were then treated with either CsA or Debio-025 followed by HIV-1 NL4.3 infection. No difference between CsA or Debio-025 treatment was observed for any investigated cell line (Figure 11), which is in agreement with the literature [199]. These findings exclude an impact of the immunosuppressive role of CsA on the type I IFN-induced block to HIV-1 infection and support the hypothesis, that an additional CsA target aside from CypA is involved in HIV-1 infection.

8.1.2 Knockouts of CypB, CypC or CypD in THP-1 cells do not influence the type I IFN-induced block to HIV-1 infection

Further, the influence of additional members of the cyclophilin family on the type I IFN-induced block of HIV-1 infection was investigated. To this end, CRISPR/Cas9 knockout cell lines of CypB, CypC, CypD, CypE and CypH were generated. Respective gRNA encoding DNA sequences (listed in 7.1.9) were cloned into plentiCRISPRv2 vector and the vector RNA was packaged into lentiviral vectors (described in 7.2.6). If possible, gRNAs targeted the first exon of the respective protein. This ensures the introduction of early frame shifts upon CRISPR/Cas9 editing and avoids the production of partly functional shorter protein versions. THP-1 target cells were transduced with the respective lentiviral constructs and after puromycin selection single cell clones of CypX -/- cells were generated.

For CypB -/- cells, the knockout was validated by Western blot. An exemplary blot is shown in Figure 12A. The gRNA used (SB3/SB4; 7.1.9) targeted CypB within the first 15 amino acids, thus the epitope of the used antibody is C-terminal of the CRISPR/Cas9 editing site, making it unlikely that a destroyed epitope is responsible for the absent CypB band in the presented immunoblot analysis of the tested knockout cells (Figure 12A). Further validation through sequencing failed due to the lack of suitable primer sets. Although several different primer pairs for shorter and longer amplification products were tested, no specific PCR product could be obtained. Changing the polymerase, varying annealing temperatures and DMSO concentrations as well as switching to a high GC-content DNA optimized buffer and testing several gDNA samples was likewise unsuccessful.

Upon infection with HIV-1 LV (Figure 12B) CypB knockout cells showed 27.5 % infection, whereas for THP-1 wt cells 38.8 % infection was detected. However, a reduced permissivity to

HIV-1 NL4.3 for CypB -/- cells compared to THP-1 parental cells could not be observed. In fact, for CypB -/- cells 16.7 % GFP positive cells could be obtained whereas THP-1 wt cells showed an infection of 12.6 % (Figure 12E).
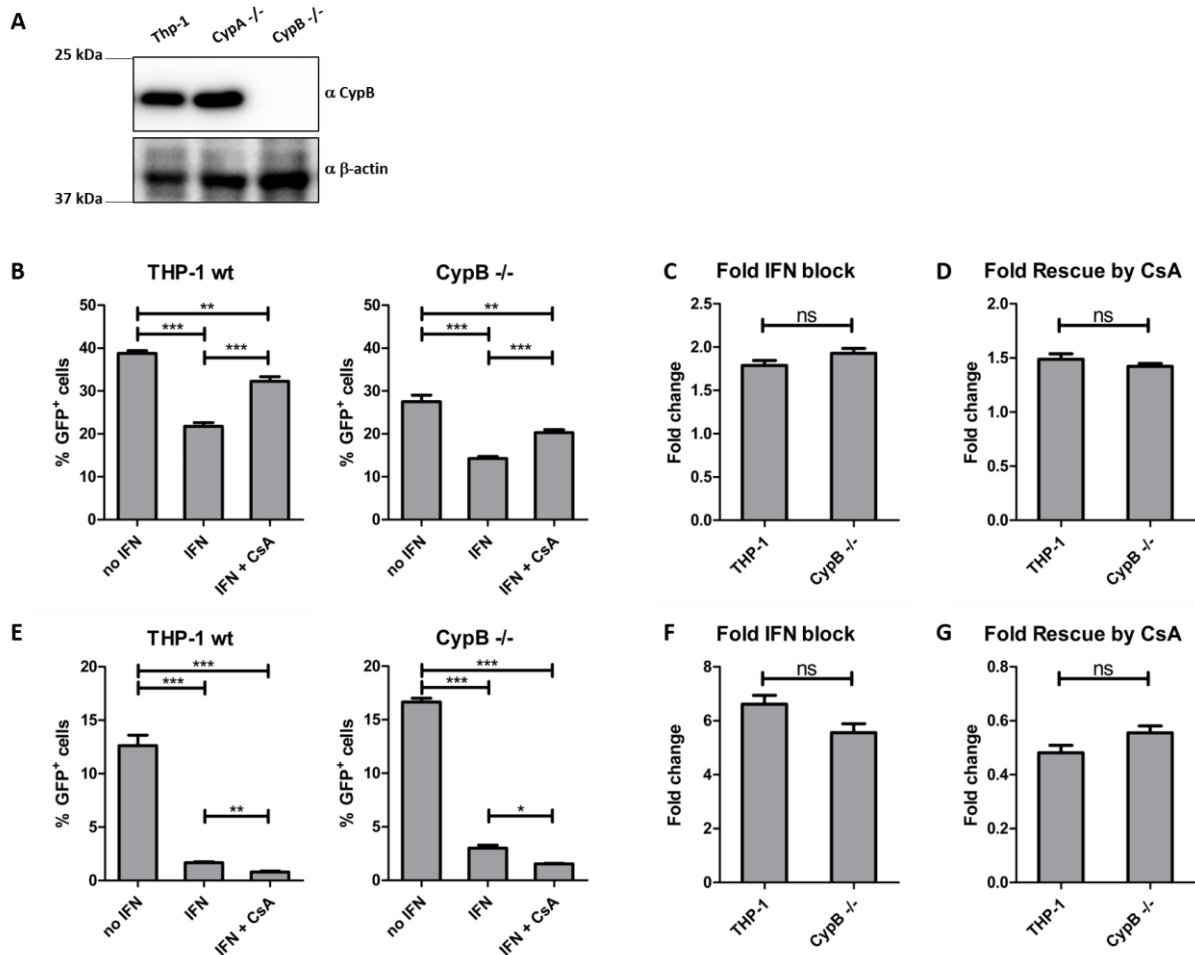

Figure 12: Cyclophilin B knockout does not influence the IFN-induced block to HIV-1 infection or its rescue by CsA.
A: THP-1 wt, CypA -/- and THP-1 based Cyclophilin B knockout cell lines (CypB -/-) were analyzed by Western blot for CypB or β-actin expression. **B:** THP-1 wt cells or CypB -/- cells were treated or not with 500 U/ml IFNα2. 24 h post IFN stimulation cells were treated with 2.5 µM CsA. At the time of CsA addition, cells were infected with VSV-G pseudotyped HIV-1 LV for 48 h. Percentage of GFP-positive cells was determined by flow cytometry. Bars indicate the average infectivity determined from three independent experiments and error bars indicate standard deviation. Unpaired two-tailed t test was performed (**, $p < 0.01$; ***, $p < 0.001$). **C:** Calculated fold changes of IFNα2 induced block to HIV-1 LV infection. Bars represent the average fold changes and error bars indicate standard deviation. Unpaired two-tailed t test was performed (ns, not significant). **D:** Calculated fold changes of the rescue from the IFN-induced block to HIV-1 LV infection by CsA. Bars represent the average fold changes and error bars indicate standard deviation. Unpaired two-tailed t test was performed (ns, not significant). **E:** THP-1 wt cells or CypB -/- cells were treated or not with 500 U/ml IFNα2. 24 h post IFN stimulation cells were treated with 2.5 µM CsA. At the time of CsA addition, cells were infected with VSV-G pseudotyped NL4.3 for 48 h. Percentage of GFP positive cells was determined by flow cytometry. Bars represent the average infectivity determined from at least three independent experiments and error bars indicate standard deviation. Unpaired two-tailed t test was performed (*, $p < 0.05$; **, $p < 0.01$; ***, $p < 0.001$). **F:** Calculated fold changes of IFNα2 induced block to NL4.3 infection. Bars indicate the average fold changes and error bars show standard deviation. Unpaired two-tailed t test was performed (ns, not significant). **G:** Calculated fold changes of the rescue from the IFN-induced block to NL4.3 infection by CsA. Bars indicate the average fold changes and error bars indicate standard deviation. Unpaired two-tailed t test was performed (ns, not significant).

Yet, IFNα2 and CsA treatment showed the same effect in CypB -/- cells than for THP-1 wt cells, independently of the virus construct used (Figure 12C, D, F and G). This indicates no function of CypB in the type I IFN-induced block of HIV-1 infection or the rescue phenotype observed in CypA -/- cells upon CsA treatment (Figure 10). Next, CypC was examined. Analogous to the analysis performed for CypB, knockout validation was limited to Western blot analysis (Figure 13A). Based on the protein size of CypC, the lowest band observed for THP-1 wt cells using an anti-CypC antibody was the corresponding CypC band. This band was absent for CypC -/- cells suggesting a successful CypC knockout in these cells. Given that the gRNA used (SB5/SB6; 7.1.9) targeted the first exon of CypC, it is unlikely, that only the epitope of the antibody in the second exon is destroyed and thus responsible for the missing signal in the CypC knockout cells.
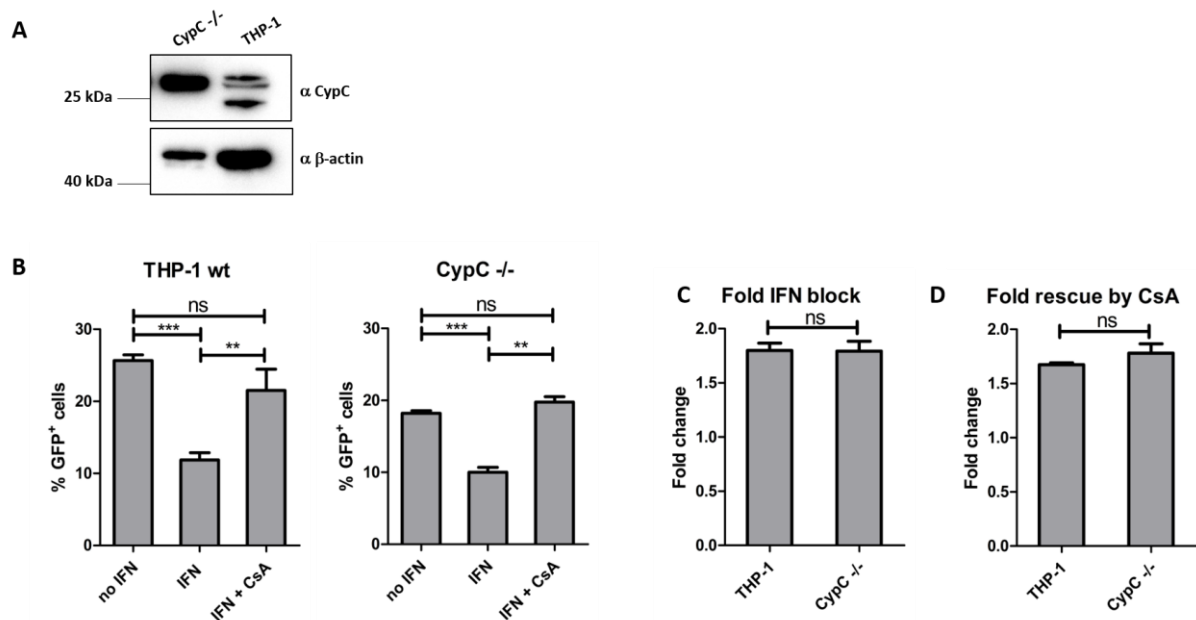

Figure 13: Cyclophilin C does not influence the IFNα2 induced block to HIV-1 infection.

A: THP-1 wt and THP-1 based Cyclophilin C knockout cell lines (CypC -/-) were analyzed by Western blot for CypC and β-actin expression. **B:** THP-1 wt cells or CypC -/- cells were treated or not with 500 U/ml IFNα2. 24 h post IFN stimulation cells were treated with 2.5 μM CsA. At the time of CsA addition, cells were infected with VSV-G pseudotyped HIV-1 LV for 48 h. Percentage of GFP positive cells was determined by flow cytometry. Bars indicate the average infectivity determined from three independent experiments and error bars represent standard deviation. Unpaired two-tailed t test was performed (**, p< 0.01; ***, p< 0.001; ns, not significant). **C:** Calculated fold changes of IFNα2 induced block to HIV-1 LV infection. Bars indicate the average fold changes determined from three independent experiments and error bars indicate standard deviation. Unpaired two-tailed t test was performed (ns, not significant). **D:** Calculated fold changes of the rescue from the IFN-induced block to HIV-1 LV infection by CsA. Bars indicate the average fold changes and error bars indicate standard deviation. Unpaired two-tailed t test was performed (ns, not significant).

HIV-1 LV infection of CypC -/- cells showed a phenotype similar to CypB -/- cells. Infection of CypC -/- cells was reduced compared to THP-1 parental cells (18.2 % and 25.7 %, respectively, Figure 13B). Indeed, the response of CypC -/- cells to IFNα2 and CsA stimulation

showed no significant changes compared to THP-1 wt cells as seen for CypB -/- cells (Figure 13 B - D).

After CypB and CypC have been tested and are most likely not the searched for CsA target responsible for the CsA induced effects observed in CypA -/- cells (Figure 10), CypD was evaluated as the responsible CsA target. CRISPR/Cas9 CypD knockouts were generated as described above (7.3.3). Sequencing of one exemplary cell clone revealed a heterozygous knockout phenotype. One allele of CypD shows a deletion of 17 nucleotides and the second one a deletion of 29 nucleotides as shown in Figure 14B. Both deletions resulted in frameshifts of the CypD ORF and generated premature stop codons. Therefore, synthesis/translation of full-length CypD failed in both cases. This was confirmed by Western blot analysis (Figure 14A). The used anti-CypD antibody targeted an epitope within the amino acids 356 and 370 of human CypD protein. The gRNA used (SB7/SB8; 7.1.9) targeted the amino acids 15 to 22, thus the antibody binds C-terminal of the CRISPR/Cas9 editing site and a destroyed antibody epitope is unlikely for the missing CypD protein band in immunoblot analysis (Figure 14A).
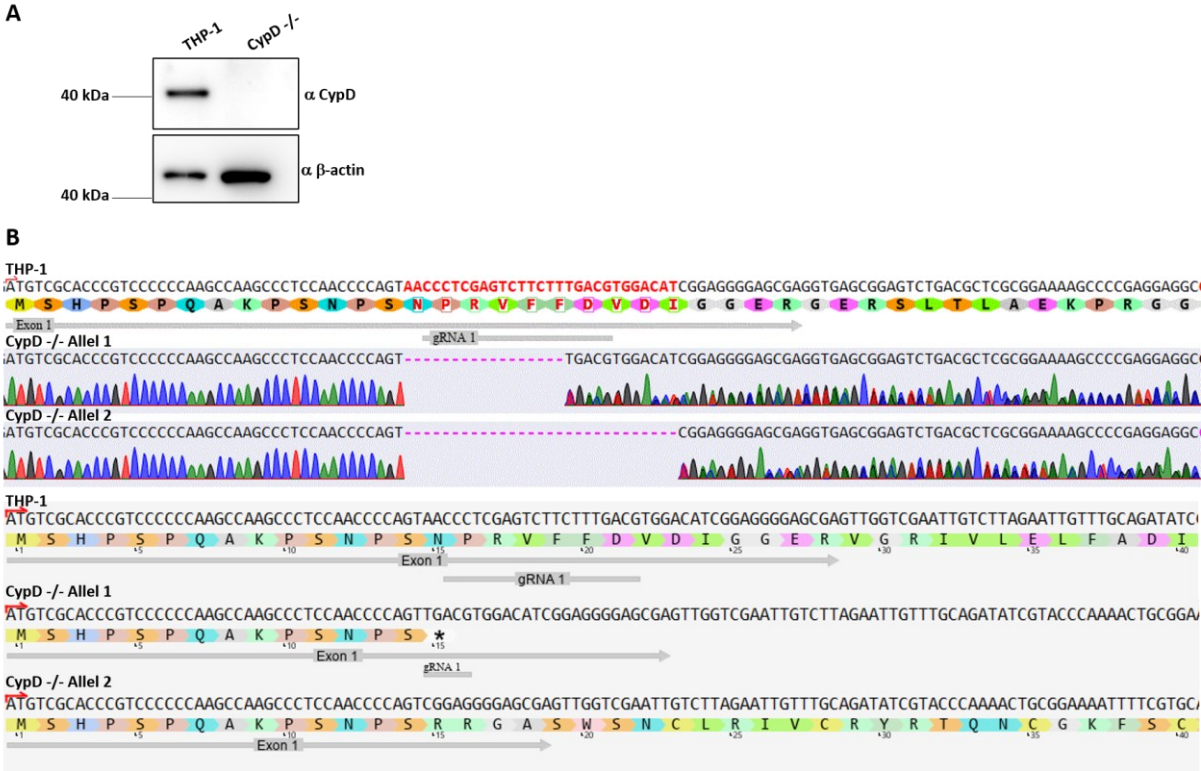
Figure 14: Validation of CRISPR/Cas9 Cyclophilin D knockouts (CypD -/-) in THP-1 cells.

A: THP-1 wt and a THP-1 based CypD knockout cell line (CypD -/-) were analyzed by Western blot for CypD or β-actin expression. **B:** PCR amplification of the CypD gene from genomic DNA of THP-1 wt and CypD -/- cells revealed the disruption of the CypD gene in CypD -/- cells. Analysis was performed with the ICE tool from synthego.com and DNADynamo.

Like CypB and CypC knockout cells, CypD -/- and THP-1 wt cells were challenged with HIV-1 LV with equal viral doses. Comparison of CypD -/- cells with THP-1 parental cells revealed

an elevated infection rate for CypD -/- cells (38.8% for THP-1 wt and 47% for CypD -/- cells; Figure 15A), indicating an involvement of CypD in HIV-1 infection. Roughly the same increase in infection was observed for CypA -/- cells (Figure 10A). However, the response to IFNα2 stimulation revealed no involvement of CypD in the type I IFN-induced block to HIV-1 LV infection (Figure 15B). Furthermore, CypD is presumably not the CsA target responsible for the rescue phenotype observed for CypA -/- cells, as no significant changes were observed between CypD -/- cells and THP-1 wt cells in response to CsA (Figure 15C).
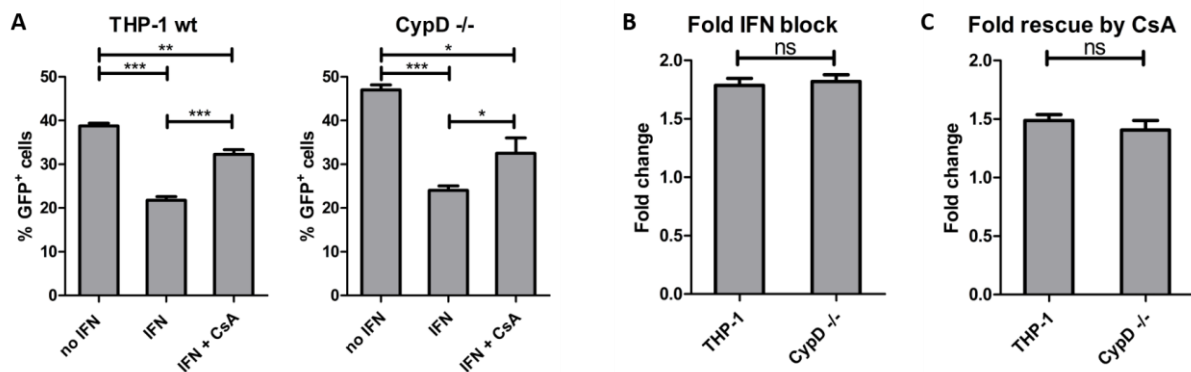
Figure 15: CypD is not involved in the type I IFN-induced block to HIV-1 infection.

A: THP-1 wt or CypD -/- cells were treated or not with 500 U/ml IFNα2. 24 h post IFN stimulation cells were treated with 2.5 μM CsA. At the time of CsA addition, cells were infected with VSV-G pseudotyped HIV-1 LV for 48 h. Percentage of GFP positive cells was determined by flow cytometry. Bars indicate the average infectivity determined from three independent experiments and error bars represent standard deviation. Unpaired two-tailed t test was performed (*, $p < 0.05$; **, $p < 0.01$; ***, $p < 0.001$). **B:** Calculated fold changes of IFNα2 induced block to HIV-1 LV infection. Bars represent the average fold change and error bars indicate standard deviation. Unpaired two-tailed t test was performed (ns, not significant). **C:** Calculated fold changes of the rescue from the IFN-induced block to HIV-1 LV infection by CsA. Bars indicate the average fold changes and error bars indicate standard deviation. Unpaired two-tailed t test was performed (ns, not significant).

8.1.3 CypE -/- cells show reduced infectivity and hypersensitivity to type I IFN-induced block of HIV-1 infection

CRISPR/Cas9 mediated CypE knockout in THP-1 cells was successfully achieved. Sequencing of the corresponding cell clone revealed an insertion of one nucleotide resulting in a frameshift and the generation of an early stop codon (Figure 16B). This result was confirmed by immunoblot analysis (Figure 16A). CypE expression was only observed for THP-1 wt but not for CypE -/- cells, whereas β-actin expression was not altered in CypE -/- cells. The gRNA against human CypE protein used targeted the protein within the first 10 amino acids (SB9/SB10; 7.1.9) and the used CypE antibody was generated using a recombinant fragment corresponding to the region within amino acids 1 to 249 of human CypE. Despite the overlap between the CRISPR/Cas9 editing site and the used immunogen used for antibody production, it is unlikely that a destroyed epitope is responsible for the different band pattern observed for CypE -/- and THP-1 parental cells in Western blot analysis (Figure 16A).

To investigate whether CypE is involved in HIV-1 infection, CypE -/- cells were infected with VSV-G pseudotyped HIV-1 GFP LV or HIV-1 NL4.3 GFP as described above (7.3.4).


Figure 16:Validation of CRISPR/Cas9 CypE knockout (CypE -/-) in THP-1 cells.

A: THP-1 wt and a THP-1 based CypE -/- were analyzed by Western blot for CypE β-actin expression. **B:** PCR amplification of the CypE gene from genomic DNA of THP-1 wt and CypE -/- cells revealed disruption of the CypE gene in CypE -/- cells. Analysis was performed with the ICE tool from synthego.com and DNADynamo.

HIV-1 LV infected CypE -/- cells showed a reduced infection by 10 % to 15.8 % compared to what was observed for THP-1 wt cells (25.7 %) (Figure 17A). A similar phenotype was observed for CypB and CypC knockout cells (Figure 12B and Figure 13B, respectively). The type I IFN-induced block of HIV-1 LV infection was significantly increased to 2.6-fold in CypE -/- cells compared to THP-1 parental cells (1.8-fold; Figure 17B). Interestingly, IFNα2 had a greater effect in CypE -/- cells than observed for CypA -/- cells (2.2-fold infection block; Figure 10B), indicating an involvement of CypE in the type I IFN response to HIV-1 infection. CsA treatment of CypE -/- cells resulted in a rescue of the IFN-induced block to HIV-1 LV infection up to infection rates observed without IFN treatment (Figure 17C, 15.8 % without treatment, 16.8 % with IFN and CsA stimulation). This suggests the complete inhibition of the type I IFN-induced CsA sensitive factor in CypE -/- cells. Thus, it is unlikely that this factor is CypE. However, reduced HIV-1 infection of CypE -/- cells suggests a contribution of CypE to HIV-1 infection.

To confirm these results in a more relevant context, CypE -/- cells were infected with the HIV-1 full-length virus NL4.3 (Figure 17D). Again, infection was reduced in CypE -/- cells compared to THP-1 parental cells (12.6 % for THP-1 wt and 9.8% for CypE -/- cells; Figure 17D). As shown for all used knockout cell lines, the capacity of IFNα2 to block HIV-1 infection

was intensified for HIV-1 NL4.3 compared to HIV-1 LV infection (compare Figure 17B and E). Although the capacity of IFNα2 to block NL4.3 infection was not significantly changed between THP-1 wt and CypE -/- cells, a tendency of increased sensitivity in CypE -/- cells can be observed (6.6-fold compared to 7.2-fold; Figure 17E). For HIV-1 LV infection a significantly increased block of infection in CypE -/- cells was detected (1.8-fold for THP-1 and 2.6-fold for CypE -/- cells; Figure 17B). This argues for HIV-1 accessory proteins possibly playing a role in impeding IFN-induced antiviral mechanisms during HIV-1infection and highlights the complexity of the Cyclophilin-IFN interplay.
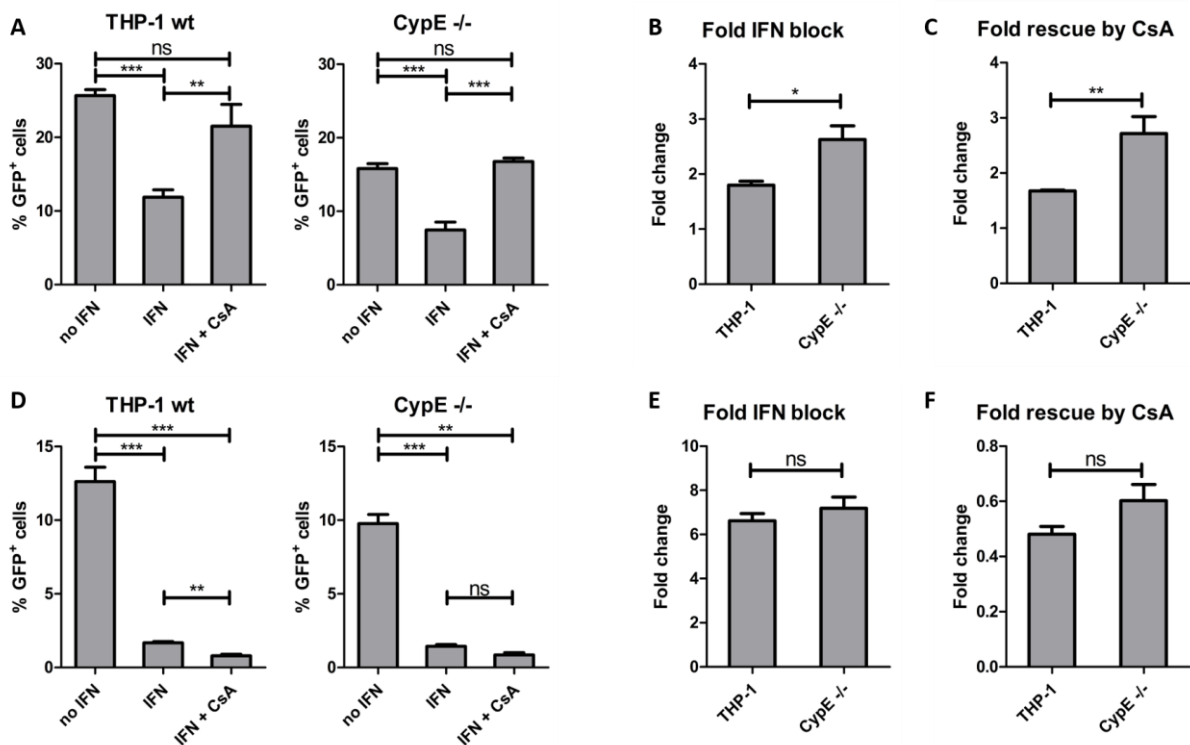

Figure 17: CypE -/- show reduced infectivity of HIV-1 and hypersensitivity to CsA.

A: THP-1 wt or CypE -/- cells were treated or not with 500 U/ml IFNα2. 24 h post IFN stimulation cells were treated with 2.5 µM CsA. At the time of CsA addition, cells were infected with VSV-G pseudotyped HIV-1 LV for 48 h. Percentage of GFP positive cells was determined by flow cytometry. Bars represent the average infectivity determined from three independent experiments and error bars indicate standard deviation. Unpaired two-tailed t test was performed (**, $p< 0.01$; ***, $p< 0.001$, ns, not significant). **B:** Calculated fold changes of IFNα2 induced block to HIV-1 LV infection. Bars indicate the average fold change and error bars represent standard deviation. Unpaired two-tailed t test was performed (*, $p< 0.05$). **C:** Calculated fold changes of the rescue from the IFN-induced block to HIV-1 LV infection by CsA. Bars indicate the average fold changes and error bars indicate standard deviation. Unpaired two-tailed t test was performed (**, $p< 0.01$). **D:** THP-1 wt cells or CypE -/- cells were treated or not with 500 U/ml IFNα2. 24 h post IFN stimulation cells were treated with 2.5 µM CsA. At the time of CsA addition, cells were infected with VSV-G pseudotyped NL4.3 for 48 h. Percentage of GFP positive cells was determined by flow cytometry. Bars indicate the average infectivity determined from three independent experiments and error bars indicate standard deviation. Unpaired two-tailed t test was performed (**, $p< 0.01$; ***, $p< 0.001$; ns, not significant). **E:** Calculated fold changes of IFNα2 induced block to HIV-1 NL4.3 infection. Bars represent the average fold change and error bars indicate standard deviation. Unpaired two-tailed t test was performed (ns, not significant). **F:** Calculated fold changes of the rescue from the IFN-induced block to HIV-1 NL4.3 infection by CsA. Bars indicate the average fold changes and error bars indicate standard deviation. Unpaired two-tailed t test was performed (ns, not significant).

To better understand the individual roles of Cyps on HIV-1 infection, knockouts of CypF and CypG in THP-1 cells were carried out. CRISPR/Cas9 lentivectors with gRNAs targeting CypF (SB45/SB46; 7.1.9) or CypG (SB47/SB48; 7.1.9), respectively, were cloned as described previously (7.2.6). Unfortunately, a CypF specific antibody was not available due to frequent unspecific cross-reactions with the similar CypA protein. This is not unsurprising, as CypF has the highest similarity of all Cyps with CypA and the immunogen used for CypF antibody production was a recombinant fragment within amino acids 21 and 207 of human CypF, which is almost the complete protein. As knockout clone pre-screening by Western blot was unsuccessful, validation of possible knockout clones via sequencing could be tried in future studies. Validation of CypG knockout cells was likewise unsuccessful. The tested CypG antibody directed towards the C-terminal region of human CypG produced no signal in diverse cell lines for all tested conditions. Thus, like for CypF, a pre-screening of possible CypG knockout cells by Western blot was not possible and a sequencing approach could be tried in future studies. With lacking information about the knockout status of the produced single cell clones, no further experiments using CypF and CypG knockout cells were conducted. However, these are interesting candidates as mentioned below (9.2) and should be investigated in future studies.

8.1.4 Knockout of CypH has no effect on HIV-1 infection

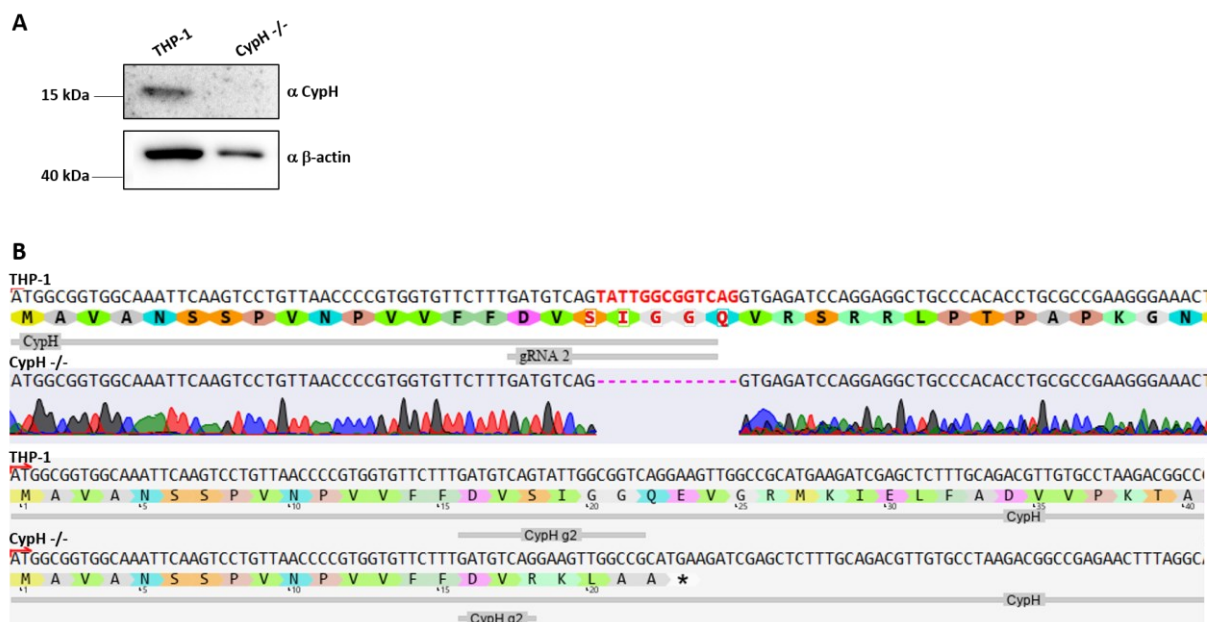**Figure 18: Validation of CRISPR/Cas9 CypH knockout (CypH -/-) in THP-1 cells.**

A: THP-1 wt and THP-1 based CypH -/- cells were analyzed by Western blot for CypH or β-actin expression. **B:** PCR amplification of the CypH gene from genomic DNA of THP-1 wt and CypH -/- cells revealed disruption of the CypH gene in CypH -/- cells. Analysis was performed with the ICE tool from synthego.com and DNADynamo.

The generation of CypH knockout in THP-1 cells was successfully validated via Western blot and sequencing analysis (Figure 18). The gRNA used binds between amino acids 16 and 22 of human CypH (SB12/SB13; 7.1.9) and the antibody used for detection was produced by taking the full CypH protein as an immunogen. Thus, no information on the exact antibody epitope was available and the missing protein band observed for CypH -/- cells could be due to an destroyed epitope and not due to successful CRISPR/Cas9 editing (Figure 18A).

However, the knockout was confirmed by sequencing. A 13 nt deletion within the first exon coding for CypH was found. In-depth sequence analysis revealed a frame shift leading to the generation of an early stop codon within exon one and thus, an incomplete translation (Figure 18B). Therefore, CypH detection by immunoblot analysis was impossible in CypH -/- cells. To investigate the role of CypH in HIV-1 infection, CypH -/- cells were infected with HIV-1 LV. As can be seen in Figure 19A, CypH knockout did not influence HIV-1 infection. The same percentage of GFP positive cells could be obtained for CypH -/- cells as for THP-1 parental cells. Although the comparison of the type I IFN-induced infection block was significant as shown in Figure 19B, the observed values are similar (1.8-fold for THP-1 wt cells and 2.1-fold for CypH -/- cells), suggesting no involvement of CypH in the type I IFN-mediated block to HIV-1 infection. CsA treatment increased HIV-1 infection of IFN stimulated CypH -/- cells to a similar extend than THP-1 parental cells, thus no significant changes between wt and knockout could be observed. eased infection rates. Therefore, it is unlikely, that CypH is the responsible CsA target.
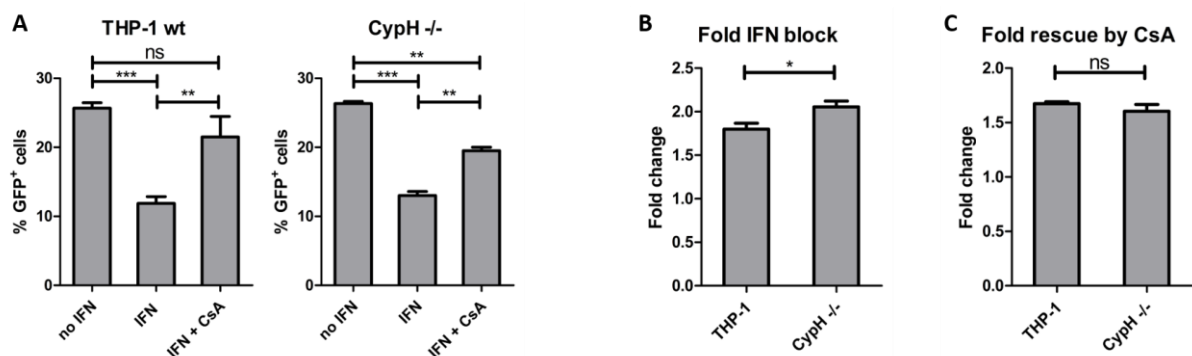
Figure 19: CypH -/- cells show hypersensitivity to the IFNα2 induced infection block.

A: THP-1 wt or CypH -/- cells were treated or not with 500 U/ml IFNα2. 24 h post IFN stimulation cells were treated with 2.5 µM CsA. At the time of CsA addition, cells were infected with VSV-G pseudotyped HIV-1 LV for 48 h. Percentage of GFP positive cells was determined by flow cytometry. Bars indicate the average infectivity determined from three independent experiments and error bars indicate standard deviation. Unpaired two-tailed t test was performed (**, $p < 0.01$; ***, $p < 0.001$, ns, not significant). **B:** Calculated fold changes of IFNα2 induced block to HIV-1 LV infection. Bars indicate the average fold change and error bars indicate standard deviation. Unpaired two-tailed t test was performed (*, $p < 0.05$). **C:** Calculated fold changes of the rescue from the IFN-induced block to HIV-1 LV infection by CsA. Bars indicate the average fold changes and error bars indicate standard deviation. Unpaired two-tailed t test was performed (ns; not significant).

8.1.5 CypA-CypB -/- results in a hypersensitive IFN-induced block of HIV-1 infection

Cyclophilins share a high sequence similarity due to the conserved cyclophilin core domain. Although investigated in diverse research fields, a clear distinction on functions for single Cyps remains elusive. To shed some light on redundancy within Cyps, double knockout cell lines based on the used CypA -/- cell line were generated. In Figure 20A the Western blot analysis of CypA-CypB -/- double cell clones can be seen. For Western blot analysis the antibodies described above were used (8.1.1 and 8.1.2), thus antibody epitopes were C-terminal from the respective CRISPR/Cas9 editing positions. Parental THP-1 wt cells expressed CypA and CypB. CypA -/- cells showed only CypB expression as well as a CRISPR/Cas9 double knockout control cell line based on CypA -/- cells (CRISPR Ctr). Interestingly, CypB expression levels were not changed in CypA -/- cells compared to THP-1 wt or Ctr cells, which were generated in parallel to the double knockout cells using a non-targeting gRNA (SB23/Sb24; 7.1.9). CypB single knockout cells showed only CypA expression in comparable amounts to THP-1 wt cells. The generated CypA-CypB -/- cell bulk after blasticidin selection already showed a strong reduction in CypB expression levels and indeed single cell clones that were negative for CypA and CypB expression could be obtained. Unfortunately sequencing of this double knockout cell line was not possible due to the reasons mentioned for the CypB single knockout cell line (8.1.2).

Next, the influence of the double knockout on HIV-1 infection was investigated. In Figure 20B a comparison of HIV-1 LV infected THP-1 wt, CypA -/- and CypA-CypB -/- cells is shown. Whereas CypA -/- cells showed an increase in infection from 38.8 % to 46.8 % compared to THP-1 parental cells, a slight reduction of infection to 35.5 % was observed for the double knockout cell line compared to THP-1 wt cells. However, CypB single knockout cells showed only 27.5 % HIV-1 LV infection (Figure 12B). Therefore, the changes in infection might be explained by the contribution of the other Cyp, respectively. However, the response to IFNα2 and CsA of CypA-CypB -/- cells in HIV-1 LV infection was comparable to CypA -/- cells. CypA single knockout and CypA-CypB double knockouts both showed a significantly increased type I IFN-induced block of HIV-1 LV infection (Figure 20C) and a significantly lower rescue of this block with CsA treatment compared with THP-1 wt cells (1.5-fold compared to 1.2-fold; Figure 20D). However, no changes were observed between single and double knockouts in response to IFNα2 and CsA (Figure 20C and D). For CypB single knockout cells, no significant changes to THP-1 wt cells were detected. This suggests an involvement of CypB in HIV-1 infection only but not in the type I IFN-induced block to HIV-1 LV infection.
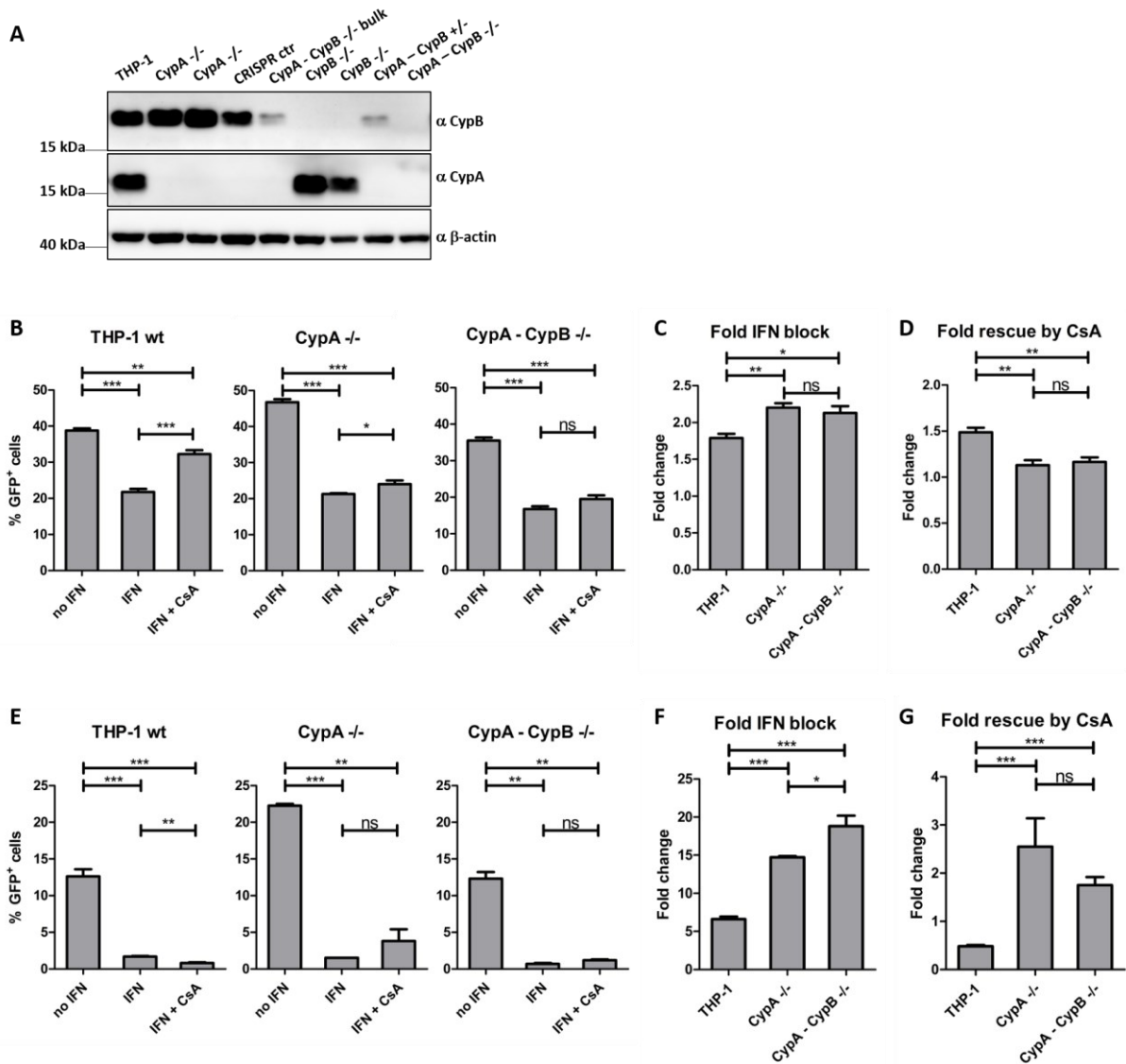
Figure 20: CypA-CypB double knockout enhances hypersensitivity of IFNα2 induced block to HIV-1 infection.

A: THP-1 wt, CypA -/-, CypB -/-, CRISPR control cells and THP-1 based CypA-CypB double knockout cell lines (CypA-CypB -/-) were analyzed by Western blot for CypA, CypB and β-actin expression. **B:** THP-1 wt, CypA -/- or CypA-CypB -/- cells were treated or not with 500 U/ml IFNα2. 24 h post IFN stimulation cells were treated with 2.5 μM CsA. At the time of CsA addition, cells were infected with VSV-G pseudotyped HIV-1 LV for 48 h. Percentage of GFP positive cells was determined by flow cytometry. Bars indicate the average infectivity determined from at least two independent experiments and error bars indicate standard deviation. Unpaired two-tailed t test was performed (*, p< 0.05; **, p< 0.01; ***, p< 0.001; ns, not significant). **C:** Calculated fold changes of IFNα2 induced block to HIV-1 LV infection. Bars indicate the average fold change and error bars represent standard deviation. Unpaired two-tailed t test was performed (*, p< 0.05; **, p< 0.01; ns, not significant). **D:** Calculated fold changes of HIV-1 LV infection levels upon CsA treatment compared to IFN stimulated cells. Bars indicate the average fold change and error bars indicate standard deviation. Unpaired two-tailed t test was performed (**, p< 0.01; ns, not significant). **E:** THP-1 wt, CypA -/- or CypA-CypB -/- cells were treated or not with 500 U/ml IFNα2. 24 h post IFN stimulation cells were treated with 2.5 μM CsA. At the time of CsA addition, cells were infected with VSV-G pseudotyped HIV-1 NL4.3 for 48 h. Percentage of GFP positive cells was determined by flow cytometry. Bars indicate the average infectivity determined from three independent experiments and error bars indicate standard deviation. Unpaired two-tailed t test was performed (**, p< 0.01; ***, p< 0.001; ns, not significant). **F:** Calculated fold changes of IFNα2 induced block to NL4.3 infection. Bars indicate the average fold change and error bars indicate standard deviation. Unpaired two-tailed t test was performed (*, p< 0.05; ***, p< 0.001). **G:** Calculated fold changes of NL4.3 infection upon CsA treatment. Bars indicate the average fold change and error bars indicate standard deviation. Unpaired two-tailed t test was performed (***, p< 0.001; ns, not significant).

60

To determine the role of the HIV-1 accessory proteins, THP-1 parental, CypA single and CypA-CypB double knockout cells were infected with VSV-G pseudotyped full-length NL4.3 GFP HIV-1. As can be seen in Figure 20E the double knockout cell line showed the same infection as THP-1 wt cells (12.3 % compared to 12.6 %, respectively), whereas CypA knockout showed 22.3 % infection. For CypB single knockout 16.6 % infection was observed, which was slightly higher than for parental cells (Figure 12E). This suggests that antiviral activity of CypA is higher than the one of CypB, but both Cyps contribute to the effects. Stimulation of cells with IFNα2 24h prior to infection with NL4.3 GFP resulted in a significant reduction of infection for all cell lines. As observed for all knockout cell lines, reduction in infection was stronger for NL4.3 infection than for HIV-1 LV infection (compare e.g. Figure 20C and F). For CypB single knockouts no significant changes in response to IFNα2 for NL4.3 infection in comparison to THP-1 wt cells was observed (Figure 12F), indicating no involvement of CypB in the type I IFN-induced block to infection. Interestingly, for CypA-CypB double knockouts a significant increase of the infection block caused by type I IFN treatment even compared to CypA -/- cells was obtained. For CypA -/- cells a 14.7-fold block and for double knockouts a 18.8-fold type I IFN-induced infection block to HIV-1 NL4.3 was observed (Figure 20F). Thus, absence of CypB alone has no effect on the type I IFN-induced block, but parallel knockout of two Cyps heightens restriction of HIV-1 NL4.3 infection by type I IFN-induced antiviral factors. This suggests that CypB contributes to protecting HIV-1 from the type I IFN-induced block and that CypA can compensate for this effect since no increase was observed in CypB -/- cells (Figure 12).

To confirm, that this effect was induced by a CsA sensitive factor, IFNα2 stimulated NL4.3 infected cells were treated with CsA. For THP-1 wt cells and CypB single knockout cells a significant reduction of infection compared to IFNα2 stimulated cells was observed (Figure 12E and G), indicating the inhibition of a CsA target promoting HIV-1 infection, which most likely is CypA. Interestingly, CsA treatment of CypA -/- cells showed an increased infection by 2.6-fold. A similar effect was observed for CypA-CypB -/- cells (1.8-fold infection increase; Figure 20E and G). The difference between CypA -/- and double knockout cells was not significant, suggesting a similar effect of CsA in both cell lines. If CypA is the only CsA target involved in HIV-1 infection, no difference upon CsA treatment in infection levels would be expected resulting in infection fold changes around 1, but even double knockouts showed an infection increase upon CsA treatment. Thus, another CsA target besides CypA and CypB is likely to be involved in an early step of HIV-1 infection.

8.1.6 CypA-CypE -/- show hypersensitivity to IFN-induced block of HIV-1infection

Therefore, a double knockout of CypA and CypE based on CypA knockout cells was generated. Figure 21A shows the Western blot analysis of the double knockout cell line using the same antibodies discussed above (8.1.3). THP-1 wt cells served as control for both CypA and CypE expression. CypA -/- cells served as a control for CypE expression and served as an input for the double knockout cell line production. CypE -/- cells were a control for CypA expression. The CypA–CypE double knockout cell line showed no expression of either Cyp. For comparison of the input material, β-actin expression levels were detected. As this study shades some light on Cyp redundancy, it is worthwhile to mention, that knockout of one Cyp did not alter the expression levels of other Cyps as shown in Figure 21A as well as in Figure 20A. Further immunoblot analysis of CypA -/- cells for several other Cyps confirmed this observation (data not shown).

Figure 17A shows that CypE single knockout cells had a reduced infection (15.8 %) of HIV-1 LV compared to THP-1 parental cells (25.7 %). Furthermore, a higher potency of IFNα2 to block infection (2.6-fold) and an increased ability of CsA to rescue infection from the IFN-induced block for HIV-1 LV infection (2.7-fold) was observed for CypE -/- cells. In CypA-CypE double knockout cells an intermediate phenotype between CypA and CypE single knockouts was observed in response to HIV-1 LV challenge (Figure 21B). Infection levels were increased for CypA -/- (46.8 %) compared to the double knockout cell line (35.3 %). Thus, the opposite effects of CypA and CypE single knockouts were almost compensated for in the double knockout cell line. IFNα2 again had a higher potency to block HIV-1 LV infection in the absence of at least one Cyp. CypA -/- cells showed the smallest increase in the infection block (2.2-fold compared to 1.8-fold for THP-1 wt cells) whereas CypE -/- showed an 2.6-fold block to HIV-1 LV infection and CypA-CypE double knockout cells showed a 2.4-fold reduction of infection (compare Figure 17B and Figure 21C). The double knockout showed a significantly enhanced rescue ability compared to THP-1 wt cells, but not significantly different to single knockout cells (Figure 21C). However, an additive effect, as observed for infection without any additional treatment, was not observed. Interestingly, the rescue ability of CsA on the type I IFN-induced block of HIV-1 LV infection was neither intermediate nor additive to the single knockouts. The double knockout cell line copied the CypA -/- phenotype showing a 1.1-fold and 1.2-fold rescue, respectively (Figure 21C). CypE -/- knockout however showed a significantly increased rescue ability of 2.7-fold (Figure 17D). These results indicate an involvement of both proteins on HIV-1 LV infection and the type I IFN-mediated block to HIV-1 LV infection.
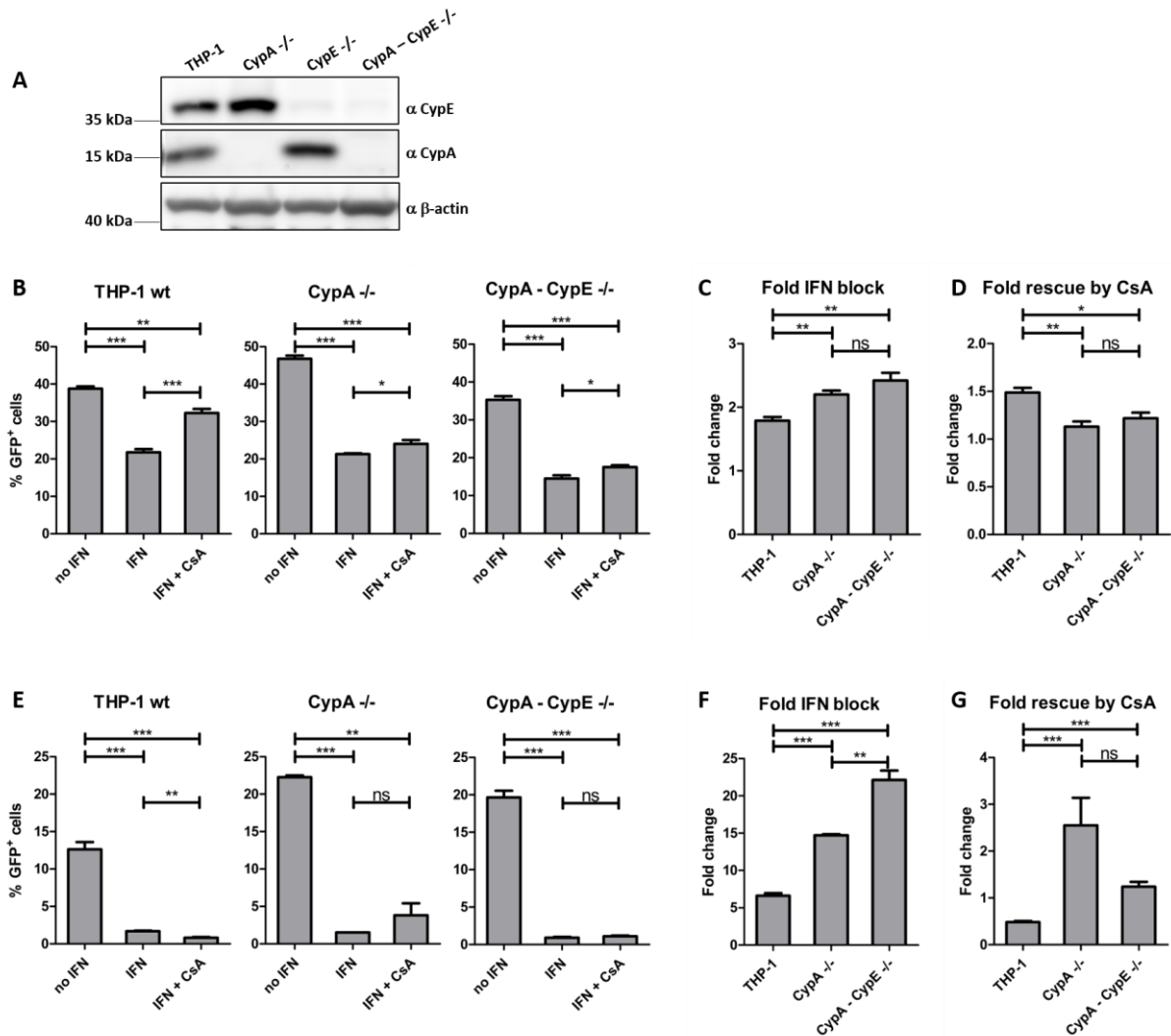
Figure 21: CypA-CypE -/- cells show enhanced hypersensitivity to the type I IFN-induced block.

A: THP-1 wt, CypA -/-, CypE -/- and THP-1 based CypA-CypE double knockout (CypA-CypE -/-) cell lines were analyzed by Western blot for CypA, CypE and β-Actin expression. **B:** THP-1 wt, CypA -/- or CypA-CypE -/- cells were treated or not with 500 U/ml IFNα2. 24 h post IFN stimulation cells were treated with 2.5 μM CsA. At the time of CsA addition, cells were infected with VSV-G pseudotyped HIV-1 LV for 48 h. Percentage of GFP positive cells was determined by flow cytometry. Bars indicate the average infectivity determined from at least three independent experiments and error bars indicate standard deviation. Unpaired two-tailed t test was performed (*, p< 0.05; **, p< 0.01; ***, p< 0.001). **C:** Calculated fold changes of IFNα2 induced block to HIV-1 LV infection. Bars indicate the average fold change and error bars indicate standard deviation. Unpaired two-tailed t test was performed (**, p< 0.01; ns, not significant). **D:** Calculated fold changes of HIV-1 LV infection levels upon CsA treatment compared to IFN stimulated cells. Bars indicate the average fold change and error bars indicate standard deviation. Unpaired two-tailed t test was performed (*, p< 0.05; **, p< 0.01; ns, not significant). **E:** THP-1 wt cells, CypA -/- or CypA-CypE -/- cells were treated or not with 500 U/ml IFNα2. 24 h post IFN stimulation cells were treated with 2.5 μM CsA. At the time of CsA addition, cells were infected with VSV-G pseudotyped HIV-1 NL4.3 for 48 h. Percentage of GFP positive cells was determined by flow cytometry. Bars indicate the average infectivity determined from three independent experiments and error bars indicate standard deviation. Unpaired two-tailed t test was performed (**, p< 0.01; ***, p< 0.001; ns, not significant). **F:** Calculated fold changes of FNα2 induced block to NL4.3 infection. Bars indicate the average fold change and error bars indicate standard deviation. Unpaired two-tailed t test was performed (**, p< 0.01; ***, p< 0.001). **G:** Calculated fold changes of NL4.3 infection upon CsA treatment. Bars indicate the average fold change and error bars indicate standard deviation. Unpaired two-tailed t test was performed (***, p< 0.001; ns, not significant).

NL4.3 infection had the same effect on infectivity in CypE depleted cells as observed for HIV-1 LV infection. THP-1 parental cells showed 12.6 % infection, CypE single knockout cells

9.8 % infection and CypA-CypE double knockout cells 19.7 % infection (compare Figure 17D and Figure 21E). For CypA single knockout cells 22.3 % HIV-1 NL4.3 infection was observed, and assuming an additive effect in the CypA-CypE double knockout cells as observed for LV infection, roughly 19 % infection was expected and was observed for the double knockouts (Figure 21E). However, in response to IFNα2, an alternate phenotype to HIV-1 LV infection could be detected. As observed before, IFN- induced infection blocks were greater in HIV-1 NL4.3 full-length infection, than observed for HIV-1 LV infection. For HIV-1 LV infection, IFNα2 treatment showed the highest potency to block infection in CypE single knockout cells (2.7-fold; Figure 17B). For NL4.3 infection the highest reduction of infection upon IFNα2 treatment was observed for CypA-CypE -/- cells, where a reduction of 22.1-fold was monitored (Figure 21F). In CypE single knockout cells, which showed the strongest effect in LV infection, type I IFN blocked NL4.3 infection by 7.2-fold, which was a non-significant increase compared to THP-1 wt cells. In contrast to LV infection, for HIV-1 NL4.3 full-length virus the potency of IFNα2 to block infection in single Cyp knockout cells was additive in double knockouts (7.2-fold for CypE -/- and 14.7-fold for CypA -/- compared to 22.1-fold, respectively). Therefore, CypA and CypE may likely play different roles in HIV-1 early infection steps.

CsA treatment of CypA-CypE -/- cells showed for both viral constructs no significant changes compared to CypA -/- cells (Figure 21D and G) and the fold change of infection levels observed was 1.2-fold. However, the response of CypA-CypE -/- cells to CsA was significantly different for both viral constructs to what was observed for THP-1 parental cells. This makes CypE a possible candidate for the CsA target contributing to the CsA induced increase in infection after type I IFN treatment observed in CypA -/- cells.

Taken together, I have shown that various cyclophilins are able to modulate the type I IFN response to HIV-1 and are therefore immune modulators of HIV-1 infection. An overview of the various responses to the two viral HIV-1 strains of cyclophilin knockout cells used are listed in Table 1. CypA, CypD and CypH knockout increased HIV-1 LV infection compared to the THP-1 parental control experiment. Involved in the type I IFN-induced block to HIV-1 LV infection are most likely all tested Cyps except CypC and CypD and for CypE knockout cells the biggest impact for CsA on HIV-1 LV infection was found (2.7-fold infection increase upon CsA addition, see Table 1 and Figure 17C). For full length HIV-1 NL4.3 infection Cyp knockouts showed alternate phenotypes, indicating an involvement of HIV-1 accessory proteins on the functions of Cyps. Except for CypE knockout cells all tested cell lines showed increased HIV-1 NL4.3 infection compared to THP-1 cells. Furthermore, the block to infection by IFNa2 was greater than observed in HIV-1 LV infection. CypA single and the two double knockout

cell lines showed the highest impact on the type I IFN response to HIV-1 NL4.3 infection. CsA treatment increased HIV-1 NL4.3 infection for all tested knockout cell lines compared to THP-1 parental cells with the highest impact observed for CypA -/- cells.

Table 1: Overview of HIV- 1 infection phenotypes in Cyclophilin knockout cells.
Summary of all observed effects in the above discussed CRISPR/Cas knockout cells. Listed are % GFP positive cells for the indicated condition of HIV-1 LV and HIV-1 NL4.3 infection or the calculated fold changes in response to IFNα2 and CsA. Knockout indicates, which protein is knocked out. CypA-B is the double knockout of CypA and CypB, CypA-E is the double knockout of CypA and CypE. - = infection without any stimulation; IFN = infection with previous IFNα2 stimulation (see 7.3.4); IFN + CsA = infection with IFNα2 and CsA stimulation (see 7.3.4); Fold block = calculated fold block to infection upon IFNα2 treatment; Fold rescue = calculated change of infection between IFNα2 and IFNα2-CsA stimulated cells. Bold numbers indicate an increase compared to THP-1 parental cells.

Knock-out	HIV-1 LV infection					HIV-1 NL4.3 infection				
	-	INF	INF + CsA	Fold block	Fold rescue	-	INF	INF + CsA	Fold block	Fold rescue
CypA	**46.8**	21.3	24.0	**2.2**	1.1	**22.3**	1.5	**3.8**	**14.7**	**2.6**
CypB	27.5	14.3	20.3	**1.9**	1.4	**16.7**	**3**	**1.6**	5.6	**0.6**
CypC	18.2	10.0	19.8	1.8	1.8					
CypD	**47.0**	**24.0**	**32.5**	1.8	1.4					
CypE	15.8	7.5	16.8	**2.6**	**2.7**	9.8	1.4	**0.9**	7.2	**0.6**
CypH	**26.3**	**13.0**	19.5	**2.1**	1.6					
CypA-B	35.5	16.8	19.5	**2.1**	1.2	**12.3**	0.7	**1.2**	18.8	**1.8**
CypA-E	35.3	14.5	17.5	**2.4**	1.2	**19.7**	0.9	**1.1**	22.1	**1.2**

These varying phenotypes lead to the assumption, that another type I IFN-induced CsA sensitive factor except cyclophilins is involved in modulating the immune response against HIV-1. Therefore, we performed a recently developed unbiased mass spectrometry screen to identify novel CsA sensitive targets based on their thermal stability [322], [323].

8.2 CETSA identifies possible novel CsA targets

Thermal protein stability is measured as a protein melting point. Binding of drugs, co-factors or interacting proteins can stabilize or destabilize a protein and affect thermal protein stability, thus causing an increase or decrease of the protein melting point [322], [323]. Exactly this effect was used as a readout for the conducted cellular thermal shift assay (CETSA) experiments. THP-1 CypA -/- cells were treated with 500 U/ml IFNα2 for 24 h. The next day, cells were treated with CsA or DMSO for 90 min, respectively. The CypA -/- cells were used, as an

increase of HIV-1 NL4.3 GFP infection by CsA from an IFN-induced block was observed, although CypA is absent in these cells (Figure 10F).
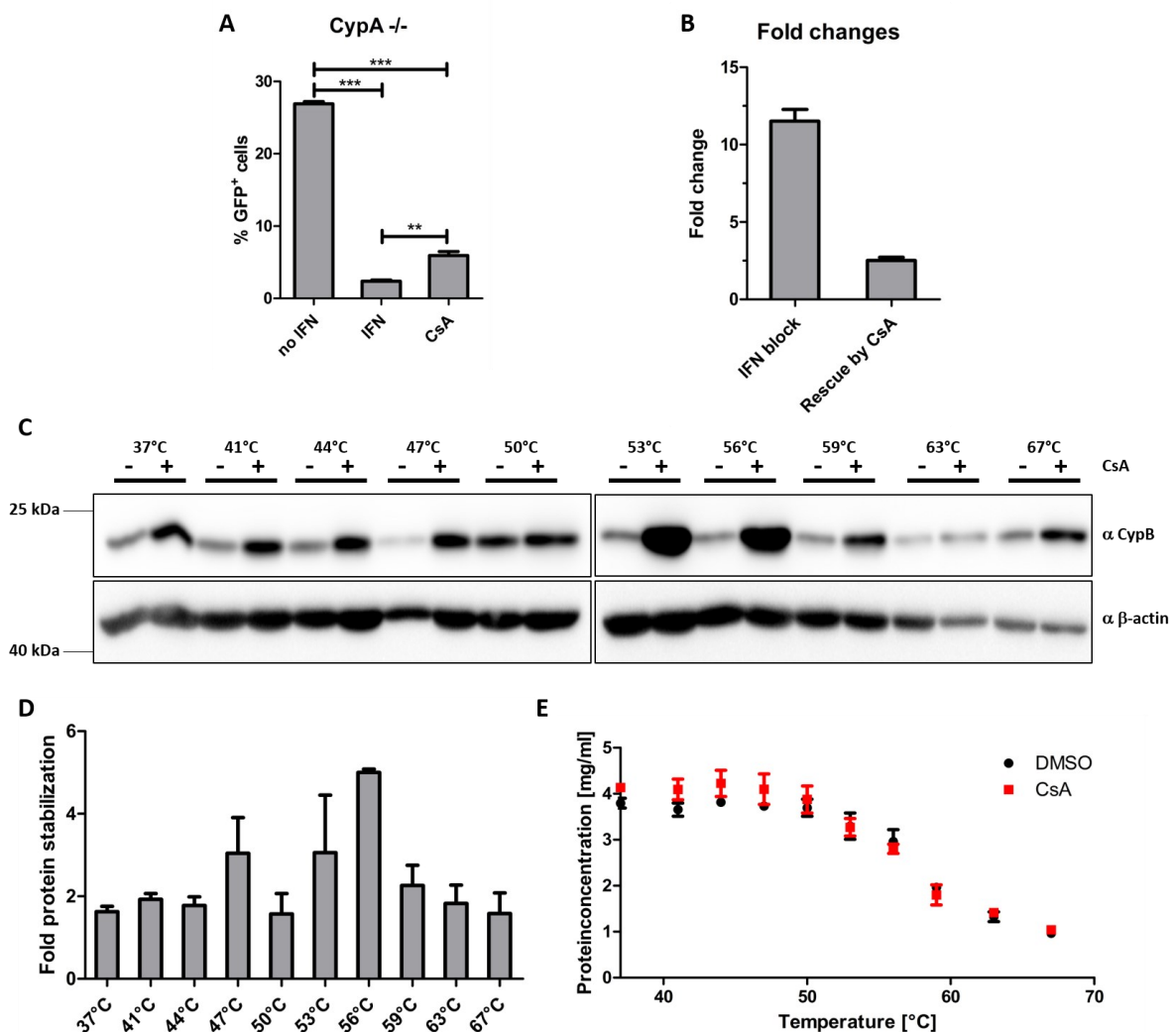

Figure 22: Cellular thermal shift assay (CETSA).

A: CypA -/- cells were treated or not with 500 U/ml IFNα2. 24 h post IFN stimulation cells were treated with 2.5 μM CsA. At the time of CsA addition, cells were infected with VSV-G pseudotyped HIV-1 NL4.3 for 48 h. Percentage of GFP positive cells was determined by flow cytometry. Bars indicate the average infectivity determined from two experiments with three replicates, respectively. Error bars indicate standard deviation. Unpaired two-tailed t test was performed (*, p< 0.05; ***, p< 0.001). **B:** Fold changes of IFNα2 induced block to NL4.3 infection and the fold rescue from this block by CsA were calculated. Bars indicate the average fold changes determined from three technical replicates. **C:** CypA -/- cells were treated with 500 U/ml IFNα2 for 24 h, followed by incubation with 2.5 μM CsA or DMSO in duplicates for 90 min. Cells were aliquoted and incubated at 10 different temperatures ranging from 37°C to 67°C for 3 min followed by 3 min at 25°C. Denatured proteins were removed by centrifugation. CETSA supernatants were used for Western blot analysis. CypB and β−actin protein expression was analyzed at each temperature for DMSO and CsA treated samples. **D:** CypB expression from C was normalized to b-actin expression and quantified. The fold stabilization of CypB by CsA was calculated and is shown for each temperature. Calculations were performed with ImageJ. **E:** Total protein concentration at the corresponding temperature for each CETSA supernatant was measured by BCA assay.

To control if the stimulation with IFNα2 and CsA resulted in the above described phenotype (Figure 10), an aliquot of treated cells was infected with HIV-1 NL4.3 and an infection assay was performed. Figure 22A shows infection rates of CypA -/- cells similar to those observed

before (Figure 10D). Fold changes of infection upon IFNα2 and CsA stimulation were calculated and are shown in Figure 22B. These are comparable fold changes to what was detected in Figure 10 and Figure 11. Non-infected, IFNα2-treated and DMSO or CsA-stimulated cells were aliquoted into ten fractions for each stimulation condition and heated for 3 min at a specific temperature in the range of 37°C to 67°C. After heating, proteins were isolated by three cycles of freeze and thaw in liquid nitrogen. Afterwards, denatured proteins were separated from soluble proteins by centrifugation. In a next step sample handling and separation of correctly folded and denatured proteins was controlled for. Total protein concentration in the soluble fractions was measured and as expected numbers decreased at higher temperatures (Figure 22E). As a control, total protein was measured by a bicinchoninic acid (BCA)-based assay (7.4.3). No difference in total protein concentration at any temperature could be observed between CsA and mock (DMSO) treated samples. To demonstrate the stabilizing effect of CsA on Cyps, a Western blot sample form each treated aliquot was taken and analyzed for CypB and β-actin protein expression (Figure 22C). The remaining CETSA supernatants containing only soluble proteins were send for MS analysis to Rozbeh Jafari, a collaborator in Sweden[1].
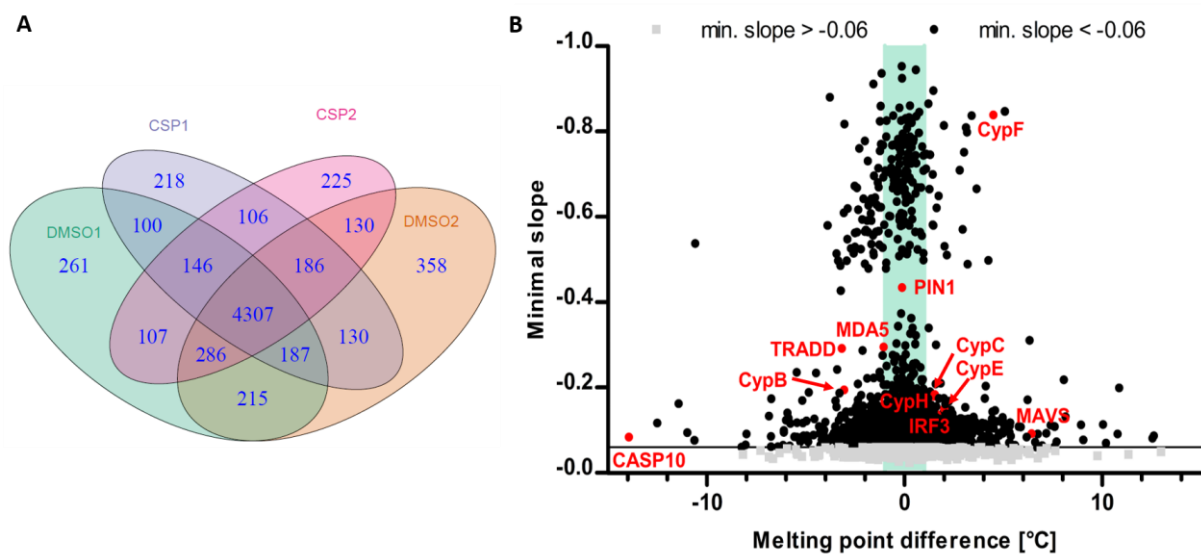
Figure 23: CETSA identifies novel CsA affected proteins.

A: CETSA supernatants containing the soluble protein fractions from two individual experiments were sent for mass spectrometry (MS) analysis. An overview of all detected proteins for DMSO and CsA treatment for both experiments is shown. **B:** All detected proteins from MS analysis are plotted for their calculated melting point shifts induced by CsA against the minimal slop of the respective melting curves. Proteins with a minimal slope greater than -0.06 are shown in grey. Highlighted in red are known CsA targets or non-targets as well as interesting hits. Marked in green is the area are proteins with a melting point shift lower than +/- 1°C.

---

[1] Division of Biophysics, Department of Medical Biochemistry and Biophysics, Karolinska Institutet, Stockholm, Sweden

Protein abundances for DMSO and CsA treated samples at all analyzed temperatures were measured by MS as described in 7.4.3. These data were used to calculate melting curves for each condition for all individual proteins detected. The melting temperature (Tm) of individual proteins for each treatment condition is defined as the temperature, where the protein abundance is half of the reference protein abundance at 37°C. To assess, whether CsA influences a protein's thermal stability, the difference of Tm between DMSO and CsA was calculated (ΔTm). An overview of all proteins detected for each treatment condition can be seen in Figure 23A. 4307 proteins could be detected in all four analyzed data sets and overall 6,962 proteins could be identified in at least one data set (DMSO 1, DMSO 2, CsA 1 or CsA 2). Not all signals from detected proteins could be used to calculate reliable melting curves and a ΔTm between DMSO and CsA treated samples. As the experiment was conducted in duplicates, two ΔTm values for each protein where obtained, when the respective protein was detected in all four datasets.

Table 2: Calculated ΔTm shifts for PPIases identified by CETSA.
Shown are calculated shifts in melting temperatures (ΔTm) induced by CsA compared to DMSO mock treated samples in two parallel experiments (Exp.1 and Exp.2). For proteins marked with a * the protein could only be detected for mock and CsA treatment in one experiment or ΔTm calculation was not possible for one experiment.

Cyclophilins			Other PPIases		
Target name	ΔTm Exp.1	ΔTm Exp.2	Target name	ΔTm Exp.1	ΔTm Exp.2
CypB	-1.41	-3.07	PPIL1	0.71	1.40
CypC*		1.53	FKBP2	1.66	1.45
CypD	-0.03	-0.26	FKBP3	0.35	2.44
CypE*		2.00	FKBP5	-0.30	-1.62
CypF	3.72	4.49	FKBP7*	2.34	
CypG	1.49	-1.09	FKBP9*		4.99
CypH	1.65	1.51	Pin1	-0.13	-0.29
			Nup358	0.06	0.79

In Figure 23B a dot plot is shown, where the minimal slope of the melting curve for each detected protein is plotted against the resulting melting point difference (exemplary for dataset 1). The bigger the minimal slope of the melting curve is, the vaguer the resulting data. Therefore, smaller minimal slopes give more accurate data than bigger slopes despite the ΔTm value. Detected proteins with a minimal slope above -0.06 are depicted with grey dots, most likely representing unreliable values and these proteins were excluded from any further analysis. Highlighted in Figure 23B are proteins detected by MS analysis, which are interesting

for several reasons: (i) all detected Cyp family members as known CsA targets, (ii) other PPIases as known non-targets for CsA and (ii) proteins which belong to an type I IFN signaling pathway that show high calculated ΔTm values in at least one experiment analyzed. The most obvious targets were cyclophilins. These are known targets for CsA binding, and an effect on thermal protein stability upon CsA treatment was expected. CypA could not be detected, as CypA -/- cells were used to perform the experiment. The calculated ΔTm shifts for all other detected PPIases are listed in Table 2. For CypB an effect on thermal protein stability by CsA was observed. Western blot analysis revealed a clearly visual stabilization of CypB by CsA at various temperatures (Figure 22C and D). Relative protein amounts were obtained and normalized to β-actin expression levels.
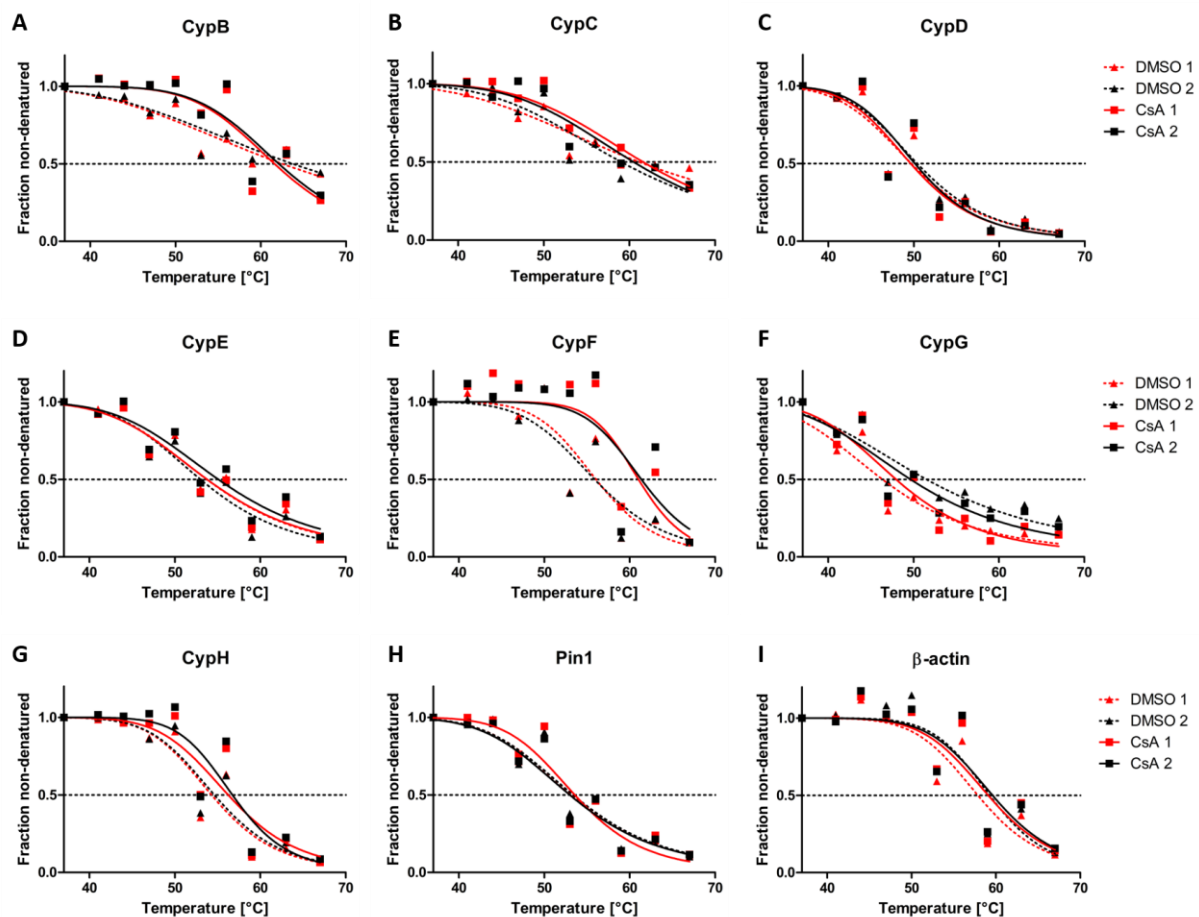
Figure 24: CsA influences the thermal stability of Cyclophilins.

CypA -/- cells were stimulated with 500 U/ml IFNα2 and 2.5 µM CsA or DMSO, respectively. The experiment was conducted in duplicates and LC-MS/MS - CETSA was performed. For each temperature protein fold changes were computed relative to the protein abundance at 37°C. These fold changes represent the relative amount of non-denatured protein at the corresponding temperature. CETSA derived melting curves for individual proteins are shown in **A-I**. DMSO control samples are shown with triangles, CsA treated samples are represented in squares. The first dataset is represented in red, the second in black. The intersections of the melting curves with the dashed horizontal line indicates the melting point of the corresponding protein under the used conditions.

The fold stabilization by CsA in immunoblot analysis was calculated compared to DMSO treated controls. This resulted in a maximal stabilization of 5-fold for CypB by CsA at 56°C (Figure 22D). MS data for CypB revealed a calculated ΔTm of at least -1.4°C, thus confirming the data obtained by Western blot analysis (ΔTm values for the two MS experiments are shown in Table 2). Notably, Western blot results indicate a protein stabilization of CypB by CsA whereas the MS data suggest a destabilizing effect (negative ΔTm values). However, this seemingly contradicting results could be explained by the melting curves obtained from the MS analysis. The melting curves for CypB obtained in the MS experiments are shown in Figure 24A. Under ideal conditions, protein abundance at the highest temperature used should be towards zero. For CypB, especially in the DMSO controls, roughly 40 % of the CypB amount detected at 37°C was still present. This makes ΔTm calculations more difficult and imprecise. Ideally, one more dataset at higher temperatures would confirm a lower CypB abundance at high temperatures. For example, the melting curve observed for CypD clearly shows low protein abundancy at high temperatures making these calculations more precise (Figure 24C). Therefore, the differences between stabilization of CypB observed by Western blot analysis and apparent destabilization observed in MS analysis can be explained by the relatively high protein abundance of CypB protein at 67°C in the DMSO control. It is notable to mention, that overall, most detected proteins had a ΔTm shift around 59°C. This is in agreement with results from other CETSA experiments and justified the chosen temperature range [322], [323]. The seemingly contradicting results between MS and immunoblot analysis for CypB also make clear, that a visual comparison of the melting curves must be done to control for those samples with high protein abundance.

For β-actin no effect of CsA on protein stability could be observed independently of the methods used. Western blot analysis (Figure 22C) showed no alterations in β-actin protein stability between DMSO and CsA treatment. This was confirmed by the melting curves (Figure 24I) and the calculated ΔTm for β-actin in MS analysis (0.98°C and 0.2°C for the two experiments, respectively; Table 4).

8.2.1 Various proteins are affected by CsA

The CETSA experiment detected a lot of proteins of the human proteome. The most obvious candidates to be detected in the CETSA experiment were Cyps, as they are known targets for CsA. Therefore, Cyps should be stabilized or destabilized by CsA resulting in a detectable ΔTm shift upon CsA treatment. The largest Cyp, Nup358, has been suggested to be insensitive to CsA binding [207], [265], [266] and also in the MS analysis shown small ΔTm shifts below

1°C were observed (Table 2), arguing, that CsA does not bind and effect the Cyp domain of Nup358. Other PPIases like FKBPs and parvulin like PPIase on the other hand should be unaffected by CsA and melting curves for these proteins should not differ in the DMSO control or the CsA treated samples. In Table 2 all calculated ΔTm values for detected PPIases are listed. For Cyps and Pin1 all melting curves are shown in Figure 24. A stabilization or destabilization was observed for all Cyps except CypD (ΔTm is -0.03°C and -0.26°C) and as mentioned above Nup358 (ΔTm is 0.06°C and 0.79°C; melting curve not shown). CypD -/- cells also did not show any changes in the type I IFN-induced block of HIV-1infection and its rescue by CsA compared to THP-1 wt cells (Figure 15). Why CypD does not show a ΔTm shift in response to CsA is unclear. However, previous studies clearly identified CypD as a CsA binding protein [257], [324], [325]. The biggest difference in ΔTm is observed for CypF (ΔTm is 3.72°C and 4.49°C; Table 2) as can be seen in the obtained melting curved shown in Figure 24E. Although CypF shows the highest homology to CypA, it located in the mitochondrion and is therefore unlikely, to resume CypA functions in the cytoplasm. Unfortunately, no CypF knockout data is available, thus a comparison with the HIV-1 related phenotype is not possible.

Table 3:Targets identified in CETSA with the highest calculated ΔTm shifts.
Shown are calculated shifts in melting temperatures (ΔTm) induced by CsA compared to DMSO mock treated samples in two parallel experiments (Exp.1 and Exp.2). Restraints for target identification were a.) calculated ΔTm has the same sign b.) minimal slope is less than -0.06 c.) the plateau of each melting curve is lower than 0.3 and d.) ΔTm in both experiments of CsA vs. control is greater than ΔTm for control 1 vs. control 2.

Target name	ΔTm Exp.1	ΔTm Exp.2	Target name	ΔTm Exp.1	ΔTm Exp.2
AP4B1	-3.33	-3.47	PRPS1L1	-2.77	-9.17
CENPU	6.75	3.75	RAB31	2.20	3.30
CFD	9.04	7.83	RBM47	-3.21	-4.21
EIF4G1	-3.45	-5.40	SASS6	2.82	7.09
ENGASE	3.51	3.19	TMEM165	-4.84	-7.11
FAM49A	-4.93	-5.96	TTC5	12.61	8.51
MACF1	-5.44	-4.29	UBTD2	2.94	3.47
CypF	3.72	4.49	VAT1	3.23	3.99

Apparently not only known Cyps are influenced by CsA. Some Cyp pseudogenes were also identified in the CETSA experiment. Peptidyl-prolyl peptidase like protein 1 (PPIL1) is one of them showing a slight stabilizing effect induced by CsA (ΔTm is 0.71°C and 1.40°C as listed in Table 2). For other PPIase family members no effect of CsA is known so far. Surprisingly all detected FKBPs which should be unaffected by CsA showed a CsA induced ΔTm shift.
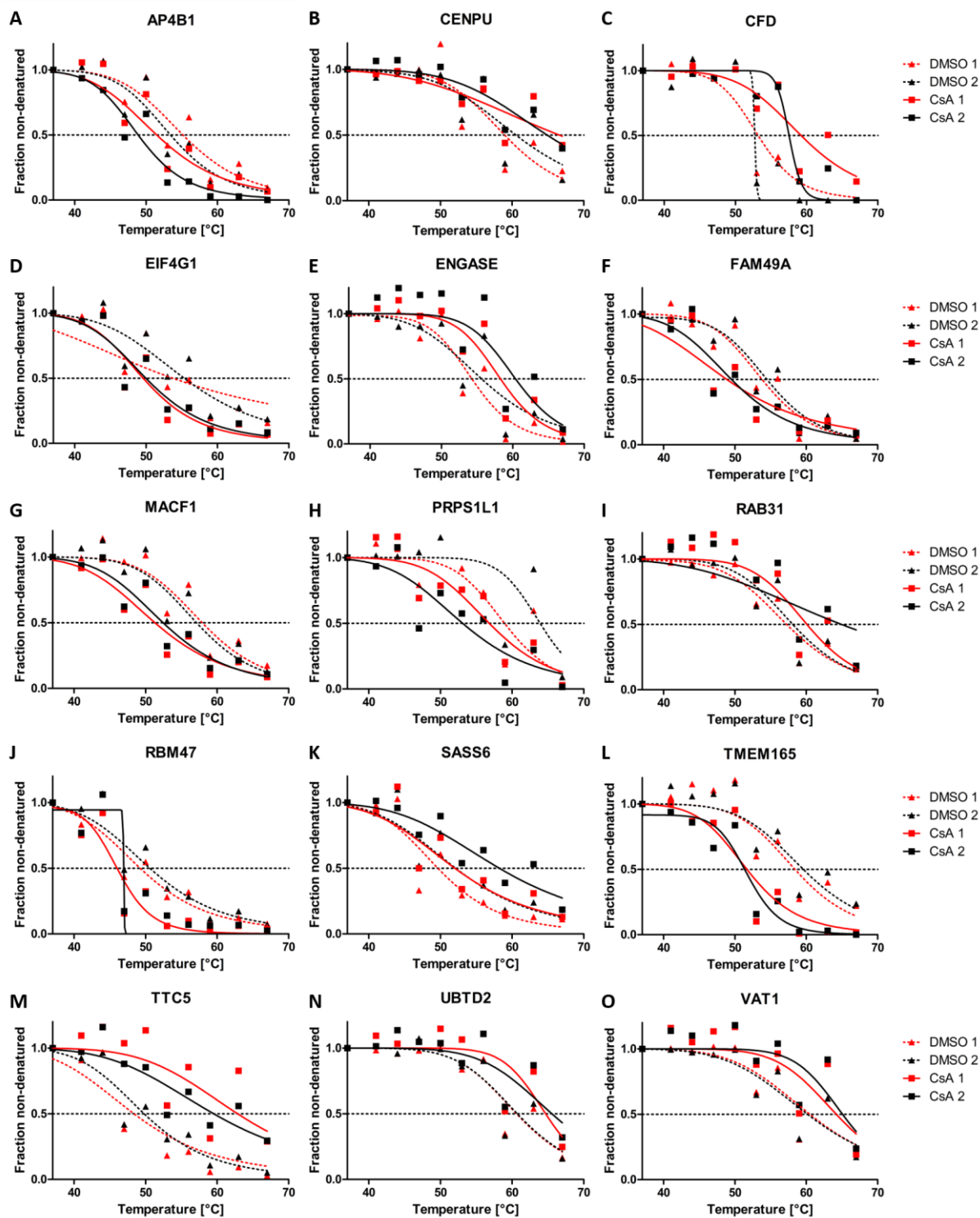
Figure 25: Melting curves of proteins with the highest ΔTm shift upon CsA treatment identified by CETSA.

CypA -/- cells were stimulated with 500 U/ml IFN☐2 and 2.5 µM CsA or DMSO, respectively. The experiment was conducted in duplicates (1 and 2, respectively) and LC-MS/MS-CETSA was performed. For each temperature protein fold changes were computed relative to the protein abundance at 37°C. These fold changes represent the relative amount of non-denatured protein at the corresponding temperature. CETSA derived melting curves for individual proteins are shown (A-O). DMSO control samples are shown with triangles, CsA treated samples are represented in squares. The first dataset is represented in red, the second in black. The intersections of the melting curves with the dashed horizontal line indicates the melting point of the corresponding protein under the used conditions. Calculated ΔTm values can be found in Table 3.

However, not all known FKBPs could be detected. All detected FKBPs with a ΔTm shift greater than $\pm$ 1°C for at least one experiment are listed in Table 2.

For other proteins like the PPIase Pin1 belonging to the CsA independent parvulin-like PPIases no ΔTm shift was observed. The melting curves for Pin1 can be seen in Figure 24H. No discrimination between DMSO and CsA treated curves can be detected and calculated ΔTm shifts are -0.13°C and -0.29°C as listed in Table 2. In the overview of all detected proteins in Figure 23B, Pin 1 is highlighted and positioned in the green shaded area. This marks proteins whose thermal stability is not influenced by CsA and which therefore, most likely are not affected by CsA and thus not the searched for type I IFN-induced CsA sensitive factor affecting HIV-1 infection.

After evaluating the MS dataset with known CsA targets and off-targets, proteins that showed the highest ΔTm shift upon CsA treatment and met all quality control restrains were identified. These restrains are (i) the calculated ΔTm shift had the same direction; (ii) the minimal slope of any melting curve was -0.06; (iii) the plateau of each melting curve was below 0.3 at the highest measured temperature and (iv) the ΔTm in both experiments between DMSO and CsA was greater than the ΔTm for DMSO1 vs DMSO2. The proteins identified by CETSA with the highest ΔTm shifts are listed in Table 3. These proteins fulfilled all quality control parameters but were not chosen as candidates for knockout cell lines. For some of them specific functions are unknown like FAM49A, a family with sequence similarity 49 member, RBM47, a RNA binding motif containing protein, or UBTD2, a ubiquitin domain containing protein as well as TTC5, a tetratricopeptide domain containing protein that is involved in the formation of large protein complexes. Other proteins are involved in vesicular transport like AP4B1, RAB31, TMEM165 and VAT1 or cell division like CENPU or SASS6 protein. The other highly affected proteins are CFD, complement factor D, which activates complement factor B to facilitate proliferation of pre-activated B-lymphocytes, EIF4G1, a translation initiation factor, MACF1, a protein that crosslinks actin and microtubules, ENGASE, an acetyl-glycosaminidase involved in the production of free oligosaccharides and PRPS1L1, a phosphoribosyl pyrophosphate synthase. Interestingly, of the known CsA targets only CypF made this list. As mentioned above (8.2), other cyclophilins are affected as well, but do not meet all four stringent criteria. Melting curves of the proteins listed in Table 3 are shown in Figure 25 except the one for CypF, which is shown in Figure 24E along with melting curves for all other detected cyclophilins.

To better understand the complex interplay of Cyps and HIV-1 the CETSA experiments were further analyzed in respect to PPIase interaction partners mentioned in this study (see section 5.2). These proteins and their corresponding ΔTm shifts are listed in Table 5. Most of these

proteins are not affected by CsA like Arp2 or MEK7. Other proteins known to play a crucial role in HIV-1 infectivity were detected during MS, but ΔTm shifts only occurred in one experiment like for CPSF6 or MX2. Other proteins, like e.g. APOBEC3G, APOBEC3F, ASK1 and TRIM5 were only detected by MS in one of the two experiments.

Table 4: Selected additional identified proteins in CETSA relevant for this study.
Shown are calculated shifts in melting temperatures (ΔTm) induced by CsA compared to DMSO mock treated samples in two parallel experiments (Exp.1 and Exp.2). For proteins marked with a * the protein could only be detected for mock and CsA treatment in one experiment or ΔTm calculation was not possible for one experiment. ** individual proteins of this protein family could not be identified clearly, shown data is for IFITM1, IFITM2 and IFITM3 combined.

Target name	ΔTm Exp.1	ΔTm Exp.2	Target name	ΔTm Exp.1	ΔTm Exp.2
APOBEC3F*		-2.06	MEK7	0.18	-0.14
APOBEC3G*	1.11		MEKK1	1.82	2.82
Arp2	0.83	0.36	MEKK2	-0.47	-1.58
Arp3	1.18	1.17	MTK1	0.60	-0.36
ASK1*	-0.44		MX2	-1.84	-0.07
β-actin	0.98	0.20	NFAT	3.25	1.47
β-catenin	5.33	1.29	NFκB	-2.22	-0.98
Casp1	-0.27	-0.95	N-WASP	0.26	1.20
Casp2	-0.34	-3.77	p65	-0.89	0.01
Casp4	0.30	0.86	Pinin	2.01	4.23
Casp7	0.29	2.35	PDZD8	-0.18	-4.15
CPSF6	1.91	0.47	STAT2	-1.84	-1.30
Calcineurin	1.24	1.47	STAT3	-0.40	-0.55
ERK1	1.58	0.22	STAT5A	5.30	1.64
ERK2	0.29	0.32	STAT5B	-0.80	-9.50
IFITIMs**	1.36		TRIM11	2.57	1.29
IRF5	0.11	0.88	TRIM21	-0.61	-0.60
IRF8	0.96	0.66	TRIM22	1.85	2.76
IRF9	-0.76	-1.30	TRIM24	0.48	1.75
MAP3K3	1.75	0.71	TRIM28	-0.32	-0.53
MAP3K7	1.25	-0.01	TRIM32	-3.64	-1.30
MAP4K5*	-6,17		TRIM38*	6.72	
MEK5*	-2.08		TRIM5*	-0.69	
MEK6	3.23	0.28	WNT	-1.51	-2.72

The known CsA binding proteins calcineurin and NFAT were both stabilized by CsA (Table 4), which was expected. Interestingly, β-catenin was stabilized and WNT was destabilized. It was shown that β-catenin interacts with CypA but no other Cyp and thereby enhances WNT target genes. In the absence of CypA these results are unexpected and might indicate that β-catenin may have other Cyp binding partners than CypA. More Cyp interaction partners were identified as positive hits, like Pinin, a CypG interacting protein [260] with a positive ΔTm shift or several STAT proteins that have been described before as CypB interacting partners [326]. In the infection assays with HIV-1 LV and HIV-1 NL4.3 a possible type I IFN-dependent function of CsA was observed, as CsA was able to rescue HIV-1 infection from a type I IFN-induced block in CypA -/- cells (Figure 10). Therefore, the CETSA data were carefully analyzed and cross referenced with known type I IFN-induced proteins. This analysis revealed amongst other pathways an enrichment of affected proteins involved in the RIG-I-signaling pathway. An schematic overview of the signaling pathway is shown in Figure 7 and proteins involved in this signaling pathway detected in the CETSA experiments are listed with their corresponding ΔTm values in Table 5.

Table 5: Calculated melting temperature shifts from CETSA experiment for Rig-1 signaling pathway proteins.
Shown are calculated shifts in melting temperatures (ΔTm) induced by CsA compared to DMSO mock treated samples in two parallel experiments (Exp.1 and Exp.2). For proteins marked with a * the protein could only be detected for mock and CsA treatment in one experiment or ΔTm calculation was not possible for one experiment.

Target name	ΔTm Exp.1	ΔTm Exp.2	Target name	ΔTm Exp.1	ΔTm Exp.2
RIG-I	0.92	0.31	IRF3	0.07	1.36
MDA5	-1.00	-1.06	IRF7	-2.45	-0.28
TRIM25	0.01	0.07	TRAF2	0.89	0.15
MAVS	4.44	8.42	TRAF6	0.83	0.02
TRADD	-3.17	-1,67	Casp8	-0.01	0.29
FADD	-2.50	-0.17	Casp10*	-13.93	
RIP1	-1.21	-0.07	p38	1.17	0.63
NFκB	-2.22	-0.98	JNK	0.04	-0.88
Tbk1	-0.58	-1.30			

Upon viral infection viral RNA is detected by cytosolic pattern recognition receptors and the innate immune response is initiated including type I and type III IFN expression and NFκB-dependent pro-inflammatory cytokine expression. The most affected proteins of the RIG-I signaling pathway detected were MDA5 with ΔTm shifts of -1.00 and -1.06°C, MAVS with ΔTm shifts of 4.44°C and 8.42°C, TRADD with ΔTm shifts of -3.17°C and -1.67°C, NFκB

with ΔTm shifts of -2.22°C and -0.98°C and Caspase10 (Casp10) with a ΔTm shift of -13-93°C, respectively. In addition to these five proteins, which showed a great ΔTm shift in all detected experiments, a few other pathway members were affected in at least one experiment. These were RIG-I, MAVS, FADD, RIP1, IRF3, IRF7 and p38. MDA5 is involved in PAMP recognition, TRADD is the first protein recruited by MAVS, the major scaffold protein at the mitochondria to induce downstream signaling. NFκB, a well-known transcription factor regulating expression of various ISGs and Casp10, a procaspase that is activated by Casp8 and that activates Casp3 and Casp7 to induce apoptosis, are two late acting proteins in the RIG-I signaling pathway.
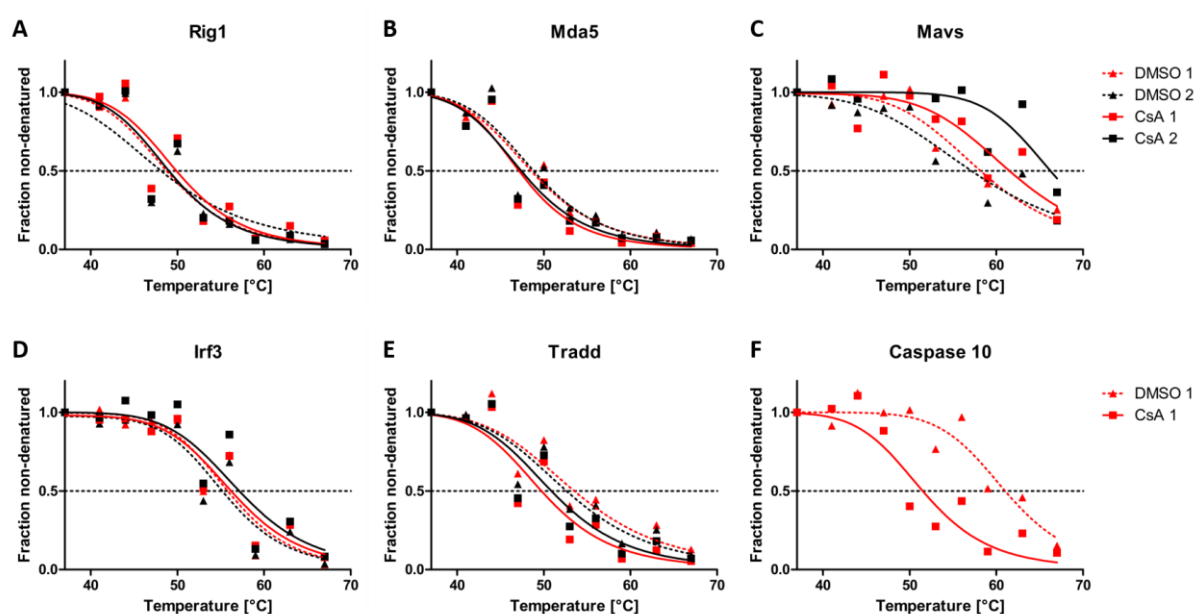

Figure 26: Melting curves of CETSA hits from the RIG-I signaling pathway chosen for in-depth analysis.

CypA -/- cells were stimulated with 500 U/ml IFNα2 and 2.5 µM CsA or DMSO, respectively. The experiment was conducted in duplicates (DMSO1/CsA1 and DMSO2/CsA2, respectively) and LC-MS/MS-CETSA was performed. For each temperature protein fold changes were computed relative to the protein abundance at 37°C. These fold changes represent the relative amount of non-denatured protein at the corresponding temperature. CETSA derived melting curves for individual proteins are shown (A-F). DMSO control samples are shown with triangles, CsA treated samples are represented in squares. The first dataset is represented in red, the second in black. The intersections of the melting curves with the dashed horizontal line indicates the melting point of the corresponding protein under the used conditions. Calculated ΔTm values can be found in Table 5.

The biggest shifts were observed for MAVS with 8.42°C ΔTm change upon CsA treatment and for Casp10 (ΔTm = -13.93°C, Table 5, melting curves in Figure 26). Although the minimal slope for Casp10 was just slightly over the threshold of -0.06 the resulting ΔTm was big enough to assume reliable data (Figure 23B). Unfortunately, this protein could only be detected in one of the two experiments as shown in Table 5 and Figure 26F. However, some proteins involved in this pathway were unaffected by CsA. For example, TRIM25, which plays a role in RIG-I activation is unaffected as no ΔTm shift could be observed (0.01°C and 0.07°C). Other

unaffected proteins were TNF receptor-associated factor 2 (TRAF2) and TRAF6 or Casp8. These proteins are involved in signal transduction facilitated through the MAVS protein.

After careful evaluation of the CETSA data for RIG-I signaling pathway proteins a few targets were chosen for CRISPR/Cas9 knockout cell lines based on CypA -/- cells. The chosen candidates were RIG-I and MDA5 as sensing proteins of viral RNA, MAVS, as a highly affected protein and the central point of signal transduction in the pathway. Furthermore, IRF3 and TRADD as two downstream proteins representing different signaling routes and Casp10 with one of the greatest shifts in melting points induced by CsA treatment. Melting curves of all chosen targets are shown in Figure 26. Taken together, the CETSA experiment could identify several interesting hits. In this study the aim was to identify a type I IFN-induced target protein affected by CsA that might be involved in the CsA-mediated increase of HIV-1 infection in type I IFN-stimulated THP-1 cells. Therefore, the RIG-I signaling pathway with several affected IFN-induced proteins was chosen to be investigated further.

8.2.2   Knockout of Rig-1 in CypA -/- cells reduces effects of CypA -/- to HIV-1 infection

Several members of the RIG-I signaling pathway could be identified as interesting candidates in the CETSA experiments as described above. Initially 6 key players of this pathway were chosen for in depth analysis. To further study the effects of these proteins, CRISPR/Cas-induced knockout cell lines were generated. Unfortunately, knockout of Casp10 in THP-1 CypA -/- could not be achieved, although the used gRNA has been previously used (7.1.9, [314].

The other chosen targets were RIG-I, MDA5, MAVS, IRF3 and TRADD. All these proteins are key players of the RIG-I signaling pathway. RIG-I, a cellular sensor for viral RNA, which is involved in initiation of the signaling cascade was investigated first. Its expression is regulated by IFNs and the recognition of HIV-1 derived RNA fragments by RIG-I was previously proposed [327]. Although in the CETSA experiments only minimal differences could be observed for ΔTm (0.92°C and 0.31°C, see Table 5) RIG-I was chosen as a target. The calculated melting curves for RIG-I are shown in Figure 26A. As can be seen, the relative low Tm of around 50°C indicates, that more data points at lower temperatures would be needed for a more precise result. Therefore, the low changes of ΔTm did not exclude RIG-I as a possible CsA affected protein.

In a next step RIG-I CRISPR/Cas9 knockouts of THP-1 CypA -/- were generated. Figure 27A shows the Western blot analysis of CypA-RIG-I -/- cells and several control cells.
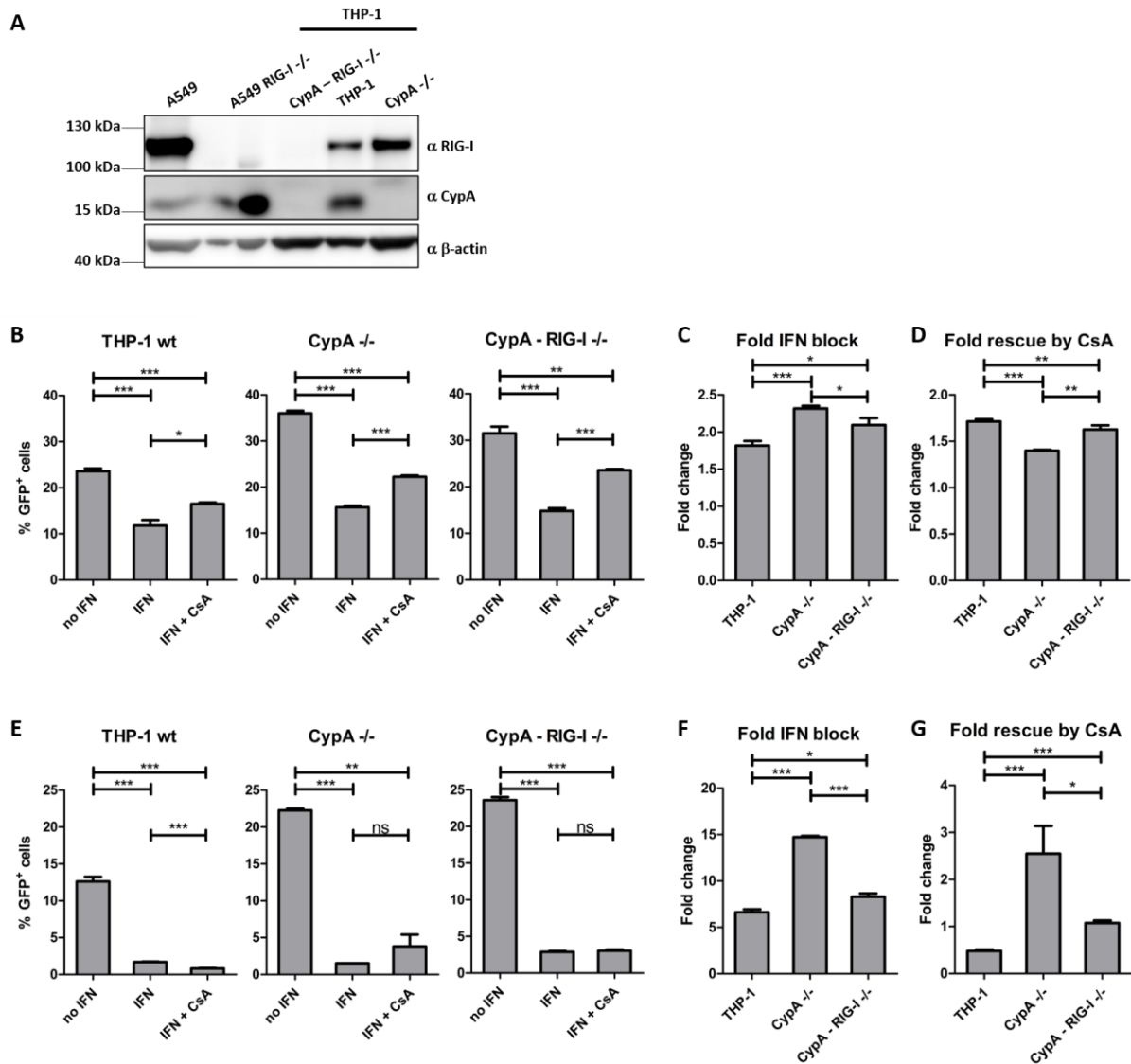
Figure 27: Knockout of RIG-I in CypA -/- cells shows enhanced infectivity and increased sensitivity to type I IFN and CsA.

A: THP-1 wt, CypA -/- and THP-1 based CypA and RIG-I double knockout (CypA-RIG-I -/-) cell lines were analyzed by Western blot for CypA, RIG-I and β-actin expression. A569 parental cells and a RIG-I -/- in these cells served as controls. **B:** THP-1 wt, CypA -/- or CypA-RIG-I -/- cells were treated or not with 500 U/ml IFNα2. 24 h post IFN stimulation cells were treated with 2.5 µM CsA. At the time of CsA addition, cells were infected with VSV-G pseudotyped HIV-1 LV for 48 h. Percentage of GFP positive cells was determined by flow cytometry. Bars indicate the average infectivity determined from at least three independent experiments and error bars indicate standard deviation. Unpaired two-tailed t test was performed (*, p< 0.05; **, p< 0.01; ***, p< 0.001). **C:** Calculated fold changes of IFNα2 induced block to HIV-1 LV infection. Bars indicate the average fold change and error bars indicate standard deviation. Unpaired two-tailed t test was performed (*, p< 0.05; ***, p< 0.001). **D:** Calculated fold changes of HIV-1 LV infection levels upon CsA treatment compared to IFN stimulated cells. Bars indicate the average fold change and error bars indicate standard deviation. Unpaired two-tailed t test was performed (**, p< 0.01; ***, p< 0.001).**E:** THP-1 wt cells or CypA-RIG-I -/- cells were treated or not with 500 U/ml IFNα2 for 24 h. Prior to infection with VSV-G pseudotyped HIV-1 NL4.3 for 48 h, cells were treated with 2.5 µM CsA. Percentage of GFP positive cells was determined by flow cytometry. Bars indicate the average infectivity determined from at least three independent experiments and error bars indicate standard deviation. Unpaired two-tailed t test was performed (**, p< 0.01; ***, p< 0.001; ns, not significant). **F:** Calculated fold changes of IFNα2 induced block to NL4.3 infection. Bars indicate the average fold change and error bars indicate standard deviation. Unpaired two-tailed t test was performed (*, p< 0.05; ***, p< 0.001). **G:** Calculated fold changes of NL4.3 infection levels upon CsA treatment compared to IFN stimulated cells. Bars indicate the average fold change and error bars indicate standard deviation. Unpaired two-tailed t test was performed (*, p< 0.05; ***, p< 0.001).

A549 and A549 RIG-I-/- cells served as a control for antibody specificity. These cells lysates were a kind gift from the group of Marco Binder[2] and were previously evaluated and are confirmed parental and knockout cells [328], [329]. In these cells and THP-1 wt cells CypA levels were not altered. Therefore, these served as controls and expression level comparison for single cell knockout clones. CypA -/- cells served as a control for normal RIG-I expression. CypA-RIG-I -/- clearly showed no CypA or RIG-I expression (Figure 27A). After knockout cell generation the above described infection assays (7.3.4) were performed. HIV-1 LV infected CypA-RIG-I -/- cells showed slightly reduced infection (31.5 %) compared to CypA -/- cells (36 %) (Figure 27B). However, both cell lines showed increased infection compared to THP-1 wt cells (23.6 %). The type I IFN-induced block to infection was also significantly reduced compared to CypA -/- cells (2.3-fold for CypA -/- compared to 2.1-fold in RIG-I -/- cells, Figure 27C), although significantly increased compared to THP-1 parental cells (1.8-fold; Figure 27C). In response to CsA, a similar phenotype to IFNα2 stimulation was observed. CypA-RIG-I double knockout cells showed significantly different responses compared to THP-1 and CypA single knockout cells Figure 27D. However, the response in CypA-RIG-I -/- cells was closer to wild type than CypA -/- cells (Figure 27D).

For HIV-1 NL4.3 infection higher infection in CypA-RIG-I double knockout cells was observed compared to THP-1 wt and CypA single knockout cells, however the differences to CypA -/- cells were only minor (23.6 % compared to 22.3 %, Figure 27E). For the response to IFNα2 and CsA stimulation a similar trend as for HIV-1 LV infection was observed. Figure 27F shows significant changes in the fold IFN-induced infection block compared to THP-1 and CypA -/- cell lines. As seen before, the fold changes of infection were much higher than observed for HIV-1 LV infection (compare Figure 27C and F). Knockout of RIG-I in CypA -/- cells significantly reduced the ability of IFNα2, to block NL4.3 infection compared to CypA single knockout cells. In CypA -/- cells a 14.7-fold block was observed whereas CypA-RIG-I double knockouts showed a 8.3-fold reduction. Interestingly, CsA treatment of the double knockout cells had almost no effect on the infection (Figure 27E and G). In CypA -/- cells CsA rescued infection from the type I IFN-induced block by 2.6-fold, indicating an additional IFN-induced target for CsA. As the effect is diminished by knocking out RIG-I in CypA -/- cells, this candidate could be involved in the CsA-induced increase of HIV-1 infection in type I IFN-stimulated THP-1 cells.

---

[2] German Cancer Research Center (DKFZ), Heidelberg, Germany

8.2.3   Knockout of MDA5 reverses CypA -/- effects on HIV-1 infection

The second protein of interest was MDA5. Together with RIG-I it senses viral RNA in the cytoplasm and initiates the signaling cascade to produce IFNs and induce ISG expression. The CETSA experiments revealed ΔTm shifts of -1.00°C and -1.06 °C in the two experiments, respectively (Table 5). The calculated melting curves shown in Figure 26B revealed a clear destabilizing effect of CsA on MDA5. The generation of CRISPR/Cas9 knockouts in THP-1 based CypA -/- cells was successful, as was judged in Western blot analysis shown in Figure 28A. As for RIG-I knockout cells, A549 cell lines served as a reference for MDA5 knockout in immunoblotting (Figure 27A and Figure 28A). These cells were previously characterized for MDA5 knockout (unpublished work by the group of Marco Binder[3]) and indicate that the lower band observed in the anti-MDA5 blot is the MDA5 corresponding band. As can be seen for THP-1 and CypA -/- control cells, MDA5 expression was observed in THP-1 cells, however to a lesser extent than observed in A549 cells. Based on CypA -/- THP-1 cells a MDA5 double-knockout was created. As can be seen in Figure 28A not all single cell clones had the knockout phenotype, but some CypA-MDA5 -/- cell lines could be created (Figure 28A).

Infection assays were performed with several MDA5 knockout clones to control for clonal effects (data not shown). For the following infection assays, one representative double knockout cell line is shown (Figure 28 B-G). In HIV-1 LV infection a reduced infection of CypA-MDA5 double knockout cells compared to the two reference cell lines could be observed (15.1 % infection), as shown in Figure 28B. Infection of CypA -/- resulted in 36 % infection and THP-1 parental cells showed 23.6 % infection. Additional knockout of MDA5 reverses this effect and infectivity was lower than in THP-1 wt cells. Infection of IFNα2 and CsA stimulated cells was also lower compared to CypA single knockouts or THP-1 parental cells (Figure 28C and D, respectively). Infection after IFNα2 pre-stimulation was almost completely lost in double knockout cells resulting in a 12.9-fold block to HIV-1 LV infection, indicating strong effects of MDA5 in the type I IFN response to HIV-1 infection. This magnitude of infection block by IFNα2 was only observed in HIV-1 NL4.3 infection in this study. The effects of CsA were also enhanced in the double knockout cell line. CypA-MDA5 -/- cells showed a rescue of 4.1-fold (see Figure 28D) whereas CypA single knockouts only showed a rescue of HIV-1 LV infection of 1.4-fold. This suggests an inhibiting effect of CsA on MDA5, which might be direct or indirect.

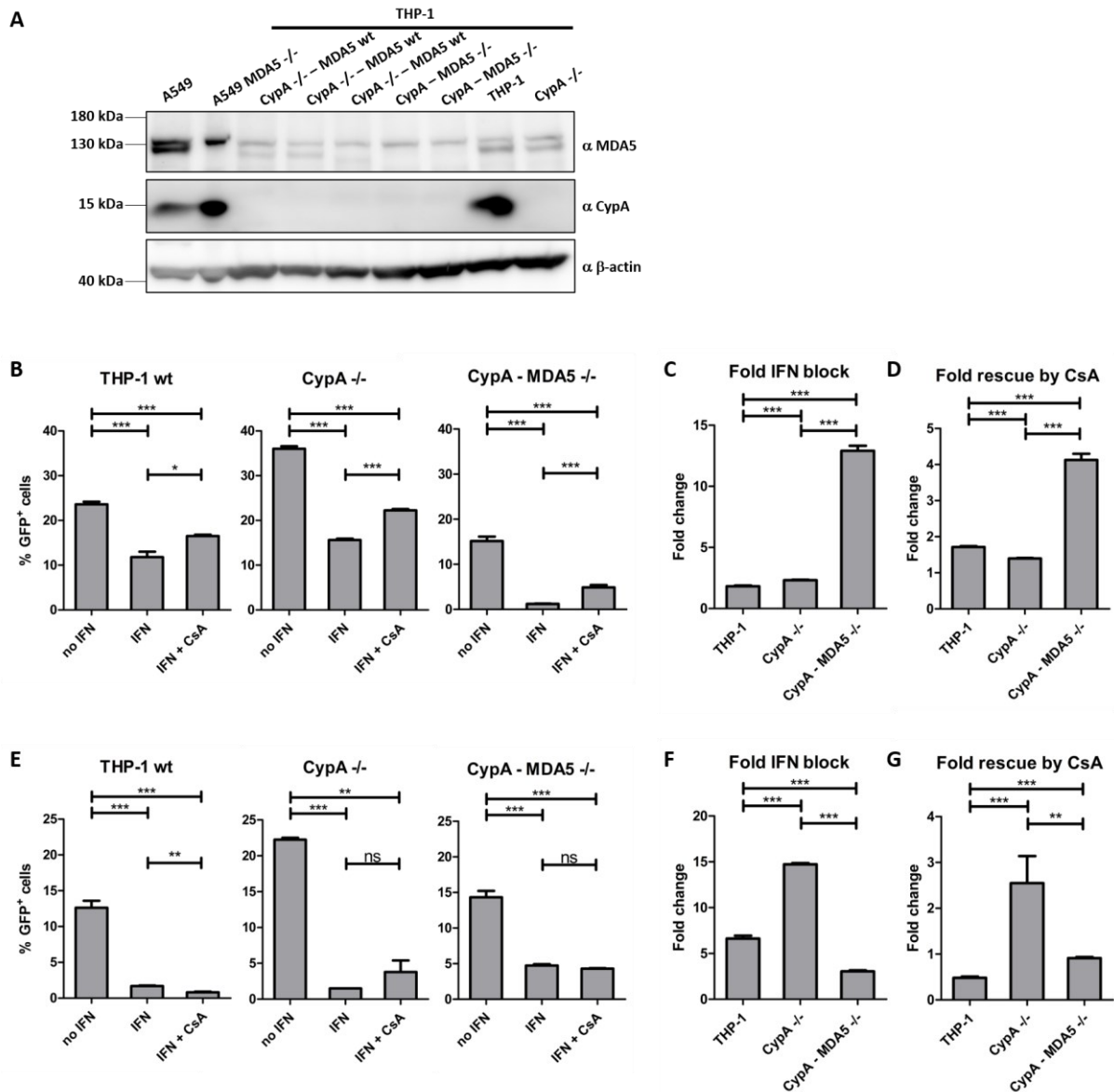---

[3] German Cancer Research Center (DKFZ), Heidelberg, Germany

Figure 28: CypA-MDA5 -/- show reduced HIV-1 infectivity, a strong response to IFNα and hypersensitivity to the rescue of this block by CsA.

A: THP-1 wt, CypA -/- and CypA and MDA5 double knockout (CypA-MDA5 -/-) cell lines were analyzed by Western blot for CypA, MDA5 and β-actin expression. A569 parental cells and MDA5 -/- in these cells served as controls. **B:** THP-1 wt, CypA -/- or CypA-MDA5 -/- cells were treated or not with 500 U/ml IFNα2 for 24 h. Prior to infection with VSV-G pseudotyped HIV-1 8.91 LV for 48 h, cells were treated with 2.5 µM CsA. Percentage of GFP positive cells was determined by flow cytometry. Bars indicate the average infectivity determined from three independent experiments and error bars indicate standard deviation. Unpaired two-tailed t test was performed (*, p< 0.05; ***, p< 0.001). **C:** Calculated fold changes of IFNα2 induced block to HIV-1 LV infection. Bars indicate the average fold change and error bars indicate standard deviation. Unpaired two-tailed t test was performed (***, p< 0.001). **D:** Calculated fold changes of HIV-1 LV infection levels upon CsA treatment compared to IFN stimulated cells. Bars indicate the average fold change and error bars indicate standard deviation. Unpaired two-tailed t test was performed (***, p< 0.001). **E:** THP-1 wt cells or CypA-MDA5 -/- cells were treated or not with 500 U/ml IFNα2. 24 h post IFN stimulation cells were treated with 2.5 µM CsA. At the time of CsA addition, cells were infected with VSV-G pseudotyped NL4.3 for 48 h. Percentage of GFP positive cells was determined by flow cytometry. Bars indicate the average infectivity determined from independent experiments and error bars indicate standard deviation. Unpaired two-tailed t test was performed (**, p< 0.01; ***, p< 0.001; ns, not significant). **F:** Calculated fold changes of IFNα2 induced block to NL4.3 infection. Bars indicate the average fold change and error bars indicate standard deviation. Unpaired two-tailed t test was performed (***, p< 0.001). **G:** Calculated fold changes of NL4.3 infection levels upon CsA treatment compared to IFN stimulated cells. Bars indicate the average fold change and error bars indicate standard deviation. Unpaired two-tailed t test was performed (**, p< 0.01; ***, p< 0.001).

Surprisingly, these effects were reversed in HIV-1 NL4.3 infection, pointing to a possible involvement of HIV-1 accessory proteins. A reduction of infection was observed in CypA-MDA5 -/- cells compared to CypA -/- cells (14.3 % compared to 22.3 %) but no difference in infection to THP-1 wt cells was found (12.6 %; Figure 28E). Interestingly, the type I IFN-induced block to infection was only 4.7-fold for CypA-MDA5 double knockout cells, which was significantly lower than the block observed in parental THP-1 cells or CypA -/- cells (6.6-fold and 14.7-fold, respectively; Figure 29F). Additionally, no rescue of this type I IFN-induced block to infection was observed upon CsA treatment in CypA-MDA5 -/- cells whereas CsA treatment of THP-1 parental cells reduced HIV-1 NL4.3 infection further. As CsA has no effect on IFNα2 treated CypA-MDA5 double knockout cells, MDA5 is a possible candidate for a type I IFN-induced CsA affected protein involved in HIV-1 infection. However, CypA-MDA5 -/- cells were less sensitive to the type I IFN-mediated HIV-1 infection block and effects of CsA could be masked due to the smaller IFN-induced block. Nonetheless, MDA5 is an interesting candidate for further analysis. MDA5 effects could be investigated more thoroughly with MDA5 single knockout cells, which were already generated but remain to be screened.

8.2.4 CypA-MAVS -/- and CypA-IRF3 -/- cells show hypersensitivity to type I IFN-induced block of HIV-1infection

The central player of the RIG-I signaling pathway is MAVS, an antiviral signaling molecule located at the mitochondria. MAVS serves as a scaffold protein which links all involved players together. Dependent on which downstream factors are recruited, either apoptosis, IRF3-mediated or NFκB-mediated signaling can be induced. As downstream signaling is activated independent of the viral RNA sensing factor involved, MAVS serves as the bottleneck of this pathway making it an ideal candidate to investigate.

In the CETSA experiments a clear influence of CsA on MAVS thermal stability was observed. As shown in Figure 23B and Figure 26C major ΔTm shifts were observed for MAVS (4.44°C and 8.42°C in the two experiments, respectively, see also Table 5). However, a few more data points at higher temperatures would be ideal for a more substantiated statement as there is a relative high protein abundance left at 67°C. Nevertheless, CypA -/- based CRISPR/Cas9 CypA-MAVS double knockout cells were created. In Figure 29A the Western blot analysis of the generated knockout cell lines is shown. A confirmed knockout in A549 cells served as MAVS knockout control (lane 2 and wt cells in lane 11, a kind gift from Binder lab[4]; [329]). CypA expression was observed for THP-1 wt cells and A549 based cells, but not in CypA single

---

[4] German Cancer Research Center (DKFZ), Heidelberg, Germany

knockout or CypA-MAVS -/- double knockout cells (Figure 29A). Parental THP-1 and CypA -/- cells as well as A549 cell served as controls for MAVS expression. As can be seen in Figure 29A several single cell clones with a CypA-MAVS -/- could be generated. Thus, the following infection assays were conducted with one representative single cell clone. For HIV-1 LV infection (Figure 29B), CypA-MAVS double knockout cells showed 32.7 % infection while only 23.6 % of THP-1 parental cells were infected. However, the infection of CypA -/- cells was not fully matched (36 % infection). The same was observed for HIV-1 NL4.3 infection (Figure 29E). Additional knockout of MAVS in THP-1 based CypA -/- cells enhanced the capacity of IFNα2 to block HIV-1 LV infection. HIV-1 LV infection was reduced 7.5-fold by IFNα2 treatment (Figure 29C), which is significantly more than observed for THP-1 parental or CypA single knockout cells (1.8-fold and 2.3-fold, respectively). This is in line with the involvement of MAVS in type I IFN-mediated signaling. In response to CsA treatment, a high rescue ability of CsA for the double knockouts was observed. CsA rescued HIV-1 LV infection from the IFNα2 induced infection block in CypA-MAVS double knockout cells by 2.6-fold. This is significantly more than what was observed for THP-1 wt or CypA -/- cells (1.7-fold and 1.4-fold, respectively).

As observed before, the phenotype was different upon HIV-1 NL4.3 infection. Infection of CypA-MAVS double knockout cells was not significantly changed upon CsA stimulation (Figure 29E). Unlike what was observed for CypA-MDA5 double knockout cells (Figure 28E and F), the IFNα2-induced block for CypA-MAVS double knockout cells was as high as observed for CypA single knockout cells (Figure 28F). Therefore, it is unlikely, that effects of CsA were masked. No further reduction of infection was observed upon CsA treatment, but a rescue of the IFN-induced block of HIV-1 NL4.3 infection as seen for CypA single knockout cells was also not observed (Figure 29G). This further punctuates the importance of the RIG-I signaling pathway on HIV-1 infection and a possible role in the CsA-induced increase of HIV-1 infection in the presence of a type I IFN-induced early block to infection.

Another protein involved in the RIG-I signaling pathway is IRF3, an IFN-induced transcription factor. IRF3 is activated upon MAVS and TRADD signaling. Activated IRF3 induces ISG expression and facilitates an antiviral state after infection of various viruses (reviewed in Mogensen 2019). CRISPR/Cas9 IRF3 double knockouts based on CypA -/- cells were obtained as described in section 7.3.3. In Figure 30A the Western blot analysis of CypA-IRF3 -/- cells is shown. A549 and A549 IRF3 -/- served as wt and knockout controls and were obtained from the lab of Marco Binder[5] (unpublished). THP-1 wt and CypA -/- cells served as controls for

---

[5] German Cancer Research Center (DKFZ), Heidelberg, Germany

CypA and IRF3 expression, respectively. As can be seen in lanes 4 to 9 several different single cell clones could be obtained. Infection assays were performed with all of them and the results of one representative cell line is shown in Figure 30B - G. HIV-1 LV infection of CypA-IRF3 double knockout cells showed increased infection compared to THP-1 wt cells (35.8 % and 23.6 %, respectively; Figure 30B), but no difference to CypA single knockout cells could be observed (Figure 30B).
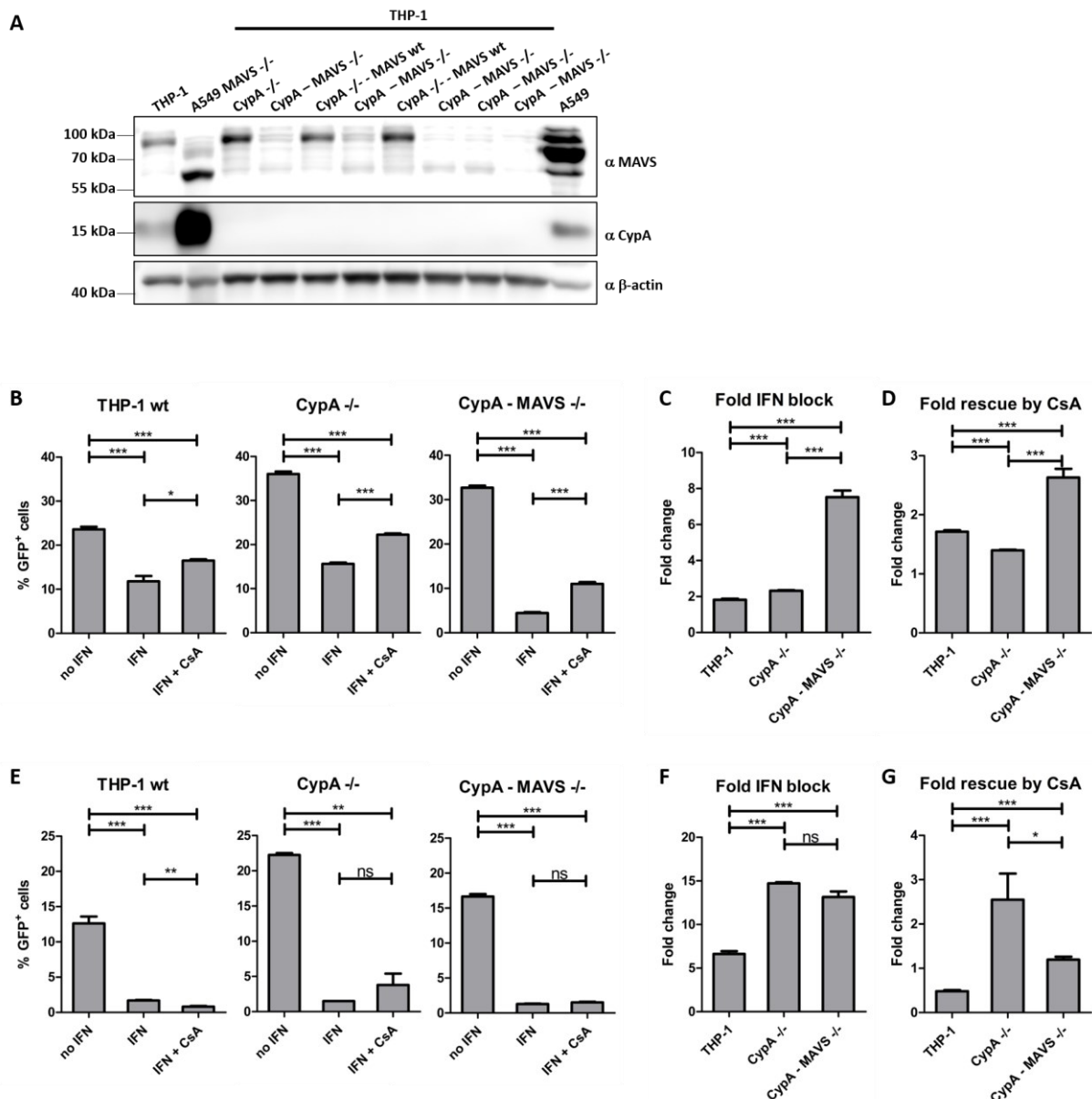

Figure 29: CypA-MAVS knockout (CypA-MAVS -/-) cells are hypersensitive to the type I IFN-induced block of HIV-1infection.

A: THP-1 wt, CypA -/- and THP-1 based CypA and MAVS double knockout (CypA-MAVS -/-) cell lines were analyzed by Western blot for CypA, MAVS and β-actin expression. A569 parental cells and MAVS -/- in these cells served as controls. **B:** THP-1 wt, CypA -/- or CypA-MAVS -/- cells were treated or not with 500 U/ml IFNα2 for 24 h. Prior to infection with VSV-G pseudotyped HIV-1 8.91 LV for 48 h, cells were treated with 2.5 µM CsA. Percentage of GFP positive cells was determined by flow cytometry. Bars indicate the average infectivity determined from two independent experiments and error bars represent standard deviation. Unpaired two-tailed t test was performed (*, p< 0.05; ***, p< 0.001). **C:** Calculated fold changes of IFNα2-induced block

to HIV-1 LV infection. Bars indicate the average fold change and error bars indicate standard deviation. Unpaired two-tailed t test was performed (***, p< 0.001). **D:** Calculated fold changes of HIV-1 LV infection levels upon CsA treatment compared to IFN stimulated cells. Bars indicate the average fold change and error bars indicate standard deviation. Unpaired two-tailed t test was performed (***, p< 0.001). **E:** THP-1 wt cells or CypA-MAVS -/- cells were treated or not with 500 U/ml IFNα2. 24 h post IFN stimulation cells were treated with 2.5 µM CsA. At the time of CsA addition, cells were infected with VSV-G pseudotyped NL4.3 for 48 h. Percentage of GFP positive cells was determined by flow cytometry. Bars indicate the average infectivity determined from three independent experiments and error bars indicate standard deviation. Unpaired two-tailed t test was performed (**, p< 0.01; ***, p< 0.001; ns, not significant). **F:** Calculated fold changes of IFNα2 induced block to NL4.3 infection. Bars indicate the average fold change and error bars indicate standard deviation. Unpaired two-tailed t test was performed (***, p< 0.001; ns, not significant). **G:** Calculated fold changes of NL4.3 infection levels upon CsA treatment compared to IFN stimulated cells. Bars indicate the average fold change and error bars indicate standard deviation. Unpaired two-tailed t test was performed (*, p< 0.05; ***, p< 0.001).

Stimulation with IFNα2 prior to HIV-1 LV infection resulted in a 7.3-fold infection block, which is significantly higher than the block observed for the two control cell lines (Figure 30C, 1.8-fold for THP-1 wt and 2.3-fold for CypA -/- cells). The increased effect of the stimulating drug on the double knockout cells compared to the two control cell lines could also be observed for CsA treatment. In THP-1 parental cells and CypA single knockout cells a rescue of a type I IFN-induced block to HIV-1 infection of 1.7- and 1.4-fold, respectively was observed. In CypA-IRF3 double knockout cells CsA treatment resulted in a 2.9-fold higher infection than monitored for type I IFN treated cells. The obtained fold changes are alike the ones observed for CypA-MAVS -/-. This might indicate that the phenotype observed for MAVS and IRF3 knockouts masks the actual searched for target, as it is a protein acting downstream of both. NL4.3 GFP infection of CypA-IRF3 double knockout cells was more than doubled compared to THP-1 parental cells. THP-1 cells showed 12.6 % infection whereas CypA-IRF3 double knockout cells showed 28.7 % infection, which is also higher than what was shown for CypA -/- cells (22.3 % infection, Figure 30E). Double knockout cells also showed an enhanced response to IFNα2 stimulation compared to THP-1 wt cells (10.1-fold compared to 6.6-fold), however a 14.7-fold reduction of infection as observed for CypA single knockout cells could not be shown (Figure 30F). The response to CsA stimulation was similar to what was observed for other RIG-I signaling pathway knockout cell lines. Indeed, no reduction or enhancement of infection could be observed for the double knockout cells as observed for THP-1 parental cells or CypA single knockout cells, respectively (Figure 30G). However, a 10.1-fold type I IFN block to HIV-1 NL4.3 infection should be sufficient, that CsA effects are not masked by a minor IFN-induced block.

These results confirm the importance of the RIG-I signaling pathway for the innate immune response against HIV-1. The increased infection rates in absence of IRF3 indicate a direct involvement of IRF3 in restricting HIV-1.
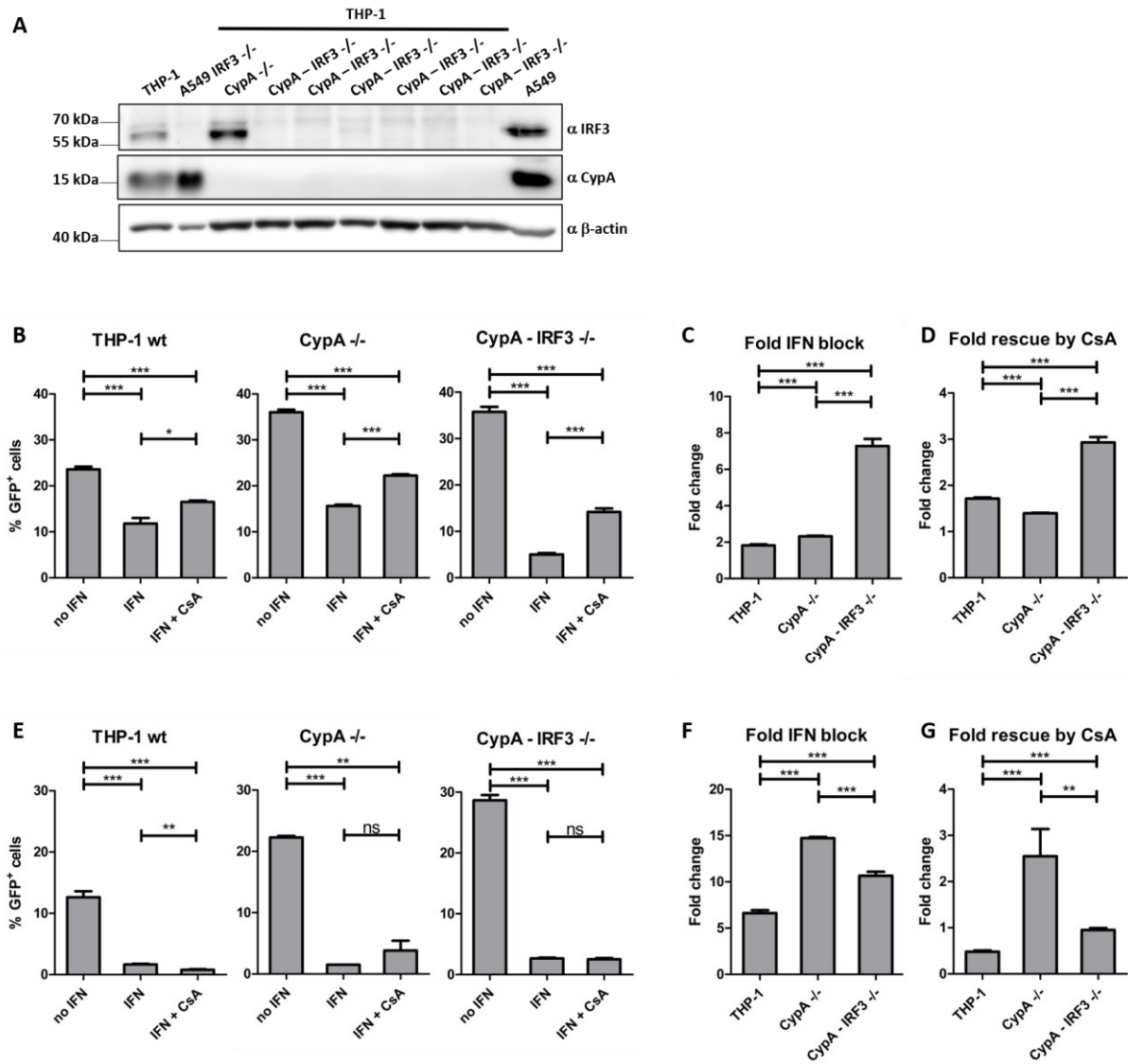
Figure 30: CypA-IRF3 knockout cells (CypA-IRF3 -/-) show hypersensitivity to type I IFN-induced block of HIV-1infection and the rescue of this block by CsA.

A: THP-1 wt, CypA -/- and CypA and IRF3 double knockout (CypA-IRF3 -/-) cell lines were analyzed by Western blot for CypA, IRF3 and β-actin expression. A569 parental cells and an IRF3 -/- in these cells served as controls. **B:** THP-1 wt, CypA -/- or CypA-IRF3 -/- cells were treated or not with 500 U/ml IFNα2. 24 h post IFN stimulation cells were treated with 2.5 μM CsA. At the time of CsA addition, cells were infected with VSV-G pseudotyped HIV-1 LV for 48 h. Percentage of GFP positive cells was determined by flow cytometry. Bars indicate the average infectivity determined from three independent experiments and error bars indicate standard deviation. Unpaired two-tailed t test was performed (*, p< 0.05; ***, p< 0.001). **C:** Calculated fold changes of IFNα2 induced block to HIV-1 LV infection. Bars indicate the average fold change and error bars indicate standard deviation. Unpaired two-tailed t test was performed (***, p< 0.001). **D:** Calculated fold changes of HIV-1 LV infection levels upon CsA treatment compared to IFN stimulated cells. Bars indicate the average fold change and error bars indicate standard deviation. Unpaired two-tailed t test was performed (***, p< 0.001). **E:** THP-1 wt cells or CypA-IRF3 -/- cells were treated or not with 500 U/ml IFNα2. 24 h post IFN stimulation cells were treated with 2.5 μM CsA. At the time of CsA addition, cells were infected with VSV-G pseudotyped NL4.3 for 48 h. Percentage of GFP positive cells was determined by flow cytometry. Bars indicate the average infectivity determined from three independent experiments and error bars indicate standard deviation. Unpaired two-tailed t test was performed (**, p< 0.01; ***, p< 0.001; ns, not significant). **F:** Calculated fold changes of IFNα2 induced block to NL4.3 infection. Bars indicate the average fold change and error bars indicate standard deviation. Unpaired two-tailed t test was performed (***, p< 0.001). **G:** Calculated fold changes of NL4.3 infection levels upon CsA treatment compared to IFN stimulated cells. Bars indicate the average fold change and error bars indicate standard deviation. Unpaired two-tailed t test was performed (**, p< 0.01; ***, p< 0.001).

86

Interestingly, a higher IFN-induced block to infection was observed. As IRF3 induces type I IFN production, the maintenance of the IFN-induced antiviral state should be diminished or at least reduced. However, the cell has various ways to induce IFN production, which could explain the stronger response to IFNα2

8.2.5 CypA-TRADD double knockout shows increased hypersensitivity to type I IFN-induced block of HIV-1 infection.

The last protein investigated in relation to this study is another adaptor protein of the RIG-I signaling pathway. TRADD is directly recruited by MAVS and facilitates the binding of several proteins to the MAVS-induced signaling platform and therefore facilitates downstream signaling of the RIG-I signaling pathway. In the CETSA experiments a clear destabilization of TRADD upon CsA treatment was observed. As listed in Table 5 ΔTm shifts of -3.17°C and -1.67°C were observed in the two experiments, respectively. The corresponding calculated melting curves are shown in Figure 26E. TRADD CRISPR/Cas9 knockout cells were generated. Unfortunately, no other TRADD knockout cell line was available as a control for Western blot analysis. Therefore, only THP-1 wt and CypA -/- cells served as controls for immunoblotting as can be seen in Figure 31A. The used gRNA against human TRADD targets the DNA sequence corresponding to amino acids 28 to 35 and the TRADD antibody used was generated with a C-terminal protein fragment. Therefore, a destroyed epitope is unlikely responsible for the absent protein bands for TRADD in the generated knockout clone. TRADD expression could not be detected for the CypA-TRADD double cell line but was observed in THP-1 and CypA -/- cells.

Next the knockout cell lines were infected with HIV-1 LV or full-length HIV-1 NL4.3, respectively. For HIV-1 LV infection lower infection than for wt cells was observed (Figure 31B, 18.7 % for the double knockout compared to 36 % for CypA -/- cells) and infection of NL4.3 in CypA-TRADD double knockout cells was in the range of what was observed for wt cells (13.3 % and 12.6 %, respectively; Figure 31E). Interestingly, infection of both used virus variants was almost completely prohibited upon IFNα2 treatment in the double knockout cells (0.9 % and 0.4 % for HIV-1 LV and HIV-1 NL4.3, respectively). This is also represented in the fold block induced by IFNα2 to HIV-1 infection. In Figure 31C and F the calculated fold changes in infection upon type I IFN treatment in response to HIV-1 LV and NL4.3 infection are shown, respectively. Both viruses showed over 20-fold reduced infection upon IFNα2 stimulation, an effect observed in this magnitude only for CypA-CypE -/- cells for NL4.3 infection (Figure 21F). For both virus variants, infection increased upon CsA treatment.
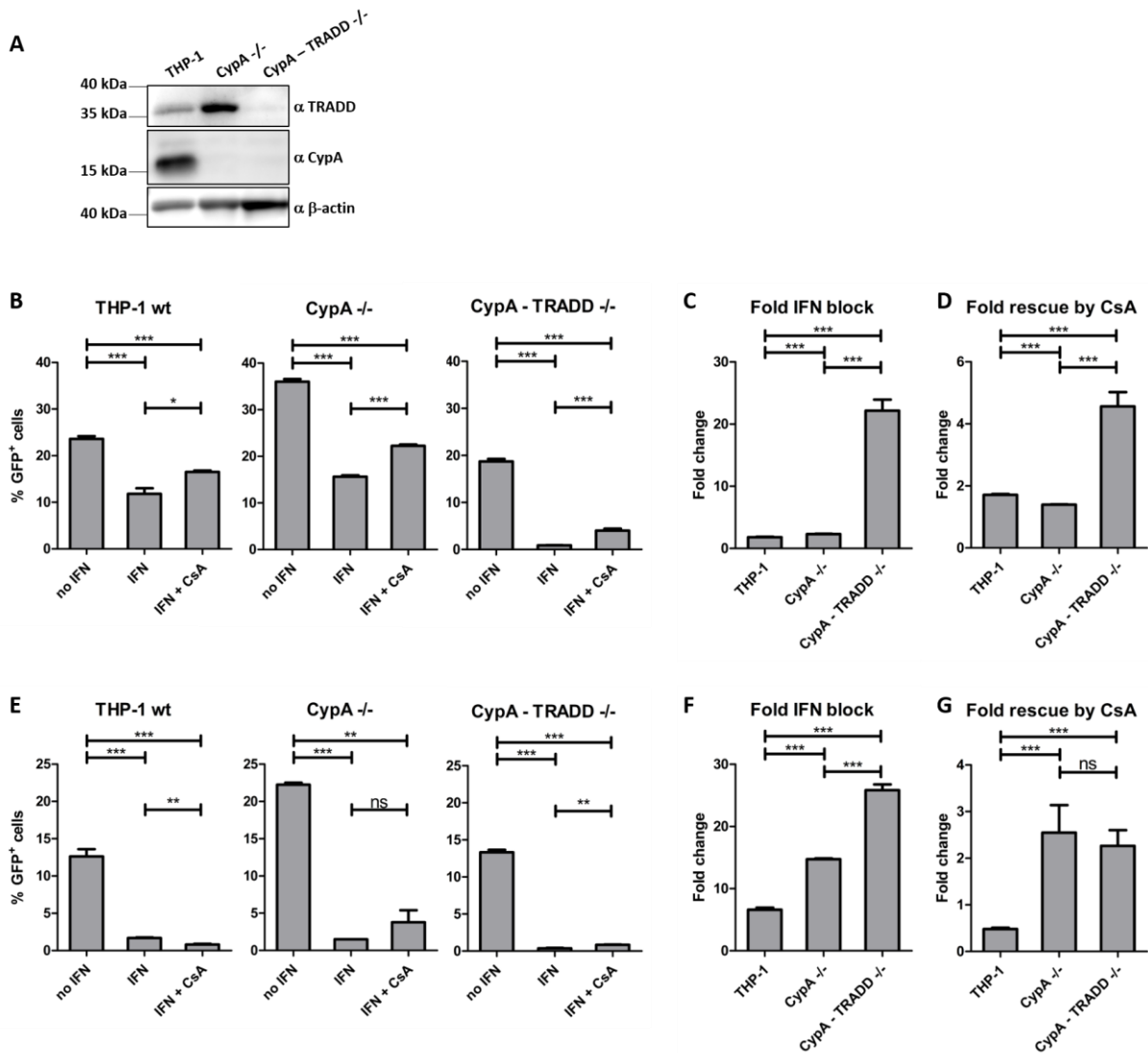
Figure 31: CypA -TRADD knockout cells shows strong hypersensitivity to the type I IFN-induced block of HIV-1 infection and an enhanced rescue from this block by CsA.

A: THP-1 wt, CypA -/- and CypA and TRADD double knockout (CypA-TRADD -/-) cell lines were analyzed by Western blot for CypA, TRADD and β-actin expression. **B:** THP-1 wt, CypA -/- or CypA-TRADD -/- cells were treated or not with 500 U/ml IFNα2. 24 h post IFN stimulation cells were treated with 2.5 μM CsA. At the time of CsA addition, cells were infected with VSV-G pseudotyped HIV-1 LV for 48 h. Percentage of GFP positive cells was determined by flow cytometry. Bars indicate the average infectivity determined from three independent experiments and error bars indicate standard deviation. Unpaired two-tailed t test was performed (*, p< 0.05; ***, p< 0.001; ns, not significant). **C:** Calculated fold changes of IFNα2 induced block to HIV-1 LV infection. Bars indicate the average fold change and error bars indicate standard deviation. Unpaired two-tailed t test was performed (***, p< 0.001). **D:** Calculated fold changes of HIV-1 LV infection levels upon CsA treatment compared to IFN stimulated cells. Bars indicate the average fold change and error bars indicate standard deviation. Unpaired two-tailed t test was performed (***, p< 0.001). **E:** THP-1 wt cells or CypA-TRADD -/- cells were treated or not with 500 U/ml IFNα2. 24 h post IFN stimulation cells were treated with 2.5 μM CsA. At the time of CsA addition, cells were infected with VSV-G pseudotyped NL4.3 for 48 h. Percentage of GFP positive cells was determined by flow cytometry. Bars indicate the average infectivity determined from at least three independent experiments and error bars indicate standard deviation. Unpaired two-tailed t test was performed (**, p< 0.01; ***, p< 0.001; ns, not significant). **F:** Calculated fold changes of IFNα2 induced block to NL4.3 infection. Bars indicate the average fold change and error bars indicate standard deviation. Unpaired two-tailed t test was performed (***, p< 0.001). **G:** Calculated fold changes of NL4.3 infection levels upon CsA treatment compared to IFN stimulated cells. Bars indicate the average fold change and error bars indicate standard deviation. Unpaired two-tailed t test was performed (***, p< 0.001; ns, not significant).

Thus, CsA rescued HIV-1 infection in CypA-TRADD double knockout cells from a type I IFN-induced block. This effect was more pronounced in HIV-1 LV infection (4.6-fold compared to 2.3-fold for NL4.3 infection, see Figure 31D and G). This demonstrates, that TRADD is most likely not the CsA target involved in the phenotype observed for CypA -/- cells.

Table 6: Overview of all observed phenotypes discussed above for CypA- RIG-I signaling pathway double knockout cell lines.
Summary of all observed effects in the above discussed CRISPR/Cas knockout cells. Listed are % GFP positive cells for the indicated condition of HIV-1 LV and HIV-1 NL4.3 infection or the calculated fold changes in response to IFNα2 and CsA. Knockout indicates, which protein is knocked out. THP-1 are parental cells, CypA is a single CypA -/- in THP-1 cells. *= all cells are THP-1 double knockout cells with CypA -/-. - = infection without any stimulation; IFN = infection with previous IFNα2 stimulation (see **7.3.4**); IFN + CsA = infection with IFNα2 and CsA stimulation (see **7.3.4**); Fold block = calculated fold block to infection upon IFNα2 treatment; Fold rescue = calculated change of infection between IFNα2 and IFNα2-CsA stimulated cells. Bold numbers indicate an increase compared to THP-1 parental cells.

Knockout	HIV-1 LV infection					HIV-1 NL4.3 infection				
	-	INF	IFN + CsA	Fold block	Fold rescue	-	INF	IFN + CsA	Fold block	Fold rescue
THP-1	23.6	11.8	16.5	1.8	1.7	12.6	1.7	0.8	6.6	0.5
CypA	**36.0**	15.6	**22.3**	**2.3**	1.4	**22.3**	**1.5**	**3.8**	**14.7**	**2.6**
RIG-I*	**31.5**	14.8	**23.6**	**2.1**	1.6	**23.6**	2.9	**3.1**	**8.3**	**1.1**
MDA5*	15.1	**1.2**	4.9	**12.9**	**4.1**	14.3	4.7	**4.3**	3.1	**0.9**
MAVS*	**32.7**	4.5	11.0	**7.5**	**2.6**	16.7	**1.3**	1.5	**13.2**	**1.2**
IRF3*	**35.8**	5.0	14.2	**7.3**	**2.9**	28.7	2.7	2.5	**10.1**	**1.0**
TRADD*	18.7	**0.9**	4.0	**22.2**	**4.6**	13.3	**0.4**	0.9	**25.9**	**2.3**

Taken together, a lot of different knockout cell lines could be generated within this study. These cell lines are excellent tools to study various functions of cellular proteins involved in innate immune signaling pathways and the involvement of the targeted proteins not only in viral infection but every disease related function. Double knockouts of Cyps can be used to study redundancy amongst Cyps and might shed some light on cellular functions of specific Cyps. The effects of targeted cyclophilins on HIV-1 infection are summarized in Table 1. Most Cyps increased the type I IFN-induced block to HIV-1 infection, thus modulate immunity against HIV-1. However, some like CypA or CypE are more relevant to HIV-1 infection than others. Interestingly, a CsA-sensitive factor aside from CypA is involved in modulating the type I IFN-induced responses to HIV-1 infection. Further knockouts of RIG-I signaling pathway proteins showed an increased IFNα2 block compared to parental cells. An overview of the observed phenotypes is shown in Table 6. As the CETSA experiments identified RIG-I signaling proteins as possible CsA-sensitive factors, it was not surprising, that knockout of these proteins

influenced the responses to CsA stimulation in an IFNα2 dependent manner. The double knockout cell lines provided an interesting insight into crosstalk between proteins and pathways, but further experiments are necessary to provide a concluding statement regarding their effects in HIV-1 infection.

9 Discussion and perspective

In the early nineties CypA was found to be incorporated into HIV-1 particles [141]. Since then, extensive research regarding the role and function of CypA in HIV-1 infection was conducted. Several studies found that despite CypA is incorporated into HIV-1 virions during virus production, target cell CypA is crucial for viral infection [188], [189]. However, cell type specific differences were observed and evidence that CypA influences HIV-1 infection at multiple stages was found. Interestingly, up until now, the involvement of other cyclophilins on HIV-1 infection was investigated only briefly. With this study we provide evidence, that besides CypA at least one other CsA sensitive factor is involved in early post-entry events during HIV-1 infection. With a CRISPR/Cas9 based approach different members of this protein family were investigated as possible HIV-1 host factors and factors involved in innate antiviral immune pathways. Furthermore, an unbiased proteomics approach was used to identify novel IFN-induced CsA-sensitive factors. Besides possible candidates involved in the IFN-induced block and the CsA-induced increase of HIV-1 infection under IFN-stimulated conditions, many other cellular factors were identified for the first time to change in protein thermo-stability in the presence of CsA, indicating possible new direct or indirect targets of CsA.

9.1 CypA -/- show hypersensitivity to IFNα during HIV-1 infection

I have shown that a homozygous knockout of CypA in THP-1 cells slightly elevates HIV-1 infection in THP-1 cells (Figure 10). These effects are independent of general CRISPR/Cas9 effects, as CRISPR control cells do not show an altered response to HIV-1 infection (Figure 11). Many studies observed stabilizing effects of CypA on HIV-1 CA [194], [195]. In CD4$^+$ T cells CypA binding to the CA core prevents premature uncoating, circumvents innate sensing of retroviral DNA, and thus ensures normal infection levels [197]. Furthermore, a study on a South African patient cohort revealed upregulation of CypA following HIV-1 infection. This was accompanied by enhanced viral replication suggesting an involvement of CypA in HIV-1 uncoating [331]. Knockout of CypA in THP-1 cells did not reduce HIV-1 infection upon CypA depletion [209]. The differences in infection might be explained by cell type specific differences and the amount of virus used. It was proposed, that knockout of CypA only reduced infection levels at low viral loads [189], hence differences in viral loads used in the independent studies may account for the different results.

Many groups have discovered the potency of type I IFNs to suppress viral infections, amongst other viruses also HIV-1. IFNα pretreatment could block HIV-1 infection during reverse

transcription in CD4$^+$ T-cells and MDMs [72]. Furthermore, reduction of viral load was observed in clinical trials during IFNα treatment. Unfortunately, HIV-1 RNA rebound after several weeks indicated an escape or desensitization to IFN-induced antiviral effectors [332]. Recent studies suggest that IFNα may induce two early blocks to HIV-1 infection, the first one at the level of reverse transcription and a second one at the level of nuclear import. The first block is sensitive to changes in CA [72], the second one is most likely dependent on MX2 [98]. Bulli and colleagues observed an increased MX2-independent sensitivity of HIV-1 to type-I IFN treatment in CypA -/- cells [209]. Here I show that IFNα2 stimulation of CypA -/- cells reduced HIV-1 infectivity by more than 8-fold compared to wt cells (Figure 10). This magnitude is similar to published data and suggests a protective role of CypA against IFN-induced cellular restriction factors during reverse transcription also proposed by the previous study [209]. This might be due to alterations in the capsid structure upon CypA loss and may provoke or alter interactions with IFNα-induced antiviral effectors. Preventing these stabilizing effects of CypA by introducing the CypA-binding deficient CA mutant P90A also increased sensitivity of HIV-1 to the IFN-induced infection block. Furthermore, depletion of CypA had no additional effects on HIV-1 P90A infection confirming CypA as the responsible factor [209]. Additionally, CypA binding to HIV-1 CA can be prevented by CsA, a cyclophilin inhibitor. Here I have shown, that without IFNα2 stimulation, CsA treatment had no effect on any tested cell line (Figure 11). However, upon IFNα2 treatment, HIV-1 infection could be increased by CsA treatment in CypA knockout cells at least partially rescuing HIV-1 infection from the IFNα2-induced infection block (Figure 10). This is consistent with previous observations showing a rescue of HIV-1 P90A infection [209]. An impact of the immunosuppressive function of CsA was excluded, as a non-immunosuppressive analogue of CsA, Debio-025, showed the same results (Figure 11). These data suggest that an additional host cell cyclophilin other than CypA may directly or indirectly be involved in the type I IFN-induced block to early HIV-1 infection.

Interestingly, the two viral constructs used in the infection assays showed varying results. For infection assays a HIV-1 lentiviral vector lacking the accessory proteins Vpr, Vpu, Vif and Nef and the full-length HIV-1 laboratory strain NL4.3 were pseudotyped with VSV-G. Without pseudotyping, no detectable infection was observed due to low expression levels of CD4 and CCR5 in the cell line used (data not shown). Therefore, switching to an R5 tropic virus strain failed as well. Although the route of entry was altered by pseudotyping, previous results suggest effects of CypA or other CsA targets in the cytosol after cell entry up until nuclear import [72], [98], thus possibly independent of the route of entry. Differences in the viral constructs used

may be explained by 23-point mutations in the HIV-1 GagPol sequence. Some of these mutations are silent. However, three mutations are found in the CA coding region. Given that two of them are silent, an amino acid substitution on position 83 from Leucin in NL4.3 to Valin in 8.91 LV may explain the differences observed between the investigated virus strains. HIV-1 CA is a crucial component for effective viral infection and restriction of HIV-1 by host factors. CA L83 is in close proximity to the CypA-binding loop. Fischer et al. identified the L83V change as causative for differences in HIV-1 NL4.3 and HIV-1 Lai infection differences and apparently residue 83 is crucial for the modulation of TRIM5α restriction [333], [334]. Human TRIM5α was reported to restrict HIV-1 infection dependent on CypA levels [111], [335]. CypA may shield the HIV-1 capsid from human TRIM5α and in CypA depleted cells infection is blocked at a step prior to reverse transcription [111]. However, TRIM5α directly is not likely to be affected by CsA, as it does not show a Tm difference in the CETSA experiment performed within this study (Table 4). Whether the differences between the used virus variants are due to the L83V amino acid change or the HIV-1 accessory proteins are causative for the altered behavior of the used virus variants may be solved by creating CA identical strains of the used viruses and/or constructs with added accessory proteins. However, this was beyond the scope of this study.

9.2   Impact of other Cyclophilins

In human cells at least 17 different Cyps can be expressed. For some Cyps, interaction with HIV-1 proteins has been suggested like CypB [182], CypE and CypF [256] as well as for CypH [336]. Additionally, genome wide screens discovered a high number of Cyp related pseudogenes [171], [337]. Some of these pseudogenes have intact open reading frames and may be expressed under certain conditions [171], [338]. High sequence similarity amongst human Cyp proteins provided an additional challenge. For this study I used a CRISPR/Cas9 based approach to individually target different Cyps in THP-1 cells. THP-1 cells were chosen as a surrogate model for monocyte/macrophage infection of human cells. Unfortunately, CypF and CypG knockouts could not be verified due to the lack of suitable antibodies to detect protein expression. Furthermore, overexpression and knockout of PPIAL4, a CypA pseudogene, remained unsuccessful (data not shown). For the cyclophilins B, C, D, E and H single cell knockout clones could be generated although confirming the genomic phenotype by sequencing proved to be difficult for some of them. For some Cyps gene amplification was impossible, despite several attempts. For others, sequencing results remained ambiguous, as several overlaying sequencing traces could be detected (Figure 9; Figure 14 ;Figure 16; Figure 18). The

parental THP-1 cell line has diploid chromosomes, thus polyploidy effects can be ruled out [339]. However, sequence variations between the two alleles and pseudogenes have not been considered during analysis. Additionally, heterozygous CRISPR/Cas9 knockouts are quite common. The CRISPR/Cas9 approach used in this study generated sequence-specific double strand breaks in the host genome, which are repaired by nonhomologous end joining. This is an error-prone process leading to diverging repairs for the two alleles [340]. For all experiments performed within this study, eliminating functional protein expression of the respective proteins was crucial. This was achieved independent of a homozygous or heterozygous knockout as shown for every cell line used by Western blotting.

Systematic infection of Cyp knockout cell lines revealed variable effects not only on infectivity and sensitivity to IFN but also on the ability of CsA to increase HIV-1 infection from the IFN-induced block. Interestingly, the observed effects were dependent on the viral construct used (e.g. Figure 10) as discussed above. Here I have shown, that despite slight changes in HIV-1 infection, type I IFN and CsA had no influence on infection of CypB knockout cells (Figure 12). However, in the past decades, CypB was reported in various studies to impact HIV-1 infection. CypB can bind to HIV-1 CA [182] and increased nuclear CypB amounts were detected in HIV-1 infected cells [341]. DeBoer and colleagues found that increased CypB but not CypA expression enhanced HIV-1 infection [211]. Furthermore, it was found that CsA treatment reduces the PPIase activity of CypB and promotes CypB secretion [228], [342]. This agrees with our finding, that CsA stimulation affects the thermal stability of CypB (Table 5 and Figure 24). This is reasonable, as CsA is a general PPIase inhibitor and CypB shares high sequence similarity with CypA apart from N- and C-terminal flanking sequences containing an endoplasmic reticulum signal sequence and an nuclear translocation signal [342], [343]. These findings suggest a role of CypB in HIV-1 biology independent of CypA. It was suggested, that CypB increases nuclear import of HIV-1 DNA, as the N-terminal region containing the nuclear localization sequence is crucial for its effects on HIV-1 infection [211], [326]. Using the newly created CypA-CypB double knockout cell line, additive effects of CypA and CypB as well as redundancy amongst these Cyps were investigated. For both viral constructs used (lentiviral vector as well as full-length NL4.3 HIV-1 lab strain), no changes in infection compared to parental THP-1 cells or CRISPR/Cas9 control cells could be observed, whereas for single knockout cells slight differences were observed (Figure 20). In response to type I IFN and CsA, double knockout cells behaved like CypA single knockout cells. This may agree with the finding, that CypB may have a CypA independent role on HIV-1 nuclear import [211]. These effects are most likely only dependent on the nuclear translocation signal of CypB, thus

independent of the CsA binding site. To substantiate these observations, further experiments regarding the impact of CypA, CypB and knockout of both proteins on reverse transcription and nuclear import are necessary. One could use reverse transcription and nuclear import inhibitors as well as 2-LTR circle quantification experiments, a readout for sufficient nuclear import. However, the data presented here provide evidence, that CypB can be excluded as the factor responsible for the CsA-induced HIV-1 infection increase in CypA knockout cells, as in double knockout cells HIV-1 infection is still increased by CsA from the IFN-induced block to infection (Figure 20).

For the cyclophilin family member CypC no direct interaction with HIV-1 is known. CypC is found in the cytosol and a specific function for CypC in ER-redox homeostasis has been proposed [236], [238]. Furthermore, CypC was suggested to modulate immunity by degrading MHC I [239] and CypC was shown to be inhibited by CsA and to form the CsA-dependent complex with Calcineurin [236], [237]. I could confirm this by the Tm shift observed for CypC upon CsA stimulation in the CETSA experiment, although CypC could only be detected in one of the two datasets analyzed (Table 5). Therefore, CypC was included within this study as the potential CsA target responsible for CsA effects observed in CypA knockout cells after type I IFN stimulation. Knockout of CypC in THP-1 cells was successfully accomplished although several sequencing attempts of the obtained knockout clones failed, likely for the reasons discussed above (Figure 13). A reduction in HIV-1 LV infection by nearly 20 % was observed. However, IFN or CsA did not alter the response to HIV-1 compared to THP-1 wt cells (Figure 13). These results imply a function of CypC on HIV-1 infection independent of ISGs or the PPIase domain of CypC. Therefore, it is unlikely that CypC is the CsA-sensitive factor responsible for the rescue effects observed in CypA knockout cells. This could be analyzed with a CypA-CypC double knockout cell line. To further investigate the inhibitory effects of CypC depletion on HIV-1 infection, quantification of reverse transcription products and efficiency of nuclear import in these cells could provide interesting insights into HIV-1 kinetics in the absence of CypC. For CypD, another cytosolic cyclophilin, no distinct function and so far, no evidence for an involvement in HIV-1 infection is known. CypD knockout cells were successfully created and genomic information confirming gene disruption by sequencing was successfully obtained (Figure 14). CypD knockout cells showed a slight increase in HIV-1 infection compared to THP-1 parental and CRISPR/Cas9 control cells. However, no changes in response to IFNα2 or CsA by contrast with parental and control cells were observed (Figure 15). Like CypC, CypD was shown to bind CsA, thus depletion of CypD could potentially have altered the response to CsA [344]. However, CETSA results do not reveal thermal stabilization

of CypD by CsA indicating no effect of CsA on CypD. Given that CypD knockout had only mild effects on HIV-1 infection, CypD can likely be excluded as the CsA sensitive factor this study tried to identify.

Cyclophilin E is an interesting candidate as it shares over 80 % sequence identity with CypA [250]. The size difference between both Cyps is mainly due to a N-terminal RNA binding sequence in CypE, enabling poly(A)+RNA binding [250], [251]. Knockout of CypE in THP-1 cells strongly reduced infection for both, LV as well as full-length NL4.3 (Figure 17). Besides CypA, CypB and CypF, CypE was found to bind HIV-1 CA [256], [345] thus varying responses to altered CA sequences are reasonable. As shown for all used knockout cell lines discussed so far, the capacity of IFNα2 to block HIV-1 infection is intensified for HIV-1 NL4.3 compared to HIV-1 LV and this is also the case in CypE knockout cells. Thus, independent of the cell line used, HIV-1 NL4.3 is more sensitive to type I IFN-induced factors than LV. CypE is a nuclear protein inhibited by CsA as several studies have proposed [237], [249]. Here, I indirectly confirmed the influence of CsA on CypE, as CypE was stabilized in one out of two data sets in the CETSA experiment (Table 5). Therefore, it was not surprising that for LV infection an increase of HIV-1 infection by CsA for CypE knockouts was observed (Figure 17). However, CsA treatment did not increase HIV-1 NL4.3 infection as observed for THP-1 parental cells (Figure 17). This is a reversed effect to what was observed for CypA -/- cells where a 2.6-fold increase was observed. One might speculate that HIV-1 accessory proteins counteract CsA targets, as the effects of CsA were much lower for HIV-1 NL4.3. CypE was previously identified as part of the spliceosome complex [252], but so far evidence for CypE participating in HIV-1 RNA processing is lacking. However, all HIV-1 mRNAs provide the CypE binding feature, a Poly(A) tail [346]. Besides small differences in the CA protein between the two viral constructs used, the NL4.3 genome codes for all HIV-1 accessory proteins, including Vpr. Vpr has been shown to promote viral gene expression [347], [348]. Thus, one can speculate whether Vpr actions make CypE inactivation by CsA irrelevant. Despite the fact that so far no evidence for an involvement of CypE in HIV-1 infection is known, CypE has been discussed as a possible host factor for HCV and IAV infection. CypE plays a role in HCV replication and can bind the nucleoprotein of IAV which results in the inhibition of viral replication and transcription [237], [255]. Interestingly double knockout of CypA and CypE in THP-1 cells provided a phenotype varying only slightly from the one observed for CypA knockouts (Figure 21). CypA-CypE -/- cells showed the strongest block to HIV-1 infection by IFNα2 treatment of all generated Cyp knockout cells, possibly indicating that both Cyps play differential roles in protecting HIV-1 against IFN-induced restriction factors. As CypA is predominantly cytoplasmic and CypE is a

nuclear Cyp, these two could therefore execute protective roles in these two cellular compartments. The absent increase of NL4.3 infection by CsA is surprising, as CsA binding to CypE was shown [237] and thus CsA treatment should either increase or decrease HIV-1 infection in CypE knockout cells. However, I found that infection of CypA-CypE knockout cells did not show a phenotype significantly different to THP-1 parental and CypA single knockout cells except in response to IFNα2 (Figure 21). Although CypE is mainly present in the nucleus, it was recently found in human plasma, similar to CypA [324]. Furthermore, unpublished data from Luis Apolonia indicate redundancy between these two Cyps (L. Apolonia, personal communication, May 2018). The knockout cells created within this study provide an interesting tool to investigate cellular localization of these Cyps. Given the availability of functional and specific antibodies for CypA and CypE in immune fluorescence, changes in cellular localization of these Cyps in the presence or absence of the other could indicate relevant modes of function. As sequence similarity between these Cyps is high, one could also use HA- or Flag-tagged constructs to re-express these proteins in the knockout cell lines. To establish endogenous protein levels, a doxycycline inducible or similar system could be used for controlled protein expression, however, this was beyond the scope of this study. Knocking out CypF and CypG proved to be difficult. Although suitable gRNAs against these two proteins were available, judging protein expression by Western blot was impossible due to the lack of working antibodies. However, CypF expression is upregulated upon IFN treatment (dataset IFM30) [349] making it a suitable candidate responsible for the effects of CsA in type I IFN treated cells. For CypG the effects observed in the CETSA experiment were unclear. In the first dataset analyzed a stabilization of CypG was observed, whereas the second data set suggested a destabilization of CypG by CsA (Table 5). Nonetheless, CypG is influenced by CsA, which is in agreement with previous studies [344], [350]. Furthermore, literature suggests a function of CypG in splicing events [260], [261]. The nuclear localization and a CypG-dependent localization of several SR-rich proteins as well as the direct binding of CypG to RNA Pol II suggest a role in splicing events [260], [261]. Interestingly, TNPO3, a nuclear import receptor for SR-rich proteins promotes HIV-1 infection in an CsA-sensitive manner. Upon CsA addition in TNPO3 depleted Hela cells an HIV-1 infection increase of 4-fold could be observed [195]. Shah and colleagues demonstrate a dependence of TNPO3 function on CypA, but whether another nuclear Cyp may be involved remains elusive [195]. Furthermore, it would be interesting to know if the functions of CypE and CypG are redundant or whether these Cyps influence viral gene expression. Thus, a CypG knockout cell line could be used as a tool to address these questions. The last Cyp of interest for this study was CypH, a cytoplasmic and

nuclear PPIase. Like CypE and CypG its suggested function lies within splicing events [263], [264]. Thus, it may possibly execute a role in HIV-1 gene expression. In line with these results is the significantly reduced HIV-1 infection observed in CypH knockout cells (Figure 19). As these knockout cells do not show an altered infection increase by CsA compared to parental THP-1 cells, a function of CypH independent of its PPIase domain could be possible. Previous studies of CypH revealed additional functions beside its PPIase activity. Although CypH is equally small as CypA, it has a differential binding site for the U4/U6 snRNP complex [264]. Working with CypH knockout cells revealed the importance of suitable antibodies for knockout validation. Starting with single knockouts of CypH a specific antibody for Western blot was available to identify knockout clones. These results could be confirmed by a successful genome sequencing approach across the gRNA target site, verifying the knockout (Figure 18). In the progress of this study CypA-CypH double knockout cells were created. Unfortunately, knockout validation by Western blot was no longer possible due to a new aliquot of the previously used antibody. Using CypA knockout cells as a specificity control, no CypH specific signal could be obtained from the second antibody aliquot used (data not shown). As PCR amplification followed by sequencing of PPIases was not straight forward, this approach was very time consuming and not feasible to use as a first screening method. Therefore, this technique was only applied to confirm Western blot results. Previous studies reported a significantly reduced PPIase activity of CypH compared to CypA possibly indicating a reduced affinity for CsA [262]. This observation could not be confirmed here, as CETSA results revealed a stabilization of CypH for both data sets (Table 5). These results are confirmed by a study from Gaither and colleagues demonstrating the comparative inhibition by CsA and non-immunosuppressive analogues [237]. HIV-1 LV infection of CypH -/- cells revealed an increased sensitivity to type I IFN, indicating a possible involvement of CypH in type I IFN-mediated immunity against HIV-1. So far CypH has not been reported to be upregulated upon IFN stimulation or to exert a function in immunity. Unfortunately, due to time limitations and instrument malfunction, experiments with full-length HIV-1 for CypC, CypD and CypH knockout cells were not possible within the time of this project. These infection assays would provide a better understanding of the differences between the two viral constructs used and give a better understanding for the roles of the respective cyclophilins.

9.3   CETSA identifies novel CsA sensitive factors

To identify the IFN-inducible CsA sensitive factor involved in HIV-1 early infection events, we applied the previously developed cellular thermal shift assay (CETSA). It provides an

excellent unbiased approach for this task [299], [322], [351]. This method has been proven to reveal the proteotype of diverse cell lines, a term reflecting the proteomic state of a cell that links the genotype to the cellular phenotype. As an *in situ* method, this approach can be used to determine the influences of splice isoforms, post-translational modifications, and alternate subcellular localizations, as well as mutational differences and ligand bound states on drug targets. Especially the possibility to detect alternate splicing variants could provide insight into the contribution of pseudogenes or alternatively processed cyclophilin variants to the observed knockout phenotypes. Furthermore, CETSA is an interesting method to reveal effects of a specific drug on the whole proteome containing more than 10,000 expressed gene products at varying expression levels [303]. These findings agree with the results presented here, as almost 7,000 proteins could be successfully detected in the CETSA experiment. Performing the experiment in duplicates as recommended in previous publications [299], [322] enabled more reliable data evaluation and increased the level of certainty for the generated hits. However, the experiment performed here did not include any detergent during cell lysis. As improvements of the originally published workflow showed, using mild detergents during the workflow increases the number of detected membrane proteins greatly without affecting the complete proteome [300]. However, the detergent influence needs to be carefully evaluated for every drug investigated and so far, no CETSA studies for CsA have been performed. Furthermore, the presence of detergent is not suitable for every available mass spectrometer and thus has to be carefully evaluated. The majority of known CsA target proteins are not membrane bound, so a straightforward detergent free approach was chosen. The absent detergent in the used approach resulted indeed in reduced membrane protein detection (e.g. IFITMs could not be detected individually (Table 4)), leaving an important group of proteins unconsidered.

For all proteomics studies, careful and stringent data processing is crucial for reliable conclusions of any kind. Following the advanced protocol from Franken and colleagues, several criteria must be fulfilled for significant thermal stability changes [299]. Experiments should be performed in duplicates, P values for each conducted experiment should be lower than 0.1, each protein detected for both experiments should shift in the same direction, the Tm difference of the two vehicle controls should be lower than the smallest shift observed for the vehicle versus drug experiments, and the calculated melting curves should have a certain steepness and reach a plateau below 0.3 compared to the protein amount detected at 37°C. However, using these stringent restrictions only 16 proteins could be identified to be affected by CsA (listed in Table 3). Except UBTD2 and PRPS1L1 all listed proteins have been reported to be IFN-induced, as they can be found in the interferome database. However, a link to HIV-1 infection could only

be identified for 3 proteins: CFD, EIF4G1 and VAT1. CFD expression is upregulated by HIV-1 env in mesenchymal stem cells [352], an effect most likely irrelevant for the phenotype investigated in this study here. VAT1 expression is upregulated in the presence of HIV-1 Tat or Vpr [353], [354] and the translation initiation factor EIF4G1 has been reported several times in the literature to interact with various HIV-1 proteins. EIF4G1 can be incorporated into HIV-1 Gag virus like particles and is required for the synthesis of the Gag polyprotein [355]–[357]. Furthermore, HIV-1 Tat is found to co-localize with EIF4G1 [358] and HIV-1 protease cleaves EIF4G1 leading to inhibition of protein synthesis [359]–[362]. Of the known CsA targets only PPIF was within this group. PPIF is a known type I and type II IFN-inducible cyclophilin inhibited by CsA (interferome database, entry IFM30, IFM108; IFM30 and IFM53). Unfortunately, CypF knockouts could not be obtained, but with PPIF being the strongest hit amongst all Cyps detected, it would be worthwhile to investigate the role of CypF on HIV-1 infection in future studies. Expression of HA- or Flag-tagged protein variants could overcome the lacking antibody availability, although one has to consider over-expression artefacts. In addition, the generated possible CypF knockout cells could be evaluated by establishing amplification PCR of CypF for sequencing. Although this approach is more time consuming and expensive, with no available antibody it might be the only solution. However, several attempts to amplify the CRISPR/Cas9 targeted gene region failed for the reasons discussed above (8.1.2 and 9.2). Another interesting hit which was not analyzed further within this study is SASS6. It is a type I and type II IFN-induced protein involved in cell division (interferome database, entry IFM59 and IFM35). Previous studies identified SASS6 as an antiviral factor for human papilloma virus infection [363], [364]. Furthermore, an interaction of SASS6 with TAR (HIV-1) RNA binding protein 1 (TARBP) has been proposed [365]. TARBP disengages RNA polymerase II binding from TAR, the HIV-1 Tat binding element to activate viral gene transcription. Thus, SASS6 is an interesting candidate to investigate in future analyses.

The obtained data were carefully analyzed a second and third time with less stringent restrictions providing several additional interesting candidates. For some proteins, e.g. for CypG and CypB, the chosen temperature range was not optimal (Figure 24). The protein concentration at high temperatures was still not low enough to reach the plateau required for the stringent parameters used for the first data analysis. Nonetheless, CypG and CypB were likely affected by CsA in the CETSA experiment, as Tm shifts upon CsA addition were detectable in both data sets (Figure 24 and Table 5) and this could be recapitulated by immunoblotting. For other known targets, no shift in Tm could be observed as seen for example for CypD. Despite inhibition of CypD by CsA has been previously shown [350], these results

suggest no change in thermal stability after CsA addition. However, ligand binding to a protein only results in a thermal shift when binding affects thermal stability of the protein. Especially for large proteins, binding of a small ligand often stabilizes only the binding domain rather than the whole protein per se, thus resulting in low Tm shifts [351]. Another explanation for a missing Tm shift is that unfolding of the ligand binding domain does not promote protein aggregation, thus although the ligand is binding the new protein state does not aggregate with increasing temperatures. Therefore, despite being affected by the drug, no changes in thermal stability in response to drug treatment are observed [296]. Furthermore, the drug concentration used is critical. Ideally it should be high enough to fully saturate all available binding sites. If the concentration is too low, the maximal stabilization effects cannot be detected and competition of several binding sites for one ligand can falsify the results. A simple drug titration experiment to identify the highest possible drug concentration without any cytotoxic effects on cell viability suffices. Although up to 5 µM CsA is suitable for THP-1 cells [366], [367], 2.5 µM CsA was used similar to the infection assays performed within this study, as this CsA concentration is adequate to affect the IFN-inducible CsA sensitive factor during HIV-1 infection.

Interestingly, I found that thermo stability of at least three FKBPs seemed to be affected by CsA as well (see Table 5). Usually, FKBPs are inhibited by rapamycin or FK506 but not CsA [368]. The effect of CsA on FKBPs could be through indirect interaction of CsA with this protein family. CsA clearly influences Cyps and by stabilization or destabilization of cyclophilins all their interaction partners can be affected as well. This should cause smaller shifts in Tm as observed for indirect binding partners of the used drug [299]. One binding partner of the Cyp-CsA complex is calcineurin, which can also bind FKBPs [369]. Therefore, CsA could indirectly affect FKBPs. The experimental approach used for this study only investigated one CsA concentration in living cells. To distinguish between direct and indirect binding partners of CsA amongst the possible target list, a repetition of the experiment with cell extracts could be feasible. In contrast to the performed experiment, previously generated cell extracts are treated with the drug. The remaining workflow is not altered. Thus, only direct binding partners of CsA are identified. This approach could be used in future experiments to reassure the identified targets and discriminate between early and late acting candidates in the CsA pathway. To further evaluate interesting candidates, dose-response curves for interesting targets should be obtained. Therefore, shifts in thermal stability for the respective protein are obtained using a series of varying drug concentrations. To reduce costs, analysis could be performed by immunoblotting, given that suitable antibodies against the chosen targets are

available.

The generated lists of candidates using diverse restriction parameters where analyzed in terms of gene ontology and pathway enrichment. To this end the GOrilla[6] and Enrichr[7] online tools were used. Amongst others, several members of the RIG-I signaling pathway seemed to be affected in their thermal stability upon CsA treatment. The involvement of this pathway in restricting several viruses like West Nile Virus, Influenza A Virus and Coronaviruses [286], [370] as well as the involvement of RIG-I in type I IFN signaling [59], [278] made it an interesting pathway for further analysis in search of a novel type I IFN-inducible CsA target.

9.4 RIG-I pathway and HIV-1

Overall, 17 out of 23 members of the RIG-I signaling pathway were detected in the CETSA experiment, and five of them showed strong Tm shifts upon CsA addition (Table 5), making them candidates to be involved in the CsA-induced increase of HIV-1 infection in type I IFN-stimulated THP-1 cells (pathway overview shown in Figure 7). After careful pathway analysis and with respect to the observed Tm shifts, initially seven targets were chosen for further analysis. RIG-I and MDA5 as the two cytosolic viral target sensors to initiate the pathway, although RIG-I was only mildly affected (see Table 5 and Figure 24). MAVS and TRADD, as two highly affected proteins and key players of the pathway as well as the three downstream proteins IRF3, Caspase8 and Caspase10. For all chosen candidates CRISPR/Cas9 knockouts based on THP-1 CypA -/- cells were generated. This cell line was chosen to better evaluate the effects of these proteins on HIV-1 infection and their response to CsA in the absence of CypA. In parallel single knockouts for each gene in THP-1 cells were generated. However, due to time limitations single cell clones were not investigated for their genotype or phenotype. Except for TRADD, all used gRNAs were previously published, thus knockout cells for all targets were expected to be generated [311]–[314], [371]. For the caspase targets, evaluation of the knockout status was difficult as multiple bands occurred on Western blots and despite testing over 20 clones for each target, no candidate with clearly reduced protein amounts could be obtained (data not shown). This was surprising, as the used gRNAs have been shown to work well in HeLa and Saos2 cells [314], [371]. Especially for Caspase 10, one of the highest Tm shifts of the whole data set was observed after CsA treatment, although the protein was only detected in one experiment. Establishing Caspase10 amplification to sequence the obtained single cell clones could overcome the difficult Western blot detection. Furthermore, repeating the

---

[6] http://cbl-gorilla.cs.technion.ac.il/
[7] http://amp.pharm.mssm.edu/Enrichr/

approach with another gRNA set could generate Caspase10 knockouts for further analysis. As Caspase8 does not show Tm shifts induced by CsA, the effort of generating a Caspase 8 CRISPR/Cas9 THP-1 knockout cell line probably not worth the effort. For the remaining five targets single cell clone evaluation by immunoblot was successful. All used single cell clones did not show protein expression on Western blot, however genotypic information remains elusive. To confirm gene disruption, gene amplification and sequencing should be established for RIG-I, MDA5, MAVS, TRADD and IRF3.

Infecting RIG-I, MDA5, MAVS, TRADD and IRF3 CRISPR/Cas9 knockout cells with HIV-1 revealed, that knockout of MDA5 and TRADD showed clearly reduced infection levels for both viral constructs used compared to THP-1 parental and CypA single knockout cells (Figure 28 and Figure 31, respectively), thus indicating an involvement of these two proteins in HIV-1 infection. A recent study revealed, that HIV-1 TAR and the Rev-response element interact with a complex that facilitates post-transcriptional RNA modifications to evade recognition by MDA5 and consequently avoid the induction of an antiviral state [372]. Furthermore, for TRADD and MDA5 a mRNA upregulation in response to HIV-1 is known [373]–[375]. To my knowledge, no connection between TRADD and CypA is known so far. However, CypA was recently reported to boost RIG-I mediated antiviral signaling by affecting RIG-I, MDA5 and MAVS [376]. It was shown for Sendai virus infection, that CypA knockout impaired RIG-I-mediated type I IFN production [376]. Furthermore, viral replication was promoted, and an enhanced TRIM25 activity was observed. TRIM25 mediates ubiquitination of RIG-I and MAVS, thus ensures the binding of RIG-I to MAVS and downstream signaling [376]. Furthermore, CypA is reported to activate the transcription factor IRF3, another RIG-I signaling pathway member affected by CsA (Table 5 and Figure 24) [224]. Repeating the infection assays in the presence of CypA, as for example with THP-1 based knockout cells, may reveal CypA-independent or CypA-dependent effects of these RIG-I signaling pathway proteins on HIV-1 infection. Whether MDA5 executes a CypA dependent function could also be investigated by observing the phosphorylation status of MDA5 during HIV-1 infection in the presence and absence of CypA, as MDA5 activity is strongly controlled by phosphorylation [377]–[379]. Furthermore, I observed a highly increased HIV-1 infection block after IFNα2 treatment in cells, in which members of the RIG-I signaling pathway were knocked out. At first glance, these findings are counterintuitive, as disruption of an IFN-signaling pathway should possibly not increase viral restriction upon IFN stimulation. However, IFN production and ISG expression is highly regulated, the pathway is very complex and exhibits various signaling cascades and alternative routes. The RIG-I knockouts showed the smallest block to HIV-1 LV infection

induced by type I IFN for all RIG-I signaling pathway knockout cells used. One could speculate, if MDA5, the second cytosolic viral recognition protein could compensate RIG-I signaling function, whereas vice versa RIG-I is unable to resume MDA5 function. Interestingly, CypA-MDA5 double knockout cells are the only cell line investigated in course of this study that showed a higher IFN-induced block to HIV-1 infection for LV than for NL4.3 (12.9-fold for HIV-1 LV, compared to 3.1-fold for NL4.3 infection, Figure 28). This is the smallest block to HIV-1 NL4.3 infection observed within all investigated cell lines and it is significantly lower than observed in THP-1 parental cells. The differential response of MDA5 -/- cells to type I IFN suggests the involvement of HIV-1 accessory proteins in MDA5 function during infection. How exactly type I IFN stimulation modifies the response of RIG-I signaling pathway knockout cells to HIV-1 should be evaluated by quantifying ISG production in future studies. Changes between the individual cell lines and the two viral constructs could provide interesting insights into this complex signaling pathway and its function in HIV-1 infection.

Despite altered sensitivity to IFNα2, RIG-I signaling pathway knockouts showed differential responses to CsA stimulation. Only for TRADD knockouts, a significant rescue of infection upon CsA stimulation could be observed in NL4.3 infection (Figure 31). Thus, TRADD can be excluded as the IFN-inducible CsA sensitive factor responsible for the phenotype observed in IFN-stimulated THP-1 CypA -/- cells by CsA treatment. However, RIG-I, MDA5, MAVS and IRF3 knockout cells did not show a significant effect on HIV-1 infection upon CsA treatment compared to IFN treated cells, it is likely that the IFN-induced CsA-sensitive factor responsible is a member of this signaling pathway. Though, as the early acting proteins MDA5 and RIG-I are equally affected in comparison to the late acting protein IRF3, presumably downstream members of this pathway could be implicated in the investigated effect of CsA. Another interesting member of the RIG-I signaling pathway affected by CsA according to the CETSA experiment is NFκB (Table 5), a key transcription factor involved in immunity. In future studies NFκB activity could be measured in all knockout cell lines by amplification of NFκB target genes. This would not only provide insights into the effects of the investigated proteins on antiviral gene expression, but also how CsA and IFN stimulation change expression patterns. Taken together I created many excellent tools to characterize the functions of cyclophilins and RIG-I signaling pathway members in THP-1 cells. Furthermore, the CETSA provides novel insights into the complex functions of CsA in IFN stimulated THP-1 cells, which can be useful for any future study on cyclophilins.

10 Conclusion

I showed that some members of the cyclophilin protein family are immune modulators of HIV-1 early infection events and that cyclophilins may play differential roles in HIV-1 infection. First, I investigated the impact of CypA, a long-known HIV-1 co-factor, on type I IFN-mediated cellular immunity. Therefore, CRISPR/Cas9 THP-1 CypA knockout cells were infected with HIV-1. I could observe an increased infection of CypA -/- cells compared to parental or control THP-1 cells, indicating a role of CypA in HIV-1 infection. IFNa2 treatment prior to infection showed an increased block to HIV-1 infection compared to THP-1 parental cells, suggesting an involvement of CypA in type I IFN-mediated immunity against HIV-1. Interestingly, I could observe an increased HIV-1 infection upon additional treatment with CsA, a cyclophilin inhibitor. This led us to believe, that another CsA-sensitive possible type I IFN-induced factor may be involved in modulating HIV-1 infection. Therefore, CRISPR/Cas9 THP-1 CypB, CypC, CypD, CypE and CypH knockout cells were generated. Infection assays of these single knockout cells revealed that knockout of CypD could increase HIV-1 infection compared to parental THP-1 cells. However, no changes could be observed in response to IFN or CsA, thus effects of CypD on HIV-1 infection are most likely independent of IFN-induced factors. Depletion of CypB, CypC, CypE and CypH using CRISPR/Cas9 showed increased HIV-1 infection compared to parental THP-1 cells, indicating the potential involvement of several Cyps in HIV-1 infection. However, IFN or CsA treatment did not result in significant changes in HIV-1 NL4.3 infection in those cell lines compared to THP-1 parental cells. To exclude a masking effect of CypA, CRISPR/Cas9 double knockouts of CypA and CypB or CypE were generated and infected. Both cell lines showed a strong increased sensitivity to IFN treatment compared to parental THP-1 or single knockout cells, indicating a complex interplay between Cyps in modulating type I IFN-induced factors involved in HIV-1 infection. CRISPR/Cas9 single cell clones for CypF and CypG were generated, however these clones are not validated regarding their knockout status. As suitable antibodies were not available, single cell clones could be sequenced to disclose the respective genomic phenotypes and use these cell lines as a tool to investigate the role of CypF and CypG in HIV-1 infection. Furthermore, one should investigate at which stages of the HIV-1 life cycle cyclophilins play a role by observing the effect of Cyp knockout on reverse transcription, nuclear import, integration, and viral gene expression.

Since none of the investigated cyclophilins could be identified as the CsA-sensitive possibly type I IFN-inducible factor responsible for increased HIV-1 infection upon CsA treatment in

CypA knockout cells, a unbiased proteomic screen based on altered protein thermal stability upon ligand binding was conducted. Overall, 4307 proteins could be identified in all acquired data sets and several possible novel CsA targets could be identified. However, not all interesting hits could be investigated within the course of this study, but candidates like SASS6 or the previously HIV-1 related proteins CFD, EIF4G1 and VAT1 are interesting proteins for future investigations on their impact on HIV-1 infection and type I IFN modulated immunity against HIV-1.

Since several proteins of the RIG-I signaling pathway could be identified as possible IFN-inducible CsA-sensitive factors. THP-1 CypA knockout cell based CRISPR/Cas9 knockout cells for RIG-I, MDA5, MAVS, IRF3 and TRADD were generated. I could show, that MDA5 and TRADD knockout reduced HIV-1 infection, indicating an involvement of these two proteins in HIV-1 infection. Furthermore, TRADD knockout showed the highest block to HIV-1 infection compared to any other cell line used within this study, indicating TRADD is a key play in type I IFN signaling. In contrast, MDA5 knockout cells were less sensitive to IFN treatment compared to CypA single knockout or THP-1 parental cells, suggesting an involvement of MDA5 in sensing HIV-1. CsA treatment of IFN stimulated HIV-1 infected knockout cells had no impact on infection, except for CypA-TRADD double knockout cells. Thus, knocking out members of the RIG-I signaling pathway diminishes a CsA-induced rescue from an type I IFN induced block to HIV-1 NL4.3 infection in THP-1 CypA knockout cells, suggesting at least one CsA-sensitive member of the RIG-I signaling pathway, although I could not identify one factor. However, I created so far uncharacterized single cell clones for RIG-I, MDA5, MAVS, IRF3 and TRADD knockout in THP-1 parental cells, which could provide useful tools for further studies regarding the involvement of these proteins in HIV-1 infection and their function in modulating immunity.

11 Figure and table legend

12 Publications and contributions

12.1 Publications

Rudd SG, Tsesmetzis N, Sanjiv K, Paulin CBJ, Sandhow L, Kutzner J, Myrberg IH, Bunten SS, Axelsson H, Zhang SM, Rasti A, Mäkelä P, Coggins SAA, Tao S, Suman S, Branca RM, Mermelekas G, Wiita E, Lee S, Walfridsson J, Schinazi RF, Kim B , Lehtiö J, Rassidakis GZ, Pokrovskaja-Tamm K, Warpman-Berglund U, Heyman M, Grandér D, Lehmann S, Lundbäck T, Qian H, Henter JI, Schaller T, Helleday T & Herold N

Ribonucleotide reductase inhibitors suppress SAMHD1 ara-CTPase activity enhancing cytarabine efficacy

EMBO Molecular Medicine, 2020 Mar 6;12(3) doi: 10.15252/emmm.201910419 Epub 2020 Jan 17

12.2 Conference Contributions

Bunten SS, Apolonia L, Pollpeter D, Herold N, Jafari R, Lethiö J, Malim M & Schaller T

Poster presentation: **A cyclosporine-sensitive factor contributes to the type I IFN-induced early block to HIV-1.**

Retroviruses, Cold Spring Harbor Laboratory, NY, USA, 2018

12.3 Contributions

All data shown in this thesis were acquired and analyzed by me, if not stated otherwise. Contributions to this thesis are as follows:

Rozbeh Jafari conducted the CETSA sample processing from the point of protease digestion and the MS experiments. Primary MS data analysis was done by Rozbeh Jafari as well.

13 References

[1]   F. Barré-Sinoussi *et al.*, "Isolation of a T-lymphotropic retrovirus from a patient at risk for acquired immune deficiency syndrome (AIDS)," *Science (80-.).*, vol. 220, no. 4599, pp. 868–871, 1983.

[2]   R. C. Gallo *et al.*, "Isolation of Human T-Cell Leukemia Virus in Acquired Immune Deficiency Syndrome (AIDS)," *Science (80-.).*, vol. 220, no. 4599, pp. 865–867, 1983.

[3]   J. Coffin *et al.*, "Human immunodeficiency viruses," *Science (80-.).*, vol. 232, no. 4751, p. 697, 1986, doi: 10.1126/science.3008335.

[4]   D. D. Ho, A. U. Neumann, A. Perelson, W. Chen, J. M. Leonard, and M. Markowitz, "Rapid Turnover of Plasma Virions and CD4 Lymphocytes in HIV-1 Infection.," *Nature*, vol. 373, pp. 123–126, 1995.

[5]   R. Swanstrom and J. Coffin, "HIV-1 Pathogenesis : The Virus," *Cold Spring Harb. Perspect. Med.*, vol. 2, pp. 1–18, 2012.

[6]   N. G. Sandler *et al.*, "Type I interferon responses in rhesus macaques prevent SIV infection and slow disease progression," *Nature*, vol. 511, no. 7511, pp. 601–605, 2014, doi: 10.1038/nature13554.

[7]   United Nation, "Un Aids Data 2019," 2019.

[8]   Y.-C. Ho *et al.*, "Replication-competent noninduced proviruses in the latent reservoir increase barrier to HIV-1 cure," *Cell*, vol. 155, no. 3, p. 540, 2013, doi: 10.1016/j.cell.2013.09.020.

[9]   G. Hütter *et al.*, "Long-Term Control of HIV by CCR5 Delta32/ Delta32 Stem-Cell Transplantation," *N. Engl. J. Med.*, vol. 360, no. 7, pp. 692–697, 2009, doi: 10.1056/NEJMoa0802905.

[10]   R. K. Gupta *et al.*, "HIV-1 remission following CCR5Δ32/Δ32 haematopoietic stem-cell transplantation," *Nature*, vol. 568, no. 7751, pp. 244–248, 2019, doi: 10.1038/s41586-019-1027-4.

[11]   G. Simmons *et al.*, "Primary, syncytium-inducing human immunodeficiency virus type 1 isolates are dual-tropic and most can use either Lestr or CCR5 as coreceptors for virus entry.," *J. Virol.*, vol. 70, no. 12, pp. 8355–8360, 1996, doi: 10.1128/jvi.70.12.8355-

8360.1996.

[12] S. Wain-Hobson, P. Sonigo, O. Danos, S. Cole, and M. Alizon, "Nucleotide sequence of the AIDS virus, LAV," *Cell*, vol. 40, no. 1, pp. 9–17, 1985, doi: 10.1016/0092-8674(85)90303-4.

[13] L. Ratner *et al.*, "Complete nucleotide sequence of the AIDS virus, HTLV-III," *Nature*, vol. 313, pp. 277–284, 1985.

[14] S. Nyamweya, A. Hegedus, A. Jaye, S. Rowland-Jones, K. L. Flanagan, and D. C. Macallan, "Comparing HIV-1 and HIV-2 infection: Lessons for viral immunopathogenesis," *Rev. Med. Virol.*, vol. 23, pp. 221–240, 2013, doi: 10.1002/rmv.

[15] J. Hemelaar, "The origin and diversity of the HIV-1 pandemic," *Trends Mol. Med.*, vol. 18, no. 3, pp. 182–192, 2012, doi: 10.1016/j.molmed.2011.12.001.

[16] M. Schim van der Loeff and P. Aaby, "Towards a better understanding of the epidemiology of HIV-2," *AIDS*, pp. 69–84, 1999.

[17] V. Soriano *et al.*, "Epidemiology of HIV-2 infection in Spain. The HIV-2 Spanish Study Group," *Eur J Clin Microbiol Infect Dis*, vol. 15, no. 5, pp. 383–388, 1996.

[18] V. Soriano *et al.*, "Human immunodeficiency virus type 2 (HIV-2) in Portugal: clinical spectrum, circulating subtypes, virus isolation, and plasma viral load," *J. Med. Virol.*, vol. 61, no. 1, pp. 111–116, 2000.

[19] A. A. Waheed and E. O. Freed, "The role of lipids in retrovirus replication," *Viruses*, vol. 2, no. 5, pp. 1146–1180, 2010, doi: 10.3390/v2051146.

[20] N. M. Bell and A. M. L. Lever, "HIV Gag polyprotein: Processing and early viral particle assembly," *Trends Microbiol.*, vol. 21, no. 3, pp. 136–144, 2013, doi: 10.1016/j.tim.2012.11.006.

[21] R. R. Regoes and S. Bonhoeffer, "The HIV coreceptor switch: A population dynamical perspective," *Trends Microbiol.*, vol. 13, no. 6, pp. 269–277, 2005, doi: 10.1016/j.tim.2005.04.005.

[22] J. M. Coffin, S. H. Hughes, and H. E. Varmus, *Retroviruses*. Cold Spring Harbor Laboratory Press, 1997.

[23] J. A. G. Briggs, T. Wilk, R. Welker, H. G. Kräusslich, and S. D. Fuller, "Structural

organization of authentic, mature HIV-1 virions and cores," *EMBO J.*, vol. 22, no. 7, pp. 1707–1715, 2003, doi: 10.1093/emboj/cdg143.

[24] J. A. G. Briggs, K. Grünewald, B. Glass, F. Förster, H. G. Kräusslich, and S. D. Fuller, "The mechanism of HIV-1 core assembly: Insights from three-dimensional reconstructions of authentic virions," *Structure*, vol. 14, no. 1, pp. 15–20, 2006, doi: 10.1016/j.str.2005.09.010.

[25] E. M. Campbell and T. J. Hope, "HIV-1 capsid: The multifaceted key player in HIV-1 infection," *Nat. Rev. Microbiol.*, vol. 13, no. 8, pp. 471–483, 2015, doi: 10.1038/nrmicro3503.

[26] D. C. Chan and P. S. Kim, "HIV Entry and Its Inhibition," *Cell*, vol. 93, pp. 681–684, 1998, doi: 10.1021/ja01618a044.

[27] S. Bour, R. Geleziunas, and M. A. Wainberg, "The human immunodeficiency virus type 1 (HIV-1) CD4 receptor and its central role in promotion of HIV-1 infection," *Microbiol. Rev.*, vol. 59, no. 1, pp. 63–93, 1995, doi: 10.1128/mmbr.59.1.63-93.1995.

[28] E. Chertova *et al.*, "Envelope Glycoprotein Incorporation, Not Shedding of Surface Envelope Glycoprotein (gp120/SU), Is the Primary Determinant of SU Content of Purified Human Immunodeficiency Virus Type 1 and Simian Immunodeficiency Virus," *J. Virol.*, vol. 76, no. 11, pp. 5315–5325, 2002, doi: 10.1128/jvi.76.11.5315-5325.2002.

[29] P. Zhu *et al.*, "Electron tomography analysis of envelope glycoprotein trimers on HIV and simian immunodeficiency virus virions," *Proc. Natl. Acad. Sci. U. S. A.*, vol. 100, no. 26, pp. 15812–15817, 2003, doi: 10.1073/pnas.2634931100.

[30] A. Trkola *et al.*, "CD4-dependent, antibody- sensitive interactions between HIV-1 and its co-receptor CCR-5," *Nature*, vol. 384, pp. 184–187, 1996.

[31] L. Wu *et al.*, "CD4-induced interaction of primary HIV-1 gp120 glycoproteins with the chemokine receptor CCR-5," *Nature*, vol. 384, pp. 179–183, 1996, doi: 10.1038/nature02336.1.

[32] E. O. Freed, D. J. Myers, and R. Risser, "Characterization of the fusion domain of the human immunodeficiency virus type 1 envelope glycoprotein gp41," *Proc. Natl. Acad. Sci. U. S. A.*, vol. 87, no. 12, pp. 4650–4654, 1990, doi: 10.1073/pnas.87.12.4650.

[33] W. Weissenhorn, A. Dessen, S. C. Harrison, J. J. Skehel, and D. C. Wiley, "Atomic

structure of the ectodomain from HIV-1 gp41," *Nature*, vol. 387, pp. 426–430, 1997, doi: 10.1038/387426a0.

[34]   D. C. Chan, D. Fass, J. M. Berger, and P. S. Kim, "Core structure of gp41 from the HIV envelope glycoprotein," *Cell*, vol. 89, no. 2, pp. 263–273, 1997, doi: 10.1016/S0092-8674(00)80205-6.

[35]   N. Herold, M. Anders-Osswein, B. Glass, M. Eckhardt, B. Muller, and H.-G. Krausslich, "HIV-1 Entry in SupT1-R5, CEM-ss, and Primary CD4+ T Cells Occurs at the Plasma Membrane and Does Not Require Endocytosis," *J. Virol.*, vol. 88, no. 24, pp. 13956–13970, 2014, doi: 10.1128/jvi.01543-14.

[36]   R. W. Doms and J. P. Moore, "HIV-1 membrane fusion: Targets of opportunity," *J. Cell Biol.*, vol. 151, no. 2, pp. 9–13, 2000.

[37]   H. M. Temin and S. Mizutani, "RNA-dependent DNA polymerase in virions of Rous sarcoma virus. 1970.," *Biotechnology*, vol. 24, pp. 51–56, 1992.

[38]   S. G. Sarafianos *et al.*, "Structure and Function of HIV-1 Reverse Transcriptase: Molecular Mechanisms of Polymerization and Inhibition," *J. Mol. Biol.*, vol. 385, no. 3, pp. 693–713, 2009, doi: 10.1016/j.jmb.2008.10.071.

[39]   B. Maillot *et al.*, "Structural and Functional Role of INI1 and LEDGF in the HIV-1 Preintegration Complex," *PLoS One*, vol. 8, no. 4, 2013, doi: 10.1371/journal.pone.0060734.

[40]   B. K. Ganser-Pornillos, M. Yeager, and W. I. Sundquist, "The structural biology of HIV assembly," *Curr. Opin. Struct. Biol.*, vol. 18, no. 2, pp. 203–217, 2008, doi: 10.1016/j.sbi.2008.02.001.

[41]   F. Di Nunzio, "New insights in the role of nucleoporins: A bridge leading to concerted steps from HIV-1 nuclear entry until integration," *Virus Res.*, vol. 178, no. 2, pp. 187–196, 2013, doi: 10.1016/j.virusres.2013.09.003.

[42]   A. R. W. Schröder, P. Shinn, H. Chen, C. C. Berry, J. R. Ecker, and F. D. Bushman, "HIV-1 Integration in the Human Genome Favors Active Genes and Local Hotspots," *Cell*, vol. 110, no. 4, pp. 521–529, 2002.

[43]   C. M. Farnet, B. Wang, J. R. Lipford, and F. D. Bushman, "Differential inhibition of HIV-1 preintegration complexes and purified integrase protein by small molecules,"

Proc. Natl. Acad. Sci. U. S. A., vol. 93, no. 18, pp. 9742–9747, 1996, doi: 10.1073/pnas.93.18.9742.

[44]   C. Van Lint, S. Bouchat, and A. Marcello, "HIV-1 transcription and latency: An update," *Retrovirology*, vol. 10, no. 1, p. 1, 2013, doi: 10.1186/1742-4690-10-67.

[45]   M. Lusic and R. F. Siliciano, "Nuclear landscape of HIV-1 infection and integration," *Nat. Rev. Microbiol.*, vol. 15, no. 2, pp. 69–82, 2017, doi: 10.1038/nrmicro.2016.162.

[46]   S.-Y. Kao, A. F. Calman, A. Luciw, Paul, and B. M. Peterlin, "Anti-termination of transcription within the long terminal repeat of HIV -1 by tat gene product," *Nature*, vol. 330, pp. 489–493, 1987.

[47]   A. G. Fisher *et al.*, "The trans-activator gene of HTLV-III is essential for virus replication," *Nature*, vol. 320, no. 6060, pp. 367–371, 1986, doi: 10.1038/320367a0.

[48]   K. T. Jeang, H. Xiao, and E. A. Rich, "Multifaceted activities of the HIV-1 transactivator of transcription, Tat," *J. Biol. Chem.*, vol. 274, no. 41, pp. 28837–28840, 1999, doi: 10.1074/jbc.274.41.28837.

[49]   S. Schwartz, B. K. Felber, E. M. Fenyö, and G. N. Pavlakis, "Env and Vpu proteins of human immunodeficiency virus type 1 are produced from multiple bicistronic mRNAs.," *J. Virol.*, vol. 64, no. 11, pp. 5448–5456, 1990, doi: 10.1128/jvi.64.11.5448-5456.1990.

[50]   A. M. Lever and K.-T. Jeang, "Replication of human immunodeficiency virus type 1 from entry to exit.," *Int J Hematol.*, vol. 84, no. 1, pp. 223–30, 2006.

[51]   M. A. Checkley, B. G. Luttge, and E. O. Freed, "HIV-1 envelope glycoprotein biosynthesis, trafficking and incorporation," *J. Mol. Biol.*, vol. 410, no. 4, pp. 582–608, 2011, doi: 10.1016/j.jmb.2011.04.042.

[52]   T. Dorfman, F. Mammano, W. A. Haseltine, and H. G. Göttlinger, "Role of the matrix protein in the virion association of the human immunodeficiency virus type 1 envelope glycoprotein.," *J. Virol.*, vol. 68, no. 3, pp. 1689–1696, 1994, doi: 10.1128/jvi.68.3.1689-1696.1994.

[53]   P. D. Bieniasz, "Late budding domains and host proteins in enveloped virus release," *Virology*, vol. 344, no. 1, pp. 55–63, 2006, doi: 10.1016/j.virol.2005.09.044.

[54]   C. Peng, B. K. Ho, T. W. Chang, and N. T. Chang, "Role of human immunodeficiency virus type 1-specific protease in core protein maturation and viral infectivity.," *J. Virol.*,

vol. 63, no. 6, pp. 2550–2556, 1989, doi: 10.1128/jvi.63.6.2550-2556.1989.

[55] N. E. Kohl *et al.*, "Active human immunodeficiency virus protease is required for viral infectivity," *Proc. Natl. Acad. Sci. U. S. A.*, vol. 85, no. 13, pp. 4686–4690, 1988, doi: 10.1073/pnas.85.13.4686.

[56] J. Chojnacki *et al.*, "Maturation-dependent HIV-1 surface protein redistribution revealed by fluorescence nanoscopy," *Science (80-.).*, vol. 338, no. 6106, pp. 524–528, 2012, doi: 10.1126/science.1226359.

[57] H. Cheon, E. C. Borden, and G. R. Stark, "Interferons and their stimulated genes in the tumor microenvironment," *Semin. Oncol.*, vol. 41, no. 2, pp. 156–173, 2014, doi: 10.1053/j.seminoncol.2014.02.002.

[58] P. Fitzgerald-Bocarsly, J. Dai, and S. Singh, "Plasmacytoid dendritic cells and type I IFN: 50 years of convergent history," *Cytokine Growth Factor Rev.*, vol. 19, no. 1, pp. 3–19, 2008.

[59] J. W. Schoggins *et al.*, "A diverse range of gene products are effectors of the type i interferon antiviral response," *Nature*, vol. 472, no. 7344, pp. 481–485, 2011, doi: 10.1038/nature09907.

[60] J. M. Jimenez-Guardeño, L. Apolonia, G. Betancor, and M. H. Malim, "Immunoproteasome activation enables human TRIM5α restriction of HIV-1," *Nat. Microbiol.*, vol. 4, pp. 933–940, 2019.

[61] D. Blanco-Melo, S. Venkatesh, and P. D. Bieniasz, "Intrinsic cellular defenses agains HIV," *Immunity*, vol. 37, no. 3, pp. 399–411, 2012, doi: 10.1016/j.immuni.2012.08.013.INTRINSIC.

[62] M. K. Chelbi-Alix and J. Wietzerbin, "Interferon, a growing cytokine family: 50 years of interferon research," *Biochimie*, vol. 89, no. 6–7, pp. 713–718, 2007, doi: 10.1016/j.biochi.2007.05.001.

[63] K. Gibbert, J. F. Schlaak, D. Yang, and U. Dittmer, "IFN-α subtypes: Distinct biological activities in anti-viral therapy," *Br. J. Pharmacol.*, vol. 168, no. 5, pp. 1048–1058, 2013, doi: 10.1111/bph.12010.

[64] J. Bitzegeio, M. Sampias, P. D. Bieniasz, and T. Hatziioannou, "Adaptation to the Interferon-Induced Antiviral State by Human and Simian Immunodeficiency Viruses,"

J. Virol., vol. 87, no. 6, pp. 3549–3560, 2013, doi: 10.1128/jvi.03219-12.

[65]   M. B. Agy, R. L. Acker, C. H. Sherbert, and M. G. Katze, "Interferon Treatment Inhibits Virus Replication in HIV-1- and SIV-Infected CD4+ T-Cell Lines by Distinct Mechanisms: Evidence for Decreased Stability and Aberrant Processing of HIV-1 Proteins," *Virology*, vol. 214, no. 2, pp. 379–386, 1995, doi: 10.1006/viro.1995.0047.

[66]   D. D. Ho *et al.*, "Recombinant human interferon alfa-A suppresses HTLV-III replication in vitro," *Lancet*, vol. 324, no. 8400, p. 455, 1985, doi: 10.1016/S0140-6736(84)92922-2.

[67]   L. Baca-Regen, N. Heinzinger, M. Stevenson, and H. E. Gendelman, "Alpha interferon-induced antiretroviral activities: restriction of viral nucleic acid synthesis and progeny virion production in human immunodeficiency virus type 1-infected monocytes.," *J. Virol.*, vol. 68, no. 11, pp. 7559–7565, 1994, doi: 10.1128/jvi.68.11.7559-7565.1994.

[68]   M. H. Malim and P. D. Bieniasz, "HIV restriction factors and mechanisms of evasion," *Cold Spring Harb. Perspect. Med.*, vol. 2, no. 5, pp. 1–16, 2012, doi: 10.1101/cshperspect.a006940.

[69]   Y. Shirazi and P. M. Pitha, "Alpha interferon inhibits early stages of the human immunodeficiency virus type 1 replication cycle.," *J. Virol.*, vol. 66, no. 3, pp. 1321–1328, 1992, doi: 10.1128/jvi.66.3.1321-1328.1992.

[70]   V. Vieillard, E. Lauret, V. Rousseau, and E. De Maeyer, "Blocking of retroviral infection at a step prior to reverse transcription in cells transformed to constitutively express interferon β," *Proc. Natl. Acad. Sci. U. S. A.*, vol. 91, no. 7, pp. 2689–2693, 1994, doi: 10.1073/pnas.91.7.2689.

[71]   O. Yamada, N. Hattori, T. Kurihura, M. Kita, and T. Kishida, "Inhibition of Growth of HIV by Human Natural Interferon In Vitro," *AIDS Res. Hum. Retroviruses*, vol. 4, no. 4, pp. 287–294, 1988, doi: 10.1089/aid.1988.4.287.

[72]   C. Goujon and M. H. Malim, "Characterization of the Alpha Interferon-Induced Postentry Block to HIV-1 Infection in Primary Human Macrophages and T Cells," *J. Virol.*, vol. 84, no. 18, pp. 9254–9266, 2010, doi: 10.1128/jvi.00854-10.

[73]   D. Mildvan *et al.*, "Synergy, activity and tolerability of zidovudine and interferon-alpha in patients with symptomatic HIV-1 infection: ACTG 068," *Antivir. Ther.*, vol. 1, no. 2, pp. 77–88, 1996.

[74] F. J. Torriani *et al.*, "Hepatitis C Virus (HCV) and Human Immunodeficiency Virus (HIV) Dynamics during HCV Treatment in HCV/HIV Coinfection," *J. Infect. Dis.*, vol. 188, no. 10, pp. 1498–1507, 2003, doi: 10.1086/379255.

[75] A. R. Sedaghat *et al.*, "Chronic CD4+ T-Cell Activation and Depletion in Human Immunodeficiency Virus Type 1 Infection: Type I Interferon-Mediated Disruption of T-Cell Dynamics," *J. Virol.*, vol. 82, no. 4, pp. 1870–1883, 2008, doi: 10.1128/jvi.02228-07.

[76] A. S. Liovat *et al.*, "Acute Plasma Biomarkers of T Cell Activation Set-Point Levels and of Disease Progression in HIV-1 Infection," *PLoS One*, vol. 7, no. 10, pp. 1–13, 2012, doi: 10.1371/journal.pone.0046143.

[77] A. M. Sheehy, N. C. Gaddis, J. D. Choi, and M. H. Malim, "Isolation of a human gene that inhibits HIV-1 infection and is suppressed by the viral Vif protein," *Nature*, vol. 418, pp. 646–650, 2002, doi: 10.1038/nature00969.Published.

[78] R. S. Harris and J. P. Dudley, "APOBECs and virus restriction," *Virology*, vol. 479, pp. 131–145, 2015, doi: 10.1016/j.virol.2015.03.012.

[79] R. Suspène, D. Guétard, M. Henry, P. Sommer, S. Wain-Hobson, and J. P. Vartanian, "Extensive editing of both hepatitis B virus DNA strands by APOBEC3 cytidine deaminases in vitro and in vivo," *Proc. Natl. Acad. Sci. U. S. A.*, vol. 102, no. 23, pp. 8321–8326, 2005, doi: 10.1073/pnas.0408223102.

[80] R. Mahieux *et al.*, "Extensive editing of a small fraction of human T-cell leukemia virus type 1 genomes by four APOBEC3 cytidine deaminases," *J. Gen. Virol.*, vol. 86, no. 9, pp. 2489–2494, 2005, doi: 10.1099/vir.0.80973-0.

[81] D. Pollpeter *et al.*, "Deep sequencing of HIV-1 reverse transcripts reveals the multifaceted antiviral functions of APOBEC3G," *Nat. Microbiol.*, vol. 3, pp. 220–233, 2018.

[82] H. Zhang, B. Yang, R. J. Pomerantz, C. Zhang, S. C. Arunachalam, and L. Gao, "The cytidine deaminase CEM15 induces hypermutation in newly synthesized HIV-1 DNA," *Nature*, vol. 424, no. 6944, pp. 94–98, 2003, doi: 10.1038/nature01707.

[83] B. Mangeat, P. Turelli, G. Caron, M. Friedli, L. Perrin, and D. Trono, "Broad antiretroviral defence by human APOBEC3G through lethal editing of nascent reverse transcripts," *Nature*, vol. 424, no. 6944, pp. 99–103, 2003, doi: 10.1038/nature01709.

[84] M. H. Malim, "Natural resistance to HIV infection: The Vif-APOBEC interaction," *Comptes Rendus - Biol.*, vol. 329, no. 11, pp. 871–875, 2006, doi: 10.1016/j.crvi.2006.01.012.

[85] S. Kupzig, V. Korolchuk, R. Rollason, A. Sugden, A. Wilde, and G. Banting, "Bst-2/HM1.24 is a raft-associated apical membrane protein with an unusual topology," *Traffic*, vol. 4, no. 10, pp. 694–709, 2003, doi: 10.1034/j.1600-0854.2003.00129.x.

[86] N. Jouvenet *et al.*, "Broad-Spectrum Inhibition of Retroviral and Filoviral Particle Release by Tetherin," *J. Virol.*, vol. 83, no. 4, pp. 1837–1844, 2009, doi: 10.1128/jvi.02211-08.

[87] R. L. Kaletsky, J. R. Francica, C. Agrawal-Gamse, and P. Bates, "Tetherin-mediated restriction of filovirus budding is antagonized by the Ebola glycoprotein," *Proc. Natl. Acad. Sci. U. S. A.*, vol. 106, no. 8, pp. 2886–2891, 2009, doi: 10.1073/pnas.0811014106.

[88] N. Van Damme *et al.*, "The Interferon-Induced Protein BST-2 Restricts HIV-1 Release and Is Downregulated from the Cell Surface by the Viral Vpu Protein," *Cell Host Microbe*, vol. 3, no. 4, pp. 245–252, 2008, doi: 10.1016/j.chom.2008.03.001.

[89] M. S. Diamond and M. Farzan, "The broad-spectrum antiviral functions of IFIT and IFITM proteins," *Nat Rev Immunol*, vol. 13, no. 1, pp. 46–57, 2013, doi: 10.1038/jid.2014.371.

[90] J. Lu, Q. Pan, L. Rong, W. He, S.-L. Liu, and C. Liang, "The IFITM Proteins Inhibit HIV-1 Infection," *J. Virol.*, vol. 85, no. 8, pp. 4043–4043, 2011, doi: 10.1128/jvi.00312-11.

[91] A. L. Brass *et al.*, "The IFITM Proteins Mediate Cellular Resistance to Influenza A H1N1 Virus, West Nile Virus, and Dengue Virus," *Cell*, vol. 139, no. 7, pp. 1243–1254, 2009, doi: 10.1016/j.cell.2009.12.017.

[92] D. Jiang *et al.*, "Identification of Five Interferon-Induced Cellular Proteins That Inhibit West Nile Virus and Dengue Virus Infections," *J. Virol.*, vol. 84, no. 16, pp. 8332–8341, 2010, doi: 10.1128/jvi.02199-09.

[93] J. M. Weidner, D. Jiang, X.-B. Pan, J. Chang, T. M. Block, and J.-T. Guo, "Interferon-Induced Cell Membrane Proteins, IFITM3 and Tetherin, Inhibit Vesicular Stomatitis Virus Infection via Distinct Mechanisms," *J. Virol.*, vol. 84, no. 24, pp. 12646–12657, 2010, doi: 10.1128/jvi.01328-10.

[94] J. Yu *et al.*, "IFITM Proteins Restrict HIV-1 Infection by Antagonizing the Envelope Glycoprotein," *Cell Rep.*, vol. 13, no. 1, pp. 145–156, 2015, doi: 10.1016/j.physbeh.2017.03.040.

[95] J. Pavlovic, T. Zürcher, O. Haller, and P. Staeheli, "Resistance to influenza virus and vesicular stomatitis virus conferred by expression of human MxA protein.," *J. Virol.*, vol. 64, no. 7, pp. 3370–3375, 1990, doi: 10.1128/jvi.64.7.3370-3375.1990.

[96] O. Haller and G. Kochs, "Human MxA Protein: An Interferon-induced Dynamin-Like GTPase with Broad Antiviral Activity," *J. Interf. Cytokine Res.*, vol. 31, no. 1, 2011.

[97] S. Y. Liu, D. J. Sanchez, R. Aliyari, S. Lu, and G. Cheng, "Systematic identification of type I and type II interferon-induced antiviral factors," *Proc. Natl. Acad. Sci. U. S. A.*, vol. 109, no. 11, pp. 4239–4244, 2012, doi: 10.1073/pnas.1114981109.

[98] C. Goujon *et al.*, "Human MX2 is an interferon-induced post-entry inhibitor of HIV-1 infection," *Nature*, vol. 502, no. 7472, pp. 559–562, 2013, doi: 10.1038/nature12542.

[99] M. Kane *et al.*, "Mx2 is an interferon induced inhibitor of HIV-1 infection," *Nature*, vol. 502, no. 1, pp. 563–566, 2013, doi: 10.1038/jid.2014.371.

[100] M. C. King, G. Raposo, and M. A. Lemmon, "Inhibition of nuclear import and cell-cycle progression by mutated forms of the dynamin-like GTPase MxB," *Proc. Natl. Acad. Sci. U. S. A.*, vol. 101, no. 24, pp. 8957–8962, 2004, doi: 10.1073/pnas.0403167101.

[101] B. Schulte *et al.*, "Restriction of HIV-1 Requires the N-Terminal Region of MxB as a Capsid-Binding Motif but Not as a Nuclear Localization Signal," *J. Virol.*, vol. 89, no. 16, pp. 8599–8610, 2015, doi: 10.1128/jvi.00753-15.

[102] C. Goujon, R. A. Greenbury, S. Papaioannou, T. Doyle, and M. H. Malim, "A Triple-Arginine Motif in the Amino-Terminal Domain and Oligomerization Are Required for HIV-1 Inhibition by Human MX2," *J. Virol.*, vol. 89, no. 8, pp. 4676–4680, 2015, doi: 10.1128/jvi.00169-15.

[103] Z. Liu *et al.*, "The interferon-inducible MxB protein inhibits HIV-1 infection," *Cell Host Microbe*, vol. 14, no. 4, pp. 398–410, 2013, doi: 10.1016/j.chom.2013.08.015.

[104] B. Liu, X. Wen, C. Huang, and Y. Wei, "Unraveling the complexity of hepatitis B virus: From molecular understanding to therapeutic strategy in 50 years," *Int. J. Biochem. Cell Biol.*, vol. 45, pp. 1987–1996, 2013, doi: 10.1016/j.biocel.2013.06.017.

[105] R. Sakuma, A. A. Mael, and Y. Ikeda, "Alpha Interferon Enhances TRIM5 -Mediated Antiviral Activities in Human and Rhesus Monkey Cells," *J. Virol.*, vol. 81, no. 18, pp. 10201–10206, 2007, doi: 10.1128/jvi.00419-07.

[106] K. Asaoka, K. Ikeda, T. Hishinuma, K. Horie-Inoue, S. Takeda, and S. Inoue, "A retrovirus restriction factor TRIM5α is transcriptionally regulated by interferons," *Biochem. Biophys. Res. Commun.*, vol. 338, no. 4, pp. 1950–1956, 2005, doi: 10.1016/j.bbrc.2005.10.173.

[107] M. Stremlau, C. M. Owens, M. J. Perron, M. Kiessling, P. Autissier, and J. Sodroski, "The cytoplasmic body component TRIM5α restricts HIV-1 infection in Old World monkeys," *Nature*, vol. 427, no. 6977, pp. 848–853, 2004, doi: 10.1038/nature02343.

[108] X. Wu, J. L. Anderson, E. M. Campbell, A. M. Joseph, and T. J. Hope, "Proteasome inhibitors uncouple rhesus TRIM5α restriction of HIV-1 reverse transcription and infection," *Proc. Natl. Acad. Sci. U. S. A.*, vol. 103, no. 19, pp. 7465–7470, 2006, doi: 10.1073/pnas.0510483103.

[109] S. L. Sawyer, L. I. Wu, M. Emerman, and H. S. Malik, "Positive selection of primate TRIM5α identifies a critical species-specific retroviral restriction domain," *Proc. Natl. Acad. Sci. U. S. A.*, vol. 102, no. 8, pp. 2832–2837, 2005, doi: 10.1073/pnas.0409853102.

[110] R. M. Newman *et al.*, "Balancing selection and the evolution of functional polymorphism in Old World monkey TRIM5α," *Proc. Natl. Acad. Sci. U. S. A.*, vol. 103, no. 50, pp. 19134–19139, 2006, doi: 10.1073/pnas.0605838103.

[111] K. Kim *et al.*, "Cyclophilin A protects HIV-1 from restriction by human TRIM5a," *Nat. Microbiol.*, vol. 4, no. 12, pp. 2044–2051, 2019, doi: 10.1038/s41564-019-0592-5.Cyclophilin.

[112] S. D. Barr, J. R. Smiley, and F. D. Bushman, "The interferon response inhibits HIV particle production by induction of TRIM22," *PLoS Pathog.*, vol. 4, no. 2, pp. 1–11, 2008, doi: 10.1371/journal.ppat.1000007.

[113] S. L. Sawyer, M. Emerman, and H. S. Malik, "Discordant evolution of the adjacent antiretroviral genes TRIM22 and TRIM5 in mammals," *PLoS Pathog.*, vol. 3, no. 12, pp. 1918–1929, 2007, doi: 10.1371/journal.ppat.0030197.

[114] P. D. Uchil, B. D. Quinlan, W. T. Chan, J. M. Luna, and W. Mothes, "TRIM E3 ligases interfere with early and late stages of the retroviral life cycle," *PLoS Pathog.*, vol. 4, no.

2, 2008, doi: 10.1371/journal.ppat.0040016.

[115] A. J. Koletsky, M. W. Harding, and R. E. Handschumacher, "Cyclophilin : distribution and variant properties in normal and neoplastic tissues .," *J. Immunol.*, vol. 137, pp. 1054–1059, 1986.

[116] D. J. Bergsma *et al.*, "The cyclophilin multigene family of peptidyl-prolyl isomerases. Characterization of three separate human isoforms," *J. Biol. Chem.*, vol. 266, no. 34, pp. 23204–23214, 1991.

[117] E. Roydon Price, L. D. Zydowsky, M. Jin, C. Hunter Baker, F. D. Mckeon, and C. T. Walsh, "Human cyclophilin B: A second cyclophilin gene encodes a peptidyl-prolyl isomerase with a signal sequence," *Proc. Natl. Acad. Sci. U. S. A.*, vol. 88, no. 5, pp. 1903–1907, 1991, doi: 10.1073/pnas.88.5.1903.

[118] S. Hopkins and P. A. Gallay, "The role of immunophilins in viral infection," *Biochim. Biophys. Acta - Gen. Subj.*, vol. 1850, no. 10, pp. 2103–2110, 2015, doi: 10.1016/j.bbagen.2014.11.011.

[119] F. X. Schmid, "Protein folding: Prolyl isomerases join the fold," *Curr. Biol.*, vol. 5, no. 9, pp. 993–994, 1995, doi: 10.1016/S0960-9822(95)00197-7.

[120] K. P. Lu, G. Finn, T. H. Lee, and L. K. Nicholson, "Prolyl cis-trans isomerization as a molecular timer," *Nat. Chem. Biol.*, vol. 3, no. 10, pp. 619–629, 2007, doi: 10.1038/nchembio.2007.35.

[121] N. Takahashi, T. Hayano, and M. Suzuki, "Peptidyl-prolyl cis-trans isomerase is the cyclosporin A-binding protein cyclophilin," *Nature*, vol. 337, 1989.

[122] G. Fischer and F. X. Schmid, "The mechanism of protein folding. Implications of in vitro refolding models for de novo protein folding and translocation in the cell," *Biochemistry*, vol. 29, no. 9, pp. 2205–2212, 1990.

[123] T. Kiefhaber, H. Grunert, U. Hahn, and F. X. Schmid, "Replacement of a cis proline simplifies the mechanism of ribonuclease T1 folding.," *Biochemistry*, vol. 29, no. 27, pp. 6475–6480, 1990.

[124] H. P. Bächinger, "The influence of peptidyl-prolyl cis-trans isomerase on the in vitro folding of type III collagen.," *J. Biol. Chem.*, vol. 262, no. 35, pp. 17144–17148, 1987.

[125] J. Kallen *et al.*, "Structure of human cyclophilin and its binding site for cyclosporin A

determined by X-ray crystallography and NMR spectroscopy," *Nature*, vol. 353, no. 6341, pp. 276–279, 1991.

[126] G. D. Van Duyne, R. F. Standaert, P. A. Karplus, S. L. Schreiber, and J. Clardy, "Atomic structure of FKBP-FK506, an immunophilin-immunosuppressant complex," *Science (80-.).*, vol. 252, no. 5007, pp. 839–842, 1991, doi: 10.1126/science.1709302.

[127] R. . Handschumacher, M. . Harding, J. Rice, and R. . Drugge, "Cyclophilin: A Specific Cytosolic Bidg Protein for Cyclosporin A," *Science (80-.).*, vol. 226, pp. 544–547, 1984.

[128] V. Thai *et al.*, "Structural, Biochemical, and in Vivo Characterization of the First Virally Encoded Cyclophilin from the Mimivirus," *J. Mol. Biol.*, vol. 378, no. 1, pp. 71–86, 2008, doi: 10.1016/j.jmb.2007.08.051.

[129] T. J. Pemberton and J. E. Kay, "The cyclophilin repertoire of the fission yeast Schizosaccharomyces pombe," *Yeast*, vol. 22, no. 12, pp. 927–945, 2005, doi: 10.1002/yea.1288.

[130] S. F. Göthel and M. A. Marahiel, "Peptidyl-prolyl cis-trams isomerases, a superfamily of ubiquitous folding catalysts," *Cell. Mol. Life Sci.*, vol. 55, no. 3, pp. 423–436, 1999, doi: 10.1007/s000180050299.

[131] J. J. Siekierka, S. H. Y. Hung, M. Poe, C. S. Lin, and N. H. Sigal, "A cytosolic binding protein for the immunosuppressant FK506 has peptidyl-prolyl isomerase activity but is distinct from cyclophilin," *Nature*, vol. 341, pp. 755–757, 1989.

[132] J. Jain *et al.*, "The T-cell transcription factor NFATp is a substrate for calcineurin and interacts with Fos and Jun," *Nature*, vol. 365, pp. 352–355, 1993.

[133] J. Liu, J. D. Farmer, W. S. Lane, J. Friedman, I. Weissman, and S. L. Schreiber, "Calcineurin is a common target of cyclophilin-cyclosporin A and FKBP-FK506 complexes," *Cell*, vol. 66, no. 4, pp. 807–815, 1991, doi: 10.1016/0092-8674(91)90124-H.

[134] R. T. Abraham and G. J. Wiederrecht, "Immunopharmacology of Rapamycin," *Annu. Rev. Immunol.*, vol. 14, pp. 483–510, 1996.

[135] L. Hennig *et al.*, "Selective inactivation of parvulin-like peptidyl-prolyl cis/trans isomerases by juglone," *Biochemistry*, vol. 37, no. 17, pp. 5953–5960, 1998, doi: 10.1021/bi973162p.

[136] R. Thapar, "Roles of prolyl isomerases in RNA-mediated gene expression," *Biomolecules*, vol. 5, no. 2, pp. 974–999, 2015, doi: 10.3390/biom5020974.

[137] L. Bao, A. Kimzey, G. Sauter, J. M. Sowadski, K. P. Lu, and D. G. Wang, "Prevalent Overexpression of Prolyl Isomerase Pin1 in Human Cancers," *Am. J. Pathol.*, vol. 164, no. 5, pp. 1727–1737, 2004, doi: 10.1016/S0002-9440(10)63731-5.

[138] Y. C. Liou, X. Z. Zhou, and K. P. Lu, "Prolyl isomerase Pin1 as a molecular switch to determine the fate of phosphoproteins," *Trends Biochem. Sci.*, vol. 36, no. 10, pp. 501–514, 2011, doi: 10.1016/j.tibs.2011.07.001.

[139] H.-Y. Wang, J. C.-M. Fu, Y.-C. Lee, and P.-J. Lu, "Hyperthermia Stress Activates Heat Shock Protein Expression via Propyl Isomerase 1 Regulation with Heat Shock Factor 1," *Mol. Cell. Biol.*, vol. 33, no. 24, pp. 4889–4899, 2013, doi: 10.1128/mcb.00475-13.

[140] J. V. Olsen *et al.*, "Global, In Vivo, and Site-Specific Phosphorylation Dynamics in Signaling Networks," *Cell*, vol. 127, no. 3, pp. 635–648, 2006, doi: 10.1016/j.cell.2006.09.026.

[141] E. K. Franke, H. E. H. Yuan, and J. Luban, "Specific incorporation of cyclophilin a into HIV-1 virions," *Nature*, vol. 372, no. 6504, pp. 359–362, 1994, doi: 10.1038/372359a0.

[142] Z. G. Jin *et al.*, "Cyclophilin A is a secreted growth factor induced by oxidative stress," *Circ. Res.*, vol. 87, no. 9, pp. 789–796, 2000, doi: 10.1161/01.RES.87.9.789.

[143] W. M. Gwinn *et al.*, "Novel Approach to Inhibit Asthma-Mediated Lung Inflammation Using Anti-CD147 Intervention," *J. Immunol.*, vol. 177, no. 7, pp. 4870–4879, 2006, doi: 10.4049/jimmunol.177.7.4870.

[144] C. Spitzfaden, W. Braun, G. Wider, H. Widmer, and K. Wüthrich, "Determination of the NMR solution structure of the cyclophilin A-cyclosporin A complex.," *J Biomol NMR*, vol. 4, no. 4, pp. 463–482, 1994.

[145] K. Piotukh, W. Gu, M. Kofler, D. Labudde, V. Helms, and C. Freund, "Cyclophilin A binds to linear peptide motifs containing a consensus that is present in many human proteins," *J. Biol. Chem.*, vol. 280, no. 25, pp. 23668–23674, 2005, doi: 10.1074/jbc.M503405200.

[146] C. C. Calhoun, Y. C. Lu, J. Song, and R. Chiu, "Knockdown endogenous CypA with siRNA in U2OS cells results in disruption of F-actin structure and alters tumor

phenotype," *Mol. Cell. Biochem.*, vol. 320, no. 1–2, pp. 35–43, 2009, doi: 10.1007/s11010-008-9896-0.

[147] J. Colgan *et al.*, "Cyclophilin A regulates TCR signal strength in CD4+ T cells via a proline-directed conformational switch in Itk," *Immunity*, vol. 21, no. 2, pp. 189–201, 2004, doi: 10.1016/j.immuni.2004.07.005.

[148] W.-M. Yang, C. J. Inouye, and E. Seto, "Cyclophilin A and FKBP12 interact with YY1 and alter its transcriptional activity," *J. Biol. Chem.*, vol. 270, no. 25, pp. 15187–15193, 1995.

[149] M. Guo *et al.*, "Novel Role for Cyclophilin A in Regulation of Chondrogenic Commitment and Endochondral Ossification," *Mol. Cell. Biol.*, vol. 35, no. 12, pp. 2119–2130, 2015, doi: 10.1128/mcb.01414-14.

[150] M. Guo *et al.*, "Cyclophilin A (CypA) Plays Dual Roles in Regulation of Bone Anabolism and Resorption," *Sci. Rep.*, vol. 6, no. March, pp. 2–11, 2016, doi: 10.1038/srep22378.

[151] Z. Dongsheng, F. Zhiguang, J. Junfeng, L. Zifan, and W. Li, "Cyclophilin A Aggravates Collagen-Induced Arthritis via Promoting Classically Activated Macrophages," *Inflammation*, vol. 40, no. 5, pp. 1761–1772, 2017, doi: 10.1007/s10753-017-0619-0.

[152] H. Kim *et al.*, "Cyclophilin A regulates JNK/p38-MAPK signaling through its physical interaction with ASK1," *Biochem. Biophys. Res. Commun.*, vol. 464, no. 1, pp. 112–117, 2015, doi: 10.1016/j.bbrc.2015.06.078.

[153] Z. Xue *et al.*, "Cyclophilin A mediates the ox-LDL-induced activation and apoptosis of macrophages via autophagy," *Int. J. Cardiol.*, vol. 230, pp. 142–148, 2017, doi: 10.1016/j.ijcard.2016.12.042.

[154] G. Wang *et al.*, "Cyclophilin A maintains glioma-initiating cell stemness by regulating Wnt/β-catenin signaling," *Clin. Cancer Res.*, vol. 23, no. 21, pp. 6640–6649, 2017, doi: 10.1158/1078-0432.CCR-17-0774.

[155] S. Semba and K. Huebner, "Protein expression profiling identifies cyclophilin A as a molecular target in fhit-mediated tumor suppression," *Mol. Cancer Res.*, vol. 4, no. 8, pp. 529–538, 2006, doi: 10.1158/1541-7786.MCR-06-0060.

[156] K. J. Choi *et al.*, "Overexpressed cyclophilin A in cancer cells renders resistance to

hypoxia- and cisplatin-induced cell death," *Cancer Res.*, vol. 67, no. 8, pp. 3654–3662, 2007, doi: 10.1158/0008-5472.CAN-06-1759.

[157] M. J. Campa, M. Z. Wang, B. Howard, M. C. Fitzgerald, and E. F. Patz, "Protein expression profiling identifies macrophage migration inhibitory factor and cyclophilin A as potential molecular targets in non-small cell lung cancer," *Cancer Res.*, vol. 63, no. 7, pp. 1652–1656, 2003.

[158] B. A. Howard *et al.*, "Stable RNA interference-mediated suppression of cyclophilin A diminishes non-small-cell lung tumor growth in vivo," *Cancer Res.*, vol. 65, no. 19, pp. 8853–8860, 2005, doi: 10.1158/0008-5472.CAN-05-1219.

[159] M. Takahashi, S. Suzuki, and K. Ishikawa, "Cyclophilin A-EMMPRIN interaction induces invasion of head and neck squamous cell carcinoma," *Oncol. Rep.*, vol. 27, no. 1, pp. 198–203, 2012, doi: 10.3892/or.2011.1474.

[160] S. Cheng *et al.*, "Downregulation of Peptidylprolyl isomerase A promotes cell death and enhances doxorubicin-induced apoptosis in hepatocellular carcinoma," *Gene*, vol. 592, no. 1, pp. 236–244, 2016, doi: 10.1016/j.gene.2016.07.020.

[161] P. Seizer, M. Gawaz, and A. E. May, "Cyclophilin A and EMMPRIN (CD147) in cardiovascular diseases," *Cardiovasc. Res.*, vol. 102, no. 1, pp. 17–23, 2014, doi: 10.1093/cvr/cvu035.

[162] S. Ramachandran *et al.*, "Proteomic profiling of high glucose primed monocytes identifies cyclophilin A as a potential secretory marker of inflammation in type 2 diabetes," *Proteomics*, vol. 12, no. 18, pp. 2808–2821, 2012, doi: 10.1002/pmic.201100586.

[163] B. Sherry, N. Yarlett, A. Strupp, and A. Cerami, "Identification of cyclophilin as a proinflammatory secretory product of lipopolysaccharide-activated macrophages," *Proc. Natl. Acad. Sci. U. S. A.*, vol. 89, no. 8, pp. 3511–3515, 1992, doi: 10.1073/pnas.89.8.3511.

[164] B. P. Toole, "Emmprin (CD147), a cell surface regulator of matrix metalloproteinase production and function," *Curr. Top. Dev. Biol.*, vol. 54, pp. 371–389, 2003.

[165] F. Song *et al.*, "Cyclophilin A (CyPA) induces chemotaxis independent of its peptidylprolyl cis-trans isomerase activity," *J. Biol. Chem.*, vol. 286, no. 10, pp. 8197–8203, 2011, doi: 10.1074/jbc.C110.181347.

[166] N. N. Soe *et al.*, "Acetylation of cyclophilin A is required for its secretion and vascular cell activation," *Cardiovasc. Res.*, vol. 101, no. 3, pp. 444–453, 2014, doi: 10.1093/cvr/cvt268.

[167] V. Yurchenko *et al.*, "Active site residues of cyclophilin A are crucial for its signaling activity via CD147," *J. Biol. Chem.*, vol. 277, no. 25, pp. 22959–22965, 2002, doi: 10.1074/jbc.M201593200.

[168] Y. Xie, X. Li, and J. Ge, "Cyclophilin A–FoxO1 signaling pathway in endothelial cell apoptosis," *Cell. Signal.*, vol. 61, pp. 57–65, 2019, doi: 10.1016/j.cellsig.2019.04.014.

[169] J. Colgan, M. Asmal, and J. Luban, "Isolation, characterization and targeted disruption of mouse Ppia: Cyclophilin A is not essential for mammalian cell viability," *Genomics*, vol. 68, no. 2, pp. 167–178, 2000, doi: 10.1006/geno.2000.6295.

[170] Z. Zhang, P. M. Harrison, Y. Liu, and M. Gerstein, "Millions of years of evolution preserved: A comprehensive catalog of the processed pseudogenes in the human genome," *Genome Res.*, vol. 13, no. 12, pp. 2541–2558, 2003, doi: 10.1101/gr.1429003.

[171] P. M. Harrison, D. Zheng, Z. Zhang, N. Carriero, and M. Gerstein, "Transcribed processed pseudogenes in the human genome: An intermediate form of expressed retrosequence lacking protein-coding ability," *Nucleic Acids Res.*, vol. 33, no. 8, pp. 2374–2383, 2005, doi: 10.1093/nar/gki531.

[172] H. Kawasaki, E. S. Mocarski, I. Kosugi, and Y. Tsutsui, "Cyclosporine Inhibits Mouse Cytomegalovirus Infection via a Cyclophilin-Dependent Pathway Specifically in Neural Stem/Progenitor Cells," *J. Virol.*, vol. 81, no. 17, pp. 9013–9023, 2007, doi: 10.1128/jvi.00261-07.

[173] X. Liu *et al.*, "Cyclophilin A interacts with influenza A virus M1 protein and impairs the early stage of the viral replication," *Cell. Microbiol.*, vol. 11, no. 5, pp. 730–741, 2009, doi: 10.1111/j.1462-5822.2009.01286.x.

[174] F. Yang, J. M. Robotham, H. B. Nelson, A. Irsigler, R. Kenworthy, and H. Tang, "Cyclophilin A Is an Essential Cofactor for Hepatitis C Virus Infection and the Principal Mediator of Cyclosporine Resistance In Vitro," *J. Virol.*, vol. 82, no. 11, pp. 5269–5278, 2008, doi: 10.1128/jvi.02614-07.

[175] A. P. V. Castro, T. M. U. Carvalho, N. Moussatche, and C. R. A. Damaso, "Redistribution of Cyclophilin A to Viral Factories during Vaccinia Virus Infection and

Its Incorporation into Mature Particles," *J. Virol.*, vol. 77, no. 16, pp. 9052–9068, 2003, doi: 10.1128/jvi.77.16.9052-9068.2003.

[176] S. Bose, M. Mathur, P. Bates, N. Joshi, and A. K. Banerjee, "Requirement for cyclophilin A for the replication of vesicular stomatitis virus New Jersey serotype," *J. Gen. Virol.*, vol. 84, no. 7, pp. 1687–1699, 2003, doi: 10.1099/vir.0.19074-0.

[177] L. R. Keyes, M. G. Bego, M. Soland, and S. St. Jeor, "Cyclophilin A is required for efficient human cytomegalovirus DNA replication and reactivation," *J. Gen. Virol.*, vol. 93, no. 4, pp. 722–732, 2012, doi: 10.1099/vir.0.037309-0.

[178] A. A. Abdullah *et al.*, "Cyclophilin a as a target in the treatment of cytomegalovirus infections," *Antivir. Chem. Chemother.*, vol. 26, pp. 1–21, 2018, doi: 10.1177/2040206618811413.

[179] U. Chatterji, M. Bobardt, A. Tai, M. Wood, and A. Gallay, "Cyclophilin and NS5A Inhibitors, but not other Anti-HCV Agents, Preclude 1 HCV-Mediated Formation of Double Membrane Vesicle Viral Factories," *Antimicrob. Agents Chemother.*, 2015, doi: 10.1128/AAC.04958-14.

[180] T. Von Hahn *et al.*, "Hepatocytes that express variants of cyclophilin A are resistant to HCV infection and replication," *Gastroenterology*, vol. 143, no. 2, pp. 439–447, 2012, doi: 10.1053/j.gastro.2012.04.053.

[181] D. Braaten and J. Luban, "Cyclophilin A regulates HIV-1 infectivity, as demonstrated by gene targeting in human T cells," *EMBO J.*, vol. 20, no. 6, pp. 1300–1309, 2001, doi: 10.1093/emboj/20.6.1300.

[182] J. Luban, K. L. Bossolt, E. K. Franke, G. V. Kalpana, and S. P. Goff, "Human immunodeficiency virus type 1 Gag protein binds to cyclophilins A and B," *Cell*, vol. 73, no. 6, pp. 1067–1078, 1993, doi: 10.1016/0092-8674(93)90637-6.

[183] S. Yoo, D. G. Myszka, C. yah Yeh, M. McMurray, C. P. Hill, and W. I. Sundquist, "Molecular recognition in the HIV-1 Capsid/Cyclophilin A complex," *J. Mol. Biol.*, vol. 269, no. 5, pp. 780–795, 1997, doi: 10.1006/jmbi.1997.1051.

[184] T. R. Gamble *et al.*, "Crystal structure of human cyclophilin A bound to the amino-terminal domain of HIV-1 capsid," *Cell*, vol. 87, no. 7, pp. 1285–1294, 1996, doi: 10.1016/S0092-8674(00)81823-1.

[185] D. A. Bosco, E. Z. Eisenmesser, S. Pochapsky, W. I. Sundquist, and D. Kern, "Catalysis of cis/trans isomerization in native HIV-1 capsid by human cyclophilin A," *Proc. Natl. Acad. Sci. U. S. A.*, vol. 99, no. 8, pp. 5247–5252, 2002, doi: 10.1073/pnas.082100499.

[186] B. R. Howard, F. F. Vajdos, S. Li, W. I. Sundquist, and C. P. Hill, "Structural insights into the catalytic mechanism of cyclophilin A," *Nat. Struct. Biol.*, vol. 10, no. 6, pp. 475–481, 2003, doi: 10.1038/nsb927.

[187] D. Braaten, C. Aberham, E. K. Franke, L. Yin, W. Phares, and J. Luban, "Cyclosporine A-resistant human immunodeficiency virus type 1 mutants demonstrate that Gag encodes the functional target of cyclophilin A.," *J. Virol.*, vol. 70, no. 8, pp. 5170–5176, 1996, doi: 10.1128/jvi.70.8.5170-5176.1996.

[188] T. Hatziioannou, D. Perez-Caballero, S. Cowan, and P. D. Bieniasz, "Cyclophilin Interactions with Incoming Human Immunodeficiency Virus Type 1 Capsids with Opposing Effects on Infectivity in Human Cells," *J. Virol.*, vol. 79, no. 1, pp. 176–183, 2005, doi: 10.1128/JVI.79.1.176.

[189] E. Sokolskaja, D. M. Sayah, and J. Luban, "Target Cell Cyclophilin A Modulates Human Immunodeficiency Virus Type 1 Infectivity," *J. Virol.*, vol. 78, no. 23, pp. 12800–12808, 2004, doi: 10.1128/jvi.78.23.12800-12808.2004.

[190] K. Wiegers, G. Rutter, U. Schubert, M. Grättinger, and H. G. Kräusslich, "Cyclophilin A incorporation is not required for human immunodeficiency virus type 1 particle maturation and does not destabilize the mature capsid," *Virology*, vol. 257, no. 1, pp. 261–274, 1999, doi: 10.1006/viro.1999.9669.

[191] A. Fassati and S. P. Goff, "Characterization of Intracellular Reverse Transcription Complexes of Human Immunodeficiency Virus Type 1," *J. Virol.*, vol. 75, no. 8, pp. 3626–3635, 2001, doi: 10.1128/jvi.75.8.3626-3635.2001.

[192] M. Nakai and T. Goto, "Ultrastructure and morphogenesis of human immunodeficiency virus," *J. Electron Microsc. (Tokyo).*, vol. 45, no. 4, pp. 247–257, 1996, doi: 10.1093/oxfordjournals.jmicro.a023441.

[193] T. Fricke, A. Brandariz-Nunez, X. Wang, A. B. Smith, and F. Diaz-Griffero, "Human Cytosolic Extracts Stabilize the HIV-1 Core," *J. Virol.*, vol. 87, no. 19, pp. 10587–10597, 2013, doi: 10.1128/jvi.01705-13.

[194] C. Liu *et al.*, "Cyclophilin A stabilizes the HIV-1 capsid through a novel non-canonical

binding site," *Nat. Commun.*, vol. 7, pp. 1–10, 2016, doi: 10.1038/ncomms10714.

[195] V. B. Shah *et al.*, "The Host Proteins Transportin SR2/TNPO3 and Cyclophilin A Exert Opposing Effects on HIV-1 Uncoating," *J. Virol.*, vol. 87, no. 1, pp. 422–432, 2013, doi: 10.1128/jvi.07177-11.

[196] A. De Iaco and J. Luban, "Cyclophilin A promotes HIV-1 reverse transcription but its effect on transduction correlates best with its effect on nuclear entry of viral cDNA," *Retrovirology*, vol. 11, no. 1, pp. 1–15, 2014, doi: 10.1186/1742-4690-11-11.

[197] Y. Li, A. K. Kar, and J. Sodroski, "Target Cell Type-Dependent Modulation of Human Immunodeficiency Virus Type 1 Capsid Disassembly by Cyclophilin A," *J. Virol.*, vol. 83, no. 21, pp. 10951–10962, 2009, doi: 10.1128/jvi.00682-09.

[198] G. J. Towers, T. Hatziioannou, S. Cowan, S. P. Goff, J. Luban, and P. D. Bieniasz, "Cyclophilin A modulates the sensitivity of HIV-1 to host restriction factors," *Nat. Med.*, vol. 9, no. 9, pp. 1138–1143, 2003, doi: 10.1038/nm910.

[199] R. G. Ptak *et al.*, "Inhibition of human immunodeficiency virus type 1 replication in human cells by Debio-025, a novel cyclophilin binding agent," *Antimicrob. Agents Chemother.*, vol. 52, no. 4, pp. 1302–1317, 2008, doi: 10.1128/AAC.01324-07.

[200] D. Braaten, E. K. Franke, and J. Luban, "Cyclophilin A is required for the replication of group M human immunodeficiency virus type 1 (HIV-1) and simian immunodeficiency virus SIV(CPZ)GAB but not group O HIV-1 or other primate immunodeficiency viruses.," *J. Virol.*, vol. 70, no. 7, pp. 4220–4227, 1996, doi: 10.1128/jvi.70.7.4220-4227.1996.

[201] L. Yin, D. Braaten, and J. Luban, "Human Immunodeficiency Virus Type 1 Replication Is Modulated by Host Cyclophilin A Expression Levels," *J. Virol.*, vol. 72, no. 8, pp. 6430–6436, 1998, doi: 10.1128/jvi.72.8.6430-6436.1998.

[202] M. Thali *et al.*, "Thali 1994 - Functional association of CypA with HIV-1 virions," *Nature*, vol. 372, pp. 363–365, 1994.

[203] J. Rasaiyaah *et al.*, "HIV-1 evades innate immune recognition through specific cofactor recruitment," *Nature*, vol. 503, no. 7476, pp. 402–405, 2013, doi: 10.1038/nature12769.

[204] C. Aberham, S. Weber, and W. Phares, "Spontaneous mutations in the human immunodeficiency virus type 1 gag gene that affect viral replication in the presence of

cyclosporins.," *J. Virol.*, vol. 70, no. 6, pp. 3536–3544, 1996, doi: 10.1128/jvi.70.6.3536-3544.1996.

[205] M. Qi, R. Yang, and C. Aiken, "Cyclophilin A-Dependent Restriction of Human Immunodeficiency Virus Type 1 Capsid Mutants for Infection of Nondividing Cells," *J. Virol.*, vol. 82, no. 24, pp. 12001–12008, 2008, doi: 10.1128/jvi.01518-08.

[206] L. M. J. Ylinen *et al.*, "Cyclophilin A Levels Dictate Infection Efficiency of Human Immunodeficiency Virus Type 1 Capsid Escape Mutants A92E and G94D," *J. Virol.*, vol. 83, no. 4, pp. 2044–2047, 2009, doi: 10.1128/jvi.01876-08.

[207] T. Schaller *et al.*, "HIV-1 capsid-cyclophilin interactions determine nuclear import pathway, integration targeting and replication efficiency," *PLoS Pathog.*, vol. 7, no. 12, 2011, doi: 10.1371/journal.ppat.1002439.

[208] A. Saito *et al.*, "Roles of Capsid-Interacting Host Factors in Multimodal Inhibition of HIV-1 by PF74," *J. Virol.*, vol. 90, no. 12, pp. 5808–5823, 2016, doi: 10.1128/jvi.03116-15.

[209] L. Bulli *et al.*, "Complex Interplay between HIV-1 Capsid and MX2-Independent Alpha Interferon-Induced Antiviral Factors," *J. Virol.*, vol. 90, no. 16, pp. 7469–7480, 2016, doi: 10.1128/jvi.00458-16.

[210] S. Misumi *et al.*, "Uncoating of human immunodeficiency virus type 1 requires prolyl isomerase Pin1," *J. Biol. Chem.*, vol. 285, no. 33, pp. 25185–25195, 2010, doi: 10.1074/jbc.M110.114256.

[211] J. DeBoer, C. J. Madson, and M. Belshan, "Cyclophilin B enhances HIV-1 Infection," *Virology*, vol. 489, pp. 282–291, 2016, doi: 10.1016/j.physbeh.2017.03.040.

[212] T. Yuan, W. Yao, K. Tokunaga, R. Yang, and B. Sun, "An HIV-1 capsid binding protein TRIM11 accelerates viral uncoating," *Retrovirology*, vol. 13, no. 1, pp. 1–14, 2016, doi: 10.1186/s12977-016-0306-5.

[213] C. A. Guth and J. Sodroski, "Contribution of PDZD8 to Stabilization of the Human Immunodeficiency Virus Type 1 Capsid," *J. Virol.*, vol. 88, no. 9, pp. 4612–4623, 2014, doi: 10.1128/jvi.02945-13.

[214] D. M. Sayah, E. Sokolskaja, L. Berthoux, and J. Luban, "Cyclophilin A retrotransposition into TRIM5 explains owl monkey resistance to HIV-1," *Nature*, vol.

430, no. 6999, pp. 569–573, 2004, doi: 10.1038/nature02777.

[215] S. Nisole, C. Lynch, J. P. Stoye, and M. W. Yap, "A Trim5-cyclophilin A fusion protein found in owl monkey kidney cells can restrict HIV-1," *Proc. Natl. Acad. Sci. U. S. A.*, vol. 101, no. 36, pp. 13324–13328, 2004, doi: 10.1073/pnas.0404640101.

[216] F. Diaz-Griffero, A. Kar, M. Lee, M. Stremlau, E. Poeschla, and J. Sodroski, "Comparative requirements for the restriction of retrovirus infection by TRIM5α and TRIMCyp," *Virology*, vol. 369, no. 2, pp. 400–410, 2007, doi: 10.1016/j.virol.2007.08.032.

[217] G. Brennan, Y. Kozyrev, and S. L. Hu, "TRIMCyp expression in Old World primates Macaca nemestrina and Macaca fascicularis," *Proc. Natl. Acad. Sci. U. S. A.*, vol. 105, no. 9, pp. 3569–3574, 2008, doi: 10.1073/pnas.0709511105.

[218] S. J. Wilson, B. L. J. Webb, L. M. J. Ylinen, E. Verschoor, J. L. Heeney, and G. J. Towers, "Independent evolution of an antiviral TRIMCyp in rhesus macaques," *Proc. Natl. Acad. Sci. U. S. A.*, vol. 105, no. 9, pp. 3557–3562, 2008, doi: 10.1073/pnas.0709003105.

[219] C. A. Virgen, Z. Kratovac, P. D. Bieniasz, and T. Hatziioannou, "Independent genesis of chimeric TRIM5-cyclophilin proteins in two primate species," *Proc. Natl. Acad. Sci. U. S. A.*, vol. 105, no. 9, pp. 3563–3568, 2008, doi: 10.1073/pnas.0709258105.

[220] J. P. Stoye and M. W. Yap, "Chance favors a prepared genome," *Proc. Natl. Acad. Sci. U. S. A.*, vol. 105, no. 9, pp. 3177–3178, 2008, doi: 10.1073/pnas.0800667105.

[221] M. Yamashita and M. Emerman, "Cellular Restriction Targeting Viral Capsids Perturbs Human Immunodeficiency Virus Type 1 Infection of Nondividing Cells," *J. Virol.*, vol. 83, no. 19, pp. 9835–9843, 2009, doi: 10.1128/jvi.01084-09.

[222] M. Yamashita, O. Perez, T. J. Hope, and M. Emerman, "Evidence for direct involvement of the capsid protein in HIV infection of nondividing cells," *PLoS Pathog.*, vol. 3, no. 10, pp. 1502–1510, 2007, doi: 10.1371/journal.ppat.0030156.

[223] X. Lahaye *et al.*, "The Capsids of HIV-1 and HIV-2 Determine Immune Detection of the Viral cDNA by the Innate Sensor cGAS in Dendritic Cells," *Immunity*, vol. 39, no. 6, pp. 1132–1142, 2013, doi: 10.1016/j.immuni.2013.11.002.

[224] N. Manel, B. Hogstad, Y. Wang, D. E. Levy, D. Unutmaz, and D. R. Littman, "A cryptic

sensor for HIV-1 activates antiviral innate immunity in dendritic cells," *Nature*, vol. 467, no. 7312, pp. 214–217, 2010, doi: 10.1016/j.physbeh.2017.03.040.

[225] M. S. Henning, B. N. Dubose, M. J. Burse, C. Aiken, and M. Yamashita, "In Vivo Functions of CPSF6 for HIV-1 as Revealed by HIV-1 Capsid Evolution in HLA-B27-Positive Subjects," *PLoS Pathog.*, vol. 10, no. 1, 2014, doi: 10.1371/journal.ppat.1003868.

[226] D. Braaten, H. Ansari, and J. Luban, "The hydrophobic pocket of cyclophilin is the binding site for the human immunodeficiency virus type 1 Gag polyprotein.," *J. Virol.*, vol. 71, no. 3, pp. 2107–2113, 1997, doi: 10.1128/jvi.71.3.2107-2113.1997.

[227] M. M. Endrich and H. Gehring, "The V3 loop of human immunodeficiency virus type-1 envelope protein is a high-affinity ligand for immunophilins present in human blood," *Eur. J. Biochem.*, vol. 252, no. 3, pp. 441–446, 1998, doi: 10.1046/j.1432-1327.1998.2520441.x.

[228] G. Spik *et al.*, "A novel secreted cyclophilin-like protein (SCYLP)," *J. Biol. Chem.*, vol. 266, no. 17, pp. 10735–10738, 1991.

[229] F. Allain, C. Boutillon, C. Mariller, and G. Spik, "Selective assay for CyPA and CyPB in human blood using highly specific anti-peptide antibodies," *J. Immunol. Methods*, vol. 178, no. 1, pp. 113–120, 1995, doi: 10.1016/0022-1759(94)00249-V.

[230] S. González-Cuadrado *et al.*, "Expression of leucocyte chemoattractants by interstitial renal fibroblasts: Up-regulation by drugs associated with interstitial fibrosis," *Clin. Exp. Immunol.*, vol. 106, no. 3, pp. 518–522, 1996, doi: 10.1046/j.1365-2249.1996.d01-864.x.

[231] F. Allain, A. Denys, and G. Spik, "Characterization of Surface Binding Site for Cyclophilin B on a Human Tumor T-cell Line," *J. Biol. Chem.*, vol. 269, no. 24, pp. 16537–16540, 1994.

[232] M. Teng, J. Huang, Z. Zhu, H. Li, J. Shen, and Q. Chen, "Cyclophilin B promotes cell proliferation, migration, invasion and angiogenesis via regulating the STAT3 pathway in non-small cell lung cancer," *Pathol. Res. Pract.*, vol. 215, no. 6, p. 152417, 2019, doi: 10.1016/j.prp.2019.04.009.

[233] K. Bauer *et al.*, "Cyclophilins contribute to Stat3 signaling and survival of multiple myeloma cells," *Oncogene*, vol. 28, no. 31, pp. 2784–2795, 2009, doi: 10.1038/onc.2009.142.

[234] Y. Kim *et al.*, "Role of cyclophilin B in tumorigenesis and cisplatin resistance in hepatocellular carcinoma in humans," *Hepatology*, vol. 54, no. 5, pp. 1661–1678, 2011, doi: 10.1002/hep.24539.

[235] B. Wang, L. Lin, H. Wang, H. Guo, Y. Gu, and W. Ding, "Overexpressed cyclophilin B suppresses aldosterone-induced proximal tubular cell injury both in vitro and in vivo," *Oncotarget*, vol. 7, no. 43, pp. 69309–69320, 2016, doi: 10.18632/oncotarget.12503.

[236] J. Friedman and I. Weissman, "Two cytoplasmic candidates for immunophilin action are revealed by affinity for a new cyclophilin: One in the presence and one in the absence of CsA," *Cell*, vol. 66, no. 4, pp. 799–806, 1991, doi: 10.1016/0092-8674(91)90123-G.

[237] L. A. Gaither *et al.*, "Multiple cyclophilins involved in different cellular pathways mediate HCV replication," *Virology*, vol. 397, no. 1, pp. 43–55, 2010, doi: 10.1016/j.virol.2009.10.043.

[238] P. Stocki, D. C. Chapman, L. A. Beach, and D. B. Williams, "Depletion of cyclophilins B and C Leads to dysregulation of endoplasmic reticulum redox homeostasis," *J. Biol. Chem.*, vol. 289, no. 33, pp. 23086–23096, 2014, doi: 10.1074/jbc.M114.570911.

[239] D. C. Chapman, P. Stocki, and D. B. Williams, "Cyclophilin C Participates in the US2-Mediated Degradation of Major Histocompatibility Complex Class i Molecules," *PLoS One*, vol. 10, no. 12, pp. 1–28, 2015, doi: 10.1371/journal.pone.0145458.

[240] J. Friedman, M. Trahey, and I. Weissman, "Cloning and characterization of cyclophilin C-associated protein: A candidate natural cellular ligand for cyclophilin C," *Proc. Natl. Acad. Sci. U. S. A.*, vol. 90, no. 14, pp. 6815–6819, 1993, doi: 10.1073/pnas.90.14.6815.

[241] M. Trahey and I. L. Weissman, "Cyclophilin C-associated protein: A normal secreted glycoprotein that down-modulates endotoxin and proinflammatory responses in vivo," *Proc. Natl. Acad. Sci. U. S. A.*, vol. 96, no. 6, pp. 3006–3011, 1999, doi: 10.1073/pnas.96.6.3006.

[242] A. Grassadonia *et al.*, "The 90K protein increases major histocompatibility complex class i expression and is regulated by hormones, γ-interferon, and double-strand polynucleotides," *Endocrinology*, vol. 145, no. 10, pp. 4728–4736, 2004, doi: 10.1210/en.2004-0506.

[243] V. Lodermeyer *et al.*, "90K, an interferon-stimulated gene product, reduces the infectivity of HIV-1," *Retrovirology*, vol. 10, no. 1, pp. 1–18, 2013, doi: 10.1186/1742-

4690-10-111.

[244] R. Yamaguchi *et al.*, "Cyclophilin C-associated protein regulation of phagocytic functions via NFAT activation in macrophages," *Brain Res.*, vol. 1397, pp. 55–65, 2011, doi: 10.1016/j.brainres.2011.03.036.

[245] T. Ratajczak, C. Cluning, and B. K. Ward, "Steroid receptor-associated immunophilins: A gateway to steroid signalling," *Clin. Biochem. Rev.*, vol. 36, no. 2, pp. 31–52, 2015.

[246] J. Owens-Gorillo *et al.*, "The CsA binding immunophilin Cyp40 and th FK506 binding immunophilin hsp56 bind to a common site on hsp90 and exist in independent cytosolic heterocomplexes with the untransformed glucocorticoid receptor," *J. Bacteriol.*, vol. 270, no. 35, pp. 20479–20484, 1995.

[247] K. Watashi and K. Shimotohno, "Cyclophilin and Viruses: Cyclophilin as a Cofactor for Viral Infection and Possible Anti-Viral Target," *Drug Target Insights*, vol. 2, pp. 9–18, 2007, doi: 10.1177/117739280700200017.

[248] M. S. Park, F. Chu, J. Xie, Y. Wang, P. Bhattacharya, and W. K. Chan, "Identification of cyclophilin-40-interacting proteins reveals potential cellular function of cyclophilin-40," *Anal. Biochem.*, vol. 410, no. 2, pp. 257–265, 2011, doi: 10.1016/j.ab.2010.12.007.

[249] H. Mi, O. Kops, E. Zimmermann, A. Jäschke, and M. Tropschug, "A nuclear RNA-binding cyclophilin in human T cells," *FEBS Lett.*, vol. 398, no. 2–3, pp. 201–205, 1996, doi: 10.1016/S0014-5793(96)01248-3.

[250] J. O. Kim *et al.*, "Co-amplification of a novel cyclophilin-like gene (PPIE) with L-myc in small cell lung cancer cell lines," *Oncogene*, vol. 17, no. 8, pp. 1019–1026, 1998, doi: 10.1038/sj.onc.1202006.

[251] Y. Wang *et al.*, "Human CyP33 binds specifically to mRNA and binding stimulates PPIase activity of hCyP33," *FEBS Lett.*, vol. 582, no. 5, pp. 835–839, 2008, doi: 10.1016/j.febslet.2008.01.055.

[252] M. S. Jurica, L. J. Licklider, S. P. Gygi, N. Grigorieff, and M. J. Moore, "Purification and characterization of native spliceosomes suitable for three-dimensional structural analysis," *Rna*, vol. 8, no. 4, pp. 426–439, 2002, doi: 10.1017/S1355838202021088.

[253] Z. Wang *et al.*, "Pro Isomerization in MLL1 PHD3-Bromo Cassette Connects H3K4me Readout to CyP33 and HDAC-Mediated Repression," *Cell*, vol. 141, no. 7, pp. 1183–

1194, 2010, doi: 10.1016/j.physbeh.2017.03.040.

[254] S. Park, U. Osmers, G. Raman, R. H. Schwantes, M. O. Diaz, and J. H. Bushweller, "The PHD3 domain of MLL Acts as a CYP33-regulated switch between MLL-mediated activation and repression," *Biochemistry*, vol. 49, no. 31, pp. 6576–6586, 2010, doi: 10.1021/bi1009387.

[255] Z. Wang *et al.*, "Cyclophilin E functions as a negative regulator to influenza virus replication by impairing the formation of the viral ribonucleoprotein complex," *PLoS One*, vol. 6, no. 8, 2011, doi: 10.1371/journal.pone.0022625.

[256] J. Fernandez *et al.*, "Microtubule-associated proteins 1 (MAP1) promote human immunodeficiency virus type I (HIV-1) intracytoplasmic routing to the nucleus," *J. Biol. Chem.*, vol. 290, no. 8, pp. 4631–4646, 2015, doi: 10.1074/jbc.M114.613133.

[257] A. C. Schinzel *et al.*, "Cyclophilin D is a component of mitochondrial permeability transition and mediates neuronal cell death after focal cerebral ischemia," *Proc. Natl. Acad. Sci. U. S. A.*, vol. 102, no. 34, pp. 12005–12010, 2005, doi: 10.1073/pnas.0505294102.

[258] C. P. Baines *et al.*, "Loss of cyclophilin D reveals a critical role for mitochondrial permeability transition in cell death," *Nature*, vol. 435, pp. 658–662, 2005, doi: 10.1038/nature02816.

[259] F. P. Nestel, K. Colwill, S. Harper, T. Pawson, and S. K. Anderson, "RS cyclophilins: Identification of an NK-TR1-related cyclophilin," *Gene*, vol. 180, no. 1–2, pp. 151–155, 1996, doi: 10.1016/S0378-1119(96)00436-2.

[260] C. L. Lin, S. Leu, M. C. Lu, and P. Ouyang, "Over-expression of SR-cyclophilin, an interaction partner of nuclear pinin, releases SR family splicing factors from nuclear speckles," *Biochem. Biophys. Res. Commun.*, vol. 321, no. 3, pp. 638–647, 2004, doi: 10.1016/j.bbrc.2004.07.013.

[261] J. P. Bourquin *et al.*, "A serine/arginine-rich nuclear matrix cyclophilin interacts with the C-terminal domain of RNA polymerase II," *Nucleic Acids Res.*, vol. 25, no. 11, pp. 2055–2061, 1997, doi: 10.1093/nar/25.11.2055.

[262] D. Ingelfinger *et al.*, "Two protein-protein interaction sites on the spliceosome-associated human cyclophilin CypH," *Nucleic Acids Res.*, vol. 31, no. 16, pp. 4791–4796, 2003, doi: 10.1093/nar/gkg660.

[263] S. Teigelkamp *et al.*, "The 20kD protein of human [U4/U6.U5] tri-snRNPs is a novel cyclophilin that forms a complex with the U4/U6-specific 60kD and 90kD proteins," *Rna*, vol. 4, no. 2, pp. 127–141, 1998.

[264] U. Reidt, M. C. Wahl, D. Fasshauer, D. S. Horowitz, R. Lührmann, and R. Ficner, "Crystal structure of a complex between human spliceosomal cyclophilin H and a U4/U6 snRNP-60K peptide," *J. Mol. Biol.*, vol. 331, no. 1, pp. 45–56, 2003, doi: 10.1016/S0022-2836(03)00684-3.

[265] A. Dharan *et al.*, "KIF5B and Nup358 Cooperatively Mediate the Nuclear Import of HIV-1 during Infection," *PLoS Pathog.*, vol. 12, no. 6, pp. 1–24, 2016, doi: 10.1371/journal.ppat.1005700.

[266] K. Bichel, A. J. Price, T. Schaller, G. J. Towers, S. M. V. Freund, and L. C. James, "HIV-1 capsid undergoes coupled binding and isomerization by the nuclear pore protein NUP358," *Retrovirology*, vol. 10, no. 1, p. 1, 2013, doi: 10.1186/1742-4690-10-81.

[267] A. M. Meehan *et al.*, "A Cyclophilin Homology Domain-Independent Role for Nup358 in HIV-1 Infection," *PLoS Pathog.*, vol. 10, no. 2, pp. 1–17, 2014, doi: 10.1371/journal.ppat.1003969.

[268] K. E. Ocwieja *et al.*, "HIV integration targeting: A pathway involving transportin-3 and the nuclear pore protein RanBP2," *PLoS Pathog.*, vol. 7, no. 3, pp. 19–21, 2011, doi: 10.1371/journal.ppat.1001313.

[269] F. Impens *et al.*, "A catalogue of putative HIV-1 protease host cell substrates," *Biol. Chem.*, vol. 393, no. 9, pp. 915–931, 2012, doi: 10.1515/hsz-2012-0168.

[270] S. Liu *et al.*, "Measuring antiviral activity of benzimidazole molecules that alter IRES RNA structure with an infectious hepatitis C virus chimera expressing Renilla luciferase," *Antiviral Res.*, vol. 89, no. 1, pp. 54–63, 2011, doi: 10.1016/j.antiviral.2010.11.004.

[271] T. Dochi *et al.*, "Phosphorylation of human immunodeficiency virus type 1 capsid protein at serine 16, required for peptidyl-prolyl isomerase-dependent uncoating, is mediated by virion-incorporated extracellular signal-regulated kinase 2," *J. Gen. Virol.*, vol. 95, pp. 1156–1166, 2014, doi: 10.1099/vir.0.060053-0.

[272] L. Manganaro, M. Lusic, M. I. Gutierrez, A. Cereseto, G. Del Sal, and M. Giacca, "Concerted action of cellular JNK and Pin1 restricts HIV-1 genome integration to

activated CD4+ T lymphocytes," *Nat. Med.*, vol. 16, no. 3, pp. 329–333, 2010, doi: 10.1038/nm.2102.

[273] F. Fujimori *et al.*, "Crosstalk of prolyl isomerases, Pin1/Essl, and cyclophilin A," *Biochem. Biophys. Res. Commun.*, vol. 289, no. 1, pp. 181–190, 2001, doi: 10.1006/bbrc.2001.5925.

[274] K. Takahasi *et al.*, "Nonself RNA-Sensing Mechanism of RIG-I Helicase and Activation of Antiviral Immune Responses," *Mol. Cell*, vol. 29, no. 4, pp. 428–440, 2008, doi: 10.1016/j.molcel.2007.11.028.

[275] Y. M. Loo and M. Gale, "Immune Signaling by RIG-I-like Receptors," *Immunity*, vol. 34, no. 5, pp. 680–692, 2011, doi: 10.1016/j.immuni.2011.05.003.

[276] M. Yoneyama *et al.*, "The RNA helicase RIG-I has an essential function in double-stranded RNA-induced innate antiviral responses," *Nat. Immunol.*, vol. 5, no. 7, pp. 730–737, 2004, doi: 10.1038/ni1087.

[277] H. M. Liu, Y.-M. Loo, S. M. Horner, G. A. Tornetzer, M. G. Katze, and M. J. Gale, "The mitochondrial targeting chaperone 14-3-3ε regulates a RIG-I translocon that mediates membrane-association and innate antiviral immunity," *Cell Host Microbe*, vol. 11, no. 5, pp. 528–537, 2012, doi: 10.2174/157339511794474244.

[278] H. Kato *et al.*, "Differential roles of MDA5 and RIG-I helicases in the recognition of RNA viruses," *Nature*, vol. 441, no. 1, pp. 101–105, 2006, doi: 10.1038/nature04734.

[279] B. L. Fredericksen, B. C. Keller, J. Fornek, M. G. Katze, and M. Gale, "Establishment and Maintenance of the Innate Antiviral Response to West Nile Virus Involves both RIG-I and MDA5 Signaling through IPS-1," *J. Virol.*, vol. 82, no. 2, pp. 609–616, 2008, doi: 10.1128/jvi.01305-07.

[280] A. Pichlmair *et al.*, "Rig-I-Mediated Antiviral Responses to Single-Stranded RNA Bearing 5'-Phosphates," *Science (80-.).*, vol. 314, no. 5901, pp. 997–1001, 2006.

[281] H. Kato *et al.*, "Length-dependent recognition of double-stranded ribonucleic acids by retinoic acid-inducible gene-I and melanoma differentiation-associated gene 5," *J. Exp. Med.*, vol. 205, no. 7, pp. 1601–1610, 2008, doi: 10.1084/jem.20080091.

[282] I. T. Lamborn and H. C. Su, "Genetic determinants of host immunity against human rhinovirus infections," *Hum. Genet.*, 2020, doi: 10.1007/s00439-020-02137-3.

[283] J. Hiscott, J. Lacoste, and R. Lin, "Recruitment of an interferon molecular signaling complex to the mitochondrial membrane: disruption by hepatitis C virus NS3-4A protease.," *Biochem. Pharmacol.*, vol. 72, no. 11, pp. 1477–1484, 2006.

[284] Y. Wang, X. Wang, J. Li, Y. Zhou, and W. Ho, "RIG-I activation inhibits HIV replication in macrophages," *J. Leukoc. Biol.*, vol. 94, no. 2, pp. 337–341, 2013, doi: 10.1189/jlb.0313158.

[285] M. Stunnenberg *et al.*, "Synthetic Abortive HIV-1 RNAs Induce Potent Antiviral Immunity," *Front. Immunol.*, vol. 11, no. January, pp. 1–14, 2020, doi: 10.3389/fimmu.2020.00008.

[286] M. Solis *et al.*, "RIG-I-Mediated Antiviral Signaling Is Inhibited in HIV-1 Infection by a Protease-Mediated Sequestration of RIG-I," *J. Virol.*, vol. 85, no. 3, pp. 1224–1236, 2011, doi: 10.1128/jvi.01635-10.

[287] R. K. Berg *et al.*, "Genomic HIV RNA induces innate immune responses through RIG-I-dependent sensing of secondary-structured RNA," *PLoS One*, vol. 7, no. 1, pp. 1–10, 2012, doi: 10.1371/journal.pone.0029291.

[288] A. N. Harman *et al.*, "HIV Blocks Interferon Induction in Human Dendritic Cells and Macrophages by Dysregulation of TBK1," *J. Virol.*, vol. 89, no. 13, pp. 6575–6584, 2015, doi: 10.1128/jvi.00889-15.

[289] B. P. Doehle *et al.*, "Vpu-Deficient HIV Strains Stimulate Innate Immune Signaling Responses in Target Cells," *J. Virol.*, vol. 86, no. 16, pp. 8499–8506, 2012, doi: 10.1128/jvi.00424-12.

[290] S. Y. Park, A. A. Waheed, Z. R. Zhang, E. O. Freed, and J. S. Bonifacino, "HIV-1 Vpu accessory protein induces caspase-mediated cleavage of IRF3 transcription factor," *J. Biol. Chem.*, vol. 289, no. 51, pp. 35102–35110, 2014, doi: 10.1074/jbc.M114.597062.

[291] D. Hotter, F. Kirchhoff, and D. Sauter, "HIV-1 Vpu Does Not Degrade Interferon Regulatory Factor 3," *J. Virol.*, vol. 87, no. 12, pp. 7160–7165, 2013, doi: 10.1128/jvi.00526-13.

[292] L. Manganaro *et al.*, "HIV Vpu Interferes with NF-κB Activity but Not with Interferon Regulatory Factor 3," *J. Virol.*, vol. 89, no. 19, pp. 9781–9790, 2015, doi: 10.1128/jvi.01596-15.

[293] J. K. Kranz and C. Schalk-Hihi, *Protein Thermal Shifts to Identify Low Molecular Weight Fragments*, 1st ed., vol. 493. Elsevier Inc., 2011.

[294] J. J. Lavinder, S. B. Hari, B. J. Sullivan, and T. J. Magliery, "High-throughput thermal scanning: A general, rapid dye-binding thermal shift screen for protein engineering," *J. Am. Chem. Soc.*, vol. 131, no. 11, pp. 3794–3795, 2009, doi: 10.1021/ja8049063.

[295] S. N. Krishna *et al.*, "A fluorescence-based thermal shift assay identifies inhibitors of mitogen activated protein kinase kinase 4," *PLoS One*, vol. 8, no. 12, 2013, doi: 10.1371/journal.pone.0081504.

[296] D. M. Molina *et al.*, "Monitoring Drug Target Engagement in Cells and tissues Using the Cellular Thermal Shift Assay," *Science (80-.).*, vol. 341, no. July, pp. 84–88, 2013.

[297] M. Schürmann, P. Janning, S. Ziegler, and H. Waldmann, "Small-Molecule Target Engagement in Cells," *Cell Chem. Biol.*, vol. 23, no. 4, pp. 435–441, 2016, doi: 10.1016/j.chembiol.2016.03.008.

[298] M. M. Savitski *et al.*, "Tracking cancer drugs in living cells by thermal profiling of the proteome," *Science (80-.).*, vol. 346, no. 6205, 2014, doi: 10.1126/science.1255784.

[299] H. Franken *et al.*, "Thermal proteome profiling for unbiased identification of direct and indirect drug targets using multiplexed quantitative mass spectrometry," *Nat. Protoc.*, vol. 10, no. 10, pp. 1567–1593, 2015, doi: 10.1038/nprot.2015.101.

[300] F. B. M. Reinhard *et al.*, "Thermal proteome profiling monitors ligand interactions with cellular membrane proteins," *Nat. Methods*, vol. 12, no. 12, pp. 1129–1131, 2015, doi: 10.1038/nmeth.3652.

[301] K. V. M. Huber *et al.*, "Proteome-wide drug and metabolite interaction mapping by thermal-stability profiling," *Nat. Methods*, vol. 12, no. 11, pp. 1055–1057, 2015, doi: 10.1038/nmeth.3590.

[302] Y.-G. Yeung, E. Nieves, R. Angeletti, and E. R. Stanley, "Removal of detergents from protein digests for mass spectrometry analysiss," *Anal Biochem.*, vol. 382, no. 2, pp. 135–137, 2008, doi: 10.1038/jid.2014.371.

[303] M. Wilhelm *et al.*, "Mass-spectrometry-based draft of the human proteome," *Nature*, vol. 509, no. 7502, pp. 582–587, 2014, doi: 10.1038/nature13319.

[304] E. Sokolskaja and J. Luban, "Cyclophilin, TRIM5, and innate immunity to HIV-1," *Curr.*

Opin. Microbiol., vol. 9, no. 4, pp. 404–408, 2006, doi: 10.1016/j.mib.2006.06.011.

[305] S. Li *et al.*, "Hepatitis C virus NS4B induces unfolded protein response and endoplasmic reticulum overload response-dependent NF-κB activation," *Virology*, 2009, doi: 10.1016/j.virol.2009.06.039.

[306] R. B. DuBridge, P. Tang, H. C. Hsia, P. M. Leong, J. H. Miller, and M. P. Calos, "Analysis of mutation in human cells by using an Epstein-Barr virus shuttle system.," *Mol. Cell. Biol.*, vol. 7, no. 1, pp. 379–387, 1987, doi: 10.1128/mcb.7.1.379.

[307] W. S. Pear, G. P. Nolan, M. L. Scott, and D. Baltimore, "Production of high-titer helper-free retroviruses by transient transfection," *Proc. Natl. Acad. Sci. U. S. A.*, vol. 90, no. 18, pp. 8392–8396, 1993, doi: 10.1073/pnas.90.18.8392.

[308] J. W. B. Bainbridge *et al.*, "In vivo gene transfer to the mouse eye using an HIV-based lentiviral vector; efficient long-term transduction of cornealendothelium and retinal pigment epithelium," *Gene Ther.*, vol. 8, no. 21, pp. 1665–1668, 2001, doi: 10.1038/sj.gt.3301574.

[309] T. Schaller, D. Pollpeter, L. Apolonia, C. Goujon, and M. H. Malim, "Nuclear import of SAMHD1 is mediated by a classical karyopherin α/β1 dependent pathway and confers sensitivity to VpxMAC induced ubiquitination and proteasomal degradation," *Retrovirology*, vol. 11, no. 1, pp. 1–16, 2014, doi: 10.1186/1742-4690-11-29.

[310] R. Zufferey, D. Nagy, R. J. Mandel, L. Naldini, and D. Trono, "Multiply attenuated lentiviral vector achieves efficient gene delivery in vivo," *Nat. Biotechnol.*, vol. 15, 1997.

[311] S. Wang *et al.*, "YAP antagonizes innate antiviral immunity and is targeted for lysosomal degradation through IKKI-mediated phosphorylation," *Nat. Immunol.*, vol. 18, no. 7, pp. 733–743, 2017, doi: 10.1038/ni.3744.

[312] W. Ye *et al.*, "Microvesicles from malaria-infected red blood cells activate natural killer cells via MDA5 pathway," *PLoS Pathog.*, vol. 14, no. 10, pp. 1–21, 2018, doi: 10.1371/journal.ppat.1007298.

[313] G. Q. Liu *et al.*, "Nuclear-resident RIG-I senses viral replication inducing antiviral immunity," *Nat. Commun.*, vol. 9, no. 1, 2018, doi: 10.1038/s41467-018-05745-w.

[314] S. Horn *et al.*, "Caspase-10 Negatively Regulates Caspase-8-Mediated Cell Death, Switching the Response to CD95L in Favor of NF-κB Activation and Cell Survival,"

Cell Rep., vol. 19, no. 4, pp. 785–797, 2017, doi: 10.1016/j.celrep.2017.04.010.

[315] C. Goujon *et al.*, "Evidence for IFNα-induced, SAMHD1-independent inhibitors of early HIV-1 infection," *Retrovirology*, vol. 10, no. 1, pp. 1–6, 2013, doi: 10.1186/1742-4690-10-23.

[316] M. Pizzato, O. Erlwein, D. Bonsall, S. Kaye, D. Muir, and M. O. McClure, "A one-step SYBR Green I-based product-enhanced reverse transcriptase assay for the quantitation of retroviruses in cell culture supernatants," *J. Virol. Methods*, vol. 156, no. 1–2, pp. 1–7, 2009, doi: 10.1016/j.jviromet.2008.10.012.

[317] W. Chanput, J. J. Mes, and H. J. Wichers, "THP-1 cell line: An in vitro cell model for immune modulation approach," *Int. Immunopharmacol.*, vol. 23, no. 1, pp. 37–45, 2014, doi: 10.1016/j.intimp.2014.08.002.

[318] A. Billich *et al.*, "Mode of action of SDZ NIM 811, a nonimmunosuppressive cyclosporin A analog with activity against human immunodeficiency virus (HIV) type 1: interference with HIV protein-cyclophilin A interactions.," *J. Virol.*, vol. 69, no. 4, pp. 2451–2461, 1995, doi: 10.1128/jvi.69.4.2451-2461.1995.

[319] R. Saxena, S. Gupta, K. Singh, K. Mitra, A. K. Tripathi, and R. K. Tripathi, "Proteomic profiling of SupT1 cells reveal modulation of host proteins by HIV-1 Nef variants," *PLoS One*, vol. 10, no. 4, pp. 1–24, 2015, doi: 10.1371/journal.pone.0122994.

[320] S. M. Solbak *et al.*, "The intriguing Cyclophilin A-HIV-1 Vpr interaction: Prolyl cis/trans isomerisation catalysis and specific binding," *BMC Struct. Biol.*, vol. 10, pp. 1–15, 2010, doi: 10.1186/1472-6807-10-31.

[321] G. Fischer, H. Bang, and C. Mech, "Determination of Enzymatic Catalysis for the Cis-Trans-Isomerization of Peptide Binding in Proline-Containing Peptides," *Biomed Biochim Acta.*, vol. 43, no. 10, pp. 1101–11, 1984.

[322] R. Jafari *et al.*, "The cellular thermal shift assay for evaluating drug target interactions in cells," *Nat. Protoc.*, vol. 9, no. 9, pp. 2100–2122, 2014, doi: 10.1038/nprot.2014.138.

[323] A. Alshareef *et al.*, "The use of cellular thermal shift assay (CETSA) to study Crizotinib resistance in ALK-expressing human cancers," *Sci. Rep.*, vol. 6, no. 4, pp. 1–12, 2016, doi: 10.1038/srep33710.

[324] M. Schumann *et al.*, "Identification of low abundance cyclophilins in human plasma,"

Proteomics, vol. 16, no. 21, pp. 2815–2826, 2016, doi: 10.1002/pmic.201600221.

[325] A. Nicolli, E. Basso, V. Petronilli, R. M. Wenger, and P. Bernardi, "Interactions of cyclophilin with the mitochondrial inner membrane and regulation of the permeability transition pore, a cyclosporin A-sensitive channel," *J. Biol. Chem.*, vol. 271, no. 4, pp. 2185–2192, 1996, doi: 10.1074/jbc.271.4.2185.

[326] M. A. Rycyzyn and C. V. Clevenger, "The intranuclear prolactin/cyclophilin B complex as a transcriptional inducer," *Proc. Natl. Acad. Sci. U. S. A.*, vol. 99, no. 10, pp. 6790–6795, 2002, doi: 10.1073/pnas.092160699.

[327] M. Q. Wang, Y. L. Huang, J. Huang, J. L. Zheng, and G. X. Qian, "RIG-I detects HIV-1 infection and mediates type i interferon response in human macrophages from patients with HIV-1-associated neurocognitive disorders," *Genet. Mol. Res.*, vol. 14, no. 4, pp. 13799–13811, 2015, doi: 10.4238/2015.October.28.42.

[328] C. Cadena *et al.*, "Ubiquitin-dependent and -independent roles of E3 ligase RIPLET in innate immunity," *Cell*, vol. 177, no. 5, pp. 1187–1200, 2019, doi: 10.1016/j.cell.2019.03.017.Ubiquitin-dependent.

[329] T. Krischuns *et al.*, "Phosphorylation of TRIM28 Enhances the Expression of IFN-β and Proinflammatory Cytokines During HPAIV Infection of Human Lung Epithelial Cells," *Front. Immunol.*, vol. 9, no. September, p. 2229, 2018, doi: 10.3389/fimmu.2018.02229.

[330] T. H. Mogensen, "IRF and STAT transcription factors - From basic biology to roles in infection, protective immunity, and primary immunodeficiencies," *Front. Immunol.*, vol. 10, no. JAN, pp. 1–13, 2019, doi: 10.3389/fimmu.2018.03047.

[331] P. Madlala *et al.*, "Association of polymorphisms in the regulatory region of the cyclophilin a gene (PPIA) with gene expression and HIV/AIDS disease progression," *J. Acquir. Immune Defic. Syndr.*, vol. 72, no. 5, pp. 465–473, 2016, doi: 10.1097/QAI.0000000000001028.

[332] D. M. Asmuth *et al.*, "Safety, tolerability and mechanisms of antiretroviral activity of peginterferon alfa-2a in HIV-1-mono-infected subjects: a phase II clinical trial," *J. Infect. Dis.*, vol. 201, no. 11, pp. 1686–1696, 2010, doi: 10.1086/652420.Safety.

[333] P. V. Maillard, V. Zoete, O. Michielin, and D. Trono, "Homology-based identification of capsid determinants that protect HIV1 from human TRIM5α restriction," *J. Biol. Chem.*, vol. 286, no. 10, pp. 8128–8140, 2011, doi: 10.1074/jbc.M110.187609.

[334] D. K. Fischer, A. Saito, C. Kline, R. Cohen, and S. C. Watkins, "CA Mutation N57A Has Distinct Strain-Specific HIV-1 Capsid Uncoating and Infectivity Phenotypes," vol. 93, no. 9, pp. 1–19, 2019.

[335] M. Burse, J. Shi, and C. Aiken, "Cyclophilin A potentiates TRIM5α inhibition of HIV-1 nuclear import without promoting TRIM5α binding to the viral capsid," *PLoS One*, vol. 12, no. 8, pp. 1–18, 2017, doi: 10.1371/journal.pone.0182298.

[336] S. Jäger *et al.*, "Global landscape of HIV-human protein complexes," *Nature*, vol. 481, no. 7381, pp. 365–370, 2012, doi: 10.1038/nature10719.

[337] Z. Zhang, N. Carriero, D. Zheng, J. Karro, P. M. Harrison, and M. Gerstein, "PseudoPipe: An automated pseudogene identification pipeline," *Bioinformatics*, vol. 22, no. 12, pp. 1437–1439, 2006, doi: 10.1093/bioinformatics/btl116.

[338] P. G. Ferreira *et al.*, "Transcriptome characterization by RNA sequencing identifies a major molecular and clinical subdivision in chronic lymphocytic leukemia," *Genome Res.*, vol. 24, no. 2, pp. 212–226, 2014, doi: 10.1101/gr.152132.112.

[339] S. Tsuchiya, M. Yamabe, Y. Yamaguchi, Y. Kobayashi, T. Konno, and K. Tada, "Establishment and characterization of a human acute monocytic leukemia cell line (THP-1)," *Int. J. Cancer*, vol. 26, no. 2, pp. 171–176, 1980, doi: 10.1002/ijc.2910260208.

[340] E. K. Brinkman, T. Chen, M. de Haas, H. A. Holland, W. Akhtar, and B. van Steensel, "Kinetics and Fidelity of the Repair of Cas9-Induced Double-Strand DNA Breaks," *Mol. Cell*, vol. 70, no. 5, pp. 801-813.e6, 2018, doi: 10.1016/j.molcel.2018.04.016.

[341] J. DeBoer, T. Jagadish, N. A. Haverland, C. J. Madson, P. Ciborowski, and M. Belshan, "Alterations in the nuclear proteome of HIV-1 infected T-cells," *Virology*, vol. 0, pp. 409–420, 2014, doi: 10.1038/jid.2014.371.

[342] E. R. Price, M. Jin, D. Lim, S. Pati, C. T. Walsh, and F. D. Mckeon, "Cyclophilin B trafficking through the secretory pathway is altered by binding of cyclosporin A," *Proc. Natl. Acad. Sci. U. S. A.*, vol. 91, no. 9, pp. 3931–3935, 1994, doi: 10.1073/pnas.91.9.3931.

[343] S. Arber, K. H. Krause, and P. Caroni, "s-Cyclophilin is retained intracellularly via a unique COOH-terminal sequence and colocalizes with the calcium storage protein calreticulin," *J. Cell Biol.*, vol. 116, no. 1, pp. 113–125, 1992, doi:

10.1083/jcb.116.1.113.

[344] T. L. Davis *et al.*, "Structural and biochemical characterization of the human cyclophilin family of peptidyl-prolyl isomerases," *PLoS Biol.*, vol. 8, no. 7, 2010, doi: 10.1371/journal.pbio.1000439.

[345] T. Wang, C. H. Yun, S. Y. Gu, W. R. Chang, and D. C. Liang, "1.88 Å crystal structure of the C domain of hCyP33: A novel domain of peptidyl-prolyl cis-trans isomerase," *Biochem. Biophys. Res. Commun.*, vol. 333, no. 3, pp. 845–849, 2005, doi: 10.1016/j.bbrc.2005.06.006.

[346] M. Ooms, T. E. M. Abbink, C. Pham, and B. Berkhout, "Circularization of the HIV-1 RNA genome," *Nucleic Acids Res.*, vol. 35, no. 15, pp. 5253–5261, 2007, doi: 10.1093/nar/gkm564.

[347] B. Poon and I. S. Y. Chen, "Human Immunodeficiency Virus Type 1 (HIV-1) Vpr Enhances Expression from Unintegrated HIV-1 DNA," *J. Virol.*, vol. 77, no. 7, pp. 3962–3972, 2003, doi: 10.1128/jvi.77.7.3962-3972.2003.

[348] M. Hrimech, X.-J. Yao, F. Bachand, N. Rougeau, and É. A. Cohen, "Human Immunodeficiency Virus Type 1 (HIV-1) Vpr Functions as an Immediate-Early Protein during HIV-1 Infection," *J. Virol.*, vol. 73, no. 5, pp. 4101–4109, 1999, doi: 10.1128/jvi.73.5.4101-4109.1999.

[349] I. Rusinova *et al.*, "INTERFEROME v2.0: An updated database of annotated interferon-regulated genes," *Nucleic Acids Res.*, vol. 41, no. D1, pp. 1040–1046, 2013, doi: 10.1093/nar/gks1215.

[350] S. D. Frausto, E. Lee, and H. Tang, "Cyclophilins as modulators of viral replication," *Viruses*, vol. 5, no. 7, pp. 1684–1701, 2013, doi: 10.3390/v5071684.

[351] M. M. Savitski *et al.*, "Tracking cancer drugs in living cells by thermal profiling of the proteome," *Science (80-.).*, vol. 346, no. 6205, 2014, doi: 10.1126/science.1255784.

[352] D. Gibellini *et al.*, "HIV-1 and recombinant gp120 affect the survival and differentiation of human vessel wall-derived mesenchymal stem cells," *Retrovirology*, vol. 8, no. 1, p. 40, 2011, doi: 10.1186/1742-4690-8-40.

[353] C. A. Barrero *et al.*, "HIV-1 Vpr Modulates Macrophage Metabolic Pathways: A SILAC-Based Quantitative Analysis," *PLoS One*, vol. 8, no. 7, 2013, doi:

10.1371/journal.pone.0068376.

[354] M. A. Jarboui *et al.*, "Nucleolar Protein Trafficking in Response to HIV-1 Tat: Rewiring the Nucleolus," *PLoS One*, vol. 7, no. 11, 2012, doi: 10.1371/journal.pone.0048702.

[355] C. Ritchie, I. Cylinder, E. J. Platt, and E. Barklis, "Analysis of HIV-1 Gag Protein Interactions via Biotin Ligase Tagging," *J. Virol.*, vol. 89, no. 7, pp. 3988–4001, 2015, doi: 10.1128/jvi.03584-14.

[356] S. de Breyne, R. Soto-Rifo, M. López-Lastra, and T. Ohlmann, "Translation initiation is driven by different mechanisms on the HIV-1 and HIV-2 genomic RNAs.," *Virus Res.*, vol. 171, no. 2, pp. 366–381, 2013.

[357] S. De Breyne *et al.*, "In vitro studies reveal that different modes of initiation on HIV-1 mRNA have different levels of requirement for eukaryotic initiation factor 4F," *FEBS J.*, vol. 279, no. 17, pp. 3098–3111, 2012, doi: 10.1111/j.1742-4658.2012.08689.x.

[358] M. C. Lai, S. W. Wang, L. Cheng, W. Y. Tarn, S. J. Tsai, and H. S. Sun, "Human DDX3 Interacts with the HIV-1 Tat Protein to Facilitate Viral mRNA Translation," *PLoS One*, vol. 8, no. 7, pp. 1–14, 2013, doi: 10.1371/journal.pone.0068665.

[359] A. Castelló *et al.*, "HIV-1 protease inhibits cap-and poly(A)-dependent translation upon eIF4GI and PABP cleavage," *PLoS One*, vol. 4, no. 11, 2009, doi: 10.1371/journal.pone.0007997.

[360] E. Ricci, R. Soto Rifo, C. Herbreteau, D. Decimo, and T. Ohlmann, "Lentiviral RNAs can use different mechanisms for translation initiation.," *Biochem. Soc. Trans.*, vol. 4, pp. 690–693, 2008.

[361] E. Alvarez, L. Menendez-Arias, and L. Carrasco, "The Eukaryotic Translation Initiation Factor 4GI Is Cleaved by Different Retroviral Proteases," *J. Virol.*, vol. 77, no. 23, pp. 12392–12400, 2003, doi: 10.1128/jvi.77.23.12392-12400.2003.

[362] I. Ventoso, R. Blanco, C. Perales, and L. Carrasco, "HIV-1 protease cleaves eukaryotic initiation factor 4G and inhibits cap-dependent translation," *Proc. Natl. Acad. Sci. U. S. A.*, vol. 98, no. 23, pp. 12966–12971, 2001, doi: 10.1073/pnas.231343498.

[363] P. Lohavanichbutr *et al.*, "Genomewide gene expression profiles of HPV-positive and HPV-negative oropharyngeal cancer potential implications for treatment choices," *Arch. Otolaryngol. - Head Neck Surg.*, vol. 135, no. 2, pp. 180–188, 2009, doi:

10.1001/archoto.2008.540.

[364] M. Fischer, S. Uxa, C. Stanko, T. M. Magin, and K. Engeland, "Human papilloma virus E7 oncoprotein abrogates the p53-p21-DREAM pathway," *Sci. Rep.*, vol. 7, no. 1, pp. 1–11, 2017, doi: 10.1038/s41598-017-02831-9.

[365] G. D. Gupta *et al.*, "A dynamic protein interaction landscape of the human centrosome-cilium interface," *Cell*, vol. 163, no. 6, pp. 1484–1499, 2015, doi: 10.1016/j.cell.2015.10.065.A.

[366] C. T. Mai, M. M. Wu, C. L. Wang, Z. R. Su, Y. Y. Cheng, and X. J. Zhang, "Palmatine attenuated dextran sulfate sodium (DSS)-induced colitis via promoting mitophagy-mediated NLRP3 inflammasome inactivation," *Mol. Immunol.*, vol. 105, no. October 2018, pp. 76–85, 2019, doi: 10.1016/j.molimm.2018.10.015.

[367] N. Schultze, H. Wanka, P. Zwicker, U. Lindequist, and B. Haertel, "Mitochondrial functions of THP-1 monocytes following the exposure to selected natural compounds," *Toxicology*, vol. 377, pp. 57–63, 2017, doi: 10.1016/j.tox.2016.12.006.

[368] J. J. Siekierka, M. J. Staruch, S. H. Hung, and N. H. Sigal, "FK-506 , a potent novel immunosuppressive agent , binds to a cytosolic protein which is distinct from the cyclosporin A-binding protein , cyclophilin .," *J Immunol*, vol. 143, pp. 1580–1583, 1989.

[369] J. M. Bonner and G. L. Boulianne, "Diverse structures, functions and uses of FK506 binding proteins," *Cell. Signal.*, vol. 38, no. June, pp. 97–105, 2017, doi: 10.1016/j.cellsig.2017.06.013.

[370] A. M. Kell and M. Gale, "RIG-I in RNA virus recognition," *Virology*, vol. 479, pp. 110–121, 2015.

[371] P. S. Gonzalez *et al.*, "Mannose impairs tumour growth and enhances chemotherapy," *Nature*, vol. 563, no. 7733, pp. 719–723, 2018, doi: 10.1038/s41586-018-0729-3.

[372] M. Ringeard, V. Marchand, E. Decroly, Y. Motorin, and Y. Bennasser, "FTSJ3 is an RNA 2′-O-methyltransferase recruited by HIV to avoid innate immune sensing," *Nature*, vol. 565, no. 7740, pp. 500–504, 2019, doi: 10.1038/s41586-018-0841-4.

[373] E. Balestrieri *et al.*, "Apoptosis-Associated Gene Expression in HIV-Infected Patients in Response to Successful Antiretroviral Therapy," *J. Medi*, vol. 79, pp. 111–117, 2007,

doi: 10.1002/jmv.

[374] Y. Xu, J. Kulkosky, E. Acheampong, G. Nunnari, J. Sullivan, and R. J. Pomerantz, "HIV-1-mediated apoptosis of neuronal cells: Proximal molecular mechanisms of HIV-1-induced encephalopathy," *Proc. Natl. Acad. Sci. U. S. A.*, vol. 101, no. 18, pp. 7070–7075, 2004, doi: 10.1073/pnas.0304859101.

[375] M. Ghosh *et al.*, "Pathogen Recognition in the Human Female Reproductive Tract: Expression of Intracellular Cytosolic Sensors NOD1, NOD2, RIG-1, and MDA5 and response to HIV-1 and Neisseria gonorrhea," *Am J Reprod Immunol*, vol. 69, no. 1, pp. 41–51, 2013, doi: 10.1038/jid.2014.371.

[376] W. Liu *et al.*, "Cyclophilin A-regulated ubiquitination is critical for RIG-I-mediated antiviral immune responses," *Elife*, vol. 6, pp. 1–21, 2017, doi: 10.7554/eLife.24425.

[377] C. Chiang and M. U. Gack, "Post-translational Control of Intracellular Pathogen Sensing Pathways," *Trends Immunol.*, vol. 38, no. 1, pp. 39–52, 2017, doi: 10.1016/j.physbeh.2017.03.040.

[378] K. Takashima, H. Oshiumi, H. Takaki, M. Matsumoto, and T. Seya, "RIOK3-mediated phosphorylation of MDA5 interferes with its assembly and attenuates the innate immune response," *Cell Rep.*, vol. 11, no. 2, pp. 192–200, 2015, doi: 10.1016/j.celrep.2015.03.027.

[379] E. Wies *et al.*, "Dephosphorylation of the RNA sensors RIG-I and MDA5 by the phosphatase PP1 is essential for innate immune signaling," *Immunity*, vol. 38, no. 3, pp. 437–339, 2013, doi: 10.1038/jid.2014.371.